THE NON-INVASIVE QUANTIFICATION OF CUTANEOUS HAEMOGLOBIN AND ITS OXYGENATION BY REFLECTANCE SPECTROPHOTOMETRY

by

MOHSEN HAJIZADEH SAFFAR

A thesis submitted in fulfilment of the requirements

for the degree of Doctor of Philosophy

at

The University of Leeds

Department of Medical Physics

April 1988


بسم الله الرحمن الرحيم

ABSTRACT

The work detailed in this study describes the design of a rapid scanning multiwavelength reflectance spectrophotometer and its application to the measurement of cutaneous pigments. In this instrument the radiation from a 6 V, 20 W quartz halogen lamp is transmitted to the reflectance probe by fibre optics and illuminates the skin surface perpendicularly. The diffuse reflected light is then collected and transmitted to a rotating circular variable filter, CVF. The CVF is driven by a BBC Microcomputer and the spectrum from 356 to 721 nm is measured at 200 equally spaced wavelengths in 2.8 s.

Based upon the spectral differences between the absorbances of oxy and reduced haemoglobin, two indices were defined for quantifying the amount of haemoglobin, the "haemoglobin index", and oxygen saturation, the "oxygenation index", in a blood containing sample.

The haemoglobin index is derived from the spectrum of haemoglobin as the difference between two gradients calculated between three isobestic points (527.5, 544, and 573 nm). To measure the oxygenation index, two isobestic points (544 and 573 nm) and a point at 558.5 nm, where the specific absorption coefficient of oxy and reduced haemoglobin differ, are used.

Linear calibration curves of the haemoglobin index against haemoglobin content in-vitro using collimated and diffused light were obtained. The oxygenation index was converted to percentage oxygen saturation by comparing the oxygenation index of a sample with that of reduced and fully oxygenated blood. The validity of the method was examined by measuring the oxygen dissociation curve of human blood at pCO_2 of 40 mmHg, pH of 7.33, and 37 ^{o}C and comparing the results with

between measured and published curves confirms that the oxygen saturation of blood can be accurately measured by the present method.

The scattering properties of the epidermis were studied by measuring the angular distribution of light scattered by a sheet of epidermis. It was found that most of the radiation transmitted through the epidermis is forwardly orientated; 67% of the incident radiation at 630 nm remains within 22.5 degrees of the incident beam.

To facilitate the study of the absorption properties of epidermis a new index called the "melanin index" was introduced and quantified using a synthetic melanin compound for calibration purposes. The melanin index is based on the slope of the LIR spectrum of skin surface between 650 -700 nm, and was used to investigate the melanin pigmentation levels of different ethnic groups.

Reflectance spectrometry was used to study the amount of haemoglobin and oxygen saturation of the superficial blood in skin. Variations in the haemoglobin index of an arm and a finger tip were studied under different conditions of temperature and height of the limb relative to the heart. The effects of applying a topical vasodilating chemical and of the thermal regulatory function of blood at three different sites on a hand were also studied. In all these measurements the results were in good agreement with the biological prediction and confirmed the satisfactory operation of the instrument, the validity of the indices and their usefulness in quantifying "skin colour" changes.

To find the correlation between in-vivo haemoglobin index and the true amount of haemoglobin in blood in g/dl, skin reflectance measurements and blood samples were taken from patients who attended a blood clinic. The correlation coefficient between haemoglobin content

(g/dl) and the haemoglobin index as measured on the forearm and thumb of the patients were 0.4 and 0.2 respectively. The weak correlation coefficient is attributable to the difficulty of defining the volume of blood observed when measuring the haemoglobin index.

The instrument was used to measure changes in the blood content of the skin of animal and human subjects following treatment by photochemotherapy.

ACKNOWLEDGEMENT

First, I wish to express my gratitude to the late Professor Roy Parker for accepting me as a research student in the Department of Medical Physics.

I would especially like to express my sincere thanks to my supervisor, Dr. J.B. Dawson, for giving me the opportunity to select my topic for research and for his continuous support, encouragement and invaluable help and guidance throughout the work. His scientific knowledge and sincerity made it a pleasure for me to work under his supervision. In particular, I am very grateful to him and his wife, Joyce, for reading this manuscript, correcting my English and making many useful comments.

I extend my thanks to Dr. Jim Feather for continuous and helpful discussion throughout the course of this study.

I would like to thank Professor Jones, Department of Anaesthetics, for his interest in in-vivo oxygen saturation measurement and helpful co-operation and valuable scientific advice given while the oxygenation measurement was carried out.

I would also like to thank all the following:

Dr. Paul King for many helpful scientific discussions.

Duncan Ellis, Graham Fisher for being readily available with their considerable knowledge and experience to discuss any problem during my work in this laboratory.

Gary Leslie from Cookridge Hospital for the design and construction of the original reflectance spectrometer.

All my colleagues, secretarial and technical staff in the Department of Medical Physics for accepting me among them and for

their friendly help and discussions that have made the time during the course of my study a pleasure.

I gratefully acknowledge the Ministry of Culture and Higher Education of Islamic Republic of Iran for awarding me the opportunity for this study and its financial support.

Finally, thanks to my wife and children who have patiently borne with me during my study.

CONTENT

FIGURES:

TABLES:

ABBREVIATIONS

A/D	Analog to Digital converter
AVA	Arteriovenous anastomoses
CA1, CA2	Control lines for port A
CB1, CB2	Control lines for port B
C.V.	Coefficient of Variation
CVF	Circular Variable Filter
DPG	Diphosphoglycerate
E index	Erythema index
H index	Haemoglobin index
HBA	High Base Address
IER	Interrupt Enable Register
LBA	Low Base Address
LED	Light Emitted Diode
LIR	Logarithm of the Inverse Reflection
LSB	Least Significant Bit
MED	Minimum Erythema Dose
MSB	Most Significant Bit
O.D.	Optical Density
ODC	Oxygen Dissociation Curve
OP-AMP	Operational Amplifier
OX	Oxygenation index
PCR	Peripheral Control Register
PCV	Packed Cell Volume
RBC	Red Blood Cell Count
SAC	Specific Absorption Coefficient
S.D.	Standard Deviation
SEM	Standard Error of the Mean
STP	Standard Temperature and Pressure
UV	Ultraviolet (UVA and UVB)

CHAPTER 1

1 - INTRODUCTION

1 - 1 General considerations

The work detailed in this research was initiated to further develop reflectance spectrophotometric studies of the interaction of visible radiation with skin. The emphasis of the work is on the design and construction of a rapid, multiwavelength reflectance spectrophotometer and on improving methods for the simultaneous measurement of haemoglobin, melanin, and oxygen saturation of cutaneous blood by examining the optical properties of skin and blood.

Earlier work in this laboratory (Feather 1986) was directed at quantification of skin colour as a means of studying the interaction of visible and ultraviolet radiation with skin. The colour of skin is determined largely by the amount of blood in the cutaneous vascular network, the degree of oxygenation of blood, and by the presence or absence of the brown/black pigment, melanin. Observation of skin colour changes due to skin response to disease and external stimuli contribute significantly to both clinical and investigative medicine. The level of cutaneous pigment, particularly haemoglobin, is often a sensitive parameter of changes in skin state and general patient health, thus changes in skin colour are widely used in both clinical and investigative dermatology. The major advantage of objective colour measurement by reflectance spectrophotometry is that it can provide numerical indices of colour that have a basis only in the physico-chemical properties of the tissue. Other methods such as colorimetry, photography, and visual matching using colour standards

are to some extent dependent on viewing conditions and the observer.

In earlier work, reflectance spectrophotometry was used to study the changes in the haemoglobin and melanin content of the skin of patients undergoing PUVA therapy for psoriasis (Ryatt et al, 1983). At the start of the treatment the response of the lesion, in terms of its haemoglobin content, was in contrast to that of adjacent uninvolved skin, however during treatment the psoriatic lesion began to respond in a similar way to the uninvolved skin. The lesion was still present at this time and the change in response, which might define a satisfactory treatment end point, could not be detected visually. The quantitative nature of a parameter, the "melanin index" facilitated the calculation of the dose of UVA radiation reaching the target tissue and when taken in combination with an index of haemoglobin content provided a method of determining the optimum UVA dose for the treatment.

During the present study the emphasis was increasingly directed at making the method useful for non-invasive, continuous measurement of oxygen saturation of blood through measurement of the in-vivo reflectance spectrum of the skin surface. This further development of the method makes it suitable for use in several other clinical investigations such as those outlined below.

Clinical physiologists are interested in recording oxygen saturation in patients with advanced pulmonary diseases. In such patients the delicate balance of a number of respiratory mechanisms has to be regulated. Blood oxygenation is a useful and simple parameter available for this purpose. Continuous monitoring of oxygen saturation of the blood in the heart is desirable for the determination of cardiac shunts. Cardiac shunts seriously diminish the

blood flowing through the lungs and so the cells in the body as a whole often get far less oxygen than their normal requirement. When rapid and simultaneous measurement of haemoglobin and its oxygen saturation is possible it facilitates the investigation of the origin of variation in blood content of the micro- vascular bed at the site of interest. An increase in the blood content of a certain site if accompanied by an increase in the oxygen saturation may be due to more oxygenated blood entering the measurement site by dilatation of the arteries, whilst a decrease in oxygen saturation may be caused by release of oxygen due to tissue metabolic activity or obstruction of veins.

In the course of the present study reflectance spectrophotometry was applied to a number of clinical situations. In collaboration with a dermatologist, the change of blood content, and its level of oxygenation, in port wine stains after treatment by laser coagulation was measured at intervals over a period of several months in an attempt to identify the vascular changes taking place in the skin. In a research application, reflectance measurements were made on superficial tumours in human and animal subjects undergoing treatment by photochemotherapy; marked changes in blood content and oxygenation were observed. A further area of collaboration was in anaesthetics where measurement of the oxygen saturation of anaesthetized patients is necessary to prevent hypoxaemia (ie. insufficient oxygen in the arterial blood to sustain life). Lack of oxygen is the commonest cause of anaesthetic mortality and a survey of anaesthetic mishaps indicated that from one to two thirds of those that end in death or severe brain damage were the result of hypoxaemia (Keenan 1986). Our study of reflectance spectrophotometry was extended to include the development

of an oximeter for clinical use and to an examination of the metabolic activity and response of skin to change in environmental conditions.

1 - 2 Historical survey of optical studies of skin

1-2-1 Early work

When a coloured object eg. a piece of red cardboard, is exposed to white light, red light will be reflected and produce the visual stimulus in our eye, whilst the other wavelengths will be absorbed. Thus it is the spectral composition of the reflected light which induced the visual sensation of colour, but it is the selective absorption of light which provides information on the composition of the object.

It was well understood from early times that the colour of human skin, to a certain extent, serves as an index of the state of well-being or the converse, and has been interpreted as evidence of health or disease. Without doubt, variation in environmental or body temperature and psychic emotion or unrest play a part in the composite of factors which go to make up the colour of skin. In pathological conditions, in which there may be abnormalities or derangements of pigmentation and of the vascular distribution, there is a wide range of variations in the colour of the skin. Some of these changes may be recognized readily by the eye, others can not be so recognized and, if appreciated, cannot be quantified by the clinical methods.

One of the earliest attempts to measure skin colour using reflectance spectrophotometry was that reported by Brunsting and Sheard in 1929. They used a modified KeUffel spectrophotometer, which relied upon visual matching of two semicircular fields produced by monochromatic light reflected from skin and a standard magnesium

block. In this classic study they investigated reflectance spectra of subjects with different levels of melanin pigmentation in the wavelength range 430 to 700 nm. The reflectance data were converted into the attributes of colour, relative luminosity (brilliance), dominant wavelength (hue) and purity (saturation), which at that time were considered of importance in the definition of colour.

Farrington et al (1968) reported that although skin is readily accessible, measurement of any of its parameters, including colour, is difficult, largely due to its flexibility and its sensitivity to the measurement procedures. They described a method whereby observers can grade the response of skin to environmental variables. The application of the method to a study of melanin pigmentation of the skin following exposure to solar radiation was reported. Visual grading on a scale from + to +++++ was compared with reflectance measurements of skin at different wavelengths using a reflectance meter (Photovolt model 610-T). They demonstrated a linear relationship between visual grading of the skin colour and the logarithm of the reflectance of red light. They concluded that quantitative judgments based on the above scoring system could be meaningful in clinical practice. Sulzberger (1968) has also confirmed that this method can be used by logical, trained and unbiased clinicians as a sufficiently accurate measurement that can discriminate between differences and identify similarities in responses in skin. Negative grading can be used for blanching while positive grades are used for assessment of skin reddening.

A full understanding of the optics of the connective tissue is necessary for any interpretation of skin colour. As white light falls on the surface of a piece of dermis, it penetrates increasingly into

the dermis from the violet to the red end of the spectrum. In other words, more blue light is back scattered from a thinner layer of collagen than red light. If a diffuse absorber lies within the range of visible light scattered by connective tissue, the radiation absorbed will depend on the nature and depth of the absorber. In the case of a black absorber the relative intensities of the red and blue wavelengths in the back scattered spectrum will depend upon the depth of the absorber. A common example is that of a tattoo, where the black carbon particles in the white human skin produce a blue colour. This blue colour is produced by greater scattering of blue light and the deeper penetration of red.

1-2-2 Models for optical properties of skin

An early reflectance spectrophotometric study of the skin was made by Buckley and Grum (1961). They introduced the term "skin reflectance density" which they defined as Log (1/R) by simply replacing the reflectance (R) for the transmittance (T) in the law of radiation transmission. Thus from the combined laws of Bouguer-Lambert and Beer, where ε is the molar absorptivity, c, the concentration and t, the path length of light within the sample we have:

$$\text{Absorbance} = \text{Log}_{10}(1/\text{Transmittance}) = \varepsilon ct \qquad 1\text{-}1$$

This concept is equivalent to the term LIR, Logarithm to the base 10 of the Inverse of Reflectance, which was used later by Dawson et al (1980). Based upon a simplified layer model for skin composed of fibrous protein, melanin, haemoglobin and collagen/fat layer, they showed that the LIR is proportional to a sum of the absorbances of these layers, offset by an amount equal to the logarithm of the

reflectance of the collagen/fat layer (R_{coll}) with the following formula:

$$LIR = Ab_1 + Ab_2 + Ab_3 - Log_{10}(R_{coll}) \qquad 1\text{-}2$$

Ab_1, Ab_2, and Ab_3 correspond to the absorbances of the fibrous protein, melanin, and haemoglobin respectively. The parameter LIR is also used in this present study to quantify the haemoglobin and melanin content of skin and the oxygen saturation of superficial blood using the reflectance spectrum of the skin surface.

San Wan et al (1981) applied an analytical model that interrelates the optical properties of the multilayered structure of the skin. The mathematical approach is based on the relationship between diffuse reflectance and transmittance of a multilayered system and the diffuse reflectance and transmittance of each component layer. The formula can also be derived from the Kubelka -Munk theory of radiation transfer. The applicability of the model to human epidermis over the UV and visible region was verified. In the study reported in this thesis the Kubelka-Munk equations were used to analyse the intensity of light that was diffusely reflected and transmitted by simulated skin samples containing different concentrations of diluted red cells.

Feather (1986) in a reflectance spectrophotometric study of the interaction of visible and UV radiation with skin has proposed a simple optical model, based upon the layered structure of skin. It is confirmed that the two major cutaneous pigments, haemoglobin and melanin, can be identified and quantified from in-vivo LIR spectra through their characteristic absorbances. Indices of these two pigments were derived and their application in several areas of

investigative and clinical dermatology described.

Since light specularly reflected at the skin surface results from the step change in refractive index from air to tissue it contains no information on skin pigments. In reflectance spectrophotometric measurements care must be taken to exclude stray light before any calculation of an index relating to pigment content. Most of the early studies used conventional spectrophotometers converted into reflectance spectrophotometers by means of an integrating sphere attachment, hence their reflectance data includes a contribution from specular reflected light. Later studies (Dawson et al, 1980; Anderson and Parrish, 1981; Feather, 1986) employed fibre optic light guides for greater flexibility in light delivery and collection and thereby reduced this limitation as well as facilitating the measurement of a greater number of body sites.

1-2-3 Measurement of reflectance / absorbance spectra of skin

Jacquez and Kuppenheim (1955) measured the spectral reflectance of the human skin over the range 235 to 1000 nm. The contribution of skin fluorescence to the measured reflectance spectra was investigated by the use of cut-off filters to eliminate the wavelengths liable to excite the fluorescence. They concluded that the contribution of fluorescence to the reflectance signal at wavelengths greater than 300 nm is negligible and that below 300 nm, whilst small in absolute value, it may represent 10 to 20% of the measured reflectance.

Hardy et al (1956) studied the diffuse reflectance and transmittance of excised white and Negro human skin using the absolute method of goniometric spectrophotometry in the spectral region 550 - 2400 nm. They showed that for wavelengths greater than 1

μm white and Negro skin have essentially the same optical characteristic. That is, the melanin pigment has no appreciable effect on either the transmittance or reflectance of the skin. Except for absorption due to water and scattering effects, skin appeared to be almost non-absorbing in the near infra-red. They concluded that a layer of skin 0.4 mm thick is optically similar, as regards transmittance and reflectance, to four thicknesses of glass cover slips, the surfaces of which have been ground. A water cell with ground glass walls will also approximate to the transmittance and reflectance of the skin in the near infra-red. Such an optical cell was used in this study in the investigation of the optical properties of red cells.

1 - 3 The justification for this study

The development of phototherapies ie. the use of light (often in combination with exogenous chemicals) to produce a therapeutic effect, has increased the need for information on the optical properties of tissue. Development of optimun phototherapeutic regimes needs an objective method for identification and quantification of tissue response to treatment. The reflectance measurement of skin colour in terms of the chromophores producing the colour has the potential to improve the treatment regimes in clinical dermatology.

Feather (1986) concluded that the full potential of this objective measurement technique can only be realised, particularly in the clinical environment, by developing an instrument combining speed and portability with multiwavelength capability. By improving understanding of the optical properties of skin, the accuracy of measurement of indices of cutaneous haemoglobin and melanin is also

improved and may be made independent of the oxygen saturation of the blood. Simultaneous measurement of oxygen saturation along with other parameters would facilitate studies of the origin of changes in the haemoglobin content of the skin. This facility would be of great value in clinical and investigative studies.

1 - 4 Purpose and content of this work

The purpose of this work was to promote the understanding of the optical properties of tissue by developing theoretical models of light absorption and scattering, by constructing instruments for the measurement of those optical properties and by conducting experiments on tissue using the instruments to verify the models. Based on the improved understanding, reflectance spectrophotometry may then be applied to the study of physiological problems.

The research began with the design and construction of a rapid, multiwavelength skin reflectance spectrometer to improve the quantification of skin pigments. The instrument, which has a dual channel optical system, can measure the reflectance spectrum of a surface in the visible region (356 nm to 720 nm) in 2.8 seconds with 200 data points.

As melanin and haemoglobin pigments play a major role in the reflectance and transmittance of skin in the visible spectrum, a skin simulating system (a water cell with ground glass walls as proposed by Hardy (1956) for the near infra- red) was used to model non-pigmented skin. By solving the Kubelka-Munk equations for two boundary conditions the results of in-vitro LIR measurements from different concentrations of diluted red cells were analysed. Based on these measurements the computation of indices of haemoglobin and melanin

content was modified until the indices were independent of the oxygen saturation of the blood.

To facilitate measurement of skin, efforts were made to eliminate the absorption contribution of non-specific pigments eg. melanin. By using several wavelengths, the precision of the measurement of the difference between oxy and reduced haemoglobin was increased. Following considerable refinement of procedure, measurement with the new reflectance spectrophotometer now generates indices proportional to the amount of haemoglobin and melanin and gives an accurate measure of the oxygen saturation of superficial blood.

The reflectance spectrophotometer was used in a variety of applications including a study of the vascular changes in tumour and normal rat tissue induced by photodynamic therapy, and also an analysis of the skin's response to different environmental conditions such as changes in the skin temperature or different height above/below the heart. A topical vasodilator chemical was used on forearm, palm and finger tip sites, where the capillary network patterns are different. The haemoglobin index and oxygen saturation were recorded over the following 200 minutes. The observed variation of haemoglobin index and oxygen saturation could be explained in terms of the metabolic activity of the tissue in the presence of the chemical and the thermal regulatory function of the blood.

1 - 5 Summary and conclusions

A brief history of reflectance spectrophotometric studies of skin relevant to this study has been presented.

Changes in the level of cutaneous pigments are often sensitive parameters of skin state and occasionally of general patient health.

The use of skin colour measurements in the treatment of patients undergoing PUVA therapy for psoriasis has been briefly discussed to illustrate the benefit of objective measurement of skin colour changes. Finally the justification, purpose and content of this study were summarised.

The biological basis of this study and its relevance to the optical properties of the skin will be described in chapter 2. In chapter 3, the theory of light transmission and reflection spectroscopy and its application to skin will be discussed. The design and construction of an instrument based on the described theory will be presented in chapter 4.

In chapter 5, results of in-vitro reflectance and transmittance measurements of a simulated sample will be analysed. Based on these measurements the haemoglobin and melanin indices originally devised by Feather (1986) will be improved to render them independent of the oxygen saturation of the sample. A new method for oxygen saturation measurement will also be presented.

Some modifications of the reflectance probe to exclude specularly reflected light from the skin surface measurement and to maximise the collection of diffused reflected light is presented in chapter 6. The stability of the indices against biological changes will also be reported.

In chapter 7, a new index called "melanin index" will be introduced and its independence of the amount of haemoglobin and oxygen saturation in the skin will be examined. To demonstrate the use of the technique first, the melanin content of several subjects with different racial pigmentation is measured and compared and then the results of changes in blood content and oxygen saturation of in-vivo

reflectance measurements are analysed. The changes in blood content and oxygenation of the forearm, palm, and finger tip are induced either by applying a vasodilating chemical or exposure to different environmental conditions such as height above / below the heart or temperature.

Finally in chapter 8 the observations made in the course of the study will be drawn together to provide general conclusions and some indication of the direction of future studies.

CHAPTER 2

2 - BIOLOGICAL BASIS FOR THIS STUDY

To facilitate understanding of the theoretical and experimental studies to be presented in this thesis and of their relevance to clinical problems, it is appropriate that the biological and optical properties of skin and blood should be reviewed here.

First the structure and optical properties of the skin will be reviewed. Cutaneous blood flow and its significance will then be discussed. Finally the role of blood as a distributor of oxygen and methods for the measurement of oxygen saturation will be reviewed.

2 - 1 Skin

2-1-1 Structure and optical properties

Figure 2.1 is a simplified diagram of the structure of skin. The skin varies in thickness over the body between 1 and 4 mm. The upper 0.1 to 0.2 mm is called the epidermis and is composed of tightly packed cells called keratinocytes which are produced by cell division in the basal layer. Throughout their lives keratinocytes move outwards, towards the skin surface. They become flattened, dehydrate and lose their nuclei to form a tough outer protective layer called the horny layer (stratum corneum). In normal skin it is estimated to take between 28 and 45 days for the keratinocyte to travel through the epidermis. Stratum corneum has a refractive index of 1.55 (Parrish et al, 1978). Consequently a small fraction of radiation incident on the skin surface is reflected due to the step change in refractive index between air and stratum corneum. For light incident normal to the

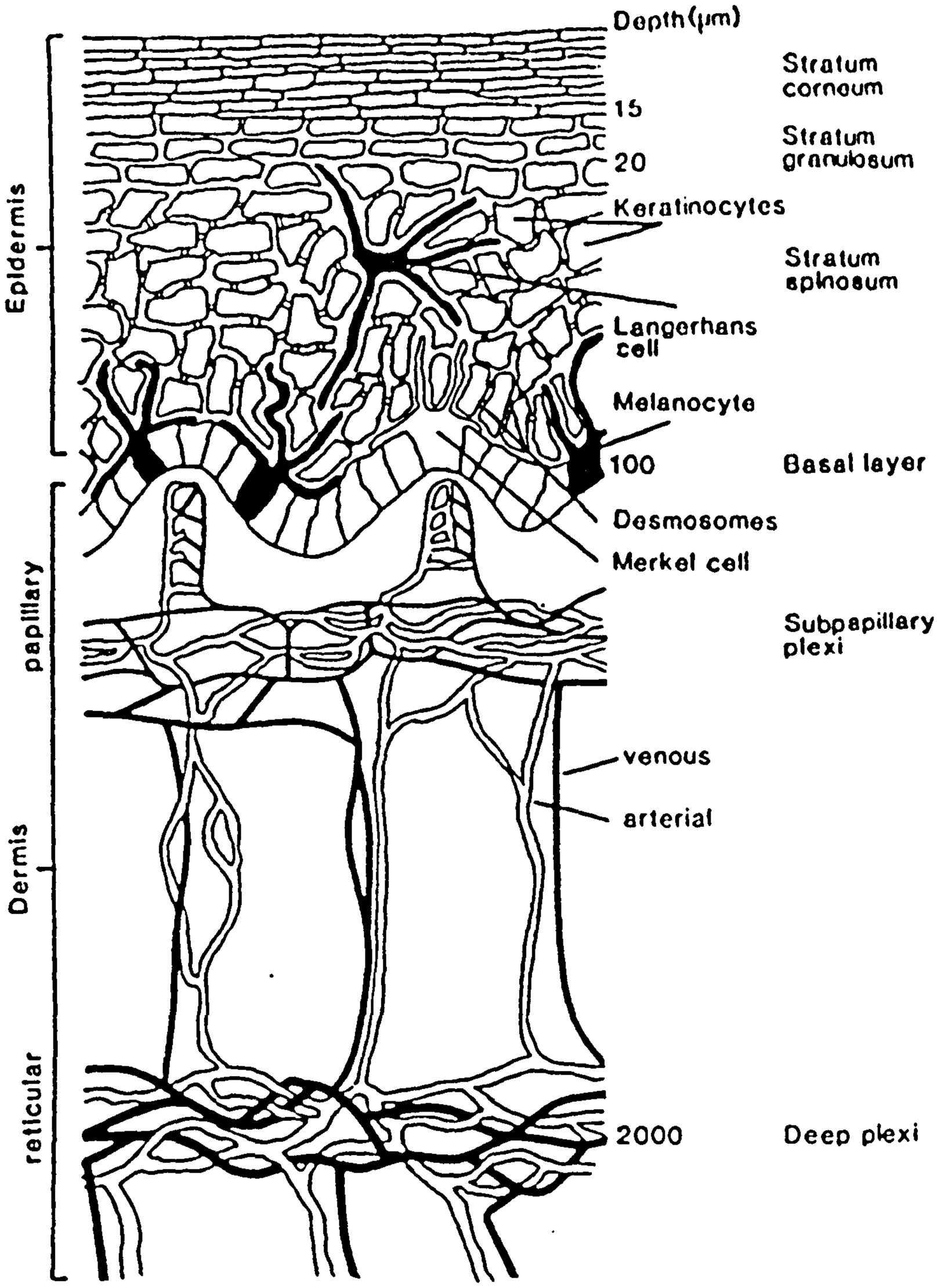

Fig. 2.1- Diagrammatic cross section of normal skin (Feather 1986).

surface, this specular reflectance lies between 4% and 7% over the entire visible spectrum, but increases for larger angles of incidence. Collimated radiation transmitted through this rough surface is refracted and therefore made somewhat diffuse.

Bruls et al (1984) measured the angular distribution of radiation on passing through the stratum corneum and epidermis. They determined the fraction of energy transmitted within an angle of 22.5 degrees of the normal at two different wavelengths. For stratum corneum this fraction ranged from 83% at 546 nm to 75% at 254 nm, and for full thickness of epidermis from 59% at 546 nm to 44% at 306 nm.

The basal layer of the epidermis contains specialised cells called melanocytes. These cells produce black and brown pigment granules called melanosomes, which contain the pigment melanin. Melanosomes are transferred through dendritic processes to the keratinocytes and are carried toward the surface of the skin, eventually appearing in the stratum corneum. Despite the continuous outward migration of melanin, its greatest concentration is in the basal cell layer. Absorption of light by melanin increases rapidly with decreasing wavelength, so that UV radiation is strongly absorbed.

The dermis contains fewer cells than the epidermis as it is composed of collagen fibres and blood vessels. Collagen makes up about 70% of the dry weight of the dermis and is optically birefringent. The scattering of light by collagen is an important feature of the optics of the dermis. Collagen molecules are about 300 nm long and 1.5 nm in diameter. Three types of collagen molecules are combined into ordered polymers called collagen fibrils; these are long (up to 10 μm), thin (10 to 300 nm in diameter), and cablelike. Such fibrils are often

grouped into larger bundles, which can be seen in the microscope as collagen fibres several μm in diameter (Alberts et al, 1983).

The uppermost dermal layer (papillary dermis) contains an extensive plexus of capillaries, lymphatics and nerves and is more cellular in appearance than the underlying reticular dermis. The reticular dermis is more fibrous, contains larger vessels and has fewer cells than the papillary dermis. The penetration and diffuse reflection of radiation in skin is a function of both scattering and absorption of light within the various tissue layers. The pigments, melanin in the epidermis and haemoglobin, oxyhaemoglobin, beta carotene and bilirubin in the dermis, are the major absorbers of visible radiation in the skin. Incident radiation is scattered within the dermis by structures with dimensions of the same order as, or greater than, the wavelength of the light (ie. collagen). Therefore scattering is expected to be wavelength dependent varying inversely with wavelength but not as strong as Rayleigh scattering.

Hardy et al (1956) have shown that for excised skin specimens with a thickness of 0.43 mm visible light became fully diffused. The back- scattered light for all thicknesses (0.3 to 2.1 mm) and for all wavelengths in the spectral range studied (550 to 2200 nm) was fully diffused and obeyed Lambert's law, ie the intensity of the reflected light decreased with the cosine of the angle between the scattered light and the normal to the surface.

In the presence of scattering, however, the effective path length of radiation within the medium is increased, which increases both the probability of absorption and of backscattering. This backscattered radiation contains information on the identity and amount of the dermal chromophores. The spatial distribution and intensity of

scattered light depends upon the size, shape, refractive index of the scattering centres, the properties of the medium, the chromophores and the wavelength of the radiation. The complicated nature of these factors in the skin layers motivated many authors to develop a phenomenological approach. Longini and Zdrojkowski (1968) suggested that multiple scattering can be described by a model of photon diffusion in the medium. A special case of this more general approach which could be applied to skin is the Kubelka -Munk theory. The theoretical aspects related to light propagation in the skin will be discussed in the next chapter.

2-1-2 Cutaneous blood flow and its significance

The minimum blood flow measured in a finger during intense vasoconstriction caused by exposure to cold is approximately 0.5 to 1 ml min^{-1} $100ml^{-1}$ tissue (Montagna & Parakkal, 1974). Even when such vasoconstriction is maintained the tissue does not necessarily become necrotic although it can be damaged when rewarmed. This minimum flow thus appears to be adequate for the physiological demands of the skin itself. The cutaneous mean blood flow and maximum flow are considerably higher than the minimum physiological flow. The mean flow is 20 to 30 times greater than the minimum and the maximum flow during vasodilatation can be more than 100 times greater (Montagna & Parakkal, 1974). These differences emphasize that cutaneous blood flow is not determined solely by the metabolic requirement of the skin which probably varies only with changes in temperature and requires, at most, only a 2 or 3 fold increase over the minimum flow to meet its metabolic needs.

Blood vessels in the cutaneous tissue are nearly always greatly

in excess of the biological needs of the tissue. The masses of interlacing small vessels in the dermis function primarily for thermal regulation, nutrition of the tissue is secondary. The major arterial and venous vessels can be divided into three categories: segmental, perforator and cutaneous, as shown in Fig. 2.2 (only arterial counterparts are shown). Branches from the segmental arteries pass through muscles as perforator arteries which divide into muscle vessels and continue peripherally to the skin. Skin is also supplied by a few direct cutaneous vessels that perforate muscle and go straight to the skin. These vessels are found mostly in the extremities and thorax and supply relatively small areas. The major trunk of direct cutaneous vessels travels parallel to the surface. The dermis and hypodermis, then, are perforated by a cutaneous arteriovenous network with meshes of different sizes and various spatial relationships. The complex distribution of vessels in the dermis is well adapted to the various changes and stresses to which the skin is exposed. The vascular beds differ widely in different areas. For example the papillary ridges on the palms and soles contain long and relatively straight capillary loops. Those on the trunk are shallower, broad, meandering and form less continuously identifiable loops.

A schematic diagram of the pattern of termination of cutaneous vessels is shown in Fig. 2.3. The most direct channels from arterial to venous circulation give off side branches called precapillary sphincters, which control the flow of the blood into the capillaries. Some capillaries consist only of an endothelial tube and anastomoses which then join the collecting venules. Thus capillary blood flow can be regulated by the contraction and dilatation of the venules and the

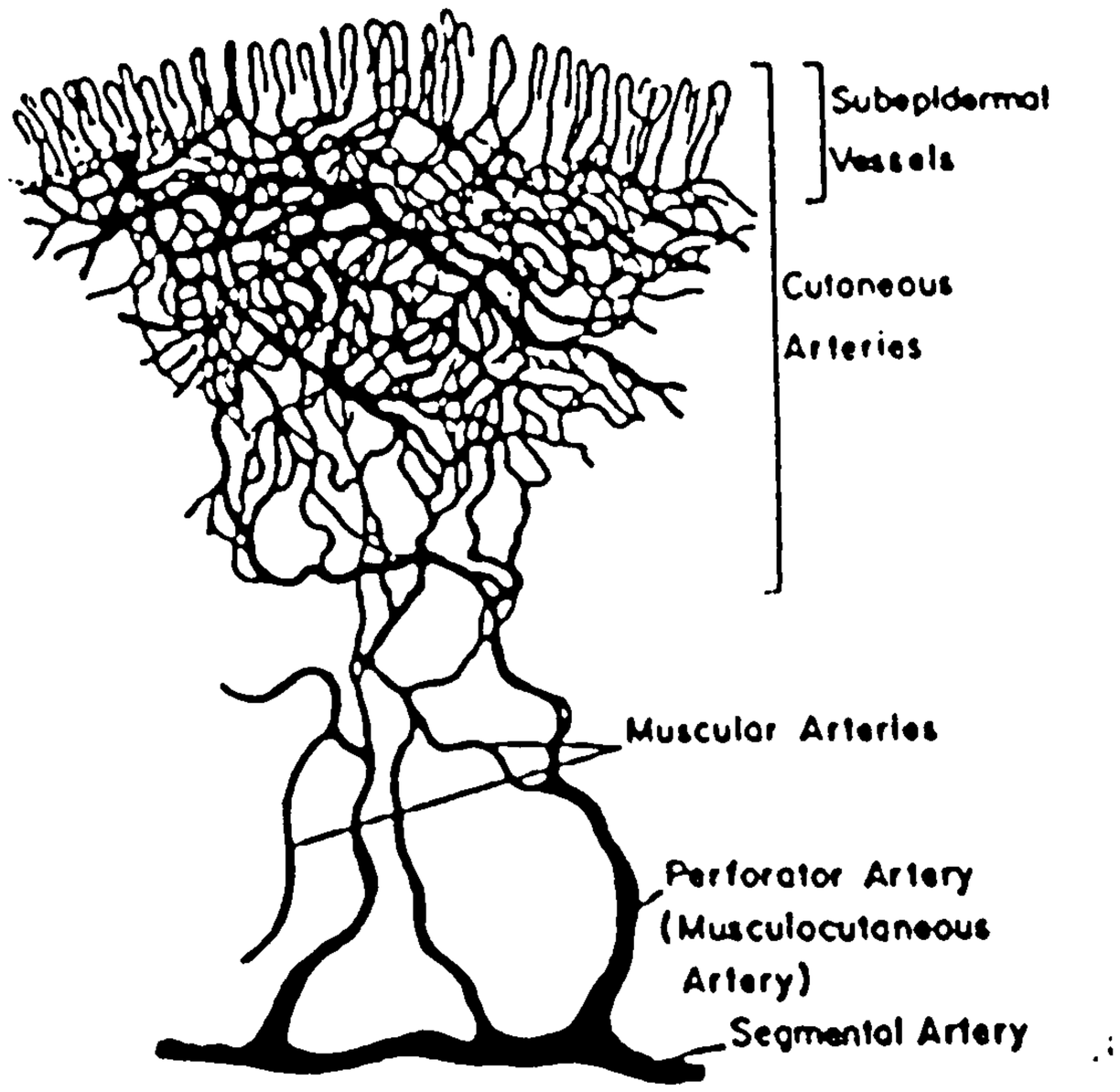

Fig. 2.2- Diagram showing the patternless cutaneous vascular system (Montagna and Parakkal, 1974).

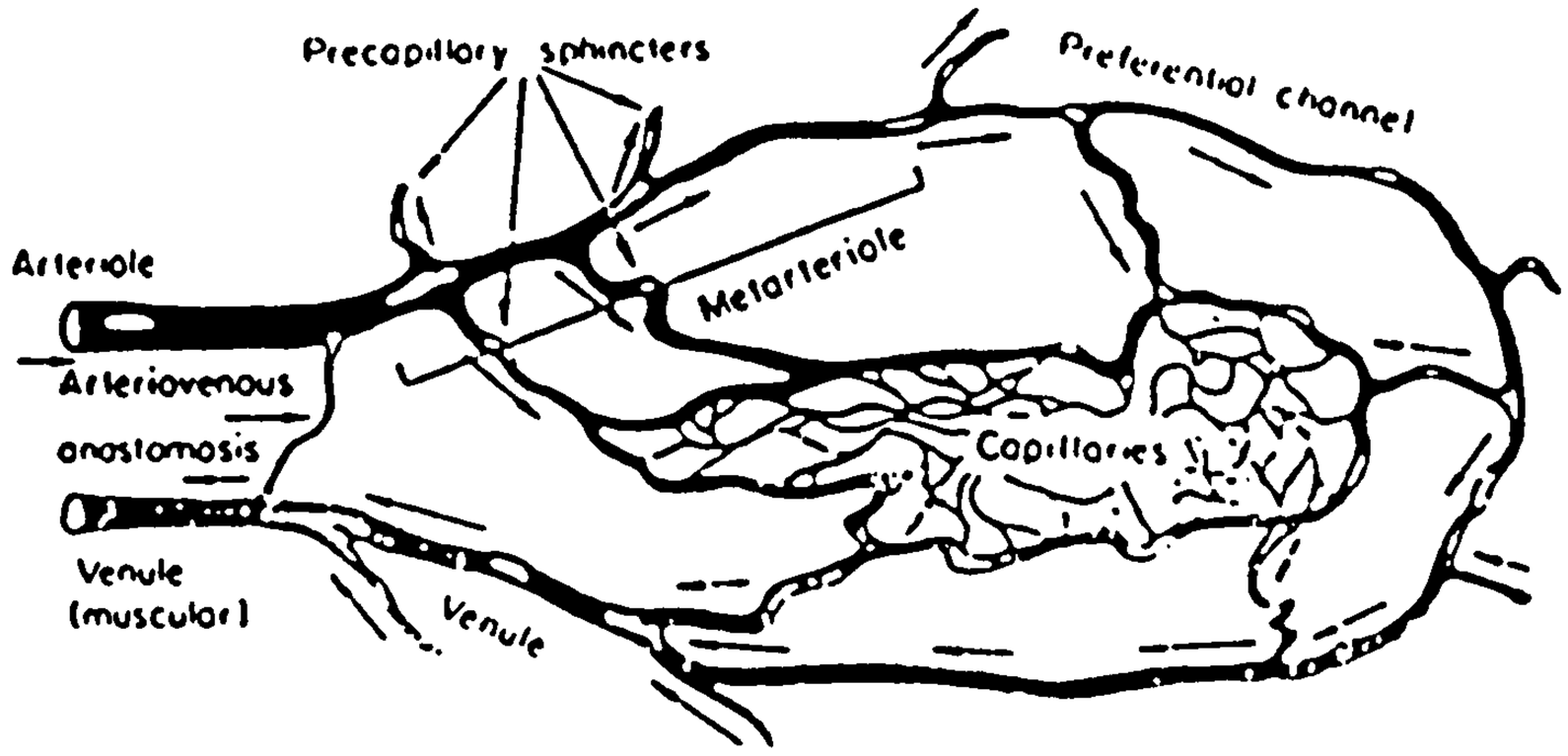

Fig. 2.3- Schematic diagram of the structural pattern of the terminal cutaneous vessels (Montagna and Parakkal, 1974).

precapillary sphincters. If only precapillary sphincters contract, blood is shunted through a preferential channel and bypasses the lateral capillary network. Contraction of the metarteriole would shunt the blood through arteriovenous anastomoses (AVA) directly to muscular venules. In man such anastomoses are found predominantly in the upper parts of the reticular dermis, especially in the skin of exposed parts of the body, such as palm, sole, lips and nose and in tissue where metabolic activity is intermittent such as the thyroid gland and the digestive system. Unlike the venules in other tissue those in the skin have a remarkable ability to contract and dilate. The major role of AVA is in blood temperature and pressure regulation. Unlike increases in capillary blood flow, increases in flow through shunts do not supply oxygen and nutrition to the skin. Thus, agents applied to skin to increase its circulation do so without a comparable improvement in the oxygen saturation of the tissue unless the metarterioles that supply the capillaries are opened as well as the shunts. (More detail of blood vasculature is given by Montagna & Parakkal, 1974).

When a finger is immersed in extremely cold water there is immediate vasoconstriction, the skin temperature falls to near freezing and there is much pain. After 4 to 5 minutes the blood flow suddenly increases in the cooled finger, the skin feels warm, and the pain subsides. This is followed by a second vasoconstriction and repeated cycles of constriction and dilatation. The fluctuations in the blood flow are the result of periodic, rhythmic responses to discharges of nervous impulses from the sympathetic vasoconstrictor nerves. This mechanism maintains blood flow at a level appropriate to the transport of an adequate amount of heat for the regulation of body temperature.

2 - 2 Blood

Blood consists of a liquid portion, the plasma, in which are suspended red cells, white cells and platelets. Human blood performs several functions: nutrition, excretion, respiration, temperature regulation, fluid and chemical balances, protection, endocrine function, and is a vital organ of the body.

This section will consider only the role of blood as a distributor of oxygen.

2-2-1 Functions of haemoglobin

Oxygen is mostly transported from the lungs to all the tissues by haemoglobin in the red cells. The red cell has the shape of a biconcave disk with a mean diameter of 7.2 $\pm$ 0.5 µm. Red cells occupy 41% of the blood volume of normal women and 47% of normal men. A count of 4-5 million cells/mm^3 of blood is considered normal for women and 4.5 to 5.5 million cells/mm^3 for men. More than half (66%) of the content of red cells is water and about 33% is the protein "haemoglobin". This protein contains a moiety, "globin", joined to a pigment "haem" . Although only 4% of haemoglobin actually consists of haem, in combination with globin it becomes strongly coloured (Ham et al 1979). If the amount of haemoglobin in circulating blood is significantly reduced, the person is said to be "anaemic". This condition can be due either to lack of red cells or lack of haemoglobin itself. Hence, the spectrophotometric measurement of this coloured pigment (haemoglobin) could be a useful criterion for diagnosis of anaemic patients.

A resting adult extracts about 5 ml of O_2 (measured at STP) from

every 100 ml of circulatory blood. During exercise this figure can increase almost 3 fold. Since the solubility of oxygen in plasma is only 0.3 ml/dl, when oxygen diffuses from lung to tissue only a small amount of it dissolves into the plasma but approximately 60 times as much combines immediately with the haemoglobin of the red cells. This is an extremely loose bond, so that the combination is easily reversible, thus allowing rapid pick up of oxygen in the lungs where the oxygen tension (pO_2) is high and an equally rapid release in the tissue where the pO_2 is low. In spectrophotometric measurement only the oxygen combined with the haemoglobin can be detected. The oxygen content of arterial blood ($C_a\ O_2$), which is defined as the total amount of oxygen carried in 100 ml of arterial blood, is then determined by the quantity and type of haemoglobin present, the amount of available haemoglobin combined with oxygen expressed as percent saturation ($\%S_a\ O_2$), and arterial pO_2. i.e.

$$C_a\ O_2 = (Hb)(1.39)(\%Sa\ O_2) + (0.003)(pO_2) \qquad 2\text{-}1$$

where "$C_a\ O_2$" is the oxygen content of arterial blood in ml/dl of blood, Hb is the haemoglobin content in g/dl, 1.39 is the oxygen carrying capacity of haemoglobin in ml/g, $\%Sa\ O_2$ is the percent oxygen saturation, 0.003 is the solubility of oxygen in plasma ml/dl blood/mmHg at 37 °C, pO_2 is arterial partial pressure of oxygen in mmHg. Haemoglobin may be bound to oxygen, unbound or functionally inert such as carboxyhaemoglobin or methaemoglobin, therefore, $\%Sa\ O_2$ can be defined as the ratio of oxyhaemoglobin to the sum of all haemoglobin present. Alternatively, $\%Sa\ O_2$ can be considered approximately to be the ratio of oxyhaemoglobin to the sum of oxyhaemoglobin and reduced haemoglobin (functional or reversible

saturation).

$$\% \text{ Sa } O_2 = \frac{\text{oxyhaemoglobin}}{\text{oxy + reduced haemoglobin}} \qquad 2\text{-}2$$

The oxygen saturation of blood may be measured instrumentally by means of an "oximeter". Most oximeters in use today consider only functional haemoglobin in their operation and the percentage of Sa O_2 depends on the haemoglobin available to bind with oxygen, the oxygen dissociation curve of haemoglobin (O.D.C) and the arterial pO_2 (Brodsky, 1986). In spectrophotometric measurement of %Sa O_2, which is based on absorption spectra of oxy and reduced haemoglobin, the functional saturation is measurable. The oxygen dissociation curve of haemoglobin is sigmoidal which is the result of co-operative binding of four successive oxygen molecules to a tetrameric haemoglobin protein. The binding of one oxygen molecule increases the affinity of the remaining sites for the next molecule. Similarly the third molecule is easier to pick up than the second and loading of the fourth is easier again (Russell et al, 1982). Therefore a haemoglobin sample with a certain oxygen saturation can be assumed to be a mixture of fully oxygenated and reduced haemoglobin. This property of haemoglobin is used in chapter 5 of this research to determine the oxygen saturation of a blood sample. The sigmoid shape of the oxygen dissociation curve (Fig. 2.4) has several physiological advantages. The flat upper portion means that even if the pO_2 in aveolar gas falls somewhat, the loading of oxygen will be little affected. The steep lower part of the dissociation curve means that the peripheral tissue can withdraw a large amount of oxygen for only a small decrease in capillary pO_2. The maintenance of blood pO_2 assists the diffusion of

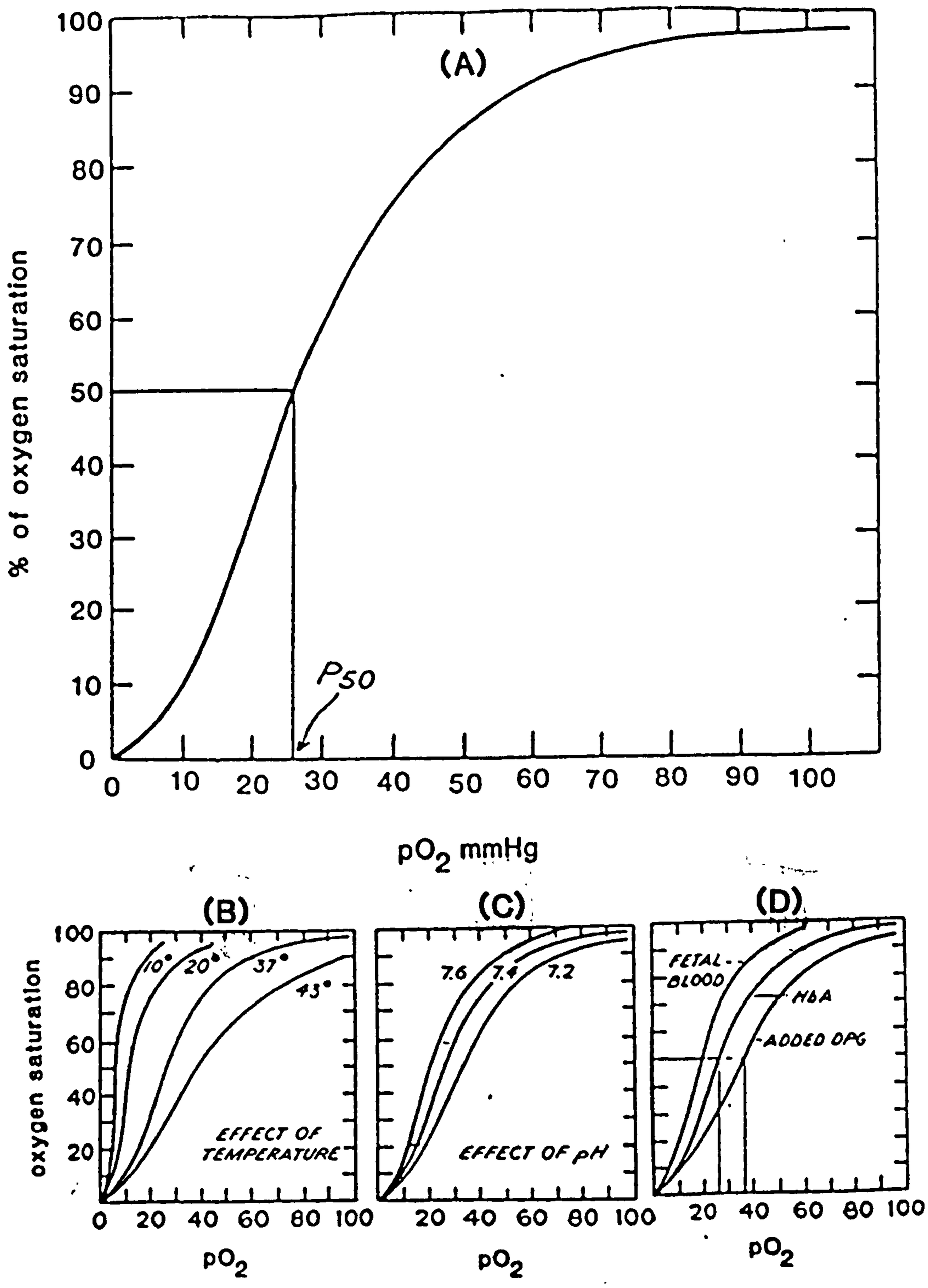

Fig. 2.4- A) Standard oxygen dissociation curve of haemoglobin in-vitro whole blood with pH =7.4, temperature 37 °C. B) effect of changes in temperature, C) effect of changes in pH, D) effect of adding DPG (diphospho-glycerate). (Comroe 1974).

oxygen into the tissue cells. The position of the O.D.C. is shifted laterally by change in pH, pCO_2, and temperature. Any fall in pH, rise in pCO_2 or temperature will shift the O.D.C. to the right as is shown in Fig. 2.4 (Comroe, 1974).

Transport of CO_2 takes place in 3 different forms, 7% as dissolved CO_2 in plasma, 70% in the form of bicarbonate ion (HCO_3-) and 23% in red cells in direct combination with haemoglobin (carbominohaemoglobin). This latter reaction does not occur at the same point on the haemoglobin molecule as the reaction between oxygen and haemoglobin. Therefore, haemoglobin can combine with both CO_2 and O_2 at the same time. Because the reaction occurs relatively slowly, this method of CO_2 transport is much less important than transport in the form of bicarbonate ions.

When the blood enters the pulmonary capillaries, all the chemical combinations of CO_2 with blood are reversed and the CO_2 is released into the alveoli.

2-2-2 Measurement of oxygen saturation

Whole human blood when well oxygenated has a brilliant red colour, while blood that is reduced or not well oxygenated is darker. The field of oximetry involves quantitative study of this visual phenomenon and uses it for in-vivo and in-vitro determination of oxygen saturation in blood. Since the survival of each cell in a living body is dependent on the supply of oxygen to it, monitoring of the oxygen saturation of blood has long been recognised to be most valuable.

The three most important methods for measuring the oxygen saturation of blood are described below:

A) Blood gas analysis

The Van Slyke method is an established method for blood gasometric analysis in which the total amount of O_2 and CO_2 are measured. In this method the blood is dispensed into an acidified air-free ferricyanide solution and subjected to a vacuum. The ferricyanide drives off the oxygen, the acid drives off the carbon dioxide and the vacuum the nitrogen. The released gas is measured volumetrically by absorbing first the carbon dioxide and then the oxygen (Bell et al, 1961). Since the Van Slyke method is a direct measurement of the extracted gases, the accuracy of other methods of oxygen saturation measurement are usually tested against this method.

In an improved blood gas analyser machine the partial pressures of blood gases, pO_2, pCO_2 and pH are measured with different electrodes and then the oxygen content or percentage saturation is calculated from the established O.D.C. curve by assuming the sample to be normal blood. Since oxygen saturation also depends on the level of carbon monoxide and 2-3 diphosphoglycerate (2-3 DPG) in blood, the calculated value of oxygen saturation may not be equal to the measured value for a patient with abnormal levels of 2-3 DPG or carbon monoxide. In practice the in-vivo analysis of arterial blood gas by this method is reliable but is invasive and can only provide intermittent information.

B) Transcutaneous oxygen tension measurement

Baumberger and Goodfriend (1951) first reported that the oxygen diffusion through the skin is sufficient to allow an estimate to be made of the arterial oxygen tension. In their experiments a finger was immersed in phosphate buffer solution at 45 ^{o}C. The high temperature

keeps the finger in hyperaemia so that the capillary blood is virtually arterial. After sufficient time (15 - 60 minutes) the pO_2 of the buffer solution also becomes equal to the pO_2 of the arterial blood. The pO_2 of the buffer was then determined by means of the polarographic method. Current practice is to attach a membrane-covered polarographic oxygen electrode on to the skin. Oxygen diffuses from the skin through the membrane and the oxygen electrode, which can be a Clark electrode, will respond linearly to the oxygen tension of the skin. To facilitate the diffusion of the oxygen through the skin it is necessary to arterialize the skin circulation. Originally this was achieved by means of vasodilators such as histamine or a nicotinic acid derivative but now vasodilatation is produced by electrically heating the electrode to a temperature of 43-44 ^{o}C.

This method provides continuous in-vivo information but requires special site preparation, an air tight probe, and a potentially harmful local heat source for increasing the blood flow at the measurement site. This method also provides pO_2 from which the oxygen content and percentage oxygen saturation can be estimated.

C) Spectrophotometric measurement

In this method the arterial oxygen saturation of haemoglobin is determined directly by using the differences between the haemoglobin and oxyhaemoglobin absorbance spectra (see Fig. 5.13). A unique advantage of this method is the continuous registration of $\%Sa\ O_2$ at any selected site in the circulation simultaneously with other continuous measurements. Further, the method may be used non-invasively. For these two reasons reflectance spectrophotometery was the preferred method in this study.

The differences in the absorbance spectra of reduced and

oxyhaemoglobin is seen in the marked difference in their colours ie "red" oxyhaemoglobin and "purple" reduced haemoglobin. Therefore, spectrophotometric oximeters usually use two wavelengths, one in the red, where the extinction coefficient of haemoglobin is 4-5 times as great as oxyhaemoglobin, the other at an isobestic point in the infra red, where the specific absorption coefficient of oxy and reduced haemoglobin are the same.

Oximeters can be divided into two groups: pulsatile and non-pulsatile. In non-pulsatile oximeters the oxygen saturation is measured from the relative absorption of light of two or more wavelengths which is directed through a vascular part of the body e.g. ear lobe, and detected either by reflection or transmission. For better performance the blood flow is usually increased by a combination of heat and chemical treatment to dilate the vascular bed in the measurement area. However, as will be demonstrated in chapter 7 any attempt to increase the blood flow is likely to change the oxygen saturation of cutaneous blood at the measurement site and this may not be a good indicator of arterial oxygen saturation. There are some intravascular reflection oximeters which are invasive and operate on the same principle.

Pulse oximeters work by positioning any pulsating arterial vascular bed (finger tip or ear lobe) between a two wavelengths light source and detector system. It is assumed that changes in blood volume as it flows in and out of the vascular bed as the heart beats causes a change in the intensity of transmitted light and thus modulates the signal. The amplitude of the variation detected depends upon the size of the arterial pulse change, the wavelength of light used and the %Sa O_2 of the arterial blood. As the detected pulsatile waveform is

produced solely by arterial blood, from measurements at each wavelength and the application of Beer's law, it is feasible to continuously calculate arterial oxygen saturation of haemoglobin with no interference from surrounding venous blood, skin, connective tissue or bone.

2 - 3 Summary and conclusions

In this chapter, the biological basis of this research work has been briefly reviewed. Skin structure and the optical properties of the constituent layers (epidermis, dermis), cutaneous blood flow and its significance in requlating body temperature, and the role of blood as a distributor of oxygen were discussed.

Scattering within the skin layers is expected to be wavelength dependent but not as strong as Rayleigh scattering. Penetration and diffuse reflection of radiation in skin is a function of both scattering and absorption of light within the various tissue layers. The pigments, melanin in the epidermis and haemoglobin, oxyhaemoglobin, beta carotene, and bilirubin in the dermis, are the major absorbers of visible radiation in the skin.

It is possible, in principle, to measure the blood content and oxygenation of the skin and superficial tissue by studying the back scattering of light from such tissue. It is normally assumed that photodiffusion theory may be used to relate reflectance measurements to the optical properties of the tissue.

The three most important methods for measuring the oxygen saturation of blood have been discussed. Reflectance spectrophotometric measurement, the preferred method in this study, is non-invasive and is capable of continuously monitoring the oxygen

saturation of blood at any selected site in the circulation; it may be carried out simultaneously with other continuous measurements.

The physical structure of skin outlined in this chapter will be used as the basis of the theoretical model to be developed in the next chapter (chapter 3) for the computation of the absorbance and scattering of light in skin. The predictions of this model will be compared with experimentally measured absorption in chapter 5. Studies on the optical properties of blood both in-vitro and in-vivo will be presented in chapters 5 and 6, and the applicability of the theoretical models developed in chapter 3 tested.

CHAPTER 3

3 - THEORY OF TRANSMISSION AND REFLECTANCE SPECTROSCOPY

In this chapter theoretical aspects of light propagation in a scattering and absorbing medium are reviewed and their relevance to the optical properties of in-vivo and in-vitro skin constituent layers and of blood samples discussed. The purpose of this theoretical study is to provide a basis for interpreting observations made with a reflectance spectrophotometer in terms of the optical properties of the sample.

3 - 1 Introduction

Transmission spectroscopy, which is a method of measuring spectral absorbance of substances in a transparent medium, is based on attenuation of light as it passes through the medium. When monochromatic radiation of known intensity passes through an absorbing medium, some will be absorbed so that a parameter, transmittance (T), may be defined as the ratio of transmitted to incident radiation, eqtn. 3.1.

$$T = \frac{I_t}{I_o} \qquad 3\text{-}1$$

where I_o and I_t are the incident and transmitted intensity of radiation (mW cm^{-2}) respectively.

The concept of intensity is applicable only when the source is so small that it can be treated as a point source. In this case, the intensity of a source in any given direction is defined as the rate of energy per unit solid angle radiated in that direction (mW sr^{-1}). If

the source is too large to be treated as a point, the corresponding quantity is called brightness. By definition the brightness in a given direction at any point of an extended surface is the quotient of the intensity of an element of the surface at that point divided by the area of the element projected in a plane perpendicular to the given direction (mW sr^{-1} cm^{-2}). At a point on a surface, the radiant power incident on an element of a surface divided by the area of that element is called irradiance (mW cm^{-2}). This term is commonly used as a measure of intensity, and will be used as such throughout this thesis.

A related parameter, absorbance, is defined as the logarithm to the base ten of the inverse of transmittance, eqtn. 3.2.

$$A = \mathrm{Log}_{10}(1/T) \qquad 3\text{-}2$$

The medium under consideration here, ie. skin, is composed of absorbing and scattering media with a rough surface. The radiation reflected by such media is usually composed of two distinct parts. The first of these is the specular reflection, which is of the same nature as the reflection from a smooth surface, i.e. the angle of incidence is equal to the angle of reflection. The specular reflectance (R_{spec}) from the skin surface, which is also scattered in all directions due to the roughness of the surface, is defined as the ratio of the light reflected at the surface to the total incident radiation. The skin surface can be assumed to be small flat reflectors which are randomly orientated. The specular reflectance is thus governed by the Fresnel equations. At the surface of each flat reflector, if "i" is the angle of incidence, "r" the angle of

refraction and "n" the refractive index for a medium (sin i =n sin r), then the specular reflectance of unpolarized incident light may be calculated from the following formula (Hardy and Perrin 1932);

$$R_{spec} = 0.5 \{ [\frac{\sin(i-r)}{\sin(i+r)}]^2 + [\frac{\tan(i-r)}{\tan(i+r)}]^2 \} \qquad 3\text{-}3$$

The reflected intensity varies with the angle of incidence and wavelength of the radiation, and for perpendicular incident radiation (i=0) becomes

$$R_{spec} = (\frac{n-1}{n+1})^2 \qquad 3\text{-}4$$

For radiation incident normally on the skin surface the measured specular reflectance is between 4% and 7% over the entire spectrum from 250 to 3000 nm, for both Caucasian and Negroid skin (Regan and Parrish 1982). If it is assumed that the refractive index of the horny layer is 1.55 (Parrish et al 1978) then equation 3.4 predicts a specular reflectance of only 4.65%. The difference between theory and observation results from the roughness of the skin surface and hence variable angles of incidence.

The second part of the radiation reflected from the skin is the diffuse reflectance which arises from penetration of a portion of the incident flux into the interior of the sample. Part of this radiation (I_r) is returned to the surface of the sample following partial absorption and multiple scattering in the medium of which the sample is composed. The ratio of such back scattered to incident radiation is called the remittance or diffuse reflectance (R).

$$R = \frac{I_r}{I_0} \qquad 3\text{-}5$$

I_0 and I_r are the incident and back scattered radiation (mW cm^{-2}) respectively. As a parameter which is analogous to absorbance, the logarithm of inverse of reflectance to the base ten (LIR) may be used to calculate the absorption within the medium.

$$LIR = Log_{10}(1/R) \qquad 3\text{-}6$$

In contrast to specular reflection, no general theory is completely valid for light returning from within the medium. Although all formulae for diffuse reflection incorporate Lambert's cosine law (eqtn. 3.7), this law has not been derived from first principles. It is phenomenologically formulated from the fact that a matt surface irradiated with constant intensity appears uniformly bright at all angles of observation. According to the cosine law, the emitted intensity of a non-absorbing matt surface which is perpendicularly illuminated is given by:

$$I_r = I_0 \cos\phi \qquad 3\text{-}7$$

where I_r and I_0 are the intensities of the radiation (mW cm^{-2}) in the direction of view and normal to the surface respectively and ϕ is the angle of observation relative to the normal to the surface. The Lambert cosine law is strictly valid only for small values of ϕ; for larger values, deviations occur (Wendlandt and Hecht 1966). The diffusely reflected radiation (I_r) is taken to be unpolarised, regardless of the state of polarisation of the incident radiation.

3 - 2 Propagation of light in a diffusing media

The propagation of light in scattering and absorbing media such as whole blood or skin, is of a very complicated nature. The scattering phenomena principally result from inhomogeneities in the refractive index of a medium. The spatial distribution and intensity of scattered light depends upon the size, shape, and refractive index of the inhomogeneities and on the wavelength of the light. For particles that are very large compared with wavelength, the well known phenomena of reflection, refraction and diffraction can be described by the wave theory of optics. When the particle size is comparable to the wavelength, it becomes impossible to discriminate between these three phenomena and the interaction of the particle with the incident light is summarised as scattering. Only in a few cases, restricted to single scattering of a plane incident wave, does a rigorous theory exist, for example, Rayleigh scattering which happens in small particles with dimensions less than roughly one-tenth of the wavelength. This scattering is generally weak, nearly isotropic and varies inversely with the fourth power of the wavelength. For particles with dimensions of the same order as of the wavelength, scattering is stronger than Rayleigh scattering, more forwardly directed and varying inversely with wavelength. When the particle size greatly exceeds the wavelength, scattering is highly forward directed and independent of wavelength (Mie scattering). Within the skin all of these general types of scattering occur but quantitatively scattering by the structures with dimensions of the order of the wavelength of visible radiation or somewhat larger (ie. collagen) must dominate over Rayleigh scattering.

Hardy et al. (1956) showed that the transmission scattering pattern of radiation by layers of a specimen of skin is a function of wavelength and thickness. They found that for thin samples there is a marked difference between the scattered radiation in the visible spectrum and in the infra-red. Visible light is scattered most, following Lambert's cosine law, whereas near infra-red radiation penetrates almost as if the skin were semitransparent. This wavelength dependence, which is an inverse function of wavelength, is very different from Rayleigh scattering. This is to be expected as the particle size of the scattering elements of the skin specimen is probably not less than that of the wavelength of light in the visible or near infra-red. For tissue thicknesses of 1 mm or greater, scattering becomes uniform for all wavelengths. Hardy et al (1956) also demonstrated that the scattering patterns measured in reflectance are less complex than those for transmittance and follow Lambert's cosine law for all angles and wavelengths. This fact demonstrates that the measurement of skin reflectance can be normalised by comparison with standard reflecting surfaces and was used as the basis for in-vivo measurement of the reflectance LIR spectrum of a skin surface in this study.

Because of the difficulties of developing a comprehensive fundamental theory for the propagation of light in a multiple scattering medium, many authors have attempted to develop a phenomenological approach. The most widely adopted approach to the problem of describing the behaviour of light in diffusing media is that of a solution of simultaneous differential equations of the first order, which describe the attenuation of light intensity within the sample due to the scattering and absorption. Equations of this type

were introduced by Schuster (1905) in connection with his work on the escape of radiation from a foggy atmosphere. Schuster considered the radiation to be travelling in two opposite directions, one of which being the direction of the incident or transmitted light. The loss of light energy travelling through a thin layer in these directions is defined by two parameters, the absorption and the scattering coefficients which are properties of the medium. The theory was developed further by Kubelka and Munk (1931) and by Kubelka (1948) into a very practical and commonly accepted method. Longini and Zdrojkowski (1968) suggested that multiple scattering can be described by a model of photon diffusion in the medium. The Kubelka-Munk theory can be regarded as a special case of this more general approach. Another alternative is the statistical approach of the Monte-Carlo method but this is not as convenient to apply. These methods will be introduced briefly here and the Kubelka-Munk equation will be solved for certain boundary conditions as it is to be utilised in later chapters of this thesis.

3-2-1 Photon diffusion theory

In this theory a uniform beam of collimated monochromatic light is normally incident on the surface of the sample. The photon flux at the surface is assumed to be A_0 photons per cm^2 per second, and the photons are treated as particles which are scattered and absorbed by the medium. In passing through the sample, as shown in Fig. 3.1, the transmitted flux contains two components, 1) the collimated component due to that fraction of light which has not been scattered and 2) the diffuse component. The collimated component is in the direction of the incident radiation and is reduced by both scattering and absorption as

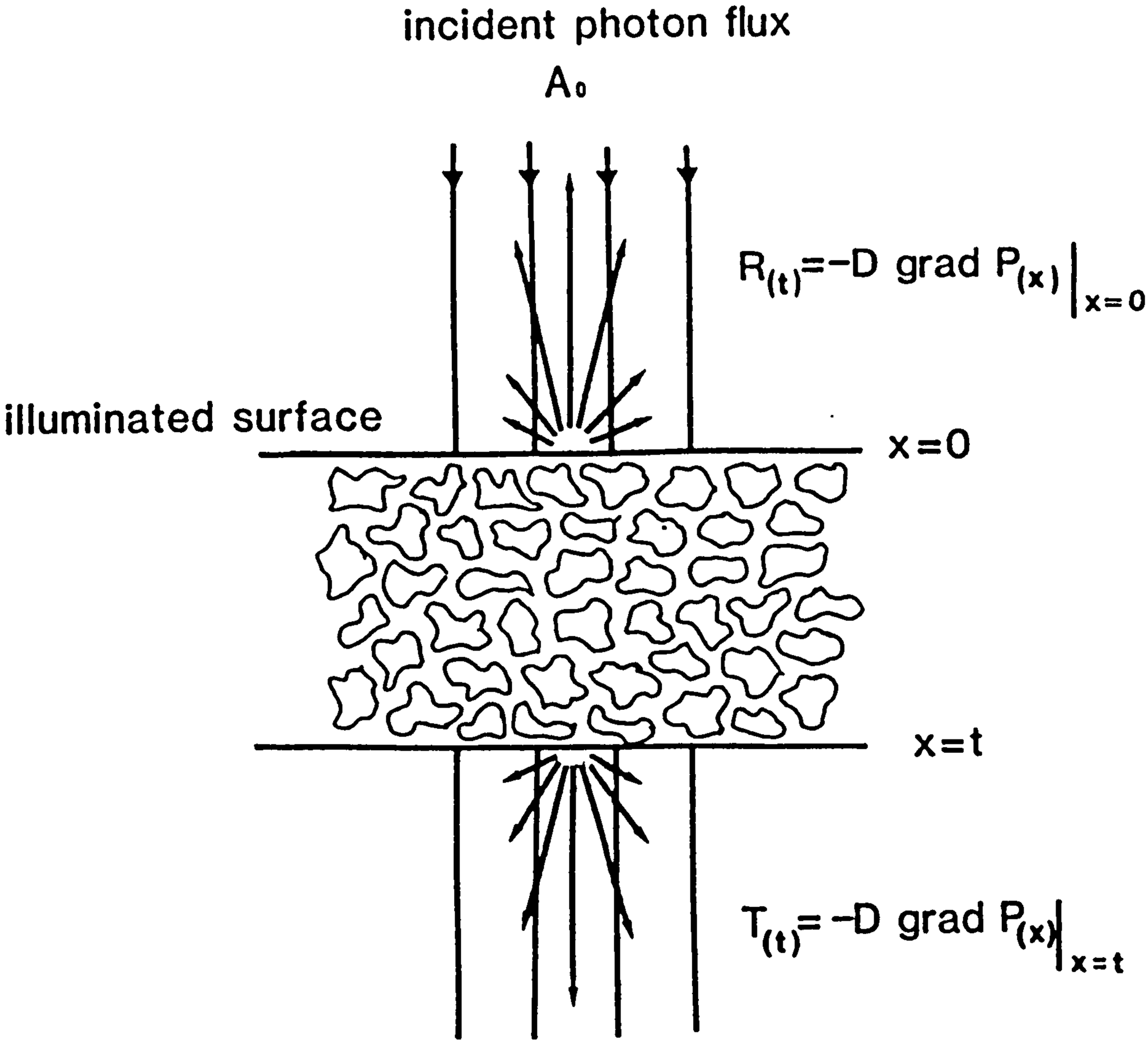

Fig. 3.1- Schematic representation of the application of diffusion theory to transmission and reflection of light by a layer of absorbing and scattering particles.

it penetrates the sample. The diffuse component which is produced by scattering of the photons, follows Lambert's cosine law. The back scattered flux is also composed of diffuse and collimated components. The latter is due to specular reflection at the illuminated surface. In the general case, the photon flux, F (photons cm^{-2} s^{-1}), at any point (x,y,z) within the medium is given by the photon diffusion equation:

$$F = -D \nabla P(x,y,z) \qquad 3\text{-}8$$

where P is the photon density (photon cm^{-3}) and D is the diffusion coefficient for the photon (cm^2 s^{-1}). Shockley (1962) has shown that the diffusion coefficient is related to the absorption and scattering coefficients of the medium by the following formula:

$$D = C/(2s + k) \qquad 3\text{-}9$$

where C is the velocity of light in the medium, k and s are the absorption and scattering coefficients of the medium, respectively. They are defined as the ratio of the amount of radiation which is removed from the incident radiation by absorption or scattering to the total original radiation on passing through unit thickness of a sample. This definition is used for a very thin sample, but for a thick sample they are defined as the inverse of the thickness which reduces the incident light intensity to one tenth either by scattering or by absorption.

In equation 3-8 only diffusing photons are considered and it can be solved by using the continuity equation of photons in the steady state ($dP(x,y,z)/dt = 0$). That is

$$\nabla.F + \frac{P(x,y,z)}{T} - G(x,y,z) = 0 \qquad 3\text{-}10$$

"T" is the photon life time and G(x,y,z) is the rate of generation of diffusing photons per unit volume. The second term on the left of equation 3.10 is the rate of photon decrease per unit volume due to absorption. The divergence of "F", which is the net outgoing photon flux per unit volume, is negative if the rate of absorption exceeds the rate of generation of scattered photons. For a simple case in one dimension, which is shown in Fig. 3.1, the incident collimated photon flux A(x) at any point within the sample may be reduced by both scattering and absorption according to the following formula suggested by Pisharoty (1971):

$$A(x) = A_o \exp\left[-\left(\frac{1}{l} + \frac{1}{m}\right) x\right] \qquad 3\text{-}11$$

where "l" is the mean optical path travelled by a photon within the sample before absorption and "m" is the mean free path before random scattering. In this case the incident collimated flux A(x) may be related to the generation function as:

$$G(x) = \frac{A(x)}{m} \qquad 3\text{-}12$$

The photon density P(x) can then be found by substitution of equations 3.11 and 3.12 in 3-10, that is:

$$\frac{d^2P(x)}{dx^2} + \frac{P(x)}{DT} = \frac{G(x)}{D} \qquad 3\text{-}13$$

McKelvey et. al. (1961) have shown that the mean free path between scattering, m, the mean optical path before absorption, l, and the photon life time, T, the parameters required for the solution of equation 3.13, are related to the absorption (k) and scattering (s) coefficients by the following formulae:

$$l = 3/4k, \quad m=3/4s, \quad T = 2/kC \qquad 3\text{-}14$$

where C is the velocity of light in the medium. Solving equation 3.13 for defined boundary conditions and sample thickness (t) will give the photon density function P(x). The diffuse transmitted flux (T), and the diffuse reflected flux (R) can be calculated by the following formulae:

$$T = - D \frac{dp(x)}{dx} \Bigg|_{x=t} \qquad 3\text{-}15a$$

$$R = - D \frac{dp(x)}{dx} \Bigg|_{x=0} \qquad 3\text{-}15b$$

Equation 3.11 and 3.12 were suggested by Pisharoty (1971) for the generation of diffused photons from a collimated photon flux in a whole blood sample. As there is doubt as to their applicability to scattering in skin and diluted blood samples, no attempt will be made to solve these equations here. The Kubelka-Munk theory, which can be regarded as a special case (one dimension) of this more general theory, will be discussed instead and its applicability to in-vitro measurements of simulated skin samples will be verified.

3-2-2 Statistical method

A statistical method based on the Monte-Carlo method of computation ie. randomised photon paths, can also be used for studying the phenomena of the propagation of light in scattering and absorbing media. The following analysis is based on the work published by Major (1980) and Groenhuis et al (1983), and is studied here to investigate the feasibility of the method for the present work.

The fundamental equation of absorption spectrometry is given by the Beer-Lambert law

$$I = I_0 \exp(-\varepsilon c t) \qquad 3\text{-}16$$

where "I_0" and "I" are the intensities of incident and transmitted radiation respectively, "ε" is the molar extinction coefficient ($cm^2\ mol^{-1}$), "c" is the concentration ($mol\ cm^{-3}$) and "t" is layer thickness (cm). This equation cannot be applied to a scattering medium as the light does not remain collimated inside the sample. However if it can be assumed that a small portion of the beam may be deviated to travel a certain path length without further deviation while passing through the absorbing medium, then the Beer-Lambert law may be written as:

$$dI = dI_0 \exp(-\varepsilon c u) \qquad 3\text{-}17$$

where "dI_0" is the small portion of the incident beam travelling through the medium with path length "u", attenuated according to absorptivity "ε" and emerging from the medium as a quantity "dI". To determine the transmitted or reflected light, all portions of the beam emerging from the sample after covering different path lengths must be

added. But this requires the knowledge of the portion of light having covered the different path lengths. In other words the density function of the path length distribution of light has to be known. Since portions of the beam may follow very different path lengths when travelling among the particles, the density function may be considered as a continuous one. Assuming the density function of path length distribution is f(u) then;

$$dI_0 = I_0 f(u)\, du \qquad 3\text{-}18$$

It is normalised by integrating over all possible path lengths as below:

$$\int_0^\infty f(u)\, du = \frac{1}{I_0} \int_0^\infty dI_0 = 1 \qquad 3\text{-}19$$

In the case of reflectance measurement the reflected light is obtained by substituting eqtn 3.18 in 3.17 and integrating as:

$$I = I_0 \int_0^\infty f(u)\, \exp(-\varepsilon c u)\, du \qquad 3\text{-}20$$

Since all measurements supply integrated data, the density function of path length distribution cannot be determined by direct or by indirect measurements. Mathematical modelling (simulation) by using the Monte-Carlo method makes it possible to investigate the phenomenon, and to get the density function for the reflection and transmission of light for different layer thicknesses. The model simulates a sample consisting of particles embedded in a medium with light being scattered and absorbed as it travels through the medium.

To construct the model the task has obviously to be restricted and simplified. It is assumed that the material is homogeneous, compact with phase boundaries and particles with surfaces at which the refractive indices differ. To effect the different path length of light travelling among the particles, the rays of light are considered as photons which travel in straight lines between the phase boundaries. At the boundary surfaces, however, they may proceed in any direction, due to the irregular shape of the particles. After change of direction they proceed linearly until reaching the next surface ie scattering points. The basic simulation steps can be explained as follows:

1) Source photon generation - The photons are generated at the surface of the sample. Their spatial and angular distribution correspond to those of the light source used in the experiment. A simple case is the one in which the photons are incident at right angles to the surface of a layer of thickness t (Fig. 3.2), while the other two dimensions of the layer are infinite.

2) Pathway generation - As the scattering particles are randomly distributed, the photons may travel in discrete steps in any direction inside the layer. The direction and size of the steps (in arbitrary unit) is calculated from three random numbers representing changes in the projection of the photon position on the x,y,z axes. Each step contributes to the free path of a photon from one scattering point to the next. The random numbers can be produced by a random number generator of uniform distribution over the range -1 to +1. Accordingly the length of the largest possible step is 1.73, ($\sqrt{3}$). Generation of three random numbers in the program gives a random free path and the generated photon will travel with this free path then .

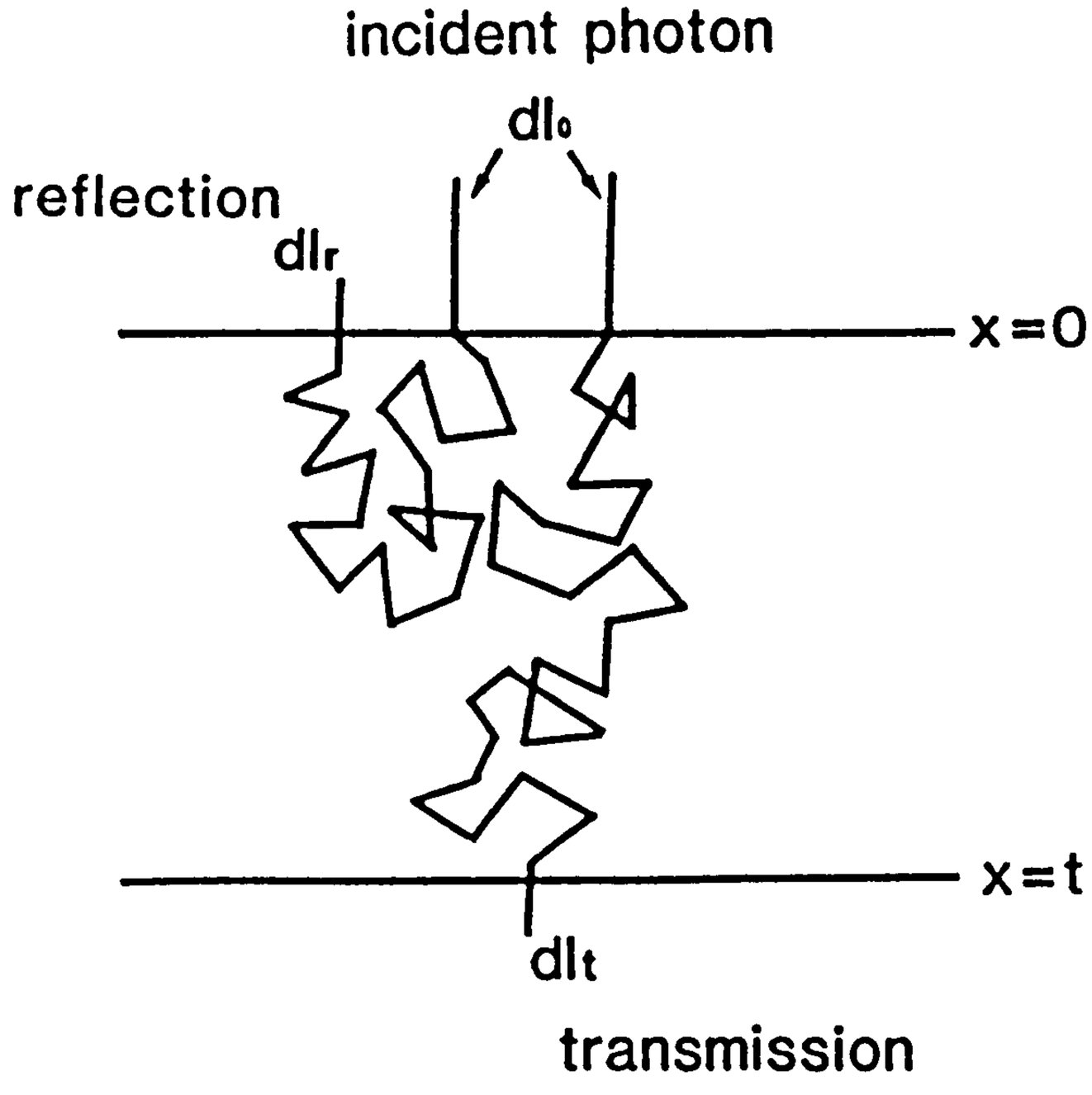

Fig. 3.2- Schematic representation of transmitted and reflected photons in the Monte-Carlo method.

scatter. If it is not eliminated, as described in steps 3 and 4 below, a new direction is determined. In a forward scattering medium the azimuth angle can be chosen randomly and the cosine of the scattering angle with respect to the old direction may be simulated by a predetermined function. The generation of new pathways and new scattering points is continued until the photon is eliminated.

3) Absorption - The incident photon when leaving the light source is assumed to have a certain energy. In the calculation it is assumed that the absorption event occurs between the scatterers, not inside the scattering particles. The absorption is taken into account by multiplying the energy of the photon by exp(-ku), where k is the absorption coefficient and u is the free path of the photon. If the sum of these terms for all paths travelled by a photon is equal to the energy of that photon, the photon is considered to be absorbed and the next photon is generated at the surface of the sample.

4) Elimination - Photons which are not eliminated due to the absorption will be scattered by a new scattering point as described in step 2. The photons whose calculated positions are above the surface or beyond the scattering volume are eliminated too. They are considered as reflected or transmitted photons respectively.

5) Detection - Traversing the plane x=0 in negative direction means reflection, and traversing the plane x=t in a positive direction means transmission. To measure reflection it is assumed that the photon is detected only by the detecting area positioned vertically over the sample surface. Since the viewing angle of the detector varies for each scattering point, the probability that the photon is detected can be computed for each point and stored in the computer. It is assumed that the summation of the probabilities yields the detected

radiance for the detector area. Numerical experience has shown that 10^4 photons are necessary to obtain results with a statistical error of 5%. Error due to elimination of the photon because the scattering point is beyond the scattering volume is considerable, especially with low absorption coefficient. This error can be reduced by enlarging the scattering volume, which increases the required computer time (Groenhuis et al 1983).

The Monte-Carlo method was not used in this study because first, in this method absorption is assumed to take place between the scattering particles while in the experimental samples, ie blood, the absorbing material, haemoglobin, is inside the scattering particles, red cells. Second, to construct the model, parameters defining the most important features of the phenomenon have to be provided. The variation of the value of "t" directly simulates the layer thickness, and considerably affects the amount of transmitted light. The variation of free path by a multiplicative factor corresponds to a change of particle size. But it is much more difficult to find a convenient parameter for modelling the refractive index, which affects the ratio of the reflected to transmitted light at the surface of the particles as well as the angle of refraction.

Therefore, a simplified case of the photon diffusion theory (one dimension) in the form of the Kubelka-Munk model was used in this research.

3-2-3 Kubelka -Munk approach

The Kubelka - Munk equations will be solved for two different boundary conditions, one is for very thick samples where diffusely reflected light is the only light returned from within the sample and

the other is the situation where light transmitted by the sample is either reflected back into the sample by a white surface or absorbed by a black surface. The first case is the one where light reflected from within the skin layers is of those wavelengths that can not penetrate deeply into the skin, ie visible wavelengths. The second situation appertains when in-vitro measurements of the LIR spectrum of diluted blood are made by placing the sample on a white or black ceramic tile. The results of the theory will then be used later in this thesis to analyse the in-vitro LIR measurement of simulated skin samples containing different concentrations of red cells (chapter 5).

3-2-3-1 Limiting conditions for the Kubelka-Munk model

The Kubelka-Munk theory was modified by Kubelka (1948) into a very practical and commonly accepted method for determining the propagation of light in a layered and multiple scattering medium. The medium is treated as a layer of absorbing and scattering particles as shown in Fig. 3.3 with the following simplifying conditions:

1) The elementary volume element is chosen such that only single scattering takes place and that the scattering is non-coherent and isotropic. In this case the back and forward scattering of an elementary layer will have a Lambertian distribution of intensity, and the amount of absorbed and scattered light is linearly dependent on the thickness of the elementary layer.

2) Conceptually the sample is presumed to have a finite thickness with an extensive area, which can be assumed to be a one dimensional geometry. In practice this can be realised by a sample holder having an area much larger than its thickness and with reflecting side walls.

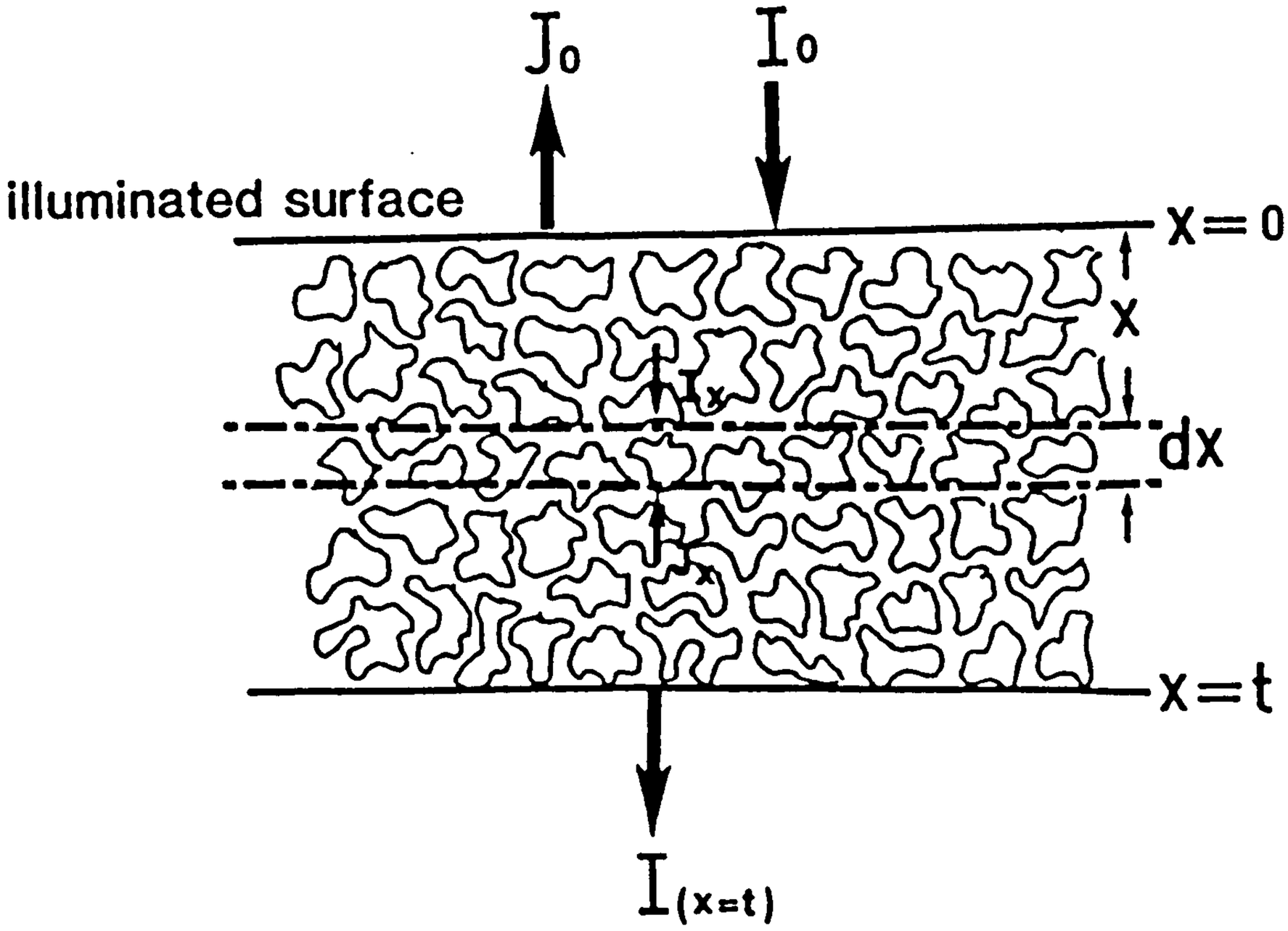

Fig. 3.3- Schematic representation of the Kubelka Munk model for the transmission and reflection of light by a layer of absorbing and scattering particles.

3) The sample is illuminated uniformly with diffuse monochromatic radiation over its entire surface. This last condition, when working with whole blood, is not a principal one because whole blood is a highly scattering medium and single scattering may be assumed to take place only in very thin samples (about 50 μm), beyond that thickness even collimated incident light will become perfectly diffuse.

Only two directions of incident and back reflected radiation are considered here, ie those perpendicular to the sample surface. The absorption coefficient (k) is defined as that fraction of the incident light flux that is removed by true absorption, and the back scattering coefficient (s) as that fraction that is reflected back in the opposite direction on passing through the elementary layer dx, per unit length of the sample. These are independent and are fundamental properties of the medium.

3-2-3-2 Average pathlength of diffused light

In the case of diffuse illumination, the light in the medium consists of rays travelling in all possible orientations with respect to the surface normal. In order to limit the analysis to only two directions of incident and back scattered radiation, the average path length of light passing through the layer should be used rather than the thickness of the layer.

To determine the average path length consider particular rays to be traversing the medium at an angle ϕ to the surface normal, as shown in Fig. 3.4. As they pass through the elementary layer, dx, their path lengths are not dx, but $dx/\cos\phi$. The average path length of all light passing through dx can be calculated by weighting each path

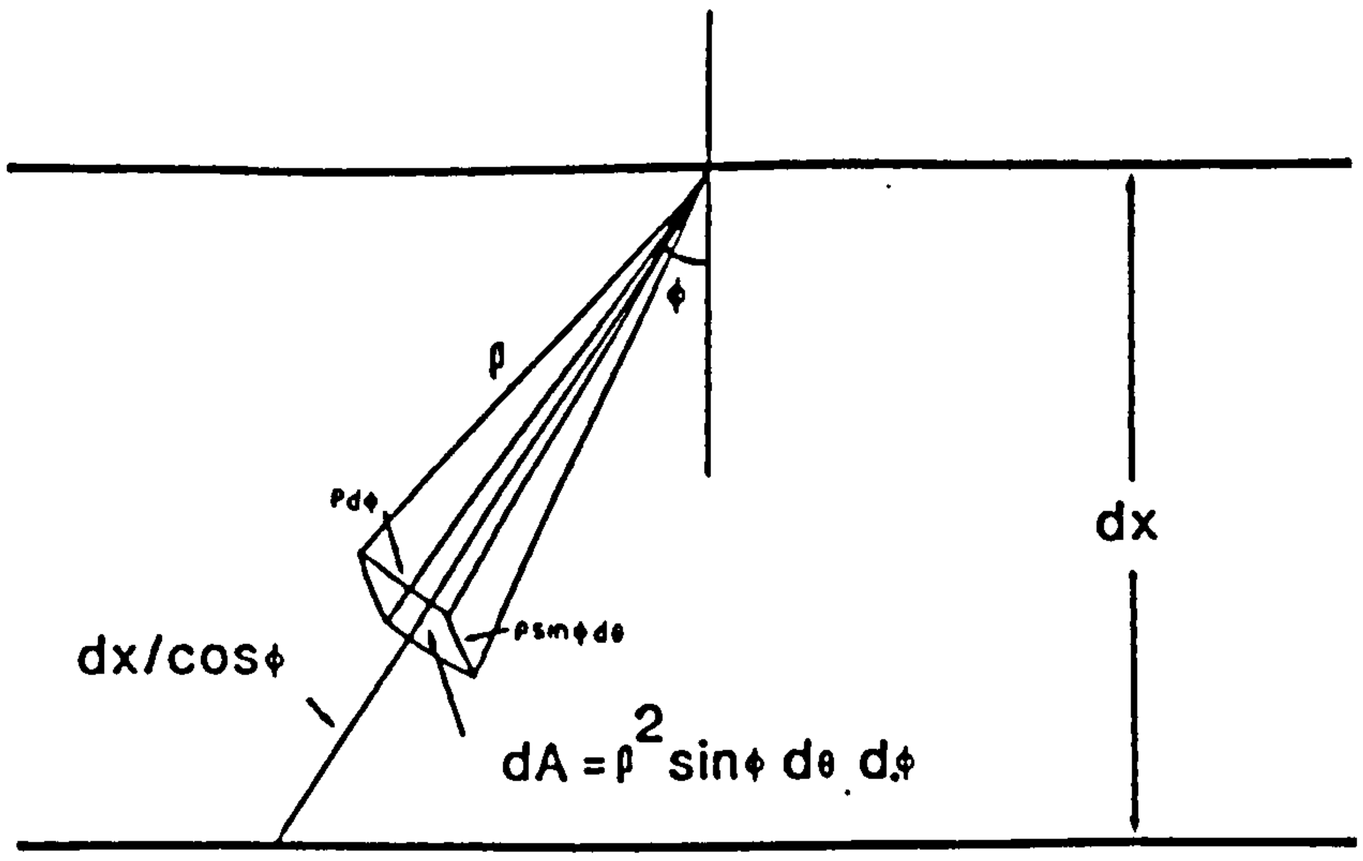

Fig. 3.4- Schematic representation of the calculation of the mean path length in an elementary layer dx of a layer of diffusing medium.

length ($dx/\cos\phi$) by the amount of light travelling in the elementary layer at that angle, ie I dA, and then integrating the function over the area of hemisphere below the surface. Assuming I_Φ is the intensity of scattered light at an angle ϕ to the surface normal, and dA is an elementary area perpendicular to the rays as shown in Fig. 3.4. The average path length is calculated from the following formula:

$$\frac{\int_0^{2\pi}\int_0^{\pi/2}\frac{dx}{\cos\phi}\, I_\Phi\, \rho^2 \sin\phi\, d\theta\, d\phi}{\int_0^{2\pi}\int_0^{\pi/2} I_\Phi\, \rho^2 \sin\phi\, d\theta\, d\phi} \qquad 3\text{-}21$$

where $\rho^2 \sin\phi\, d\theta\, d\phi$ is the elementary area dA. In order to normalise, it is divided by the total amount of light passing through the layer. The Lambertian intensity distribution of diffused light in the positive x direction in the elementary layer is given by:

$$I_\Phi = I_0 \cos\phi \qquad 3\text{-}22$$

I_Φ and I_0 are the intensity of light at an angle ϕ and normal to the surface respectively. Substitution of 3.22 in 3.21 and integration for $d\theta$ betweem 0 and 2π will give the following result;

$$\frac{dx\int_0^{\pi/2}\sin\phi\, d\phi}{\int_0^{\pi/2}\cos\phi\sin\phi\, d\phi} = \frac{dx}{1/2} = 2\,dx \qquad 3\text{-}23$$

This result indicates that, based on geometrical considerations

alone, the average path length of perfectly diffused light on passing through a layer is double the thickness of the layer.

3-2-3-3 The Kubelka -Munk equations

As was indicated above, in this theory the radiation, which is actually two Lambertian light fluxes flowing in opposite directions, can, by using the average path length, be treated as light fluxes flowing perpendicular to the sample surface and in opposite directions; one in the direction of the incident light (I), the other in the opposite direction or that of the reflected light (J) as shown in Fig. 3.3. In passing through the elementary layer dx, the light flux, I, will suffer a loss of "2kIdx" by absorption and "2sIdx" by back scattering. The light scattered backwards from J, which is "2sJdx", is added to I. Therefore the change in "I" on passing through dx is:

$$dI = -2kIdx - 2sIdx + 2sJdx \qquad 3\text{-}24$$

In an exactly analogous manner the change in J by passing through dx is:

$$-dJ = -2kJdx - 2sJdx + 2sIdx \qquad 3\text{-}25$$

The negative sign is due to the opposite direction of J with the positive x-axis. These differential equations can be readily integrated, the general solution is:

$$I = A(1 - b)\exp(qx) + B(1 + b)\exp(-qx) \qquad 3\text{-}26$$

and

$$J = A(1 + b)\exp(qx) + B(1 - b)\exp(-qx) \qquad 3\text{-}27$$

where $b = \sqrt{k/(k+2s)}$ and $q = 2\sqrt{k(k+2s)}$. A and B are constants to be determined by the boundary conditions. For a sample thickness of "t", "J" will be zero at $x = t$. The boundary conditions for a slab of sample illuminated perpendicularly are given by:

$$x = 0 \qquad I = Io$$

$$x = t \qquad J = 0$$

The solution for A and B under these conditions gives:

$$A = \frac{-(1-b)\exp(qt)\ I_o}{(1+b)^2\exp(qt) - (1-b)^2\exp(-qt)} \qquad 3\text{-}28$$

$$B = \frac{(1+b)\exp(qt)\ I_o}{(1+b)^2\exp(qt) - (1-b)^2\exp(-qt)} \qquad 3\text{-}29$$

The transmittance T and diffuse reflectance R of the layer is given by:

$$T = \frac{I(x=t)}{I_o} = \frac{4b}{(1+b)^2\exp(qt) - (1-b)^2\exp(-qt)} \qquad 3\text{-}30$$

$$R = \frac{J(x=0)}{I_o} = \frac{(1-b^2)\{\exp(qt) - \exp(-qt)\}}{(1+b)^2\exp(qt) - (1-b)^2\exp(-qt)} \qquad 3\text{-}31$$

As was mentioned earlier, in transmission and reflectance spectrophotometry the absorbance and LIR are defined as the logarithms to the base ten of the inverse of transmittance and reflectance, respectively.

In order to solve equations 3.24 and 3.25 using base ten rather

than with the natural logarithm base, apparent absorption and scattering coefficient are defined by multiplying them by Ln10 as follows:

$$K = 2.3026\ k \quad \text{and} \quad S = 2.3026\ s$$

In this case "b" does not change but $q = 4.6052\ \sqrt{k(k+2s)}$. Transmittance and reflectance may be calculated from equations 3.30 and 3.31. The dependence of LIR and absorbance, i.e. reflected and transmitted signals respectively, on the thickness, scattering and absorption coefficients, are shown in Figs. 3.5, 3.6, and 3.7. Figures 3.5a and 3.5b show the effect of thickness on the LIR and absorbance for different scattering coefficients (s = 0.001 and 1 cm^{-1}) and different absorption coefficients (k=0 to 1 cm^{-1}). It can be seen that for a constant scattering coefficient, the absorbance of the layer increases linearly with increasing absorption coefficient (Fig 3.5a). The rate of increase in absorbance is also greater when the thickness is increased. In the presence of scattering there is an absorbance value even for zero absorption coefficient and is attributable to loss of light by scattering in the sample. This absorbance value increases as the thickness and scattering coefficient increase (Fig. 3.5b). The LIR value, which is increased by increasing the k coefficient, is highly dependent on the scattering coefficient. Increase of scattering coefficient causes the LIR to decrease. For a certain scattering coefficient, change in the thickness does not change the LIR significantly except at low absorption coefficient when it will decrease with increasing the thickness. Figures 3.6 and 3.7 show the effect of changes in s and k on the LIR and absorbance for a constant thickness (t=1 cm).

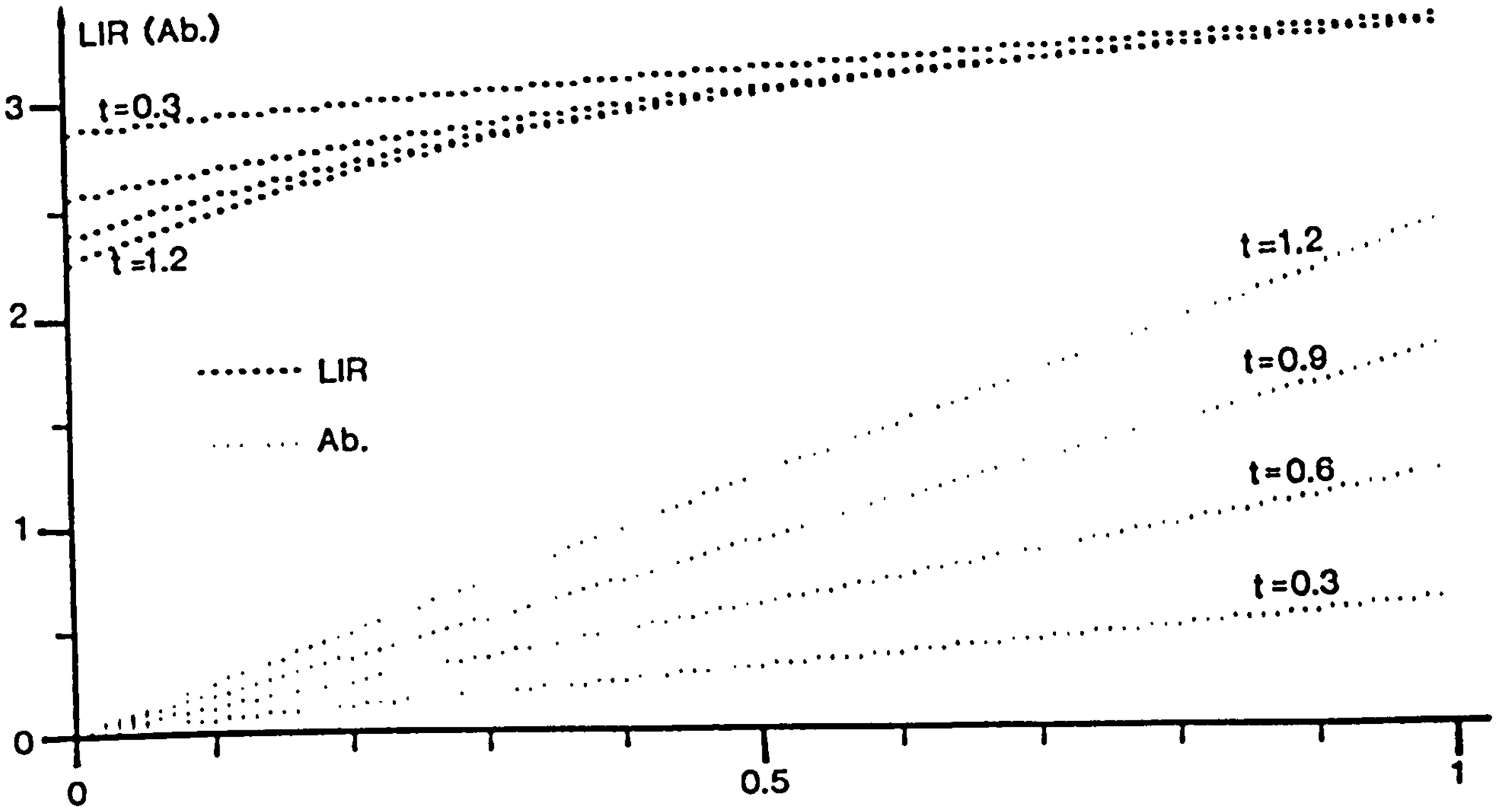

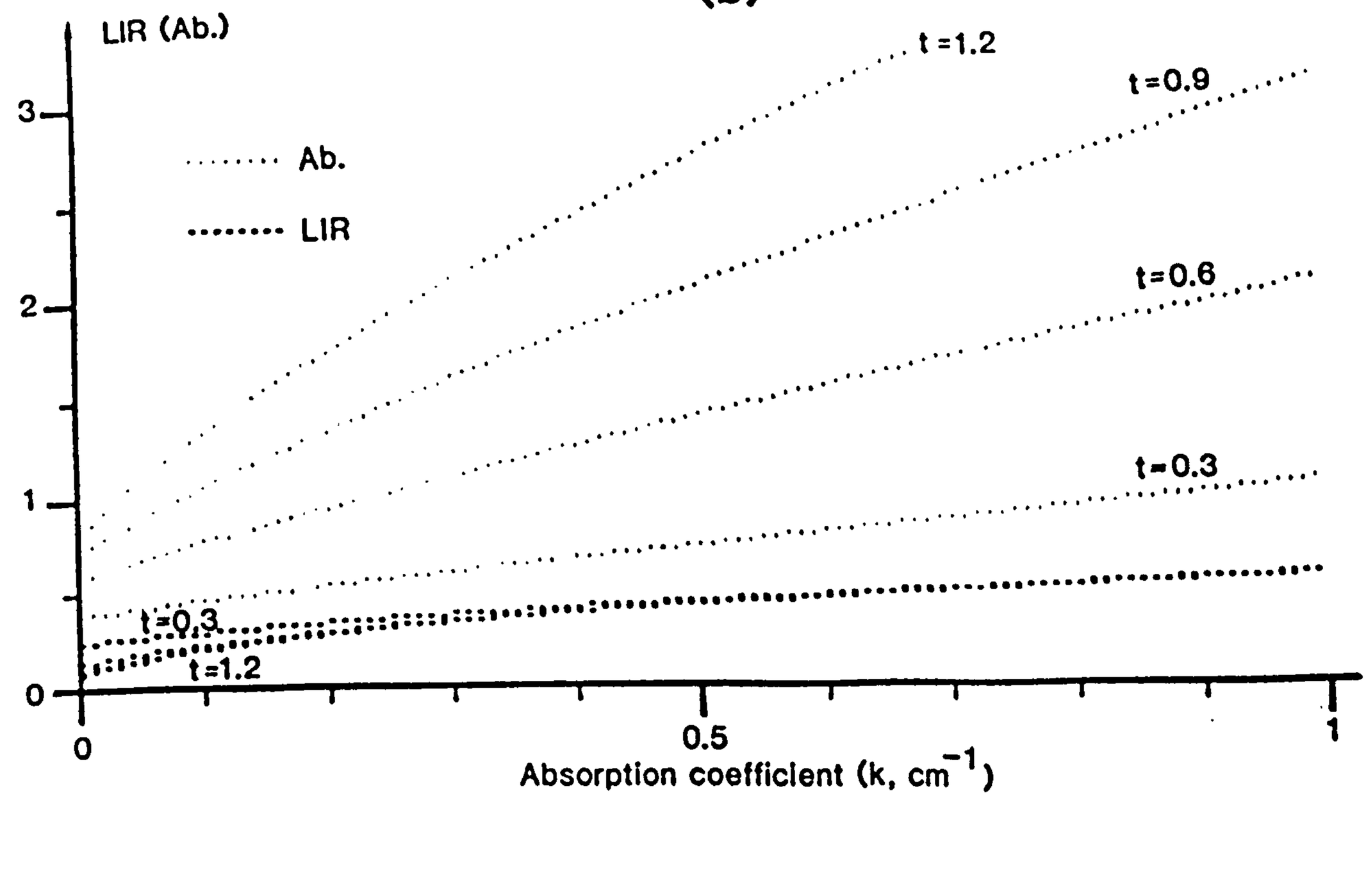

Fig. 3.5- LIR and absorbance of samples of different thickness (cm) against absorption coefficient.
a) scattering coefficient s =0.001 cm^{-1}, and
b) scattering coefficient s =1 cm^{-1}.

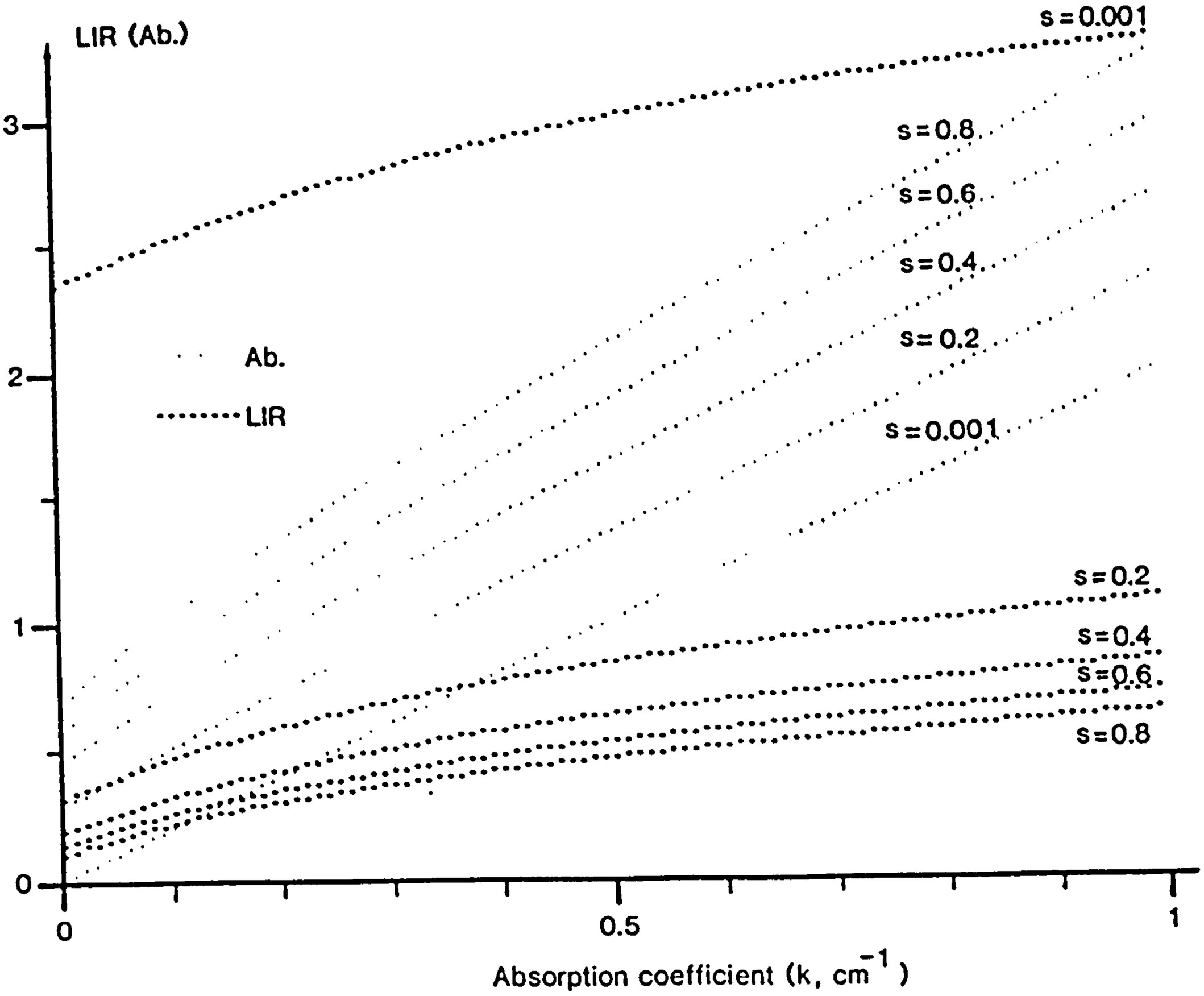

Fig. 3.6- LIR and absorbance of samples with different scattering coefficient (s, cm^{-1}) against absorption coefficient (k, cm^{-1}), (t=1 cm).

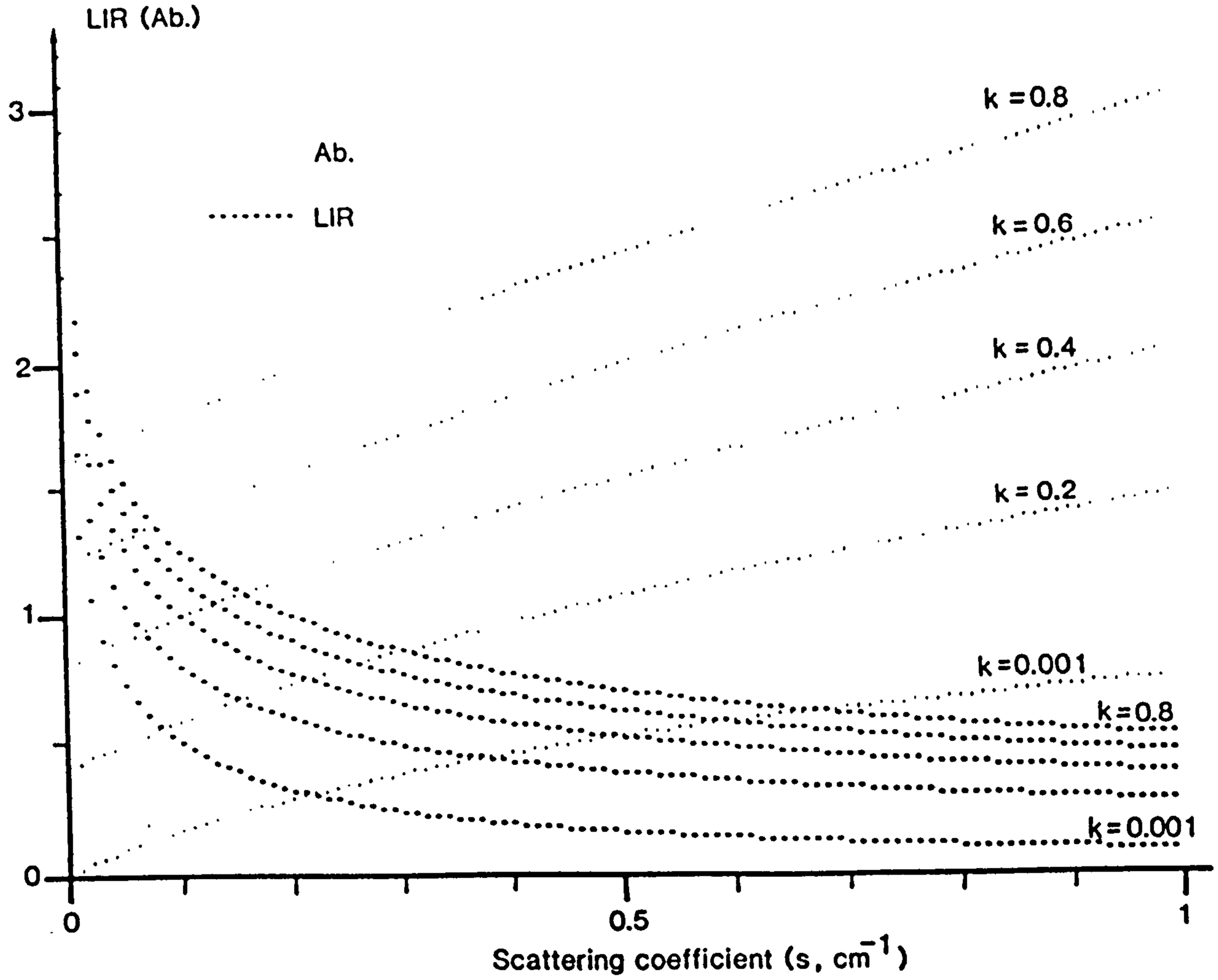

Fig. 3.7- LIR and absorbance of samples with different absorption coefficient (k, cm^{-1}) against scattering coefficient (s, cm^{-1}), (t=1 cm).

It can be seen that absorbance increases nearly linearly with increasing s and k coefficients. The rate of increase of absorbance with increased k is greater than that due to an equivalent increase in scattering coefficient, ie the slopes of the absorption curves in Fig. 3.6 are greater than those in Fig. 3.7. In contrast to the absorbance, the LIR decreases with increased scattering. This decrease as shown in Fig. 3.7 is very fast at low scattering coefficients. For a constant scattering coefficient, the LIR will increase with increasing absorption coefficient.

3-2-3-4 Kubelka -Munk theory as a special case of photon diffusion theory

To show the similarity of the Kubelka-Munk theory to the photon diffusion theory in one dimension, the differential equations 3.24 and 3.25 may be expressed in terms of photon flux (F) and photon density (P). Subtracting 3.25 from 3.24 will give the following result:

$$d(I+J) = -2(k+s)(I-J)\,dx - 2s(I-J)\,dx$$

$$= -2(I-J)\,(k+2s)\,dx \qquad 3.32a$$

Dividing the result by 2(k+2s)dx readily yields:

$$(I-J) = \frac{-1}{2(k+2s)} \times \frac{d(I+J)}{dx} \qquad 3.32$$

I and J are the light fluxes flowing perpendicularly to the sample surface in opposite directions, thus, (I -J) is the net photon flux "F" in the incident direction. Assuming the photons are travelling with the average velocity of "C", the photon density at

each point is then the sum of photons which are travelling in the incident (P_i) and opposite (P_j) directions per unit volume. It can be expressed in terms of I and J by the following formula:

$$P = P_i + P_j = (I + J)/C \qquad 3.33$$

Substituting the expression for the diffusion coefficient (D= C/(k +2s), eqtn. 3.9) and 3.33 in 3.32 will give the following formula:

$$F = -D \frac{dP}{2dx} \qquad 3.34$$

This is the photon diffusion equation, the same as eqtn. 3.8, in one dimension and has been derived from the Kubelka -Munk differential equations. The factor 2 at the denominator arises from the use of the average path length as being twice the thickness of the diffusing layer.

3-2-3-5 Application of the Kubelka -Munk formula to special cases

In the present study of reflectance spectroscopy two different situations are used. One is where the light is shone on the surface of a sample of finite thickness, while the other surface is not exposed to any light, eg. the sample is placed on a black surface. This situation fulfils the boundary conditions used to solve equations 3.24 and 3.25, hence, the reflectance is calculated from eqtn 3.31. In the situation where no light is transmitted completely through the sample, eg a very thick sample, the back scattered light from within the sample is independent of thickness. Under these circumstances

equation 3.31 will be simplified and the reflectance (R_∞) can be calculated from the following formula:

$$R_\infty = \frac{(1 - b)}{(1 + b)} = \frac{\sqrt{k+2s} - \sqrt{k}}{\sqrt{k+2s} + \sqrt{k}} \qquad 3\text{-}35$$

This equation shows that in a medium with very low absorption coefficient ($k \rightarrow 0$) all the light would be reflected back ($R_\infty \rightarrow 1$), and for a very high absorption coefficient ($k \rightarrow \infty$) the reflectance approaches zero ($R_\infty \rightarrow 0$). Increasing the scattering coefficient ($s \rightarrow \infty$) would increase the reflectance ($R_\infty \rightarrow 1$).

The above situation arises when shorter wavelength visible light (blue -violet) is shone on to the skin surface. Since this light is absorbed by the melanin and haemoglobin in the dermis and does not penetrate deeply into the skin, the diffusely reflected light is the radiation which is back scattered from superficial dermis before it penetrates to the subdermis. On the other hand longer wavelength light (red) penetrates deeper with less scattering. Measurements of the in-vivo reflectance and transmittance spectra of the ear lobe presented in chapter 6 will be analysed using this approach.

The other situation is when a significant proportion of the incident light is transmitted by the sample and reflected back into it from a white surface placed behind the sample. Such light passes again through the sample and the light reflected from the sample is the sum of light that has passed twice through the medium plus the back scattered light from within the sample. This was the arrangement used in this study for the in-vitro measurement of diluted blood samples. This situation will now be examined theoretically and then, in chapter 5, applied to the analysis of experimental results.

To calculate approximately the reflectance of a sample, assume the intensity of the incident light is I_o. The measured reflected signal (I_r) consists of the following parts:

1) Specularly reflected light at the surface (I_{spec}).

2) Diffusely back scattered light from within the sample which is $R(I_o - I_{spec})$, where R is the diffuse reflectance of the sample (eqtn 3.31).

3) The radiation which is transmitted through the sample and reflected back from the white surface. This part is $R_w T^2(I_o - I_{spec})$, where R_w is the reflection coefficient of the white surface (nearly 1 for MgO), and T is the transmittance of the sample (eqtn 3.30). Thus:

$$I_r = I_{spec} + (R + R_w T^2) x (I_o - I_{spec}) \qquad 3\text{-}36$$

From the definition of LIR (eqtn. 3.6)

$$LIR = Log_{10}\left(\frac{I_o - I_{spec}}{I_r}\right) \qquad 3\text{-}37$$

I_{spec} is equivalent to stray light in the system and is dependent on the surface texture. The LIR can be corrected for the stray light by excluding I_{spec} from I_r which gives the following formula:

$$LIR = Log_{10}\left(\frac{I_0 - I_{spec}}{I_r - I_{spec}}\right)$$

$$= Log_{10}\left(\frac{1}{R + R_w T^2}\right) \qquad 3\text{-}38$$

Since stray light reduces the gradient of the calibration curve at high absorbance and is similar to the effect of increasing the scattering coefficient, the effect of stray light (I_{spec}) and of the scattering coefficient (s) on LIR values has been studied. First, calibration curves of a non-scattering sample with unit absorption coefficient (k=1 cm^{-1}) and unit thickness were calculated for different fractions of stray light by means of equation 3.37. The values of transmittance and diffuse reflectance of the sample used to compute the LIR were calculated from equations 3.30 and 3.31. The results are shown in Fig 3.8. In this case there is no diffuse reflectance (R=0) and the transmittance is calculated from $T= 10^{-2kt}$, where t is the thickness and factor 2 arises when diffused light is used (eqtn 3.30 with s=0). The reflection coefficient of a perfect white surface (R_w) is unity. The dependence of LIR on changes in scattering coefficients (s), and absorption coefficients in the absence of stray light were next calculated from equation 3.38 and are shown in Fig. 3.9.

As can be seen from Fig. 3.8 the stray light not only decreases the LIR value but also results in its growth curve asymptotically approaching a constant value. The effect of increasing the scattering coefficient (Fig. 3.9) is dependent on the absorption coefficient and the concentration of absorber in the sample. For strongly absorbing material (Fig. 3.9a), increasing the scattering coefficient decreases the LIR value, which means that the light reflected from the white surface has been totally absorbed in passing through the sample and did not return to the surface. Therefore the reflected light is only the back scattered light from within the sample. In this case the LIR will not decrease below log{(1 +b)/(1 -b)} (eqtn. 3.35).

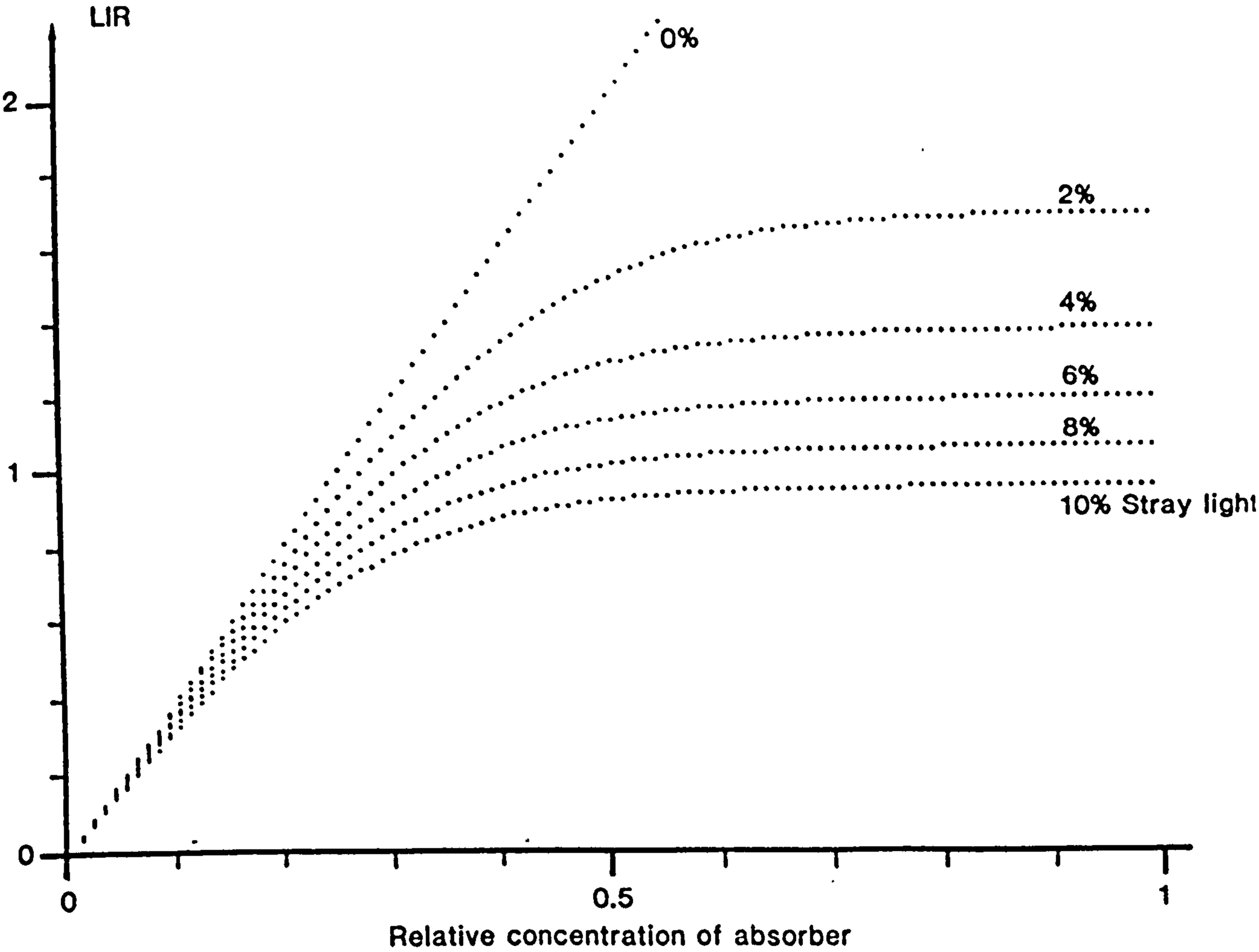

Fig. 3.8- Effect of stray light on the LIR of a sample placed on a white surface (absorption coefficient $k = 1\ cm^{-1}$, scattering coefficient $s = 0\ cm^{-1}$, thickness $t = 1$ cm).

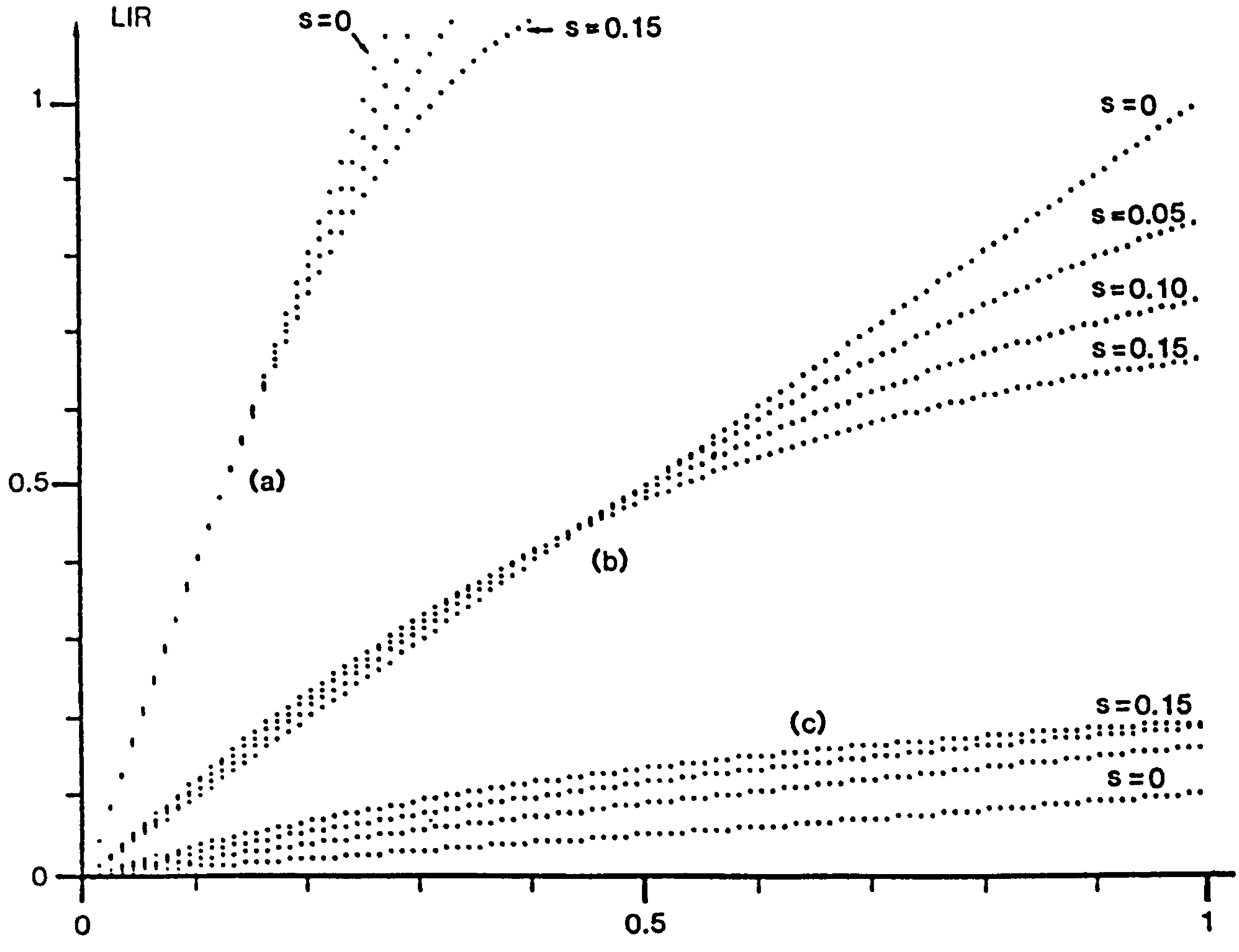

Fig. 3.9- Effect of back scattering (s, cm^{-1}) on the LIR of a sample placed on a white surface. Thickness t =1 cm, and absorption coefficient a) K =1, b) k =0.25, c) k =0.025 cm^{-1}.

In a medium with low absorption coefficient, increasing the scattering coefficient will increase the LIR value (Fig. 3.9c), owing to the loss of light by scattering and increase in the effective absorption path length. The relative enhancement will increase with decreasing absorption coefficient. The variable effect of scattering on the LIR value is clearly demonstrated in Fig. 3.9b, where increasing scattering coefficient causes first a relative increase of LIR at low concentrations but later a decrease at higher concentrations.

In the in-vitro measurements of diluted blood samples and of haemolysed cells with the same concentration of haemoglobin, the LIR value of the blood sample is increased relative to the haemoglobin sample due to the presence of scattering by red cells (Fig. 5.7). The ratio of the LIR of red cells to that of haemolysed haemoglobin varies between 1.1 and 11.3 from 540 to 670 nm, arising from the decrease in the specific absorption coefficient of haemoglobin between these two wavelengths. These observations will be considered in chapter 5.

3 - 3 Summary and conclusions

In this chapter transmittance and diffuse reflectance have been defined and absorbance and LIR introduced as parameters for quantifying the optical properties of a medium. It was noted that, due to the difficulties of a fundamental theoretical model for the propagation of light in a multiple scattering and absorbing medium, many authors have tried to develop a phenomenological approach. The most widely adopted approach to the problem of describing the behaviour of light in diffusing media is that of the solution of simultaneous differential equations of the first order, which describe

the attenuation of light intensity within the sample due to scattering and absorption. This theory was developed by Kubelka and Munk (1931) and extended by Kubelka (1948), and is known as the Kubelka-Munk theory. This theory can be regarded as a special case of the more general photon diffusion theory. In this chapter a photon diffusion equation was introduced and the relationships between photon life time, diffusion coefficient, and the absorption and scattering coefficients of the medium were demonstrated. The general solution of the equation was not attempted, instead, the special case for one dimension, which is in the form of Kubelka-Munk theory, was solved for two different boundary conditions.

One boundary condition is the situation where the light is shone onto the surface of a sample of finite thickness, while the other surface is not exposed to any light. This is the configuration that is used to measure the in-vivo transmittance and diffuse reflectance of an ear lobe. The dependence of the absorbance and LIR of a medium of sample thickness (t), absorption coefficient (k), and scattering coefficient (s) are shown in figures 3.5, 3.6, and 3.7. In this situation absorbance increased as k, s, and t increased. There is an absorbance value even when k=0 which increases with increasing s and t owing to the deflection of light out of the collimated beam by the scatterer. The LIR value, which increases with increasing k, does not change very much with the thickness of the sample for highly absorbing materials, and decreases with increasing s. The rate of decrease of LIR at low scattering coefficients is greater than that at high scattering coefficients.

The other boundary condition is the situation where the sample is placed on a white surface, so that any transmitted light is reflected

back into the sample by the white surface. This situation has been used for measuring the LIR spectra of diluted red cells and is similar to the reflection of light by "white" subcutaneous structures. For this case the dependence of LIR on k and s is shown in Fig. 3.9. For highly absorbing material, LIR will decrease with increasing s, but for low absorbing material it will increase. The prediction of the Kubelka -Munk model will be compared with the in-vivo and in-vitro measurements of skin and blood samples in chapter 5 and 6.

CHAPTER 4

4 - INSTRUMENTATION

A reflectance spectrophotometer was designed and constructed to examine and apply the theory described in Chapter 3, to the quantification of skin colour in terms of the biological pigments present. To exploit the theory, the instrument should measure only the component of light which is diffusely reflected from the skin. For this research it was necessary to collect full spectral data in order that the optimum wavelengths for the measurement of indices of skin pigments and blood oxygenation could be identified. Future instruments may operate more efficiently by making measurements at those optimum wavelengths only. As noted in chapter 1, to be of real clinical value the instrument has to be capable of rapid measurement to reduce measurement errors caused by body movement or biological changes. This requirement was met by using a rotating interference filter as the wavelength selecting device rather than a dispersive system. In this chapter the complete apparatus will be described and its performance in the measurement of in-vivo and in-vitro reflectance presented in later chapters.

4 - 1 Apparatus

The reflectance spectrophotometer which is shown schematically in Fig. 4.1a may be conveniently described in terms of its optical and electronic systems.

4-1-1 Optical system

The optical system consists of a light source, a circular

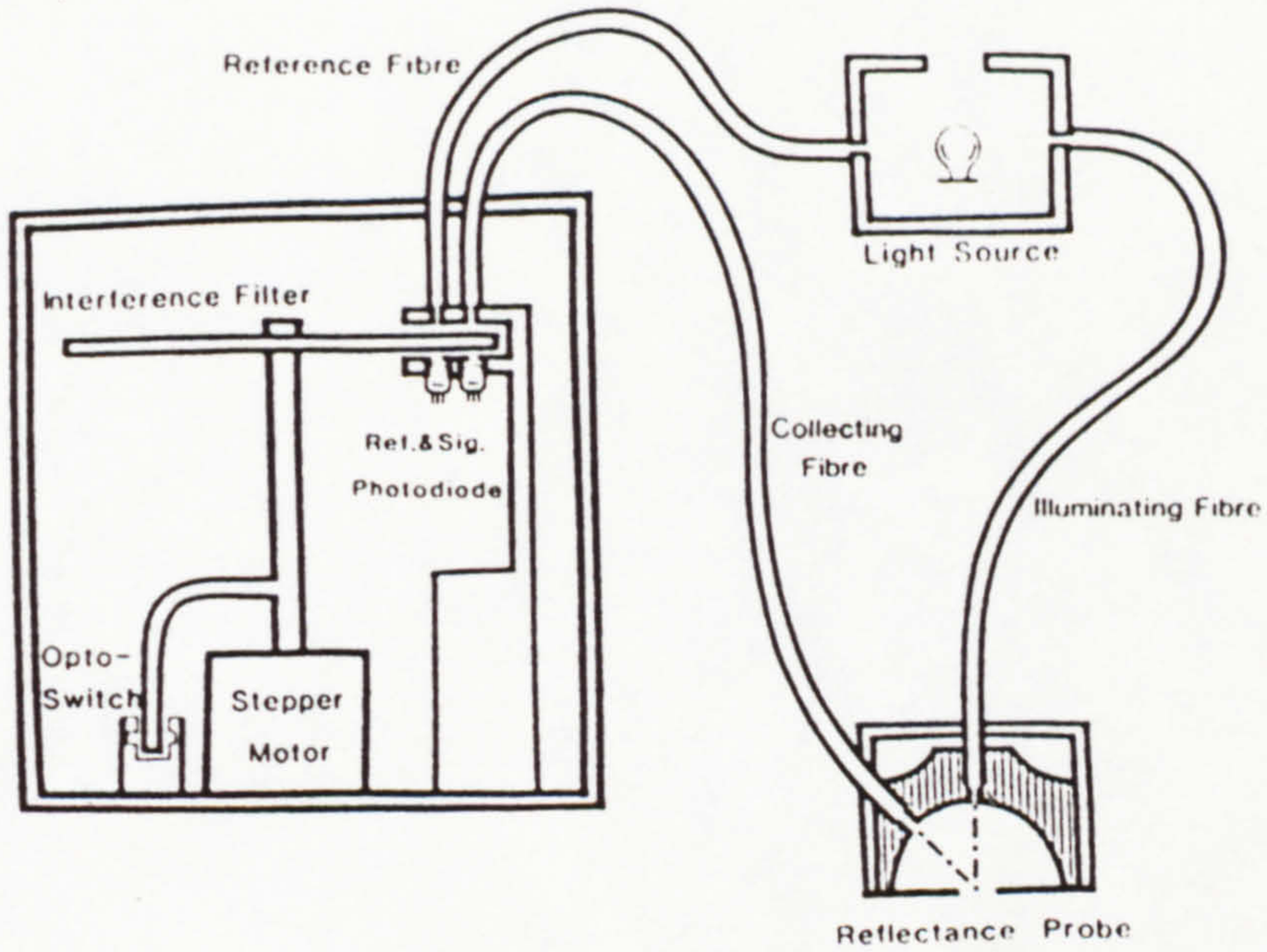

(a)

(b)

Fig. 4.1- The reflectance spectrophotometer,

a) schematic diagram, b) photograph

variable interference filter (CVF), fibre optic bundles for light delivery and collection, and two silicon (Si) photodiodes as detectors of signal and reference light.

The light source is a 6 V, 20 watt quartz halogen lamp. The interference filter (SELECTRE BAND, OCLI), is semicircular of diameter 10.2 cm and thickness 3.5 mm with an opaque black plastic semicircle completing the disc. This filter offers continuous spectral coverage from 356 to 721 nm. The band pass is wavelength dependent, varying from 9 to 16 nm from the blue to red regions of the spectrum respectively. Three 3.2 mm diameter fibre optic bundles (Ealing Electro Optics ref. Nos. 22 - 0301 and 22 - 0319) are used as light guides to carry the reflected and reference signals. The reference fibre, which is 90 cm long, guides the light from the source directly to the interference filter. After filtration the light falls on the surface of the reference photodiode (Radiospares, stock No. 308-067). The signal channel consists of two 120 cm long fibres, the first of which transfers the light from the light source to the reflection probe and illuminates the skin surface perpendicularly through a 1 cm diameter hole. The second fibre collects the light diffusely reflected at an angle of 45 degrees to the skin surface and guides it to the interference filter. This light after filtration at the same wavelength as that of the reference light excites the signal photodiode. The intensity of light in the signal fibre is maximised by mounting it as close as possible to the lamp. The use of a concave mirror positioned behind the lamp increased the light intensity at 550 nm transmitted by the fibre by almost 2.5 times. The acceptance angle of the fibre is wavelength dependent and increases with increasing wavelength.

It was found that when illuminating a surface perpendiculary and collecting the scattered light at 45 degrees the intensity was greater than that observed when illuminating at 45 degrees and collecting perpendicularly. Hence the optical fibres were mounted in the reflectance probe in the former configuration, as shown in Fig. 4.1a.

The photodiode mounting bracket was designed to minimise crosstalk between the signal and reference channels. This was achieved by minimising the distance between each fibre and its detector, by maximising the distance between two detectors on a radius from the centre of rotation of the interference filter and by mounting a small aperture in front of each photodiode. Increasing the radial distance between the detectors might be expected to cause differences in the band pass in the signal and reference channels, hence the radial separation of the photodiodes is a compromise and they are located as near to the edge of the filter as possible. It was thought that the use of a narrow slit along the radius between filter and fibres would decrease the band pass of the filter, but it was found that not only did it not effectively improve the band pass, it also decreased the signal. The slit therefore was used only in front of the reference fibre which was nearer to the centre of the filter.

The reflection probe, as illustrated in Fig. 4.1a, is a hemisphere 2.5 cm diameter with a blackened interior. The hemisphere is mounted inside a metal cylinder for ease of handling and exclusion of ambient light. For the measurement of the diffusely reflected light an integrating sphere, ie. a sphere with a whitened interior, is usually used, however in our case we wished to exclude specularly reflected light and therefore the interior surface of the reflection probe was blackened. Under these circumstances the principal

contribution to the measured signal will arise from light that has been scattered at the uneven skin surface and within the tissue.

In order to prevent saturation of the photodiode at the longer wavelength (700 nm), where the signal is 50 times greater than at shorter wavelengths (400 nm), a blue filter (Kodak, Wratten No.38) was placed in both the signal and reference channels. This filter produces maximum attenuation at 700 nm (20 fold) whilst being minimal at 400 nm (1.5 fold). Figure 4.2 shows the effect of this filter on the reflected light intensity from a white surface ($MgCO_3$). In this figure the expected spectral response of the signal channel has been calculated from the manufacturer's data of the optical components used. These data are presented in Table 4.1. The reflection coefficient of $MgCO_3$ has been calculated from the data published by Jacquez & Kuppenheim (1955), by assuming that MgO has a reflection coefficient of 100 percent for all wavelengths. As there was no specific information about the irradiance of the light source, it was not possible to predict the absolute output voltage of the photodiode. The observed value is therefore the relative spectral response of the signal channel corrected for the assumed characteristic of the light source. The spectral irradiance of the light source was taken from data published by the National Physics Laboratory for a 12 V, 100 W quartz halogen lamp at 5 m from the lamp, and was assumed to be applicable to our light source. The measured data are the output of the signal photodiode (mV), when the reflectance probe was placed on a white $MgCO_3$ surface and the filter was set at a different wavelength. A discrepancy between measured and calculated values was observed and attributed to variation of the acceptance angle of the fibre at different wavelengths. This fact was not taken into account in

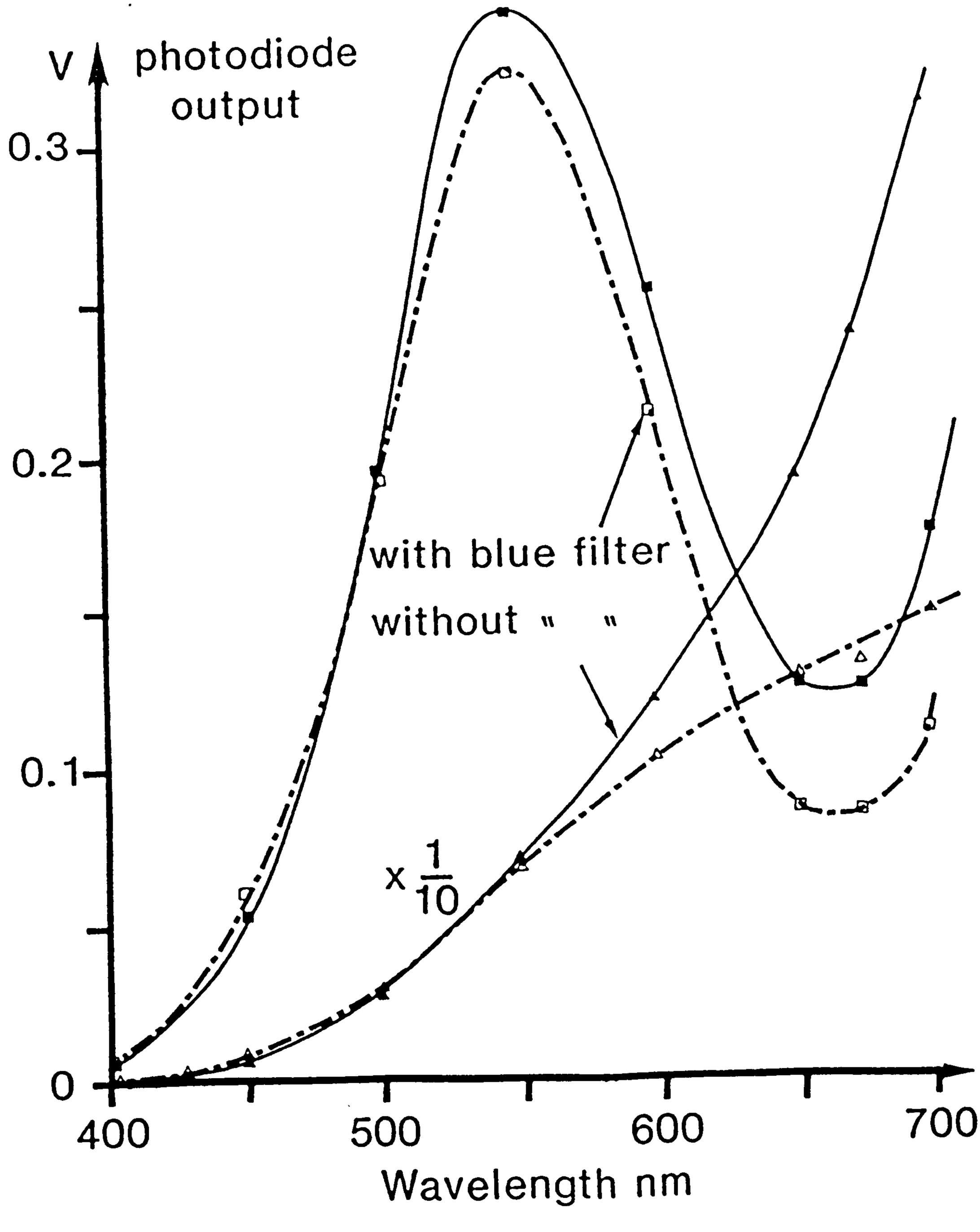

Fig. 4.2- Measured (full line) and expected (dashed line) spectral response of the signal channel with reflected light from white surface of $MgCO_3$, with and without blue filter.

Table 4.1- Spectral data of the optical components used in reflectance spectrophotometer (from manufacturer's data book).

Wavelength nm	Source Irradiance mW/cm^2	Transmission of 122 cm fibre %	Transmission blue filter %	Transmission of CVF filter %	Reflection coefficient of $MgCO_3$ %	Responsivity of photodiode mV/μW
400	3.04	23.5	60.5	22.3	0.947	2.78
425	4.48	31.3	70.0	28.4	0.948	3.00
450	6.20	36.5	75.9	31.8	0.960	3.21
500	10.38	46.1	66.7	35.8	0.974	3.75
550	15.00	51.6	48.0	41.9	0.983	4.07
600	19.53	49.6	20.9	46.6	0.984	4.61
650	23.50	47.4	6.7	48.0	0.991	5.04
675	25.25	45.9	6.4	46.6	0.991	5.30
700	26.80	45.3	7.4	48.0	0.992	5.57

deriving the calculated value of the spectral response. In Fig. 4.2 the measured signal is greater than the calculated value at longer wavelengths which is consistent with the observation that at longer wavelengths, due to a wider acceptance angle, more light has been collected by the signal fibre.

4-1-2 Electronic system

A block diagram of the electronic and computer systems is shown in Fig. 4.3. A stepper motor (STH 39C001, SHINANO KENSHI Co. Ltd. Japan) is used to rotate the interference filter which analyses the signal light. Two Si photodiodes were used as signal and reference photodiodes to convert the filtered signal and reference radiations to signal and reference voltages. A 12 bit A/D was used to convert these analog signals to digital for processing by a microcomputer. Figure 4.4 shows the circuit diagram of the electronics which have been used. It consists of two parts, one for signal processing and the other for controlling rotation of the interference filter.

4-1-2-1 Signal processing circuit

The output voltages of the signal and reference photodiodes are amplified by means of two differential amplifiers (308 OP-AMP) with appropriate gains (approximately 40 and 10 fold for the signal and reference channels respectively). In order to accommodate the wide range of signals when ranging from blue to red, and to maintain accurate measurement of the ratio of signal/reference light, the output of the reference photodiode was used to supply the reference voltage of the A/D converter. Thus when the signal voltage was applied to the input of the A/D converter, it is automatically expressed as a

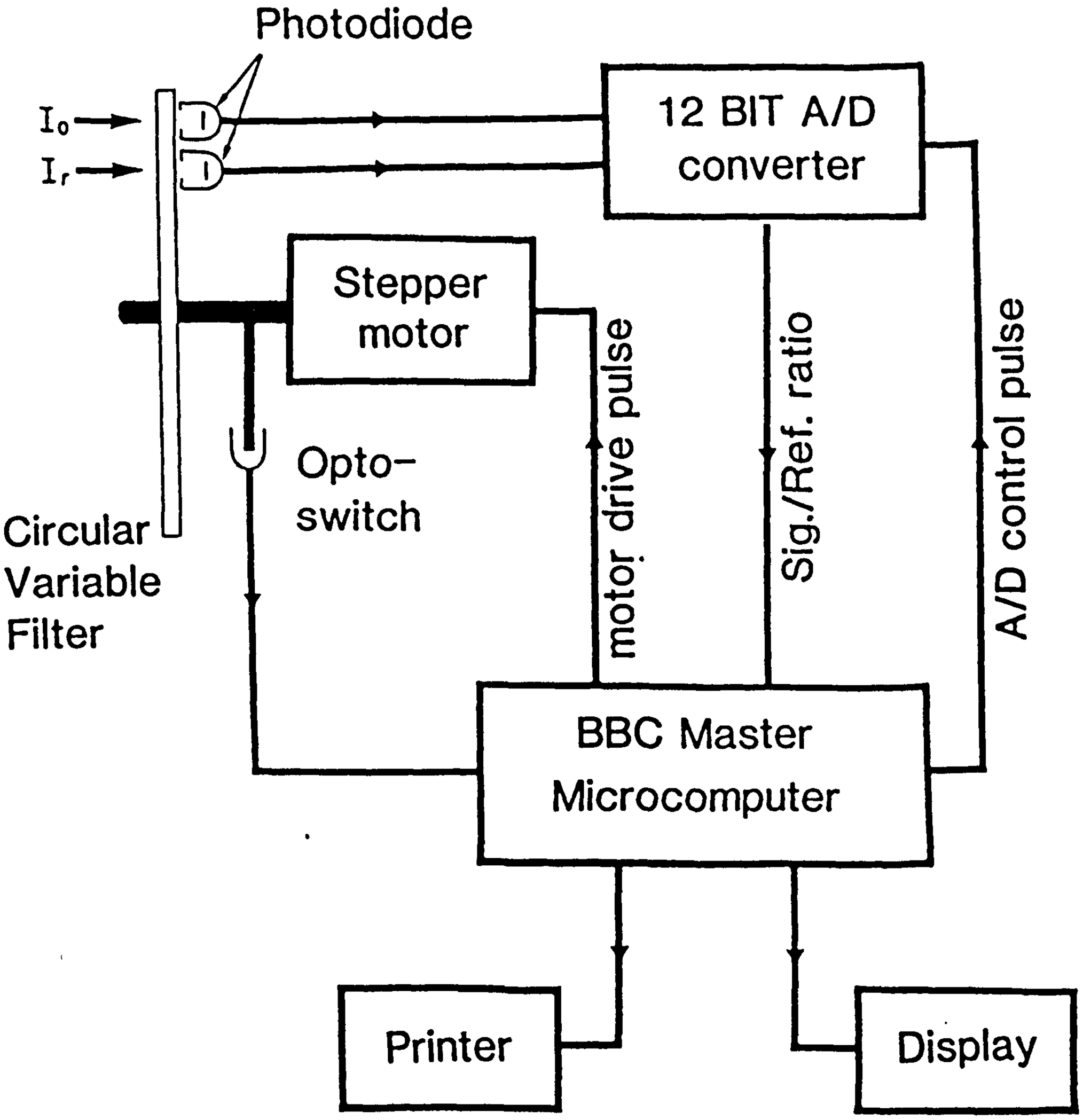

Fig. 4.3- block diagram of electronic and computer parts of reflectance spectrophotometer.

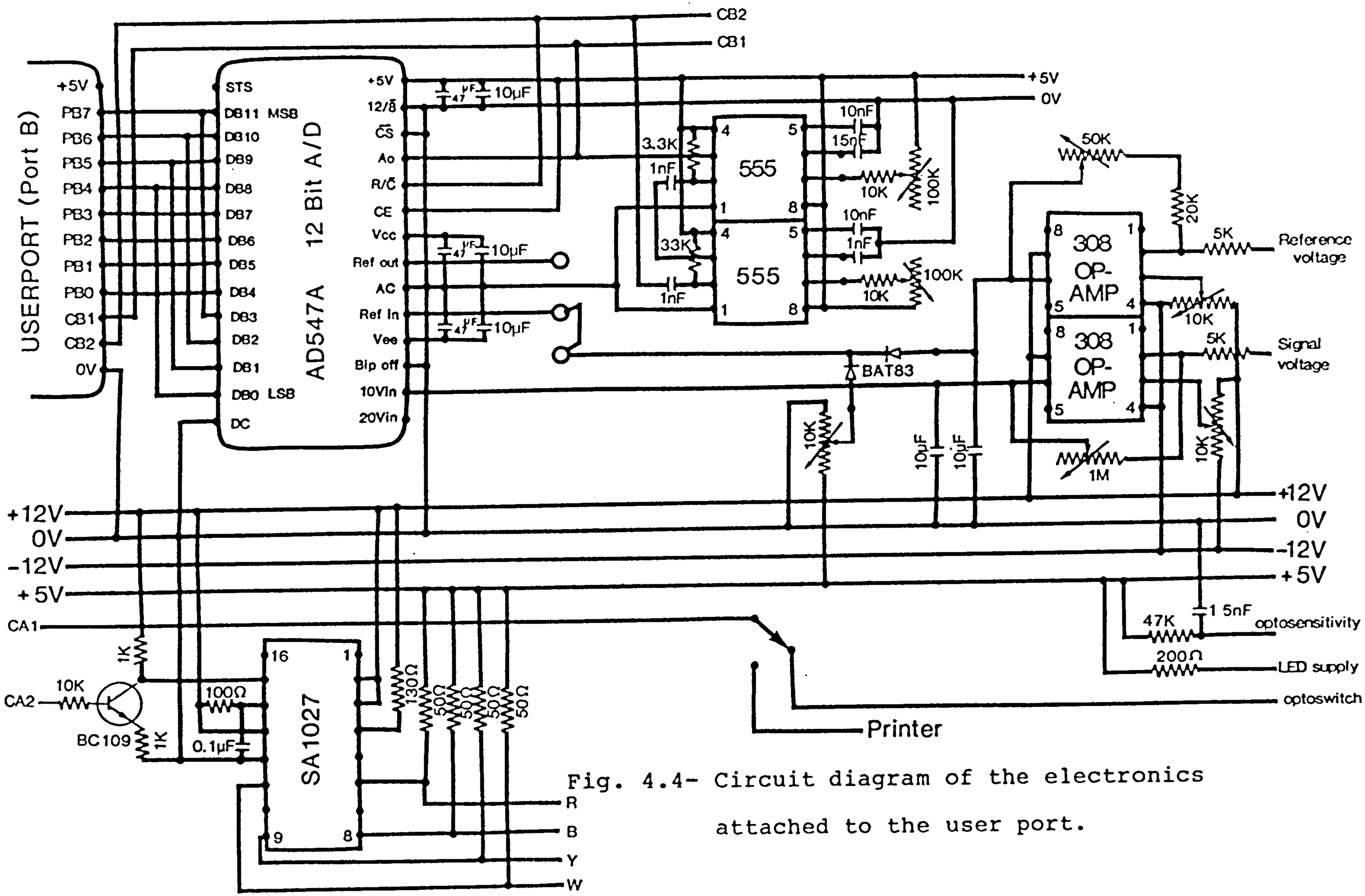

Fig. 4.4- Circuit diagram of the electronics attached to the user port.

proportion of the reference signal at any wavelength. The output of the A/D converter should therefore be independent of the emission spectrum of the lamp and the transmission characteristics of the optical system (see section 4-4). Since the A/D converter was designed to be used with a fixed reference voltage of 5 or 10 volts, and in our case the reference voltage varied between a few mV to 10 volts, its linearity had to be checked. Further, to prevent the A/D converter from saturating, the gains of the amplifiers in signal and reference channels have to be set so that, for all wavelengths, the signal voltage is less than the reference voltage. The output of each photodiode in the absence of light is slightly positive (10 mV), which on exposure to light goes negative. Since the A/D converter needs a positive input signal the OP-AMPs are used as inverting amplifiers with offsets for the dark signal.

The reference voltage of the A/D converter at short wavelengths drops to a few mV, which makes the system very sensitive to the offset of the dark signal. To prevent the reference voltage falling below 0.4V, two BAT83 diodes and a potential divider were used at the output of the reference OP-AMP as shown in Fig 4.4. The effect of these diodes on the stability of the A/D reading at low reference voltages will be shown in section 4-5. For smoothing the signal and reference voltages, two 10 μF tantalum capacitors were connected across the output of the OP-AMPs.

The linearity of the response of the instrument for different light levels of the lamp and different levels of amplification in the signal and reference channels was checked. For this purpose the reflectance probe was placed on a white surface of $MgCO_3$, and a series of measurements made. First, the amplifier gains in the signal and

reference channels were changed and then the reflected signal changed by different neutral density filters in the signal channel. In each case the signal and reference voltages at different wavelengths were measured separately and the ratio sig./ref. calculated. The result of a typical measurement is shown in Fig. 4.5. In this measurement the amplifier gains were set so that the maximum reference voltage was 8.6V and the maximum signal voltage was 7.9V, which occurred at 555 nm. The instrument responds linearly in all of the different measurements and comparison of the sig./ref. ratio derived by computer with that measured directly confirms the linearity of the A/D converter for reference voltages greater than 0.4V. Figure 4.5 shows a discrepancy between the A/D reading and corresponding measured sig./ref. ratio at short wavelength. This is because at short wavelengths, firstly the signal voltage is low and unstable and cannot be read accurately and secondly the A/D becomes more sensitive due to the low reference voltage (<0.4 V) which also fluctuates.

A BBC Master microcomputer was used as a signal processing unit to generate the pulses which drive the stepper motor and initiate the A/D conversion. The heart of the signal processing is a 6522 Versatile Interface Adaptor (VIA) chip, which is built into the microcomputer. This chip consists of two fully programmable bidirectional 8 bit I/O ports. These are designated port A and port B, each of which has two control lines called CA1, CA2, CB1 and CB2. The functions of this userport and the temporal sequence of each are described below.

Two sets of pulse trains are generated at the userport using a machine code program. One set is generated at CA2 control line for driving the stepper motor and the other is generated at the CB2 control line for driving the A/D. A timing diagram of these two sets

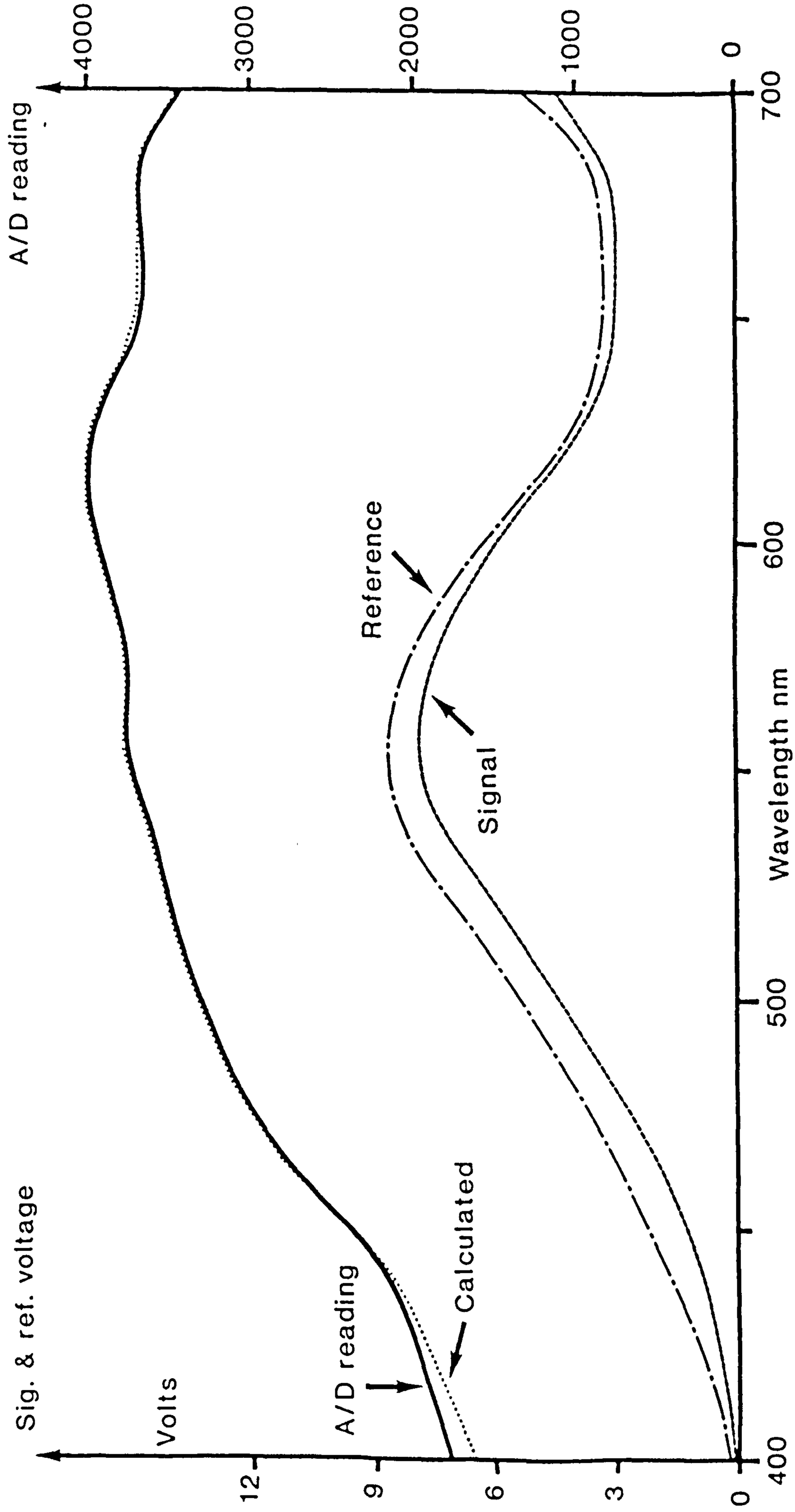

Fig. 4.5- Spectral signal (———)and reference voltage (·—·—·—), calculated signal/reference ratio (.....) and the A/D converter out put (———) using light reflected from a $MgCO_3$ surface.

of pulses with respect to each other is shown in Fig. 4.6. The motor drive pulse train has a repetition interval of 14 ms and each pulse a duration of 1 ms.

The 12 bit A/D was used to transfer the signal to the computer via 8 lines of port B of the userport. Therefore the data had to be transferred in two stages, first the 8 Most Significant Bits (MSB) and then the 4 Least Significant Bits (LSB). In order to reduce the statistical error, the A/D's output was read 16 times per step of the motor and an average value calculated for that step. The sixteen read pulses are generated by CB2. The falling edge of each pulse initiates the A/D conversion and after 34 microseconds the 8 MSB of the data are ready for transfer to the computer. Another positive pulse is generated from each pulse by means of two 555 time delay chips and is fed to line 4 of the A/D (A_0) to change its output from 8 MSB to 4 LSB. This pulse is also used to command the computer to read the 4 LSB via CB1 control line (see Fig. 4.4).

4-1-2-2 Interference filter control system

The motor drive pulses are amplified from 5 V on CA2 to 12 V with a transistor (BC 109) and then fed to a stepper motor driver chip (SAA 1027) to rotate the interference filter. This transistor is in common emitter mode and supplies the current required by the stepper motor driver chip.

The optoswitch (shown in Fig. 4.1) consists of a Light Emitting Diode (LED) which is mounted in front of a photosensor. The output voltage of the photosensor is 5 V unless the light from the LED is intercepted by an indicator arm attached to the axle of the stepper motor. The position of this indicator is adjusted so that, when the

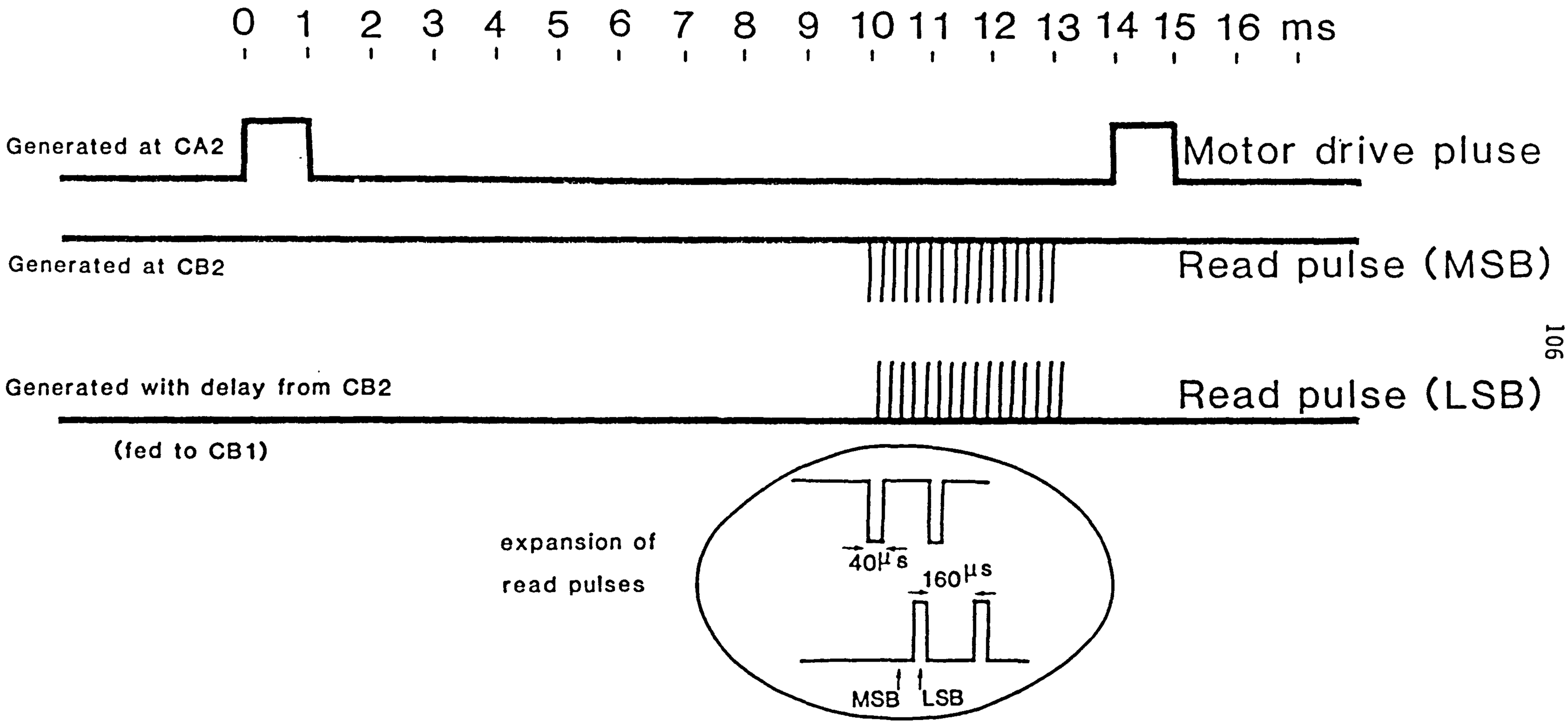

Fig. 4.6- Timing diagram of the pulse-train generated at the user port for driving the reflectance spectrophotometer.

beginning of the filter (356 nm) is located between the optical fibres and detectors, the indicator interrupts the light from the LED and causes a drop in the output of the photosensor. Thus each time the start of the filter passes the detectors a negative pulse is generated by the photosensor. This negative pulse is fed to the microcomputer via CA1 control line, which is used to locate the filter and thereafter the number of steps taken by the filter is counted.

The sensitivity of the photosensor of the optoswitch was adjusted with a 47 KΩ resistor and 1.5 μF capacitor to match the light intensity of the LED mounted in front of the photosensor. The actual sequence of the signal processing procedure ie resetting the filter, driving the stepper motor and reading the A/D's output, can be followed easily in the Basic computer program (see section 4-3).

4 - 2 Calibrating the apparatus

To calibrate the instrument, the relationship between the position of the stepper motor and the wavelength of the interference filter has to be known. This was determined by initially resetting the filter by means of the optoswitch pulse to its "start" position. The filter was then rotated to measure the spectrum of different light sources containing known emission lines. By noting the step number of the stepper motor at peaks of the known wavelengths the relationship between number of steps of the motor and wavelengths of the radiation transmitted by the interference filter may be determined. For this purpose, the emission lines of sodium (589 nm), potassium (404.5 and 495.6 nm), mercury (404.6, 435.8, 546 and 577 nm) from discharge lamps and a Helium-Neon laser (632.8 nm) were used. It was found that the interference filter transmitted radiation between 356 nm and 721 nm in

increments of 1.825 nm per step, where each step corresponds to 0.9 degree rotation of the disc. The relationship between number of steps of the stepper motor (N) and wavelength (nm) of the filter is given by:

$$\text{Wavelength (nm)} = 1.825\ N + 356 \qquad 4\text{-}1$$

In order to measure the band pass of the filter, a quartz halogen lamp was placed in front of the entrance slit of a SPEX monochromator and the signal fibre of the reflectance spectrophotometer connected to its exit slit. The SPEX monochromator was then set at different wavelengths and the spectrum at each position measured by the rotating filter. The profiles of these spectra are shown in Fig. 4.7. It can be seen that the band pass (ie full width at half maximum of the signal peak) of the interference filter increases with increasing wavelength from 9.1 nm at 400 nm to 15.5 nm at 700 nm.

It should be noted that in the spectral region in which the instrument operates (356 - 721 nm) there is no significant contribution from other orders of transmission through the interference filter.

4 - 3 Computer program

As noted earlier (section 4-1-2) a BBC Master microcomputer has been interfaced with the reflectance spectrophotometer to achieve several functions. A program was written using two different languages to meet the needs of specific functions. Basic was used for all functions which were not involved with timing operations, and Machine Code for time dependent functions such as driving the stepper motor or

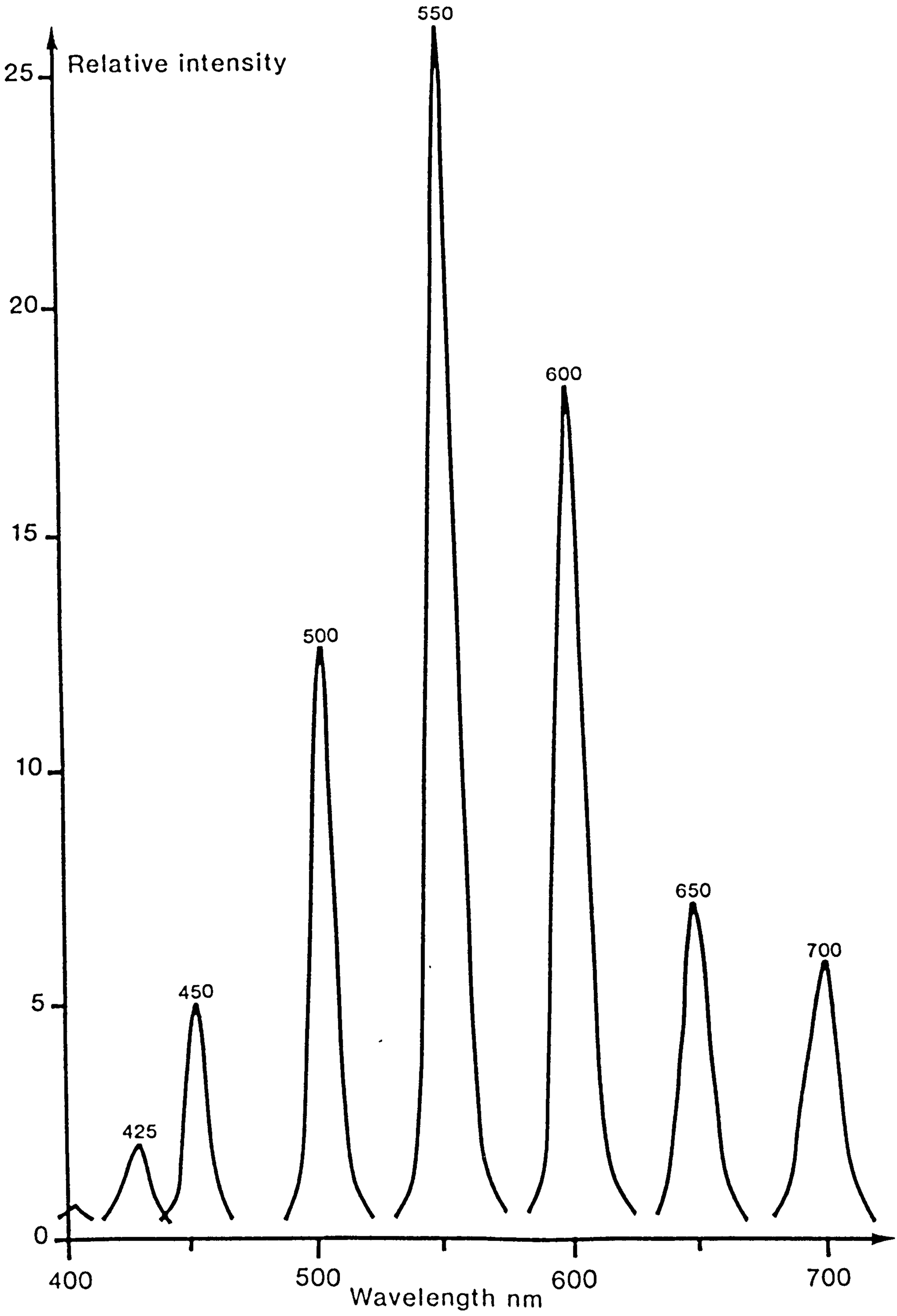

Fig. 4.7- Profiles of different monochromatic light sources measured by the rotating interference filter.

reading the A/D converter. The whole program can appropriately be described in terms of these two parts.

A : Basic program

The Basic program, in addition to carrying out all the calculations, the printing of results, plotting the spectra and saving the data on the floppy disc for future analysis, also carries out further operations as described below:

a) Prior to each measurement, the program can be set to measure the reference white and black surfaces and to keep the data for reference purposes, or it can be set to measure the sample and calculate the LIR value.

b) At the end of each measurement the program reviews all the data to determine whether or not the A/D has been saturated during measurement; if saturation occurs, the corresponding wavelength will be printed out.

c) The program also controls the measurement procedure by using different parts of the machine code program.

B : Machine code program

This part of the program, which was written in assembler language in four separate sections, drives the stepper motor, controls the optoswitch for resetting the filter, commands the A/D to start conversion and then reads the data. To carry out these functions, port B and four control lines of the userport of the computer were used. Eight lines of port B were used for transferring the data to the microcomputer, and the other 4 control lines were utilized as follows:

CA1 for checking the optoswitch

CA2 for driving the stepper motor via a stepper motor driver chip

CB1 for checking the A/D's output to change to 4 LSB

CB2 for initiating the A/D conversion and reading the 8 MSB of the data.

To avoid any interruptions generated by the microcomputer, at the beginning of each section the four control lines, CA1, CA2, CB1, CB2 are disabled by means of Interrupt Enable Register (IER). The CA1 and CB1 are set on a positive active edge, CB2 on high output, CA2 on low output by Peripheral Control Register (PCR). To simplify and be more accessible, this part of the program consists of four separate sections. Each section can be called up from within the basic program, and after execution the program counter is set to the next line of the Basic program. These four sections are as below:

a) Acquiring

In this section of the program, which is written for data acquisition, first, port B is set as input and then, by setting CA2 first high then low, a positive pulse is generated to drive the stepper motor one step forward, after which there is a loop to generate a certain number of negative pulses on CB2. This creates a read pulse to initiate the A/D start of the conversion. There is a reading after each read pulse as described in section 4-1-2-1, and all these readings are summated. At the end of this loop, the average is calculated and stored for that step. The same procedure is repeated for as many steps as are required. Special memory locations, which are used for different purposes, are described below:

90 - 91 for making indirect address as a LBA & HBA

92 - 93 for storing MSB & LSB of each reading

94 - 95 for storing the sum of 16 readings per step MSB & LSB

96 for storing the number of steps

97 for storing the number of readings per step

98 for producing a delay.

b) Resetting

The purpose of this section of the program is to locate the starting position of the filter. To achieve this, first, the CA1 flag is reset and a positive pulse on CA2 drives the stepper motor one step forward, the optoswitch will then be sought via CA1 control line, which has already been set on positive active edge. If its flag was still reset, another pulse on CA2 will drive the stepper motor a further one step forward. This procedure will be repeated until the CA1 flag was set by a pulse from the optoswitch. This pulse will be generated only when the beginning of the filter is in line with the detectors. Because CA1 is internally connected to the printer and is affected by it, the printer has to be disconnected during execution of this part of the program.

c) Driving the stepper motor forward

In order to set the interference filter at a certain wavelength or to move the non-active part of the filter past the detectors after each scan, it is necessary to drive the stepper motor forward for a predetermined number of steps. This section of the program fulfils this function by generating the required number of pulses on CA2.

d) Testing

This section of the machine code program reads only the output of the A/D converter (as described in section a). By combining this section and section "c" above with a Basic program, the input to the computer can be checked at each step. First the program will set the interference filter at a desired wavelength, the A/D is then read and the value displayed on the screen, next the program interrogates the keyboard and, if no interrupt occurs, it will continue reading. At any

interruption it will ask for the next function.

A complete program and the flowcharts of different sections of the machine code program are shown in appendix A.

4 - 4 Experimental measurement procedure

As noted earlier (section 4-1-2-1) the output of the A/D converter should be dependent only upon the reflectance characteristics of the surface being measured. However, it was found that the readings of the A/D for light reflected from a reference white surface of $MgCO_3$ were not as expected ie. a constant flat spectrum. The measured spectrum is shown in Fig. 4.5 and may be attributed to:

A) The different responses of the Si photodiodes in the signal and reference channels.

B) The different optical transmissions of the signal and reference fibres due to their different lengths and the fact that the reference fibre is continuous whereas two fibres are used in the signal channel.

C) The effect of the variable acceptance angle of the fibres with the wavelength of light transmitted. This will affect the equality of the light collection from the light source by the signal and reference fibres.

As all these factors determine the instrumental response, any absorbance spectrum measured by the instrument requires correction, by computation, for all these effects.

In practice these difficulties are overcome by measuring the diffusely reflected light from a standard white surface (assuming that to be the non-absorbed light intensity) and storing the data in the

computer memory. The diffusely reflected light from the absorbing medium is then measured and compared with the stored intensity readings. The function LIR, Logarithm of the Inverse of Reflection, is then defined as the logarithm of the ratio of the diffusely reflected light from a non-absorbing medium divided by that from an absorbing medium. Because the light reflected from a white surface and from an absorbing medium is measured with the same geometry, their ratio is independent of the geometry of the reflection probe. An array of 200 data points is provided in the computer program to store the A/D's output of the reflected light from a standard white surface. The spectral scan of a white surface is made prior to measurement of any test surface. These values, which are themselves proportional to the ratio of the intensity of light in the signal to that in the reference channel, are called I_W. When the light of the signal channel passes through an absorbing medium and is then reflected from a white surface behind the medium, the output of the A/D converter corresponding to the collected reflected light is called I_S. Using the definition of LIR at each wavelength we would have:

$$LIR = Log_{10}(I_W/I_S) \qquad 4\text{-}2$$

All the procedures required to measure a spectrum have been included in the computer program. When running the program, first there is an option for resetting the filter, then the program directs the operator to place the reflection probe on a standard white surface. Iw is then measured for all wavelengths and stored in an array for use in the successive measurements. The system is now ready to measure reflectance spectra. When the reflection probe is placed on a surface and the output of the A/D recorded, the computer then

calculates the LIR spectrum of that surface. At this stage the program offers the three options of printing, plotting or saving the spectrum on disc that can be used prior to the measurement of another spectrum.

The performance of the apparatus was examined by measuring the reflectance spectrum of different coloured cardboard. Data for a standard white surface (I_w) was taken from a smooth $MgCO_3$ surface prepared by gentle compression of the powder with a microscope slide. As is shown in Fig. 4.8, all LIR spectra decrease at short wavelengths. This decrease may be attributed to the presence of stray light. Stray light is more significant when the light intensity is low ie. short wavelengths. In order to reduce this effect, two approaches were followed. First the reflected signal was increased as much as possible, and second the intensity of the stray light was estimated and used to correct the signal. In the first approach, in addition to maximising the light intensity in the signal fibre two other approaches were tested. First, the output of the photodiodes was integrated using variable integrating times, hence, the smaller the signal, the longer the time. Second, two different levels of amplification were so used that for smaller signals higher gains were used. It was found that in both cases attempts to increase the signal increased the noise proportionately. These methods led to no improvement in the signal/noise ratio.

In the second approach the signal was corrected for instrumental stray light by creating a further 200 data point array in the computer program in which to store information from the signal channel when the reflection probe is placed on the matt black surface. These values, which are called I_b, are used to calculate the corrected LIR value

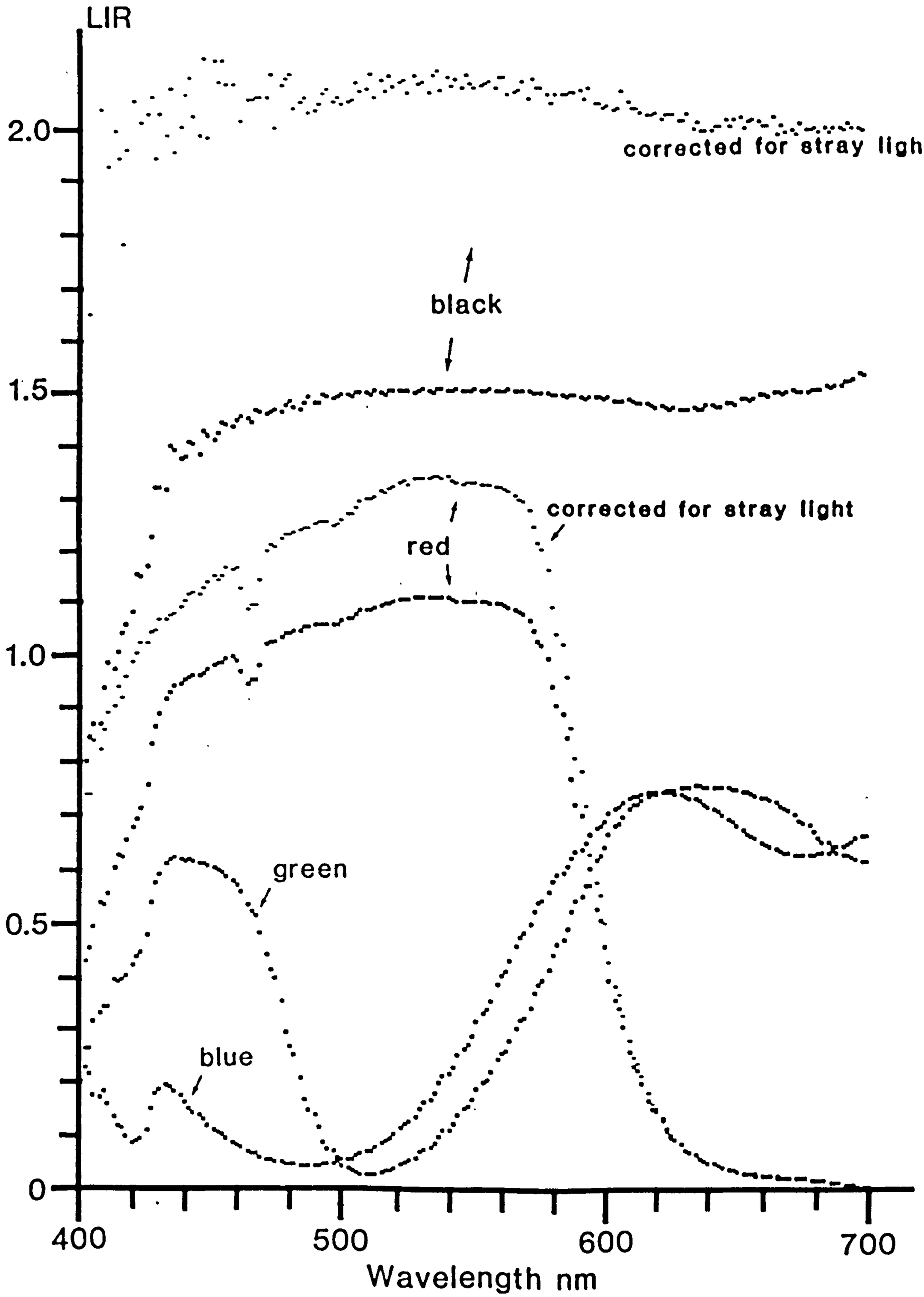

FIG. 4.8- Reflectance spectra of red, green, blue and black surfaces.

for each wavelength from the following formula:

$$LIR = Log_{10}\{(I_w - I_b) / (I_s - I_b)\} \qquad 4\text{-}3$$

This method of correction requires that the reflectance of the black surface as well as that of the white surface be measured once prior to the measurement of the surfaces under investigation. The effect of this correction on the reflected spectrum of the black surface is shown in Fig. 4.8.

4 - 5 Test of the apparatus

The reproducibility of the instrument was determined in terms of the standard deviation (S.D.) and coefficient of variation (C.V.) by measuring the reflection spectrum of a white tile 20 times. For these measurements, after measuring the reflectance of the $MgCO_3$ surface as a standard white surface, a ceramic white tile was viewed by the reflectance probe. The computer program repeatedly measured and stored the reflected light intensity as a percentage of the computed reference signal, and also computed the corresponding absorbance (LIR) spectrum, without any change in the position of the reflectance probe. At the end of 20 measurements, the standard deviation and coefficient of variation of the reflected light intensity and of the absorbance (LIR) at each wavelength was calculated and plotted in Fig. 4.9. It can be seen that at short wavelengths, where the light intensity is very low, and at 660 nm where the blue filter decreases the red light intensity, the S.D. and C.V. of both reflected intensity and LIR increase. The S.D. of the reflected intensity shows a rapid decrease between 405 and 400 nm, which may be attributed to the effect of the fixed reference voltage (0.4V) supplied to the A/D converter at the

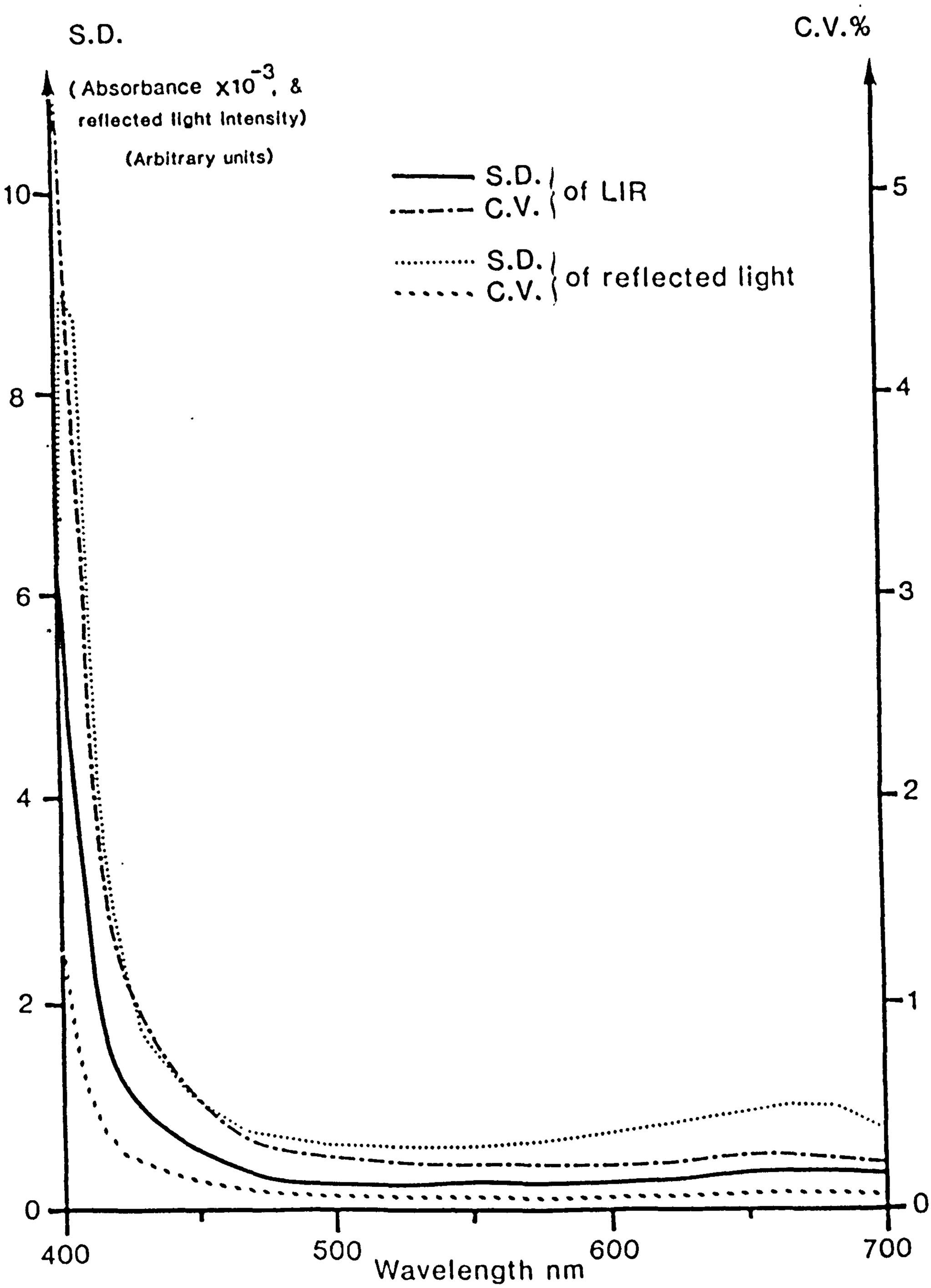

Fig. 4.9- Wavelength dependence of standard deviation (S.D.) and coefficient of variation (C.V.) of reflected light intensity and LIR from a white surface.

shorter wavelengths. The reflected signal at 400 nm (S.D.= 6.181 and C.V.= 0.015) has a maximum variation of 1.5%, while at 550 nm (S.D.= 0.544 and C.V.= 0.00048) has a variation of 0.048 percent.

From day-to-day, the precision of measurement of absorbance (LIR) will change slightly, nevertheless it is still a very reproducible measurement. The absorbance (LIR) at 400 nm (S.D.= 0.0064 and C.V.= 0.059) has a maximum variation of 5.9%, which rapidly falls to 0.18% at 550 nm (S.D.= 0.00021 and C.V.= 0.0018).

4 - 6 Summary and conclusions

Based on the theory described in chapter 3, a reflectance spectrophotometer has been designed to measure the diffusely reflected light from the surface of skin. In this instrument the radiation from the light source, a 6V, 20 watt quartz halogen lamp, is transmitted to the reflection probe by fibre optics and illuminates the skin surface perpendicularly. The diffused, reflected light is then collected at an angle of 45 degrees to the skin surface and transmitted to a rotating variable wavelength interference filter. Reference light is also passed from the light source directly to the filter. The signal and reference light after monochromation by passing through the filter are converted to an electrical signal via two Si photodiodes. The output of the reference channel photodiode was used to supply the reference voltage of the 12 bit A/D. Therefore the ratio of the signal/reference light is measured by applying the signal voltage to the input of the A/D. The linearity of the performance of the A/D converter was checked at various reference voltages, above a minimum of 0.4V. To improve the signal, equalise the band pass of the filter for signal and reference light and minimise the crosstalk between the signal and

reference channels, the distance between each fibre and its detector was minimised and the photodiodes were located on a radius as near to the edge of the filter as possible with a small aperture in front of each photodiode. In order to prevent saturation of the photodiodes at longer wavelengths a blue filter was placed in both signal and reference channels. The linearity of the response of the instrument to different intensities of the light source and different amplifier gains in the signal and reference channels was checked.

The relationship between steps of the stepper motor movement and the wavelength transmitted by the filter was determined by calibrating using the emission lines of sodium (589 nm), potassium (404.5 and 495.6 nm), mercury (404.6, 435.8, 546, and 577 nm) generated in discharge lamps and from a helium-neon laser (632.8 nm). It was found that the filter starts at 356 nm and ends at 721 nm and moves 1.825 nm per step (ie 0.9 degree rotation of the filter)

The reading of the A/D for light reflected from a reference white surface of $MgCO_3$ was not a constant flat spectrum. This irregularity was attributed to:

A) The different responses of the Si photodiodes in the signal and reference channels.

B) The different optical transmission characteristics of the signal and reference fibres due to their different lengths and the fact that the reference fibre is continuous whereas two fibres are used in the signal channel.

C) The effect of the wavelength dependence of the acceptance angle of the fibres which modifies the relative light collection efficiency of the signal and reference fibres.

Since all of these factors are incorporated into the instrumental

response, any absorbance spectrum measured by the instrument can be corrected for them by computation. In practice this is achieved by measuring the diffusely reflected light from a standard white surface and storing the data in the computer memory. The diffusely reflected light from the absorbing medium is then measured and compared with the stored data. The Logarithm of the Inverse of Reflectance, LIR, is calculated as the logarithm of the ratio of the diffusely reflected light from a nonabsorbing white surface divided by that from an absorbing medium. The LIR spectrum can also be corrected for stray light of the system by measuring the signal when the reflectance probe is placed on a black surface and storing the data in the same manner as those of a white surface. The corrected LIR can then be calculated from equation 4.3.

The instrument can measure the LIR spectrum of any diffuse reflecting surface at 200 equally spaced wavelengths between 356 to 721 nm. Each wavelength scan takes 2.8 s and is controlled by a BBC Master microcomputer. The advantages of the instrument for in-vivo measurement are:

1) Rapid measurement which minimises the possibility of biological change during the measurement.

2) Radiation in the visible spectral region is employed which is harmless and can be used with any skin disorder.

3) The use of fibre optic bundles for light delivery and collection renders all parts of the body's surface accessible to measurement.

This instrument has been used for in-vitro and in-vivo reflectance measurement of diluted blood samples and of skin surface; the results will be presented in later chapters.

CHAPTER 5

5 - IN-VITRO MEASUREMENT OF INDICES OF HAEMOGLOBIN AND ITS OXYGENATION

In this chapter, first the optical properties of diluted red cells will be investigated by in-vitro reflection spectroscopy, then a model of skin containing different amounts of blood will be made and the applicability of the Kubelka -Munk model will be tested. A new method for calculating the haemoglobin index and oxygen saturation will be suggested. Finally, the independence of these two indices with respect to each other will be verified.

5 - 1 Literature review of the optical properties of blood samples

In addition to experimental measurements of the optical properties of blood, some workers have attempted to develop a theory for the propagation of light through scattering and absorbing media such as whole blood. Non-haemolysed blood may be considered as a random distribution of particles that are large compared with the wavelength of incident radiation.

Anderson and Sekelj (1967a) applied a theory developed by Twersky (1962) to describe the scattering of radiation by whole blood. They derived the following expression for the optical density (O.D.) of a blood sample with thickness t,

$$O.D. = \varepsilon ct - Log\{10^{-sh(1-h)t} + 0.4(1 - 10^{-sh(1-h)t})\} \qquad 5\text{-}1$$

where "ε" is the specific absorption coefficient of haemoglobin, "s" is the scattering coefficient, "c" is the concentration of

haemoglobin, "h" is the haematocrit (fractional volume occupied by the red cells), 0.4 was used as the fraction of the total light scattered by a single scatterer in free space that is received by the detector. This value was calculated by Anderson and Sekelj (1967a) to be valid for sample thickness in the range 0.011 to 0.071 cm. It can be seen that the first term on the right is equivalent to Beer's law. The second term corresponds to scattering and is independent of absorption. In this theory, when the concentration and thickness of the sample are constant, the optical density of the sample is linearly related to the S.A.C. of the haemoglobin within the scattering particles and is wavelength dependent.

Longini and Zdrojkowski (1968) suggested that multiple scattering can be described by a model of photon diffusion through the medium. Janson (1972) applied the Kubelka-Munk theory, as a special case of photon diffusion theory, to blood and showed that the absorption factor for diffused light in a diffusing medium is twice that of collimated light in a clear solution having the same concentration of absorber. It was also pointed out that the scattering factor depends on the haemoglobin concentration.

Reflectance studies of non-haemolysed blood have been carried out by several workers with the aim of developing an empirical method for the estimation of oxygen saturation. Kramer et al (1956) investigated light reflectance from non-haemolysed blood with different sample thicknesses (0.13 to 1.3 cm). They demonstrated that the reflectance is inversely proportional to absorbance. It increases up to a sample thickness of about 0.3 cm and then becomes asymptotic. The relationship between reflectance and haemoglobin content is parabolic.

Anderson and Sekelj (1967b) measured reflectance and transmission

of thin films (0.25 to 0.71 mm) of flowing non-haemolysed blood at 600 to 630 nm. They confirmed the result of Kramer et al (1956) and also showed that reflectance and transmission are linearly related. They found that reflectance was exponentially related to the extinction coefficient of haemoglobin. The thickness of the sample exerts two distinct effects on reflectance, first, the absolute value of the reflectance is greater at large sample thicknesses, and second, the change in reflectance due to the wavelength dependence of the extinction coefficients is much greater when the sample thickness is larger.

Mook et al (1968) reported the reflection and transmission spectra of oxygenated and reduced blood samples measured by a fibre optic method. They found that an exact isobestic point could not be located in the reflection spectra, but there appeared to be an isobestic region between 840 and 920 nm. Their data show, however, that transmission spectra have a distinct isobestic point near 790 nm. It was suggested that the observed shift of the isobestic point was inherent in the fibre optic method of measuring the light reflected.

In the present study the reflectance spectra of diluted red cells when placed on white or black surfaces will be measured with a fibre optic probe and analysed using the Kubelka -Munk theory.

5 - 2 Preparation of blood samples

Because of the high extinction coefficent of haemoglobin at visible wavelengths, and the fact that only a small proportion of the skin tissue volume is occupied by blood, all blood samples had to be diluted, the extent of the dilution being determined by the thickness of the sample holder being used.

In most of the measurements, fresh packed red cell specimens were obtained and diluted to between 0.25 and 3% by volume with isotonic solution to prevent haemolysis of the red cells. These solutions are approximately equivalent to a 0.5 to 6% dilution of whole blood. The isotonic solution can be either plasma or 0.9% saline, the latter contains 0.9 g NaCl in 100 ml distilled water. Plasma has a slightly higher refractive index than the saline, hence the scattering properties of the red cells in plasma will be different from those of red cells in saline. This difference should be borne in mind when the results are analysed. To prepare a haemolysed sample, red cells are diluted with distilled water. In distilled water suspensions of red cells the intra- and extra-cellular osmotic pressures are not balanced, in consequence water is taken up by the red cell. The red cell then swells and its membrane ruptures allowing haemoglobin to escape into the surrounding water. The broken cell membranes can then be separated by centrifugation of the sample.

In some experiments to be reported in this chapter blood samples with different but known levels of oxygen saturation were required. To prepare such samples two different methods were used. First a chemical reagent, sodium dithionite ($Na_2S_2O_4$), was used to reduce the oxygenation and secondly a mixture of air and nitrogen gas was passed through the sample in a sealed container for a few minutes to adjust the oxygen content.

When using sodium dithionite care is necessary to prevent the haemoglobin from changing to another compound which can occur if too much sodium dithionite is used. The effect of using different amounts of dithionite with diluted red cells was investigated by deoxygenating different diluted samples with a fresh solution of 0.5 percent sodium

dithionite. The deoxygenated samples were then exposed to air to promote the change back to oxyhaemoglobin. A solution of 0.5 percent sodium dithionite contains 0.5 g $Na_2S_2O_4$ in 100 ml of 0.9% saline. This solution is unstable and in half an hour will completely lose its reducing strength, it should therefore be used immediately after preparation. It was found that when the ratio of the concentration of red cells to that of the sodium dithionite solution was approximately 50 or more, reduced haemoglobin was prepared which, on exposure to air, recombined with oxygen to produce oxyhaemoglobin. If the ratio was less than 50, haemoglobin changed to a stable compound which did not revert to oxyhaemoglobin even after long exposure to air. It is very difficult to prepare a blood sample with a predetermined level of oxygenation by this method and consequently it was not used in this work.

The second method of preparing a reduced sample is by passing a mixture of air and nitrogen gas of known composition through the sample for few minutes. In this method there is no risk of haemoglobin changing to another compound and also it is easy to achieve a known oxygenation by using specified mixtures of air and nitrogen. The instrumental arrangement used for this purpose is shown in Fig. 5.1. The flows of air and nitrogen to which 5.2% of carbon dioxide was added, are measured by passing through two rotameters. They are then mixed together and directed to the sample via a bidirectional tap A. This tap can also direct the mixed gas to an oxygen analyser machine to measure the proportion of oxygen as a check of the expected value. A small valve 'B' was used to regulate the pressure inside the flask containing the sample to be the same as atmospheric pressure. The

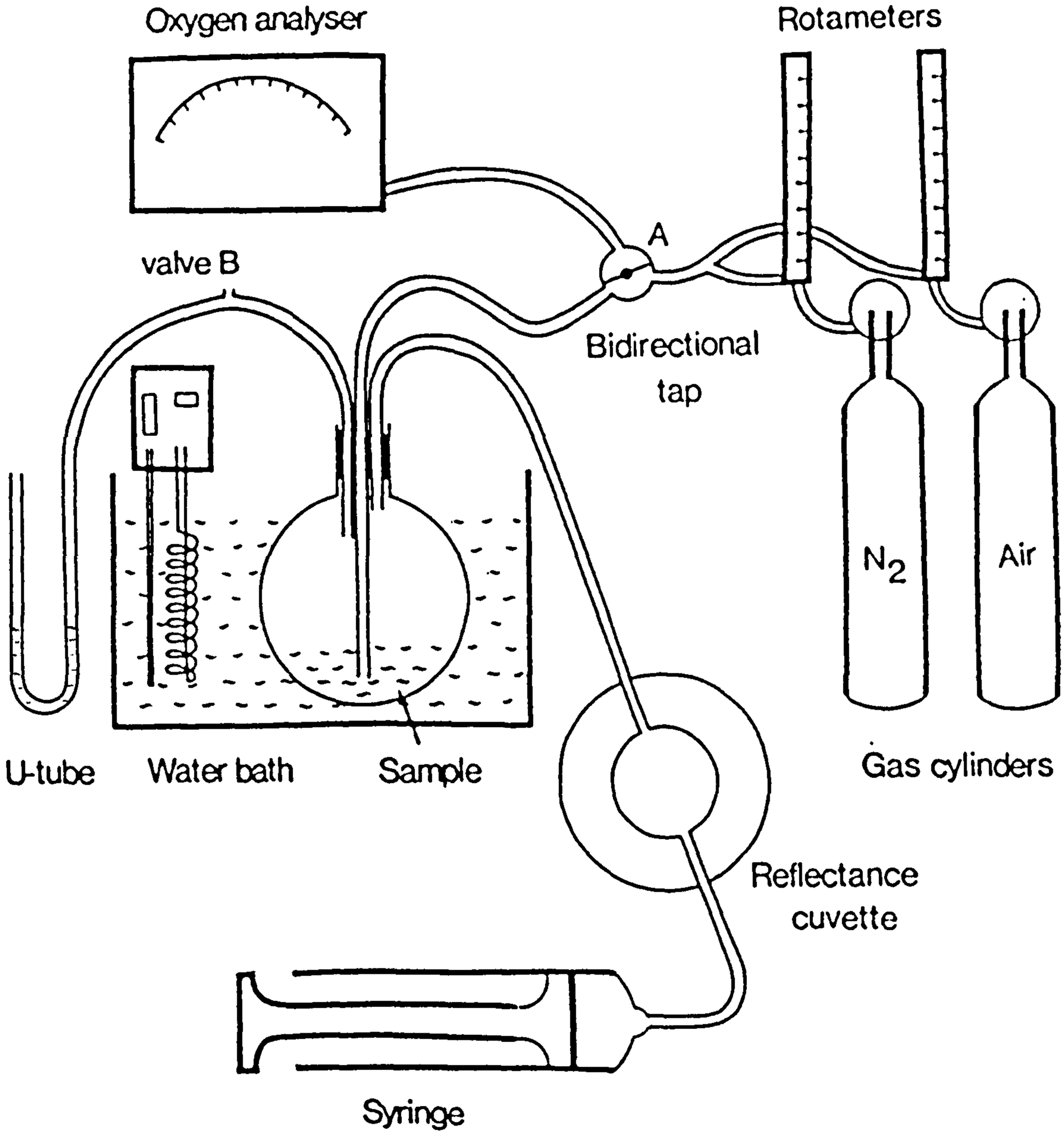

Fig. 5.1- Instrumental arrangement for achieving different levels of oxygenation of haemoglobin.

mixed gas first fills all the tubes and then goes out via valve B. Any increase in the pressure inside the flask will imbalance the water in the U tube. During any measurement the water was kept balanced in this tube by adjusting the valve B. The sample was transferred to the reflection cell by tipping the flask to one side and drawing the sample into the cell with a syringe, after measurement samples were injected back to the flask. As the oxygen affinity of haemoglobin is temperature dependent, the sample was kept in a water bath at a predetermined temperature (37 °C), and the air around the reflection cell was kept at approximately 37 °C by blowing hot air from a hair drier.

5 - 3 Measurement of the haemoglobin index

Since the LIR spectrum of a skin surface, as measured by the reflectance spectrophotometer described in chapter 4, represents the absorption characteristic of the skin's chromophores, it should therefore be possible to separate the contribution of each pigment to the LIR value and thereby quantify the amount of that pigment in the skin. The scattering property of each measurement site, by modifying the transmission of light, will affect the LIR value. Thus, the same amount of chromophore in different scattering media will lead to different LIR values. If skin chromophores are to be quantified, the measured index of skin pigment should be independent of the absolute LIR value.

A haemoglobin index was devised by Dawson et al (1980) for measuring the redness of skin. It was assumed that the presence of reduced haemoglobin in blood will modify the shape of the double peak in the spectrum of oxyhaemoglobin (Fig. 5.13) but does not

significantly alter the area under the peak. By joining the points at 510 and 610 nm on the spectrum (Fig. 5.13) an arbitrary baseline is created and the area under the curve and above the baseline is calculated by the formula:

$$E = \{(R + 1.5(Q + S) - 2.0(P + T)\} \qquad 5\text{-}2$$

where P,Q,R,S and T are the absorbance value at 510, 543, 560, 576 and 610 nm respectively. The dimension of E, which is called the "Erythema Index", is in units of absorbance x nm.

As the state of oxygenation changes the shape of the absorbance spectrum, an alternative approach is the use of isobestic points on the oxy and reduced haemoglobin spectrum, ie. where the absorption is independent of the state of oxygenation. There are 5 isobestic points in the spectral region of interest (500 - 600 nm), whose positions change slightly depending on the band pass of the measuring system. In our reflectance spectrometer they are at 500, 527.5, 544, 573 and 582.5 nm. If it is assumed that scattering affects the optical density (LIR), as described in eqtn 5.1, then differences in the LIR between two isobestic points will be proportional to the amount of haemoglobin available in the sample and independent of the state of oxygenation, if changes in scattering coefficients are negligible. Thus, a haemoglobin index can be defined, using the difference in the LIR between isobestic points. The use of a circular variable interference filter with stepper motor has limited the resolution of the instrument to 1.825 nm per step. The isobestic point at 582.5 nm, which is in a region of rapid change of absorbance with wavelength and thus produces a sensitive haemoglobin index, is not suitable for use with the present instrument. It was found that any small error in the reset

position of the filter caused a large change in measured LIR at that wavelength. The measurement wavelengths (527.5, 544 and 573 nm) and the corresponding values of the S.A.C. of haemoglobin are close to each other and any variation in the background tissue absorbance will be similar for all of them. Therefore, an index of haemoglobin (H) is calculated from the following expression:

$$H = \{(A_{544} - A_{527.5})/16.5 - (A_{573} - A_{544})/29\}\ 100 \qquad 5\text{-}3$$

where "A_x" is the LIR value at wavelength "x" nm and each term on the right hand side of the equation is the slope between two isobestic points. The dimension of this haemoglobin index is absorbance/nm. Because these slopes have different signs, subtraction of one from the other gives a more sensitive index and also, in the case of the measurement of skin in-vivo, cancels out the contribution of melanin to the LIR spectrum, as the latter has an almost linear decrease in absorbance in this region of the spectrum.

These two haemoglobin indices (eqtns. 5.2 and 5.3) will be compared in terms of their dependence on the amount of haemoglobin and independence of the state of oxygenation.

5-3-1 Calibration curve of the haemoglobin index

In order to establish the dependence of these indices on the amount of haemoglobin and to study the optical property of red cells, different concentrations of red cells in 0.9 percent saline were prepared. The reflectance spectra of 0.25, 0.5, 0.75, 1.0, 1.5 and 2.0% red cell concentrations were measured by injection of the samples into cuvettes of different thicknesses (0.654, 0.832 and 1.144 mm). The cuvette was made of two microscope slides and a rectangular

well 1.5x2.5 cm, constructed from the core of the glass fibre optics of different diameters, and glued to one of the microscope slides as shown in Fig. 5.2. The sample is injected with the top cover pulled back, after injection the cover is pushed forward again, providing a closed cuvette.

The measurement was carried out twice, first with the cuvette on a white surface of MgCO3 and then on a matt black surface. In the former measurement the transmitted light is reflected from the white surface, while in the latter, the transmitted light is absorbed by the black surface and only light back scattered by the red cells is measured. Figure 5.3 shows all these spectra for the 0.832 mm thick cell. From the lower curves, which are the LIR spectra of red cells on the white surface, it can be seen that increasing the concentration increases the haemoglobin peak i.e. the LIR values increase. The upper curves, which are the LIR spectra on a black surface, show decreasing LIR values with increasing concentration of red cells (scattering centres). This effect is a result of an increase in back scattering with concentration, particularly at longer wavelengths where the absorption coefficient is lower. The reflectance spectra from a black surface with saline only in the cell shows that there is some stray light in the system (nearly 3% of the incident light); this may be light reflected from the black background or liquid surfaces.

Figure 5.4 presents the spectra of 1% red cells using different absorbance path lengths as measured on the white and black surfaces. It shows that the LIR at the haemoglobin peak (540 nm) and the back scattered light at longer wavelengths increase with increasing thickness of the sample. The reflectance spectra of saline on the black surface with different thicknesses of cuvette are also plotted

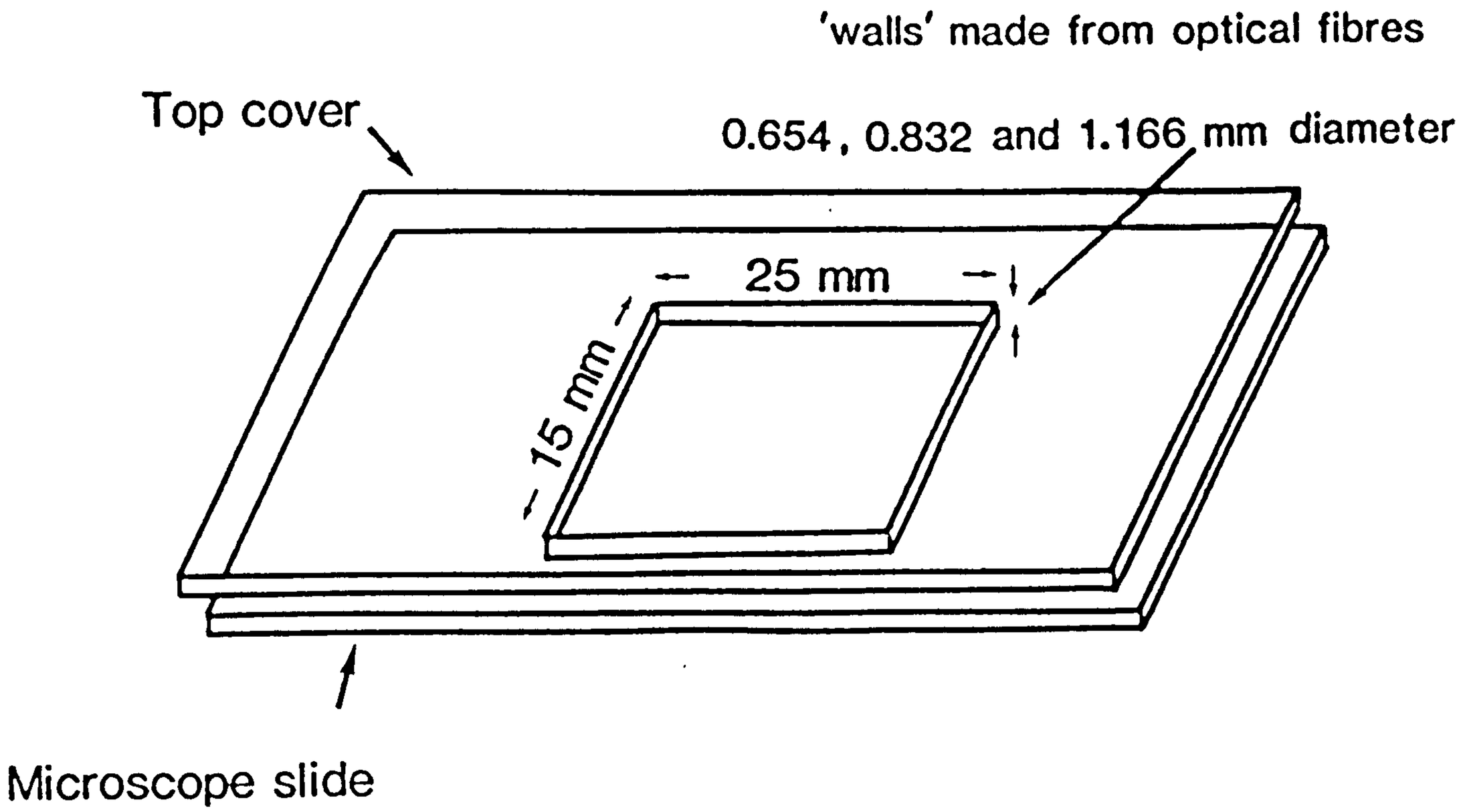

Fig. 5.2- Diagram of the reflectance cuvette.

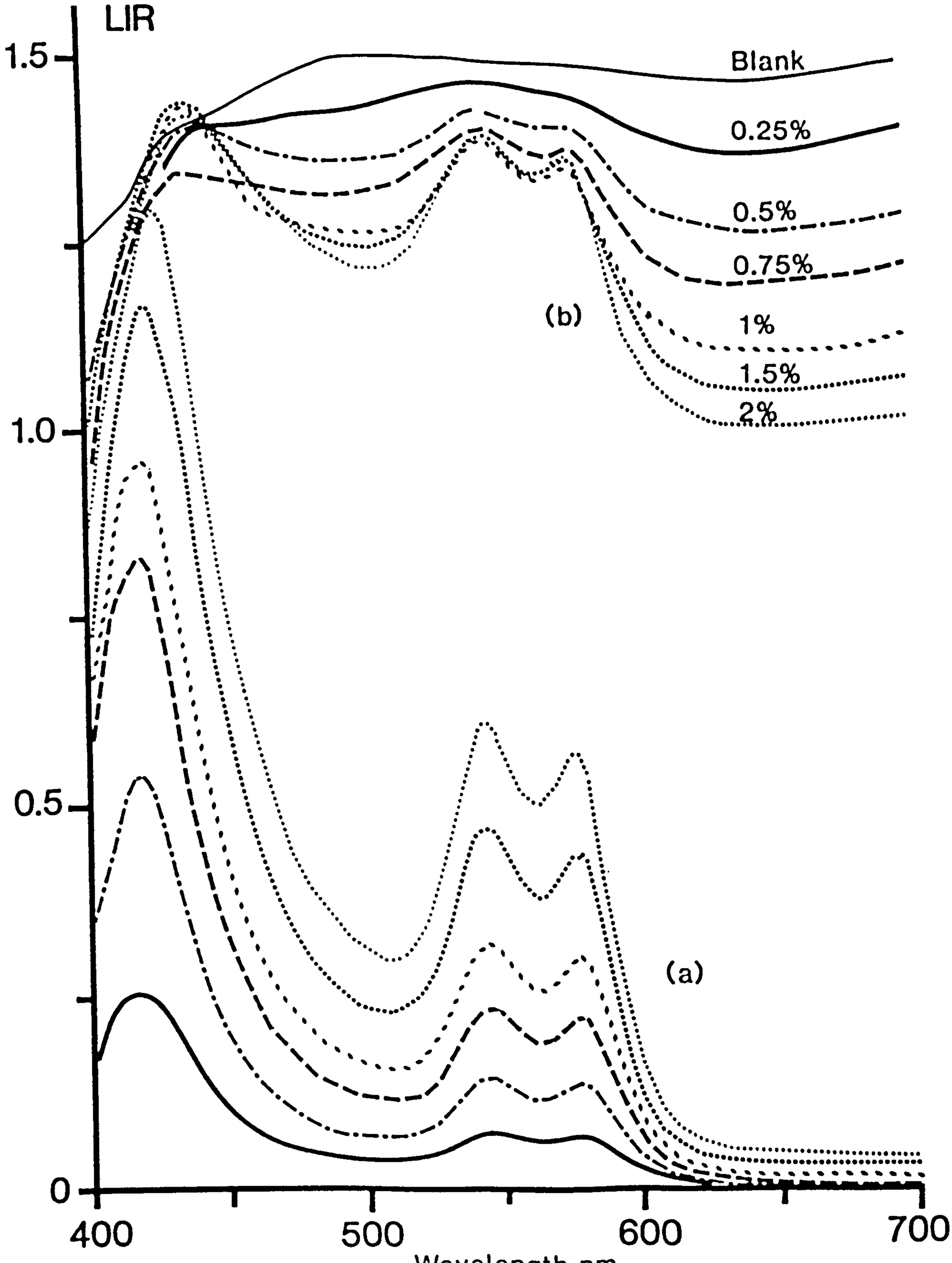

Fig. 5.3- LIR spectra of different concentration of red cells in 0.9% saline, 0.832 mm thick cuvette, a) on white tile, b) on black tile.

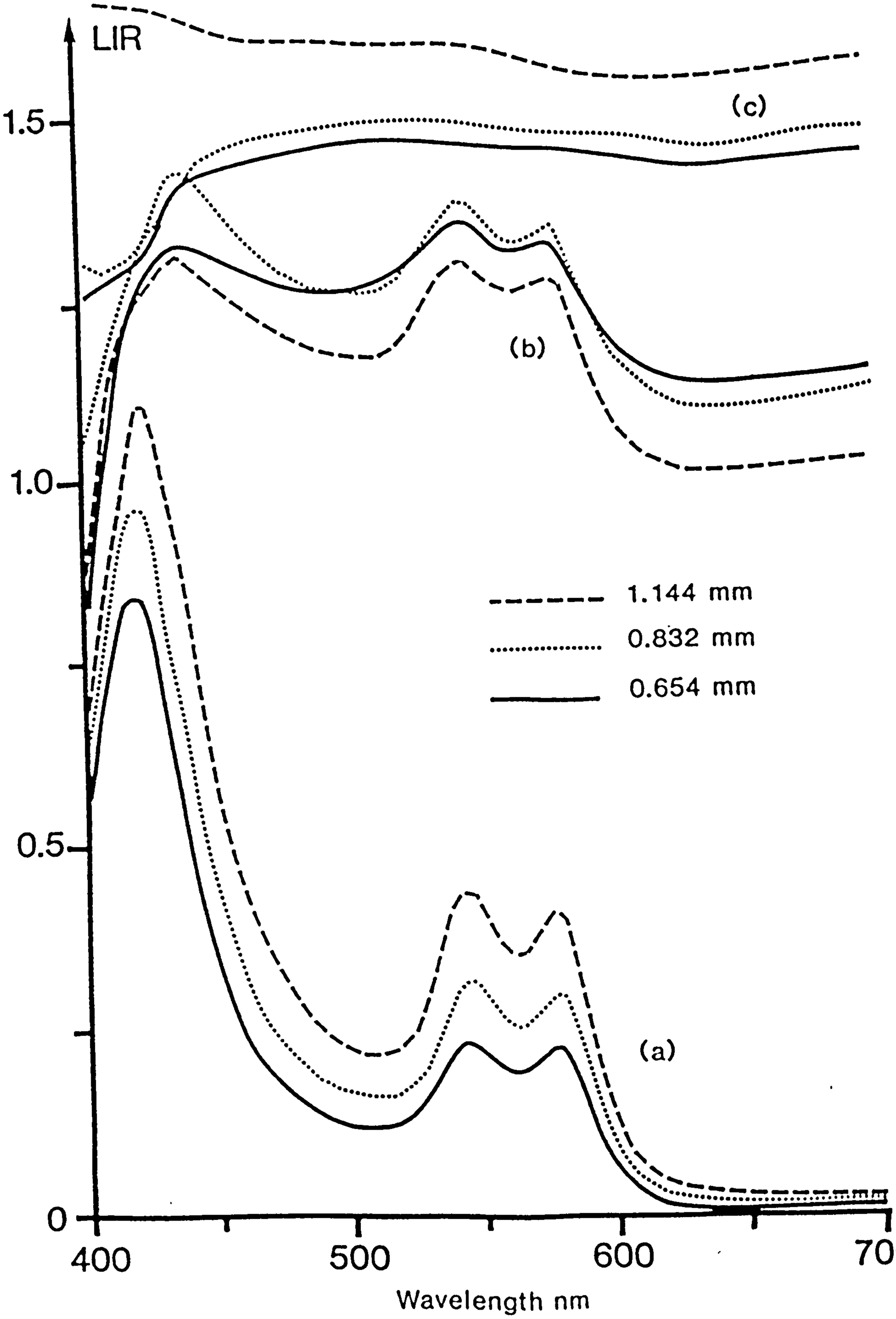

Fig. 5.4- LIR spectra of 1% red cells in 0.9% saline with different thicknesses of cuvette. Sample a) on white tile, b) on black tile, c) blank on black tile.

and the discrepancies between them are due to different heights of the reflection probe from the surface.

The haemoglobin indices calculated from reflectance spectra of blood above a white surface using eqtns. 5.2 and 5.3 are presented in Fig. 5.5 and show a near linear dependence on concentration for both indices . Although the index derived by measuring the area under the peak (eqtn. 5.2) has a steeper gradient (more sensitive) than that made by measuring the slope of the LIR spectrum between isobestic points (eqtn. 5.3), it is not independent of the oxygen saturation of blood and is more sensitive to change in oxyhaemoglobin than deoxyhaemoglobin. This dependence will be considered later in this chapter (see section 5.6).

A suspension of red cells in saline is a medium that both absorbs and scatters with the absorption occurring inside the scattering particle. The number of scattering particles will then affect the measured absorbance. To demonstrate this effect, calibration curves of absorbance (LIR) against the amount of absorber/ scatterer in the optical path at two different wavelengths, one with high and the other with low extinction coefficients, were measured using blood on a white tile. It is assumed that at wavelengths with high specific absorbance coefficient, absorption is the dominant attenuating process while at wavelengths with low specific absorbance coefficient, ie. longer wavelengths, scattering is predominant. This effect is shown in Fig. 5.6, where the absorbance at 540 nm (high specific absorption coefficient) and 670 nm (low specific absorption coefficient) is plotted against the amount (thickness x concentration) of absorber/ scatterer. The absorption of six different concentrations of red cells, was measured using three different cuvette thicknesses. The

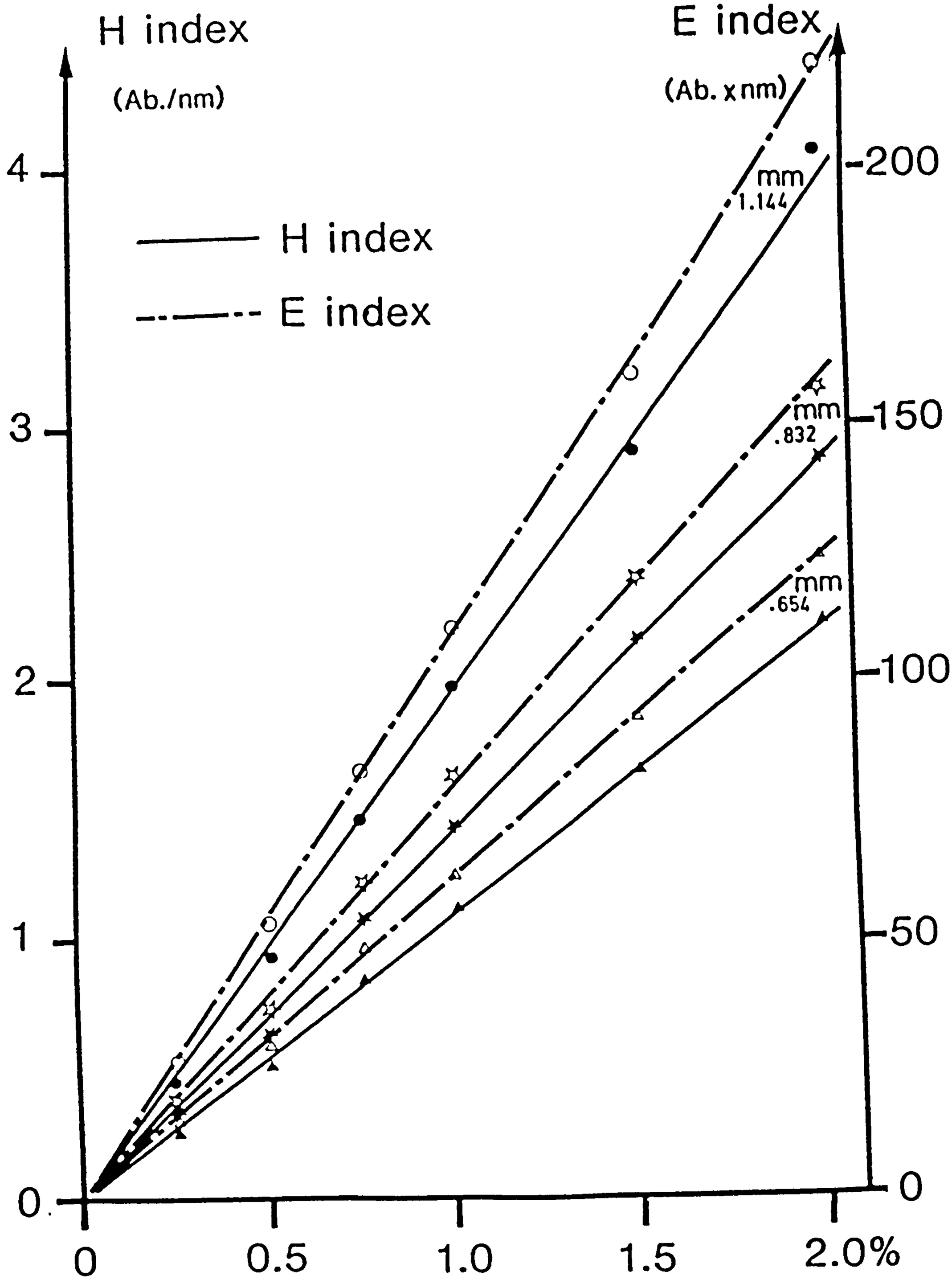

Fig. 5.5- Calibration curves of haemoglobin, H (eqtn 5.3), and erythema, E (eqtn 5.2), indices for different thickness of sample.

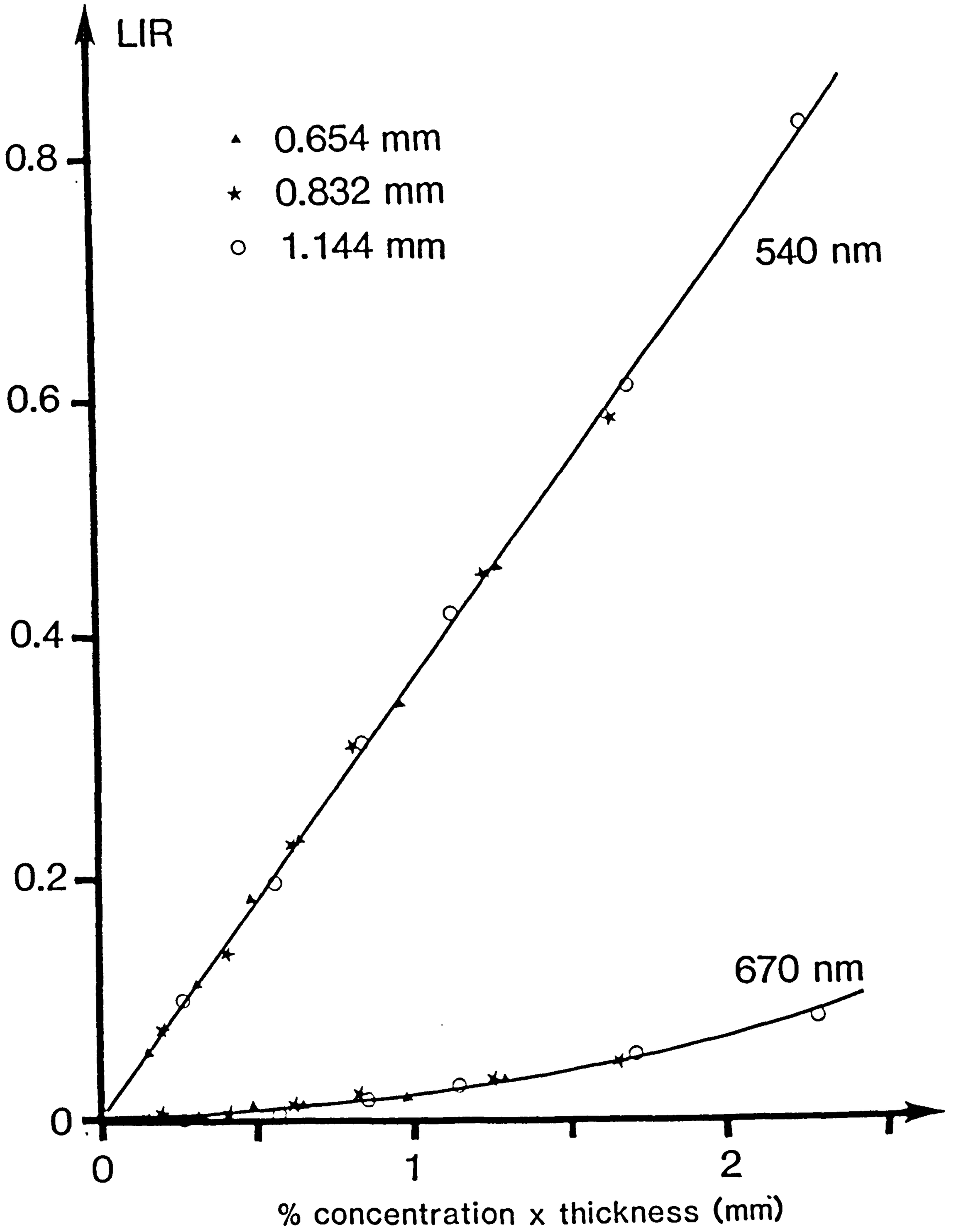

Fig. 5.6- Calibration curves of LIR of suspension of red cells in 0.9% saline, for two wavelengths against %concentration x thickness (mm).

response at 540 nm is linear but at 670 nm it increases approximately with a square law with an increasing number of absorber/scatterers. We believe this to result from a combination of the collimated nature of the incident light and the relatively greater effect scattering has on the passage of light through the sample at 670 nm, due to the decreased absorption coefficient of haemoglobin at this wavelength. Hence increasing the concentration of red cells (scattering particles) causes an increase in the effective path length of light and an almost square law increase in LIR with concentration is the result. This effect will not be seen with diffuse incident light (Fig. 5.10) or at high concentration (light becomes rapidly diffuse) because the effective path length of such diffuse light on passing through a layer is double the thickness of the layer, that is, independent of the scattering property of the sample (section 3-2-3-2).

The wavelength dependence of the relative importance of absorption and scattering of light by red cells is demonstrated when the reflected spectrum of a suspension of 2% red cells in a 1.166 mm thick cuvette is compared with the spectrum of the same concentration and thickness of haemolysed blood. As shown in Fig. 5.7, the ratio of LIR of red cells to haemolysed haemoglobin varies from 1.15 to 11.32 at 540 and 670 nm respectively. The increase in this ratio with decrease in the S.A.C. of haemoglobin confirms that at longer wavelength (670 nm), where absorption is low, the scattering of light out of the optical system by red cells is greater than its absorption by haemoglobin. This effect was observed by Kramer et al (1951) when they compared the extinction coefficient of whole blood with that of haemolysed haemoglobin. They attributed their observation to the pigments being within the cells in contrast to their uniform

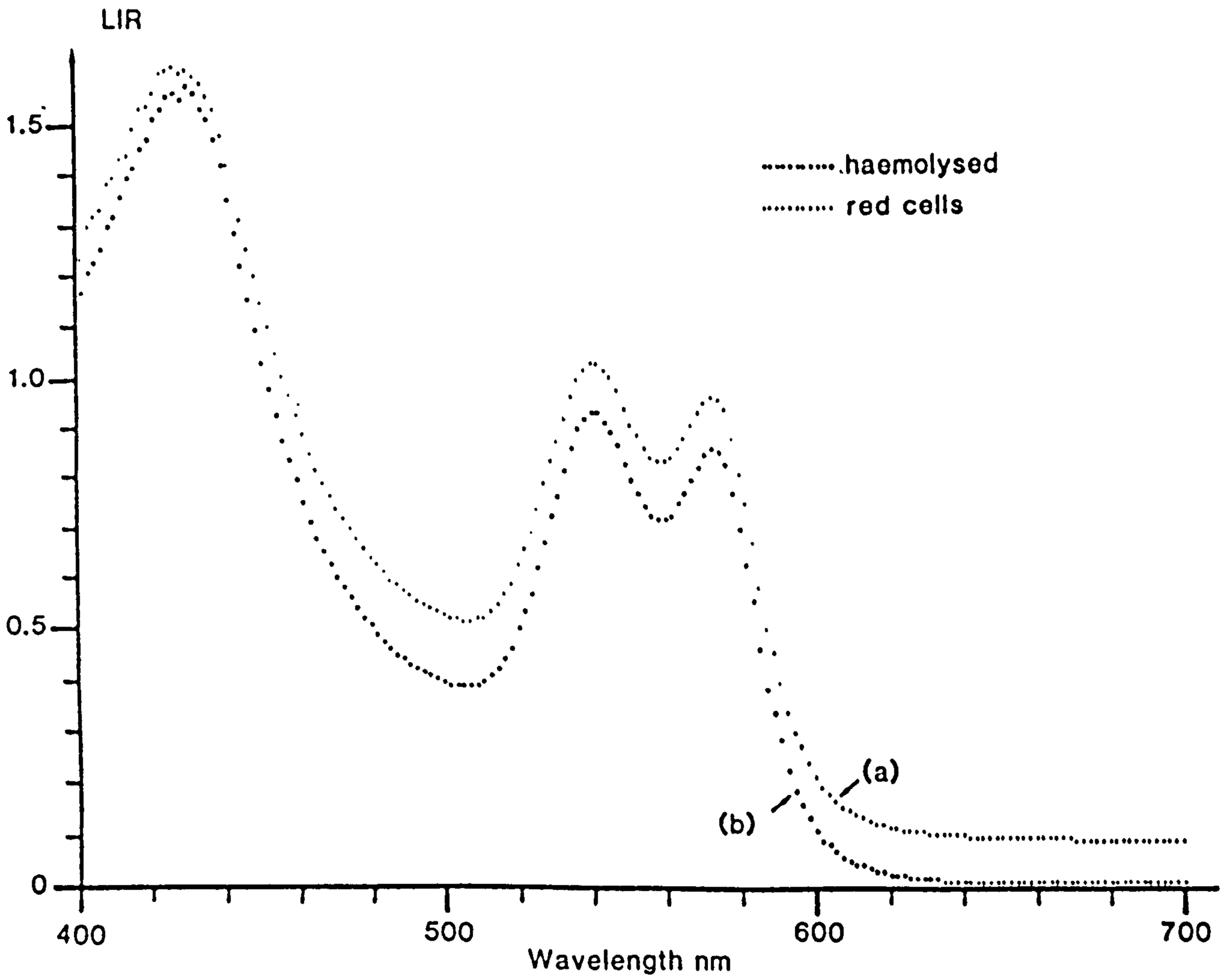

Fig. 5.7- LIR spectra of 2% red cells a) in 0.9% saline, b) in distilled water, (1.166 mm thick cuvette).

distribution in solution following haemolysis. They noted that the difference in the extinction value was influenced by the number of cells in the light path. This effect is not accommodated in the Kubelka -Munk model, in which the absorbing and scattering coefficients are independent.

5-3-2 Effect of diffused light

In order to simulate more closely the in-vivo situation, a diffusing layer rather than a clear microscope slide was used as the top cover of the cuvette. The effect of this on the haemoglobin index was then determined. Two diffusing microscope slides were made by grinding both surfaces of each of the clear microscope slides with medium carborundum powder. The reflectance spectra of a 1% solution of red cells in saline in a 0.832 mm thick cuvette was measured, first by using the diffusers separately and then by adding them together. A comparison between these LIR spectra and one taken using a clear microscope slide cover is shown in Fig. 5.8. The spectrum with two added diffusers is very similar to the in-vivo LIR spectra of reddened skin surface when the contribution of melanin has been excluded. To demonstrate the similarity, the LIR spectrum of a reddened forearm (Caucasian) is also shown in Fig. 5.8. This spectrum is displaced to higher LIR values which may be attributed to loss of light by scattering out of the optical system by the skin layers. The similarity is even closer when a decreasing base line corresponding to the melanin absorption spectrum (dashed line) is taken into account. The following conclusions can be deduced from these spectra:

a : The more diffusing the surface, the greater the reflectance. This is a "stray light" effect and may be attributed to the

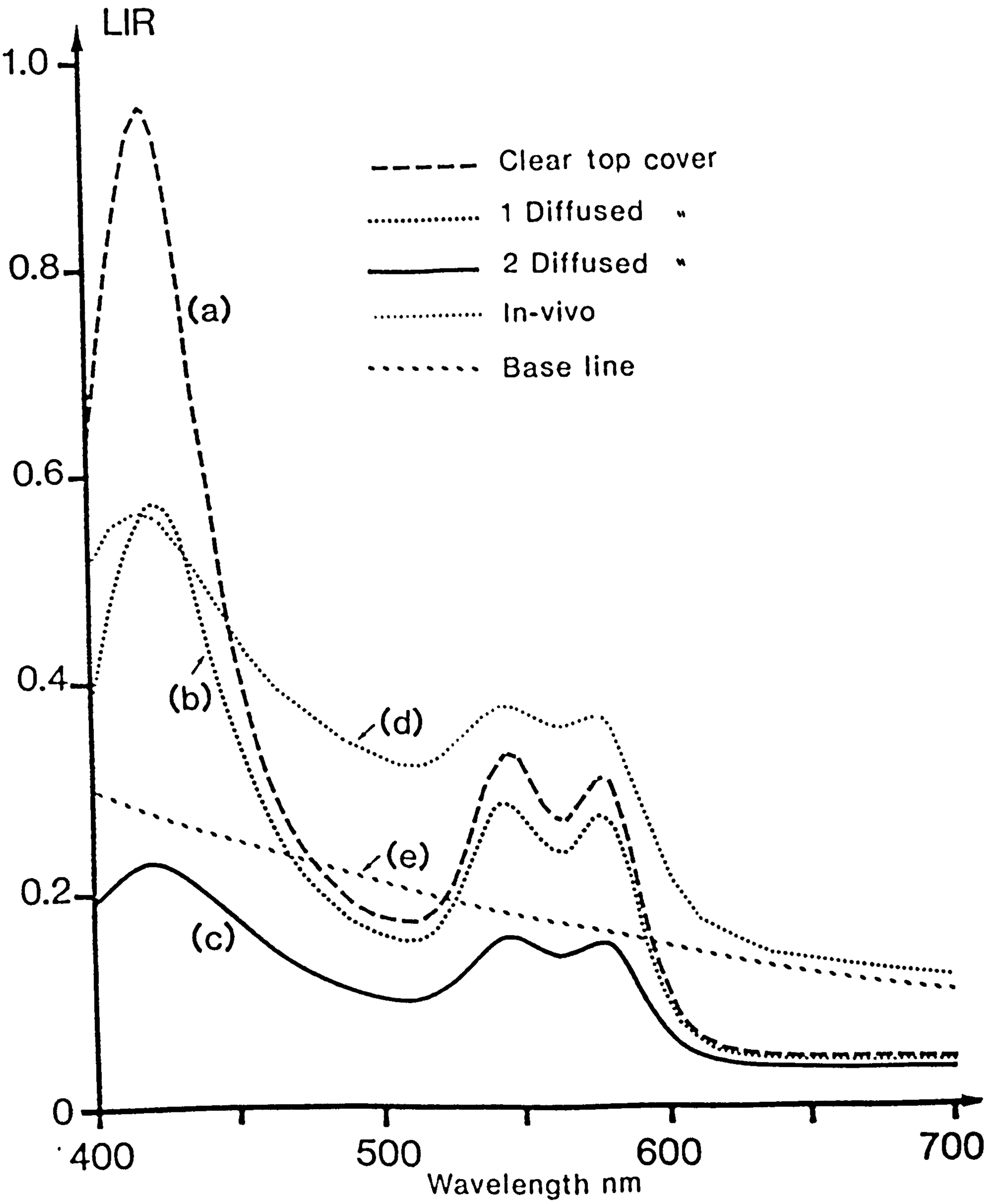

Fig. 5.8- LIR spectra of 1% red cells in 0.9% saline in 0.832 mm thick cuvette. a) with clear top cover, b) with one diffuser cover, c) with two diffuser covers, d) in-vivo spectrum of reddened Caucasian forearm, e) base line corresponding to the melanin absorption.

collection of diffusely reflected light by the signal channel from the surface of the diffuser. In this case the corrected absorbance should be calculated from the following expression:

$$\text{Absorbance} = \text{Log}\ \{(I_w - I_{dr})/(I_s - I_{dr})\} \qquad 5\text{-}4$$

where "I_s" is the intensity reflected from the sample and "I_w" is the intensity reflected from a standard white surface and I_{dr} is the diffusely reflected light intensity from the surface of the scatterer.

b : The greater the absorbance, the greater the difference between the apparent and true LIR values. This is because increases in the absorbance will decrease the intensity of the light associated with the true absorbance signal, thus the stray light I_{dr} becomes more effective in reducing the observed absorbance.

The absolute value of I_{dr} is dependent on the surface texture and the intensity of light at each wavelength. Since it is not easily measured, particularly during in-vivo measurements, a crossed polarizer method can be used to eliminate the light reflected specularly at the surface of the scatterer (I_{dr}) from the diffusely reflected signal (I_s). This method will be discussed later in chapter 6.

The accuracy of the haemoglobin index was examined using a simulated skin system with different concentrations of red cells in different thicknesses of cuvette. The reflectance measurements were repeated using a diffusing scatterer as a top cover of the cuvette. As the blood specimen was different from that used in the previous study (Fig 5.3), the absorbance spectrum of this sample was also measured in a 0.832 mm cuvette with a clear microscope slide cover so that it could be compared with that of the previous sample.

It was found that the ratio of the absorbances of the two samples at a given wavelength was constant for all concentrations. The ratio varied from one wavelength to another due to the different scattering properties of the samples. The ratio of the haemoglobin index of the first sample to the second one was 1.37 $\pm$ 0.05 for all concentrations. Calibration curves of haemoglobin indices against concentration measured under a diffusing cover using three different thicknesses of cuvette are shown in Fig. 5.9. Compared with Fig. 5.5 it can be seen, that the use of diffuse light causes non-linearity of the calibration curve at high concentration. The non-linearity also increases with increasing thickness of the cuvette. To identify the origin of this non-linearity, calibration curves of LIR at two different wavelengths, one with high, the other with low specific absorption coefficient are plotted in Fig. 5.10. In contrast to Fig. 5.6, the calibration curves at 540 nm are not linear. The nonlinearity arises from the effect of light diffusely reflected from the surface of the diffuser (I_{dr}) and back scattered light from the red cells.

The experimental results may be corrected for diffusely reflected light I_{dr} by using equation 5.4 and for red cell scattering by adapting the Kubelka-Munk theory of light transmission in scattering and absorbing media (see chapter 3). To effect the corrections, the proportion of light diffusely reflected from the surface of the diffusers (I_{dr}) and back scattered by red cells (s) per unit thickness of sample must be determined. To determine the light diffusely reflected from the surface of the diffuser (I_{dr}) as shown in Fig. 5.11a, initially the reflectance spectrum of saline on the black tile was measured with the diffuser microscope slide as the top cover of the cuvette.

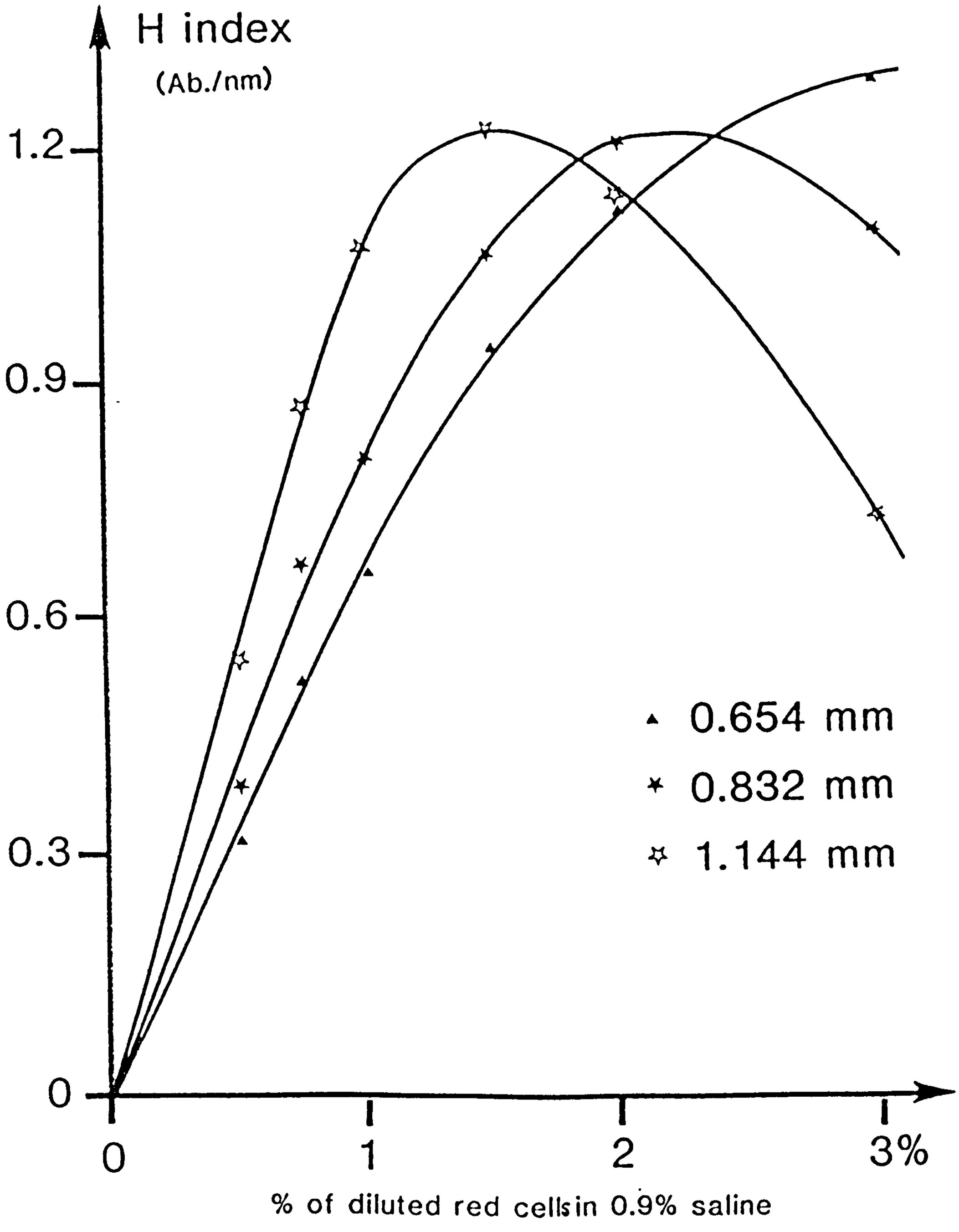

Fig. 5.9- Calibration curves of the haemoglobin index measured with diffused light, at three cuvette thicknesses.

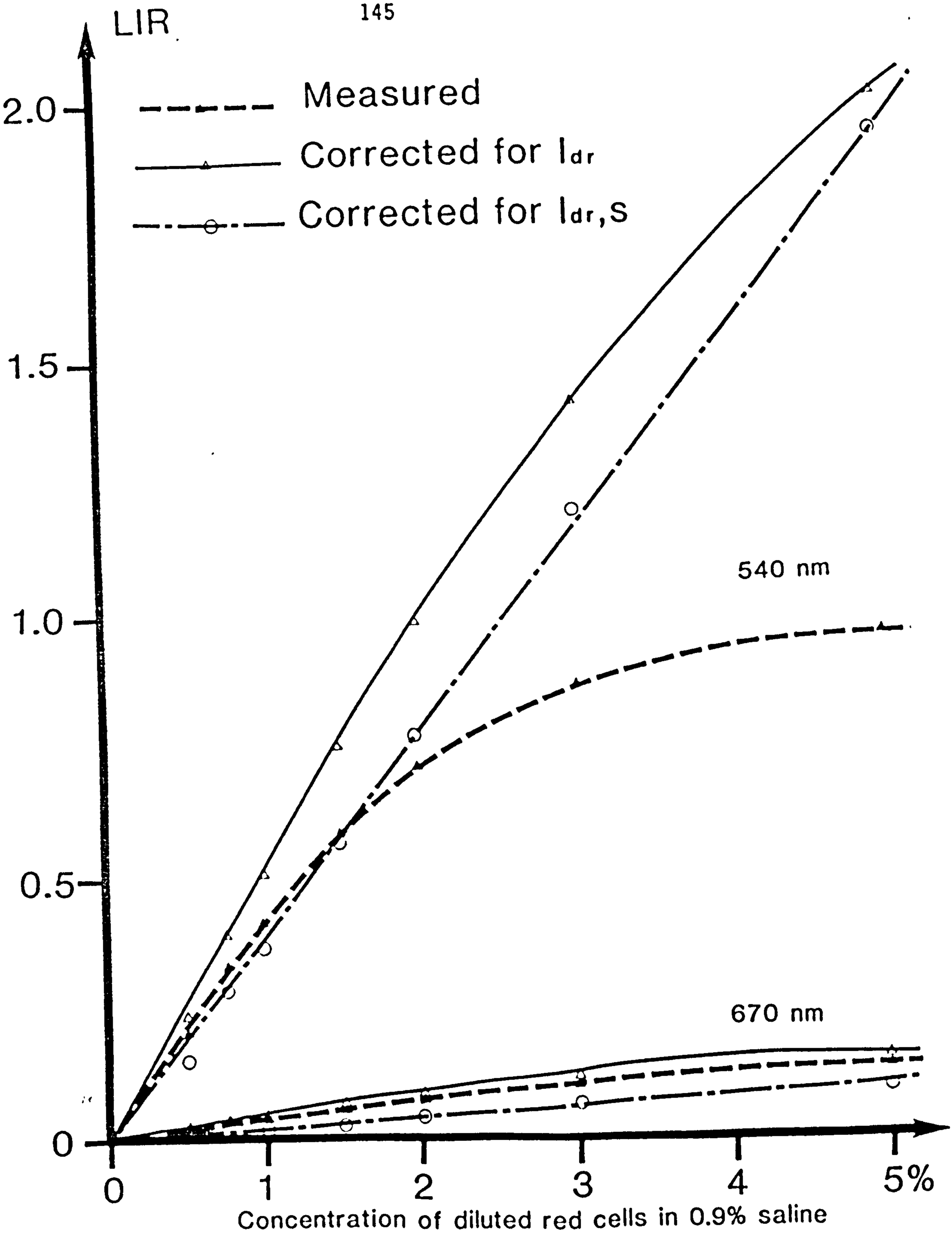

Fig. 5.10- Calibration curves of the measured, corrected for I_{dr}, and corrected for I_{dr} and scattering in a sample of red cells in 0.9% saline, with 0.832 mm thickness of cuvette, at two wavelengths.

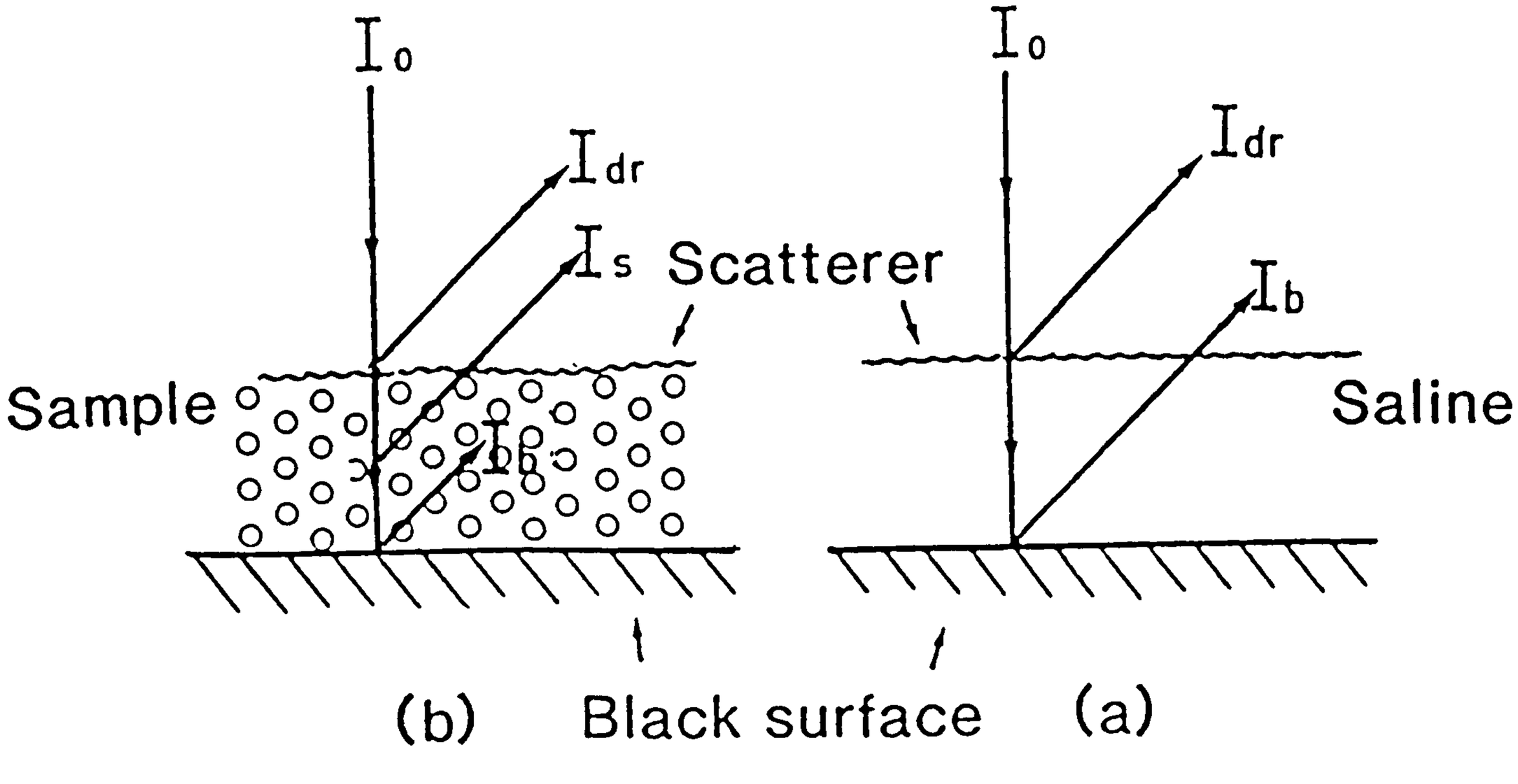

I_{dr} = Diffusely reflected light from the scatterer.

I_s = Back scattered light from the sample.

I_b = Stray light or reflected light from a black surface

Fig. 5.11- Reflected and transmitted light components from the sample and a cuvette placed on a black surface.

The stray light of the system was then calculated from the reflectance spectrum of saline on a black tile with a clear microscope slide. The amount of stray light that is attributable to the reflection of the black surface and stray light inside the reflectance probe is nearly 3% of the incident radiation. The amount of I_{dr} for three different cuvette thicknesses and at 670 nm, are calculated from the following formula:

$$I_{dr} = 10^{-A_b} - 0.03 \qquad 5\text{-}5$$

where "A_b" is the LIR value of the saline measured on the black surface at 670 nm with diffuser cover slide and 0.03 is the amount of stray light. The results are tabulated in Table 5.1. The first figure of I_{dr} (12.42%) for the thicker cuvette is more than the others (10.24%) and may be due to slight differences in the scattering properties of the diffusers.

The light back scattered by the red cells can be determined by measuring the light reflected from different samples on the black tile (Fig. 5.11b) and subtracting the results from the I_{dr}. The amount of back scattered light per unit thickness per unit concentration of red cells at 670 nm is calculated from the following formula:

$$\begin{matrix}\text{\%back scattered light} \\ \text{per mm thickness} \\ \text{per \%concentration}\end{matrix} = \frac{(10^{-A_s} - I_{dr})}{c.t} \times 100 \qquad 5\text{-}6$$

where "A_s" is the LIR value of the sample with the thickness "t" and concentration "c", measured on the black surface at 670 nm with diffusing cover slide. The results for three thicknessess and six different concentrations are also presented in Table 5.1. These

Table 5.1- Percentage of back scattered light per unit thickness per unit % concentration of red cells at 670 nm and diffusely reflected light from the surface of a diffusing microscope slide.

thickness mm \ red cell dilution %	0.5	0.75	1.0	1.5	2.0	3.0	% I_{dr}
1.144	1.95	2.65	2.12	1.18	1.59	1.65	12.42
0.832	2.03	2.03	1.84	1.74	1.62	1.57	10.26
0.654	2.22	2.37	1.85	1.73	1.66	1.23	10.22

results show that the back scattered light per unit thickness of cuvette and per unit concentration of red cells at 670 nm is nearly constant. Since the specific absorption coefficient of haemoglobin at 670 nm is not zero, these values tend to decrease for higher concentrations. Therefore the mean of the first three concentrations shown in Table 5.1, was chosen as being representative of the proportion of back scattered light found in the most common experimental condition. This is 2.12% $\pm$ 0.247 of incident light per millimetre thickness per unit %concentration of red cells. This value will change in different blood samples arising from variation in the red blood cell count (RBC).

Figure 5.10 shows the concentration dependence of the LIR of blood at 540 and 670 nm corrected for the light diffusely reflected from the surface of the scatterer (I_{dr}), and for the back scattering from red cells. Comparison of these results with the theoretical predictions made in chapter 3 (Fig. 3.9) shows that back scattering by red cells at 540 nm resembles the condition in Fig. 3.9b, ie relatively high absorption coefficient, and that at 670 nm is similar to Fig. 3.9c, ie low absorption coefficient. The presence of back scattering at 670 nm causes the LIR to be greater than the true absorption by haemoglobin. The difference between them, which increases as the concentration increases, may be attributed to loss of light by scattering in the sample. At 540 nm and low concentrations the difference also increases with concentration, but for concentrated suspensions it decreases due to absorption of the back scattered light. The calibration curves of haemoglobin indices become linear when calculated from the LIR values corrected for I_{dr}. The corrected haemoglobin indices are presented in Fig. 5.12.

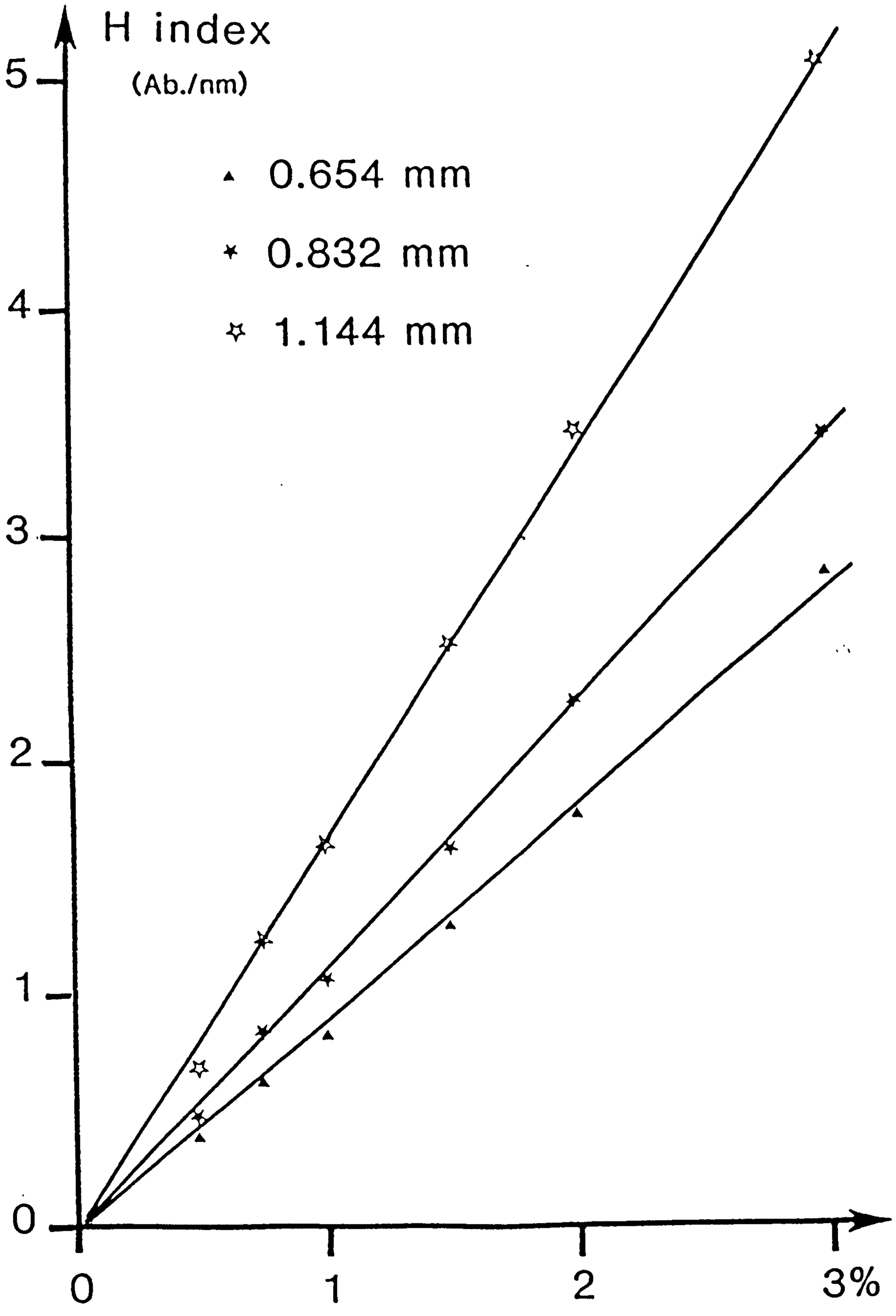

Fig. 5.12- Calibration curves of the corrected haemoglobin index (for I_{dr}) measured with diffused light, at three cuvette thickness.

5 - 4 Measurement of blood oxygenation

5-4-1 Literature review on the oxygen saturation of blood

The measurement of oxygen saturation has been reviewed in general terms earlier in this thesis (chapter 2.2.2). The technique to be used in this work, spectrophotometry, will now be examined in greater detail. Photometric measurement of oxygen saturation was developed following investigations of the absorption spectra of haemoglobin and oxyhaemoglobin (Drabkin et al (1932) and Horecker (1943)). The latter measured the absorption spectra of haemoglobin and its derivatives in the visible and near infra-red regions (400 - 1000 nm) using a laboratory constructed automatic recording spectrophotometer with a narrow band pass (0.7 to 1 4 nm over the whole spectrum). Brinkman et al (1938) and Jonxis (1938) used the difference in extinction coefficients of oxygenated and reduced haemoglobin at a single wavelength to determine the degree of oxygen saturation. As light sources, Brinkman (1938) employed a neon lamp (600 to 700 nm) and Jonxis (1938) a mercury lamp (436 nm). In both methods the samples were first haemolysed and the absorption of a thin layer (0.02 mm for Jonxis (1938) and 1.2 mm for Brinkman (1938)) was measured. The oxyhaemoglobin was then completely reduced by means of sodium hydrosulphite and the absorption of the sample measured again. The second measurement gives the amount of haemoglobin; while the first is also dependent upon the oxygenation of the sample. By knowing the ratio of the extinction coefficients of reduced to oxy haemoglobin, and by measuring the absorbance of the untreated and reduced sample, the oxygen saturation can be deduced.

Goldie (1942) and Millikan (1942) reported a method of measuring oxygen saturation of blood by means of bichromatic photometric

colorimetry of the intact human ear. Goldie used a system composed of two photocell-amplifiers with red and blue filters in front of the photocells. He found that the ratio of the photocell output currents remained constant for any given oxygen saturation irrespective of changes in the quantity of blood. For calibration of the instrument, a series of samples of known oxygen saturation were used so that a scale reading directly in oxygen saturation could be constructed. Millikan used the same method with red light (620 to 680 nm) as a colour which is sensitive to oxygen saturation and a green filter (Wratten No. 61) to select three isobestic points of oxy and reduced haemoglobin. When the Millikan oximeter was used in-vivo, compensation for the amount of ear tissue and blood in the arterial path was achieved by adjusting the instrument to indicate a known value of saturation (usually 98 to 100% when the subject was breathing air or 100% oxygen) while the earpiece was in place on the ear. The accuracy of the device, as determined by gas analysis of arterial blood samples, was from 3 to 8% for 100% to 60% saturation. Extensive calibration studies with the Millikan oximeter among white and coloured persons were carried out by Montgomery et al (1948). It was concluded that the oximeter readings were only of quantitative value in indicating changes in arterial oxygen saturation. Additionally it has been pointed out (Wood et al 1949) that films of whole blood approximately 1 mm thick transmit practically no light of wavelengths shorter than 600 nm, and the normal human ear has similar characteristics. For this reason the operation of the oximeter is best based on the red and near infra red rather than on the red and green portion of the spectrum.

Wood et al (1949) described an oximeter which could be used to

measure the absolute value of oxygen saturation and continuously follow the changes of the arterial oxygen saturation from a human ear lobe. This is accomplished by simultaneous measurement of the transmission of red and near infra red light through the normal heated-flushed ear and the squeezed bloodless ear. The light transmission of the blood alone in these spectral regions can be calculated and in turn the percentage of oxygen saturation of the blood can be derived.

In-vitro studies of oxygen saturation as well as the in-vivo study have been made using haemolysed haemoglobin or by flowing whole blood through a thin cuvette. A linear relationship between the oxygen saturation of haemolysed red cells and the ratio of the optical density of the sample at 660 to that at 805 nm was reported by Gordy and Drabkin (1957). They used a modified cuvette 0.7 mm thick with a Beckman DU spectrophotometer. They also reported that the percentage oxygen saturation as determined by both the direct spectrophotometric technique and an indirect gaseometric method agreed to within 2 percent. This latter method required haemolysis of the blood and thus necessitated an additional stage of handling of the blood sample under anaerobic conditions.

Methods for the determination of oxygen saturation based on the light absorbance of whole, non haemolysed blood have definite advantages. However, when haemoglobin is contained within cells, the relationship between optical density and haemoglobin concentration or sample thickness is not linear. Despite these difficulties successful optical methods for determining the oxygen saturation of whole blood in-vivo have been devised.

In the present study reflectance spectrophotometry in the visible

waveband is used to measure the oxygen saturation of blood. Due to the limited depth of penetration of visible radiation, in-vivo application of this method can provide information only from superficial blood.

5-4-2 Oxygenation index

Since the presence of an increasing proportion of reduced haemoglobin in the oxyhaemoglobin will modify the absorbance spectrum from the double peak of oxyhaemoglobin to the single peak of reduced haemoglobin, the state of oxygenation can be determined by measuring the gradient of the absorption spectrum in the neighbourhood of the peaks. Any method for determining the oxygen saturation of blood based on the differences in the absorption spectra of oxy and reduced haemoglobin should be independent of the amount of blood observed. According to Beer's law, the absorbance at each wavelength of the absorption spectrum of haemoglobin is proportional to the amount of haemoglobin. To obtain an index of oxygenation, first it is necessary to have an index proportional to the total amount of haemoglobin and independent of the state of oxygenation , so that the oxygenation index can be corrected for the amount of blood. The erythema index devised by Dawson et. al (1980) could not be used for this purpose because of its dependence on the oxygen saturation of the sample (see section 5.6). The new haemoglobin index which is based on measuring the slope of the LIR spectrum between isobestic points (eqtn. 5.3) can, however, be used for this purpose.

Typical absorbance spectra of 2% red cells in a 1.166 mm thick cuvette with different levels of oxygenation are shown in Fig. 5.13. The slopes of the curves between 544 -558.5 and 558.5 -573 nm are proportional to the amount of haemoglobin and to the level of

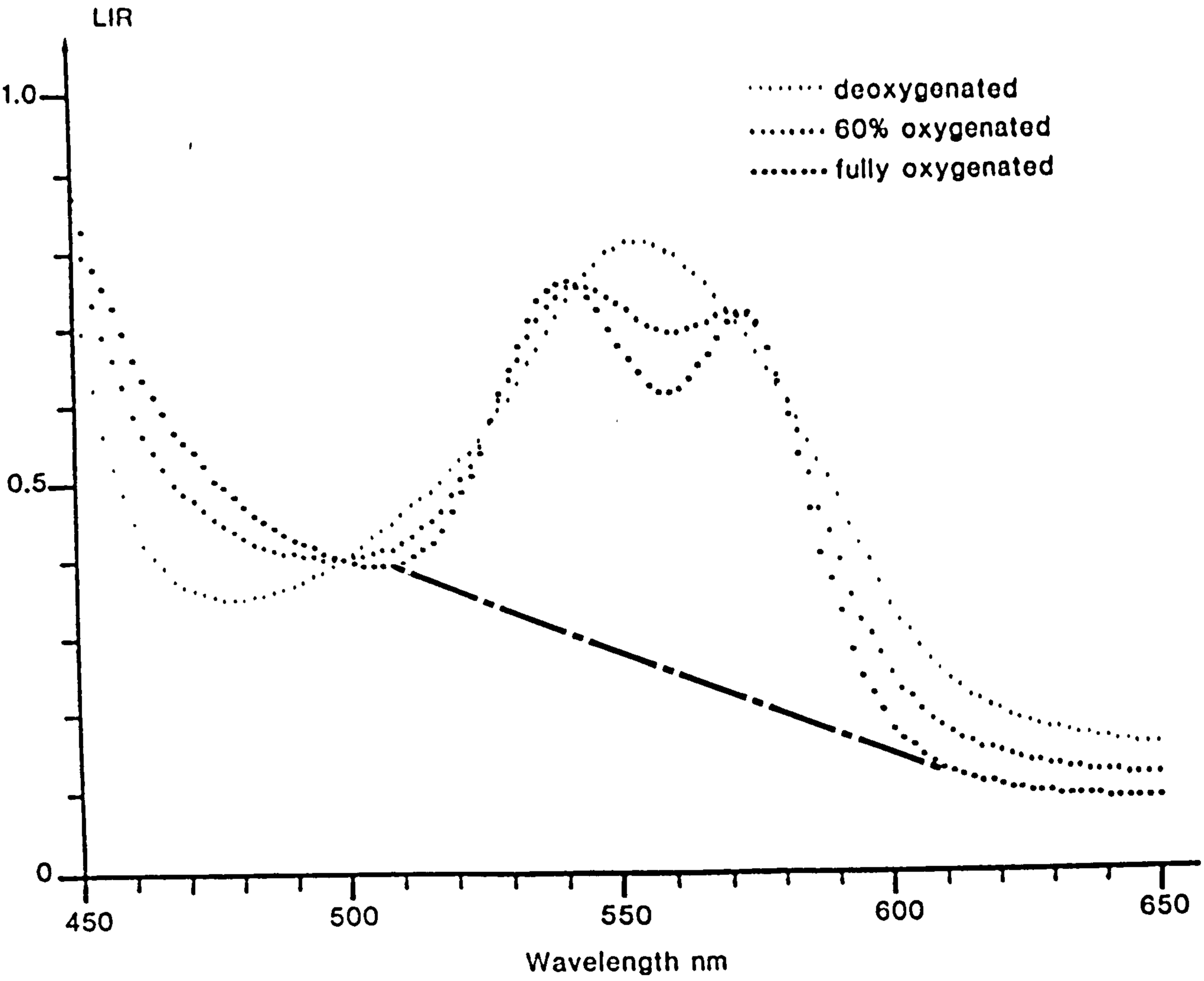

Fig. 5.13- LIR spectra of 2% red cells in 0.9% saline and a 1.166 mm thick cuvette at different levels of oxygenation.

oxygenation. An oxygenation index, OX, which is independent of the haemoglobin concentration is achieved by dividing each slope by the haemoglobin index as in the following expression:

$$OX = \{(A_{573}-A_{558.5})/14.5 - (A_{558.5}-A_{544})/14.5\} \times 100/H \qquad 5\text{-}7$$

"A_x" is the absorbance (LIR) value at wavelength "x" nm, ie 573, 558.5, and 544 nm, and "H" is the haemoglobin index as described in equation 5.3. Subtraction of two slopes, as is also incorporated in the haemoglobin index, cancels out any spectral contributions with a constant slope e.g. melanin, and is necessary for in-vivo oximetry of skin. OX is a positive value for the double peak of oxyhaemoglobin and negative for the single peak of reduced haemoglobin. In order to convert the values of oxygenation index into percentage oxygenation, the most positive value of OX from fully oxygenated haemoglobin was assumed to be 100% and the lowest negative value from reduced haemoglobin to be 0%. An index value of 1.149 was observed to be the most positive value from a sample of 2% fresh red cell in plasma, when it was exposed to air, and the value of -0.821 as the lowest negative value from the same sample when it was exposed to a mixture of nitrogen gas with 5.2% CO_2 for several minutes in a sealed container. Hence the percentage of oxygenation or oxygen saturation can be calculated from the following formula:

$$Sa\ O_2 \text{ (oxygen saturation)}\% = (OX + 0.821)\ 100/1.97 \qquad 5\text{-}8$$

In this method of measuring oxygenation only the two extreme points of fully oxygenated and fully reduced haemoglobin have been used for calibration. It is assumed that OX is linearly proportional to the state of oxygenation. This assumption is theoretically based on

the capacity of haemoglobin for binding with 4 oxygen molecules as described in Chapter 2 (section 2-2-1).

The validity of the assumption was tested experimentally by measuring the Oxygen Dissociation Curve (O.D.C.) by means of the reflected spectrometer and comparing it with published O.D.C. curves.

5 - 5 Measurement of the oxygen dissociation curve

The O.D.C. of haemoglobin is the plot of percentage saturation of haemoglobin against the partial pressure of oxygen. To obtain this curve, an experiment was set up as shown in Fig. 5.1. A small amount of diluted blood (2% red cells in plasma) was placed in a 500 ml flask and the oxygenation was changed by passing different mixtures of oxygen, nitrogen and carbon dioxide gases through the sample. The percentage saturation was then measured by the reflectance method (eqtn. 5.8) at several different partial pressures of oxygen in the mixture of gases. Since the O.D.C. is dependent upon temperature and the partial pressure of CO_2, the sample was kept at 37 °C by placing the flask in a thermostatically controlled water bath at 37 °C, and the partial pressure of CO_2 in the mixture of gases was kept constant by using two cylinders of air and nitrogen gas each containing 5.2 % CO_2. The proportions of air and nitrogen were monitored by two rotameters, the percentage of oxygen was measured by an oxygen gas analyzer machine. The mixture of gas with a known oxygen tension was then passed through the sample for at least 5 minutes. The sample was then taken into the reflectance cuvette and its reflection spectrum measured. The oxygen saturation of the sample was then calculated by means of equations 5.7 and 5.8. The pH and pCO_2 of the sample were measured with a blood gas analyser at the beginning and end of the

experiment, and were found to be constant at pH 7.33 and pCO_2 40 mmHg.

The results of eight measurements at different oxygen tensions are plotted in Fig. 5.14. The curve shows a good agreement with the O.D.C. of haemoglobin at pH 7.4 and 37 °C and exposed to a pressure of 40 mm Hg of CO_2, which was published in 'Respiratory Physiology _ The essentials' by West (1974). The oxygen affinity of haemoglobin is dependent on temperature, pCO_2 and pH, so that any fall in pH, rise in pCO_2 or rise in temperature will shift the O.D.C. laterally. The measured points are shifted slightly to the right and this may be attributed to a lower pH of the sample. During the transfer of the sample from the flask to the reflectance cuvette, the sample passes through tubes which are not at 37 °C and this causes a slight lowering in the temperature of the sample.

In order to assess the effect of temperature on the O.D.C. the oxygen saturation of a sample at a pO_2 of 30 mmHg was measured under the standard conditions. The sample, sample holder and connecting tubes were then warmed to above the temperature of the water bath by exposing to hot air from a hair drier, and the oxygen saturation again measured. The sample and apparatus were next cooled by exposing to cool air and the oxygen saturation again measured. These results are shown in Fig. 5.14 as the points identified as 'h' (heated) and 'c' (cooled). By warming the sample, the oxygen affinity of haemoglobin is decreased and some oxygen was released into the sample, as a result the oxygen saturation of the sample is decreased. By cooling the sample, the oxygen affinity is increased and the oxygen molecules again are combined with the haemoglobin and the oxygen saturation is increased, but the oxygen saturation is less than that measured before

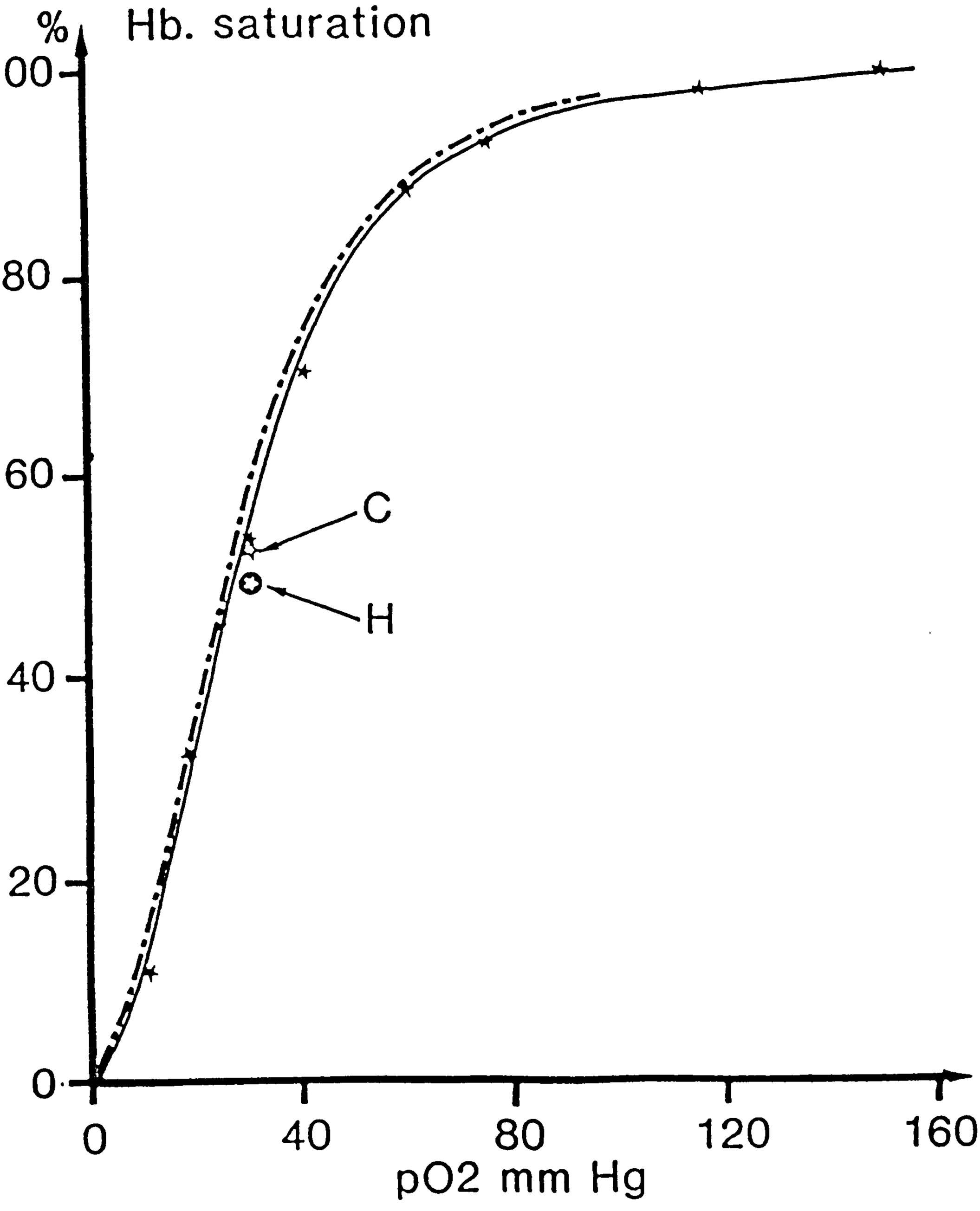

Fig. 5.14- Comparison between published (dashed line, pH=7.4, pCO_2=40 mmHg, 37 °C, West 1974) and measured (full line, pH=7.33, pCO_2=40 mmHg, 37°C) oxygen dissociation curves of haemoglobin. (points H and C show the oxygen saturation of the sample when warm (>37 °C) and cool (<37 °C), see text)

warming the sample. This is because the released oxygen molecules dispersed throughout the sample and did not recombine within the time period of the experiment. As the system is sealed and the sample is withdrawn without any bubble of gas in the tubes, any decrease in temperature of the sample due to transferring it from the flask into the reflection cuvette, while increasing the oxygen affinity of the haemoglobin, will not change the oxygen saturation of the sample as no more oxygen is available for binding to haemoglobin. During the transfer of the sample from the flask to the reflection cell the air temperature around the sample holder and connecting tubes was kept at aproximately 37 °C by blowing hot air from a hair drier. The results presented here demonstrate that the oxygenation level of red blood cell suspension can be accurately calculated from reflectance spectra using eqtns 5.7 and 5.8.

5 - 6 Dependence of the haemoglobin index on oxygenation

In theory the haemoglobin index should be independent of oxygenation, but in practice the scattering by red cells and stray light of the system have different effects on different isobestic points due to their different specific absorption coefficients. In consequence the wavelength of the isobestic points of red cells may vary from one sample to another, hence the haemoglobin index might vary slightly with changes in the oxygenation. Any variation in haemoglobin index will eventually affect the measured oxygenation index.

The dependence of the haemoglobin index on oxygenation was determined by measuring the haemoglobin indices for different oxygenated states of a sample. Data for calculating these haemoglobin

indices were taken from that obtained in the course of the experiments performed to measure the Oxygen Dissociation Curve. In this experiment the reflectance spectra of 2% red cells in a 1.166 mm thick cuvette and at different levels of oxygenation were measured. Haemoglobin indices (H) were calculated by measuring the slope of the reflectance spectrum between isobestic points (eqtn. 5.3). For comparison, the dependence of the erythema index on oxygenation was also examined. As already explained in section 5.3, erythema indices (E) are derived from the area under the haemoglobin peak (eqtn. 5.2). Both indices are presented in Table 5.2.

The average haemoglobin index is 3.02 $\pm$ 0.03 and has a coefficient of variation of 1.05%. This variation may be attributed to the effect of light scattering by red cells or stray light in the system on the observed absorbance at the isobestic points. The dependence of the erythema index on oxygenation is much greater, 257.9 $\pm$ 18.6 ie C.V. 7.2%, and thus is not suitable for use in oximetry.

In an alternative approach, the dependence of the measured oxygen saturation on the haemoglobin index was determined by measuring the apparent oxygenation of different concentrations of red cells of a sample of known oxygenation (eqtn. 5.8). Data for these calculations were taken from the reflectance spectra of different concentrations of red cells used to produce the calibration curve for the haemoglobin index (Fig. 5.5). The calculated oxygen saturation of different dilutions of red cells in 0.9% saline using three different thicknesses of sample cuvette are shown in Table 5.3. The samples were exposed to air but the oxygen saturations were less than expected. This is because the pH of the suspension of red cells in saline gradually becomes more acidic which decreases the oxygen affinity of

Table 5.2 - Haemoglobin and erythema index of different oxygenated states of 2% diluted red cells in plasma (1.166 mm thicK).

%Sa O2	0	12.8	33.0	54.8	72.3	87.5	92.2	99.9
H index	3.02	2.98	3.02	3.02	2.99	3.08	3.04	2.98
E index	227.4	235.1	248.0	259.3	264.1	283.5	278.8	267.3

Table 5.3- Oxygen saturation of different red cell concentration in 0.9% saline

thickness mm \ red cell dilution %	0.25	0.5	0.75	1.0	1.5	2.0
1.144	84.06	83.52	82.74	81.66	80.79	79.42
0.832	82.88	82.93	82.61	82.50	82.04	81.42
0.654	81.23	83.25	83.28	83.46	82.31	82.05

the haemoglobin. The average value for oxygenation, which is 82.34 ±1.102, has a coefficient of variation of 1.34%. This value is close to that measured in the first approach and represents the reproducibility of the system. It therefore can be concluded that the inter dependence of haemoglobin index and oxygenation is less than these figures, and is negligible.

5 - 7 Tests of practical accuracy

Two different approaches were used to assess the practical accuracy of the instrument. In one, the reflection and transmission spectra of a sample were compared, and in the other the specific absorption coefficient of oxy and deoxy haemoglobin were measured and compared with the published curves. The first approach uses the same instrument for measuring reflectance and transmission, but with different geometries of light illumination and collection and different path length of light through the sample.

5-7-1 Comparison of reflection and transmission spectra of a sample

The samples, suspensions of red cells in saline or plasma, are scattering media, and for measurement of their transmission spectra an integrating sphere should be used. However, an alternative method is possible using a perfect diffuser, as described by Bruls (1982). In this experiment a perfect diffuser (Comar 25 DO 00, Flashed opal disc), 2.5 cm diameter and 3 mm thick, is placed between the sample and the collecting fibre optics. The experimental arrangement is shown in Fig. 5.15. The surface of the sample is illuminated perpendicularly. The transmitted light flux falls on the diffuser at

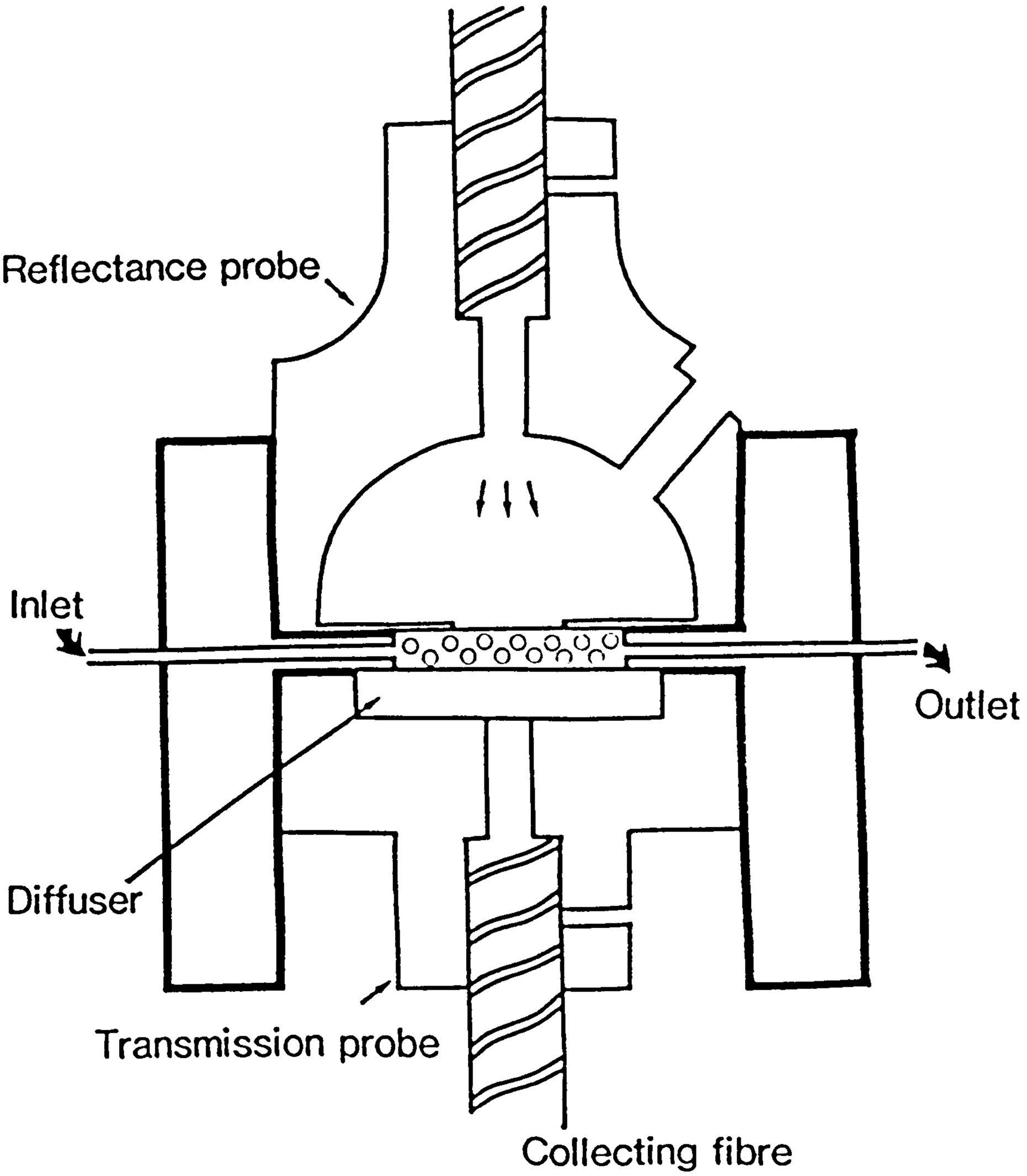

Fig. 5.15- Arrangement of an illumination and light collection system for transmission spectroscopy using a perfect diffuser.

various angles of incidence. The diffuser then transforms this flux into a completely diffuse flux. The radiant power of the flux emerging from the diffuser is proportional to the radiant power of that emerging from the sample, but does not depend on the angular distribution of the latter. In the same way, the collimated reference beam is also transformed into a diffused flux by the diffuser. As the angular distribution of the light emerging from the diffuser is the same for the sample and the reference solution, it is not necessary to measure all the light, but the constant fraction which is collected by the fibre optic is adequate. The transmission of a sample is then determined as the ratio of the measured light intensities with sample and reference solutions in the cell. By using this method, transmission spectra can be measured with the same computer program as is used for reflection spectra. In the case of transmission measurements there is no need to measure a black surface. The intensity of the diffused flux of the collimated reference beam is measured when the cuvette is filled with saline, and is stored in the computer in the same array as that where the data from the reflection of the standard white surface was kept.

Since the perfect diffuser will diffusely reflect half of the incident radiation (I_o) back and transfer half of that in a forward direction, the measured absorbance by this method is slightly underestimated. To assess the effect of that on the absorbance, assume the perfect diffuser in Fig. 5.15 reflects 50% of the incident radiation back into the cuvette. When the cuvette is filled with saline the transmitted light through the diffuser is $0.5I_o$, and when it is filled with a suspension of red cells half of the transmitted light through the sample with absorbance Ab, ($I_t = I_o \exp(-Ab)$), will be

reflected back into the sample, from which $0.5RI_t$ will again back scatter by red cells to the diffuser. Therefore, the transmitted light through the diffuser is $0.5\ I_t + 0.25\ R\ I_t$ and the measured absorbance (A_m) is calculated from the following formula:

$$A_m = \text{Log}\ \frac{0.5\ I_o}{0.5(1\ +0.5R)\ I_t} = \text{Log}\ \frac{1}{(1\ +0.5R)\ \exp(-Ab)}$$

$$= Ab\ -\text{Log}(1\ +0.5R) \qquad 5\text{-}9$$

where R is the fraction of light scattered back by the red cells. Figure 5.3b shows that for 2% red cells on a black surface, R is about 4.5% of the incident radiation at 540 nm and 10% at 670 nm. These values can reduce the measured absorbance by 0.01 at 540 nm and 0.02 at 670 nm. As R is almost the same for all isobestic points, the lower estimate of the absorbance will not affect the haemoglobin index measured by this method.

To determine the reflection and transmission spectra of red cells, a suspension of 2% red cells in saline was prepared. The sample was kept in a 500 ml sealed flask in a water bath at 37 ^{o}C. Different levels of oxygenation were produced by changing proportions of air and nitrogen gas in the atmosphere of the flask as described in section 5.1.

The computer program was modified to give two more options for measurement of reflectance and transmittance spectra. The reflected light intensity from a white surface, the stray light from a black surface, and also the intensity of the light transmitted through the diffuser with the cuvette filled with the saline were first measured and stored in the computer. This information was needed in the

reflectance and transmission measurements of LIR and absorbance spectra respectively. The reflectance spectrum of a sample was measured by setting the program on reflectance, fixing the light collecting fibre in the reflection probe and placing a white surface beneath the cuvette containing the sample. Transmission spectra of the same sample were measured by changing the program option into the transmission mode, replacing the diffuser and fixing the collecting fibre in the transmission probe as shown in Fig 5.15. The reflection and transmission spectra of the sample at different oxygen partial pressure were measured by alternating the system between its reflection and transmission modes. Figure 5.16 shows the transmission and reflectance spectra of the oxy and reduced samples measured in a 1.166 mm thick cuvette.

Haemglobin indices were calculated from both spectra and are presented in Table 5.4. In this Table the partial pressure of oxygen in the flask is also shown. The ratio of the haemoglobin index of a sample calculated from its reflectance spectrum to that calculated from its transmission spectra is approximately constant, 2.05 ± 0.15. The experimentally derived ratio of the geometrical path length of light in reflection to that in transmission, when measured with the same geometry and a clear solution of $CuSO_4$, ie no scattering particles, is 2.3.

The difference in the ratios can be explained by the fact that the reflected signal is composed of two components, one is the light back scattered by the sample before reaching the white surface, and the other is the light transmitted through the sample which is reflected back from the white surface behind the sample. The geometrical path length of the second component is 2.3 times as great

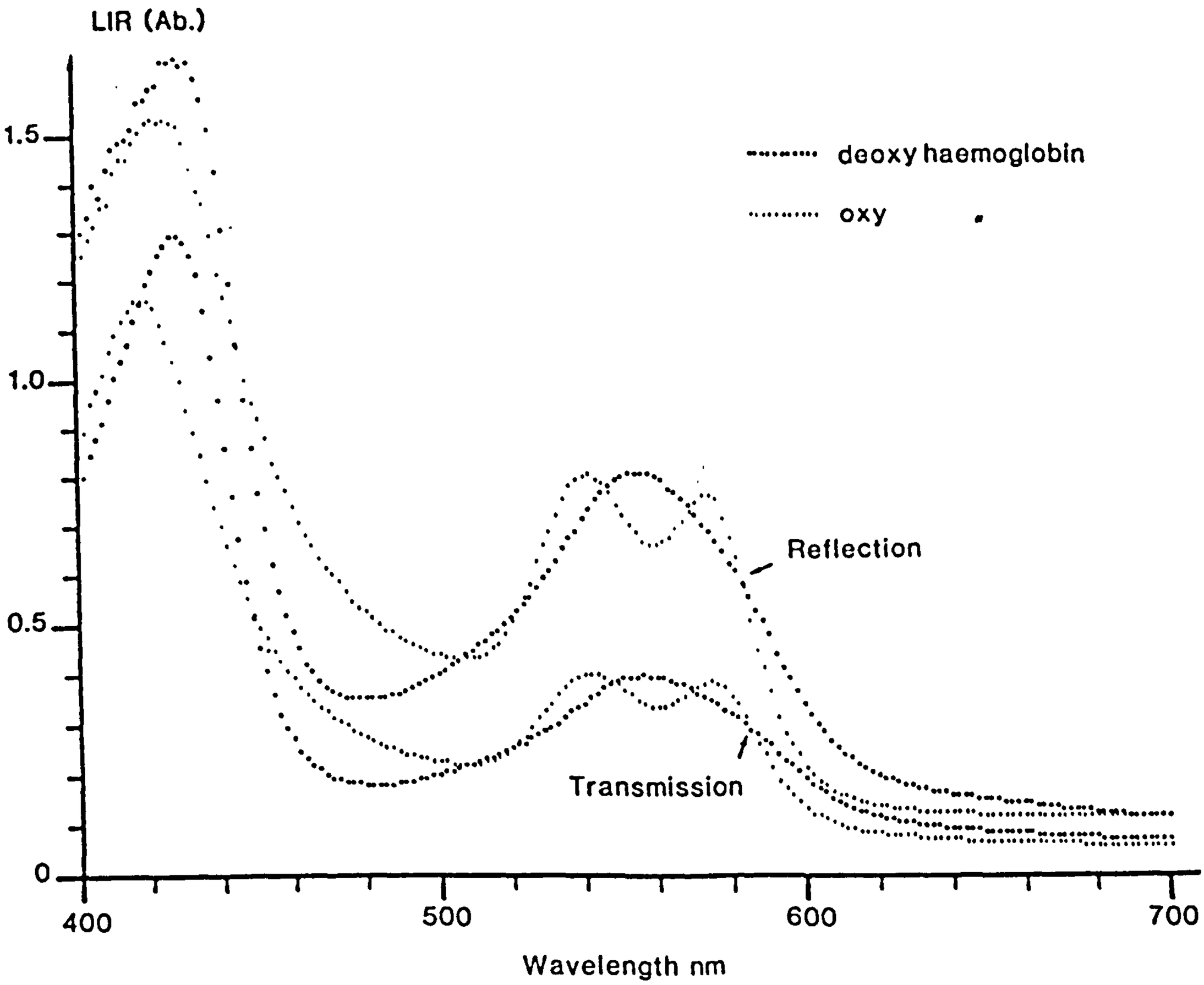

Fig. 5.16- LIR (reflection) and absorption (transmission) spectra of 2% red cells in 0.9% saline (oxygenated and reduced) in a 1.166 mm thick cuvette.

Table 5.4- Haemoglobin indices computed from reflectance and transmission spectra of samples of 2% red cells in 0.9% saline at different oxygen partial pressure using a 1.166 mm thick cuvette.

Oxygen partial pressure mmHg	H index (reflection)	H index (transmission)
0.2	2.31	0.98
9.1	2.18	1.01
19.0	2.27	1.06
31.9	2.19	1.07
42.5	2.26	1.13
62.3	2.24	1.14
85.5	2.16	1.15
159.6	2.13	1.13

as the path length of the transmitted light, but the path length of the first component is dependent upon the scattering and absorption coefficients of the sample. The contribution of the first component in the reflected signal causes the mean effective path length of light in the sample to decrease. The effective path length in the reflectance measurement can be quantified in terms of the geometrical path length by the following formula:

$$\% \text{ of effective path length} = \frac{LIR}{Ab.} \times \frac{t}{2.3t} \times 100$$

$$= 43.5\ LIR/Ab. \qquad 5\text{-}10$$

where "t" is the thickness of the cuvette. The ratio of the LIR to transmitted absorbance at two different wavelengths from the data presented in Table 5.4, when measured at the haemoglobin peak 540 nm (high absorption coefficient), is 2.026 ± 0.072, while at a longer wavelength (670 nm) where the specific absorption coefficient of haemoglobin has decreased nearly one hundred fold the ratio has decreased to 1.587 ± 0.185. These results show that the effective path length in a suspension of red cells is 69% and 88% of the geometrical path length at 670 nm and 540 nm respectively. A decrease of 97.5% in the absorption coefficient caused the transmittance to increase by a factor of 1.8 and the reflectance by a factor of 3.5 and thus produced a greater decrease in LIR than absorbance.

Since the dimensions of red cells (7 to 8 μm in diameter) are 10 to 12 times greater than the wavelength of visible light, scattering in a suspension of red cells is believed to be Mie scattering and independent of wavelength. Hence a decrease in the LIR/ Absorbance ratio is attributable to the decrease in the absorption coefficient.

The effective path length of light in the reflectance spectroscopy of red cell suspension is determined by the scattering and absorption coefficients of the sample; it will decrease by increasing the former or decreasing the latter.

The haemoglobin index derived from the transmission spectrum (Table 5.4) increases slightly with increasing oxygen saturation of the sample. This may be due to a slight shift in the isobestic points in the transmittance spectrum compared with those in reflectance (Fig. 5.16). This might be due to different characteristics in the forward and backward scattering properties of the oxygenated and reduced red cells. Flock et al (1987) reported different albedo (scattering over total attenuation coefficient) for oxygenated (>0.99) and reduced (>0.96) blood at 632.8 nm. Some discrepancy between the isobestic points in the transmission and reflection spectra of blood samples in the infra red region of the spectrum has already been noted by Mook et al (1968). However, since in the in-vivo situation the oxygen saturation does not change as much as that in this experiment, the haemoglobin index (eqtn 5.3) may be used in both transmission and reflectance measurements.

5-7-2 Measurement of specific absorption coefficient of oxy and deoxy haemoglobin

To measure the specific absorption coefficient of haemoglobin and of red cells, samples of 2% red cells in saline and 2% red cells in distilled water were prepared. As described in section 5-2, the latter produces haemolysed haemoglobin. An aliquot of this sample was centrifuged to remove the ghosts of the red cells. The amount of haemoglobin present in the red cell suspension and haemolysate was

measured using Coulter S plus IV analyser. The results were as follows:

sample	haemoglobin concentration
2% red cells	0.521 g/dl
haemolysed red cells	0.503 g/dl
haemolysed & centrifuged	0.493 g/dl

To carry out the experiment the system was set up as described in section 5.5 and the sample of 2% red cells in saline was placed in the flask. It was fully oxygenated by passing air through the flask and the reflection and transmission spectra of the oxygenated sample were measured. The samples were then deoxygenated by passing nitrogen gas through the flask for nearly 30 minutes; the reflection and transmission spectra of the deoxygenated sample were then measured again. This procedure was repeated for the sample of 2% haemolyzed red cells. The LIR and absorbance spectra of 2% red cells in saline and haemolized red cells with the same concentration for oxy and deoxy samples are shown in Fig. 5.17 and 5.18 respectively. The absorbance spectra are similar to LIR ones but with lower absorbance.

Since the concentration of haemoglobin in the haemolysed samples (c= 0.493 g/dl), the sample thickness (t= 1.166 mm), and absorbance at each wavelength are known, the specific absorption coefficient (ε) of haemoglobin can be calculated by applying Beer's law (Ab.=εct). The S.A.C. of haemoglobin is usually determined in terms of the cm^2/mol, where one mole is the amount of haemoglobin which contains 1 g atom of Fe and combines with 1 g molecule of oxygen. Haemoglobin with a molecular weight of 66800, has four iron containing groups, each of which can combine with one oxygen molecule, so, one mole haemoglobin is assumed to be 66800/4 or 16700 grams. The specific absorption coefficients of oxy and reduced haemoglobin calculated from

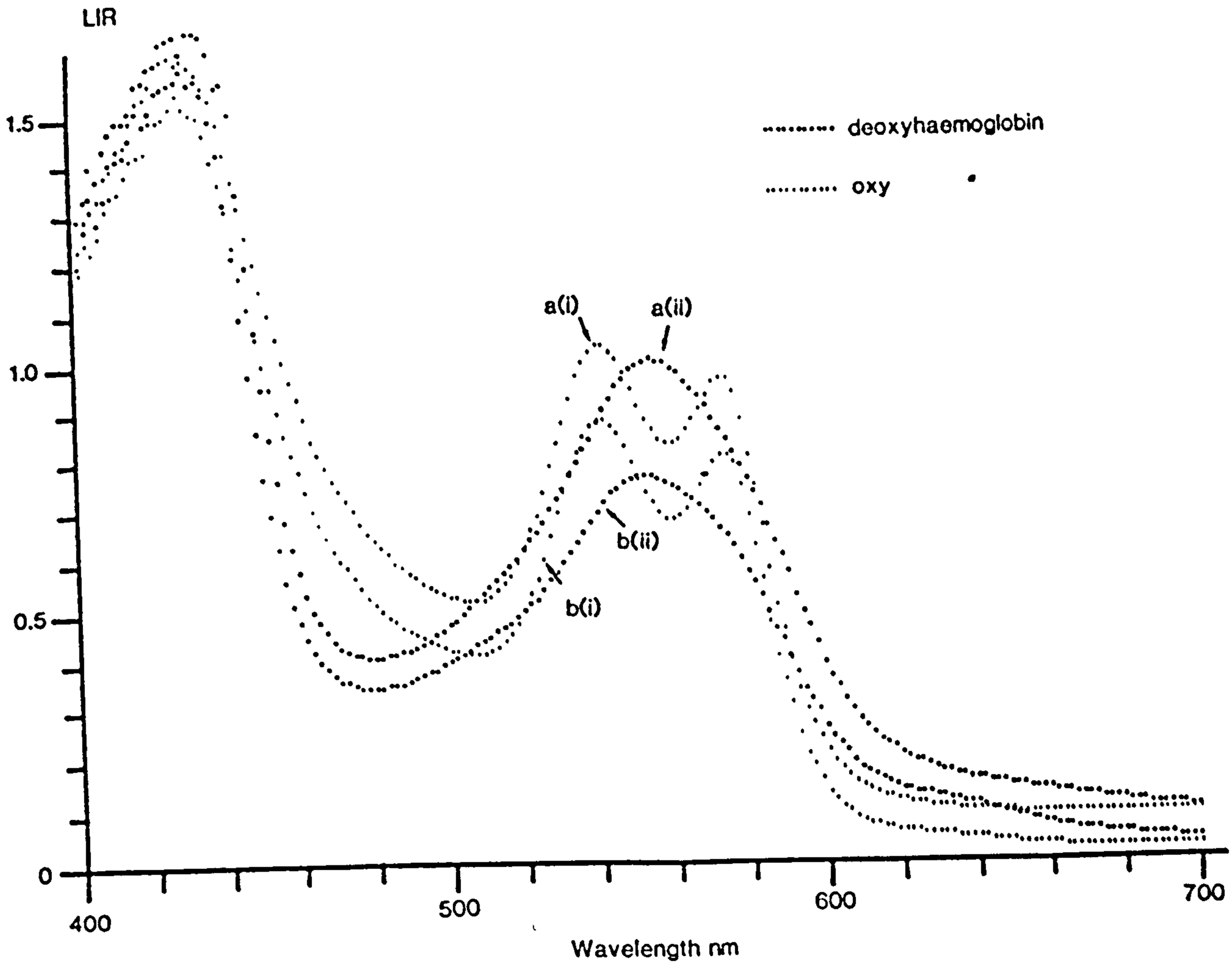

Fig. 5.17- LIR spectra of: a) 2% red cells in 0.9% saline, b) 2% haemolysed red cells, (i) oxygenated, (ii) reduced, 1.166 mm thick cuvette.

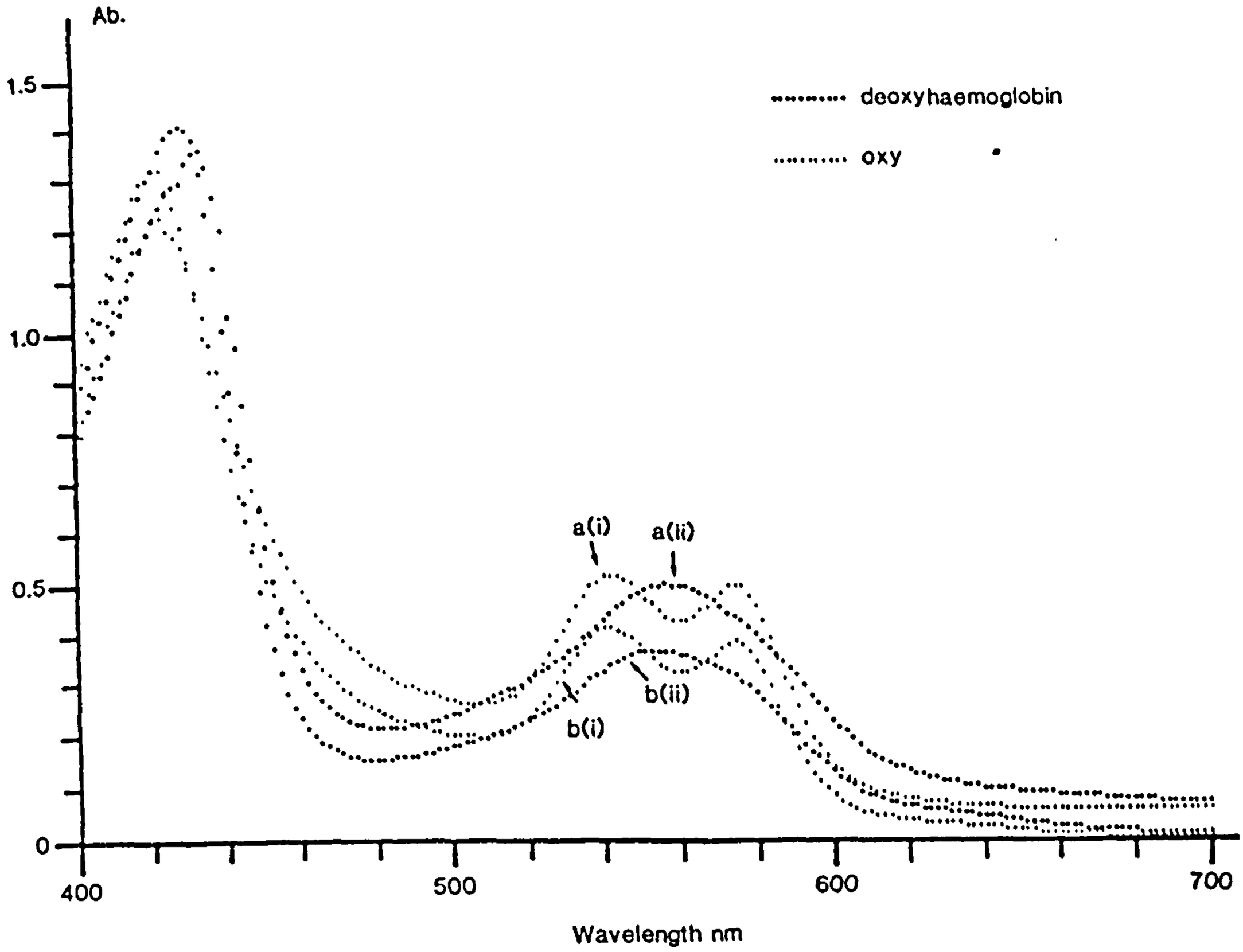

Fig. 5.18- Absorption spectra of: a) 2% red cells in 0.9% saline, b) 2% haemolysed red cells, (i) oxygenated (ii) reduced, 1.166 mm thick cuvette.

reflection and transmission measurements are in agreement with each other and they are plotted in Fig. 5.19. The LIR values at short wavelengths (400-450 nm), where the S.A.C. of haemoglobin is very high, have been suppressed due to stray light at such low reflected light intensity, therefore the S.A.C. from reflected measurements were underestimated for both oxy and deoxy samples. Figure 5.19 also compares the results of measured S.A.C. of haemoglobin with those published by Horecker (1943). The discrepancy between measured and published curves are attributed to the difference of the band pass of the system used by Horecker and the interference filter used in the present measurement. The band pass of the instrument used by Horecker was 0.7 to 1.25 nm in the visible spectrum which is nearly 13 times narrower than the band pass of the interference filter used for reflectance and transmission measurements.

The specific absorption coefficient of red cells can not be calculated because the effective path length of the light varies with the wavelength due to absorption coefficient and scattering by red cells (5.7.1).

5 - 8 Summary and conclusions

A new index has been introduced to quantify the amount of haemoglobin by means of reflectance spectra. Such an index the "Erythema index" has already been introduced by Dawson et al (1980). The erythema index was measured by calculating the area under the LIR spectrum of oxy or deoxy haemoglobin and above an arbitrary baseline created by joining the points at 510 and 610 nm on the spectrum (eqtn. 5.1). The new haemoglobin index is measured by calculating two slopes between three isobestic points of the LIR spectrum of oxy or deoxy

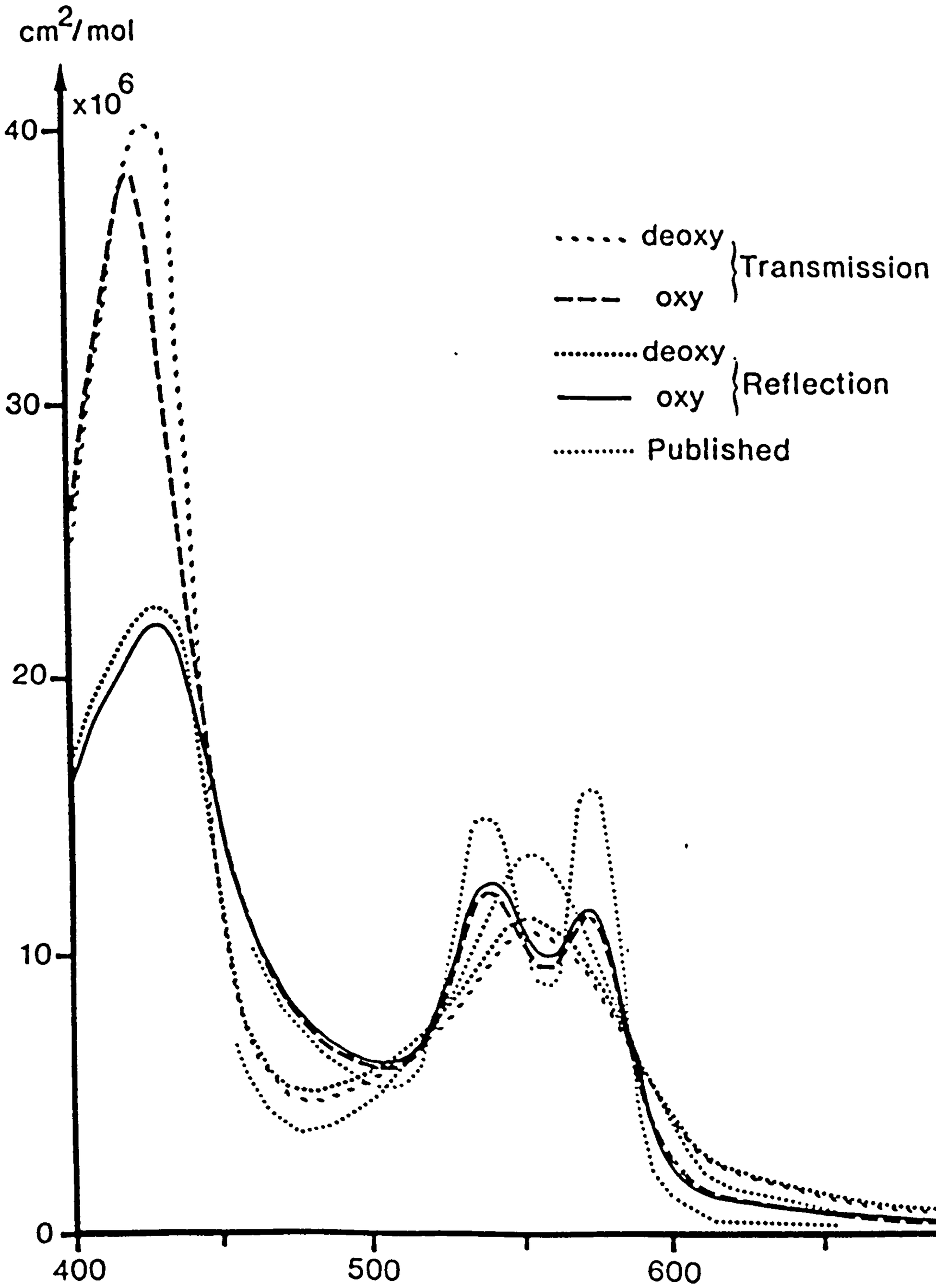

Fig. 5.19- Specific absorption coefficient of oxy and reduced haemoglobin calculated from reflectance and transmission spectra of haemolysed red cells, compared with published curves (Horecher 1943).

haemoglobin. In this index any contribution to the haemoglobin spectrum from an additional background linear spectral curve is cancelled by subtracting the two slopes (eqtn. 5.2). Such curves are generated by the melanin absorption spectrum or the effect of wavelength dependent scattering, both of which are present in in-vivo measurement of the reflection from the skin. Based on the spectral differences of oxy and reduced haemoglobin, a formula for measuring the oxygen saturation of the sample is derived.

The new and the old indices were compared in terms of: 1) their dependence on the amount of haemoglobin present and 2) the effect on the indices of the state of oxygenation of the haemoglobin. For the first criteria, the LIR spectra of six different concentrations of red cells were measured on white and black surfaces using three different cuvette thicknesses. Calibration curves of the haemoglobin and erythema indices for reflection spectra on a white surface (Fig. 5.5) showed a near linear dependence on the concentration. The erythema index has a steeper gradient than the haemoglobin index but was dependent on the oxygen saturation of the sample. The reflectance spectra measured on a black surface showed that at wavelengths with high S.A.C., absorption is the dominant attenuation process while at wavelengths with low S.A.C., ie. longer wavelengths, scattering is predominant.

To investigate the second criteria, ie independence of oxygenation, two different approaches were followed. First the dependence of the E and H indices on oxygenation were determined by measuring the indices of a sample with eight different oxygenation states. The coefficient of variation of the H index was 1.05% and that of the E index was 7.2% (Table 5.2). It was concluded that the erythma

index is not suitable for use in oximetry. Secondly, the dependence of the measured oxygenation on the H index was determined by measuring the oxygenation of different concentrations of red cells using a constant level of oxygenation. The results of six concentrations each with three different thicknesses have a C.V. of 1.34%. Hence, it is concluded that, although the H index is not as sensitive as the E index to the amount of haemoglobin, its independence of oxygenation makes it a suitable index.

To simulate the skin, a diffusing rather than clear microscope slide, was used as a top cover of the cuvette. The following conclusions were drawn from the results of this experiment:

a) The more diffusing the surface, the lower the absorbance, which may be due to diffusely reflected light from the surface of the diffuser (I_{dr}) being included in the measured intensity.

b) The greater the absorbance, the greater the difference between the apparent and true LIR values. This is because the greater absorbance will decrease the reflected signal, thus the stray light becomes more effective in reducing the calculated absorbance.

c) Calibration curves for the haemoglobin and erythema indices measured using a diffusing cover for the cuvette were not linear. The non-linearity increased with increasing thickness of the cuvette. The non-linearity arises from the effect of back scattered light by the red cells and light reflected by the diffuser (I_{dr}). By correcting the experimental results for stray light (I_{dr}) the haemoglobin index becomes linear. By adapting the Kubelka-Munk theory and assuming 2.12% back scattered light per mm thickness per unit concentration of red cells, the calibration curves based on measurements at two different wavelengths showed a good agreement with the theoretical prediction

(Fig. 5.10).

In the oximetry of blood only the H index can be used to correct the oxygenation index for the amount of blood (eqtn. 5.7). In all of the above measurements, oxygenation was calculated from equation 5.8, which is based on measuring the gradient of the absorption spectrum in the neighbourhood of the peak, and calibrating the results to 100% and 0% oxygenation with the data obtained from 2% fresh oxy and reduced red cells in plasma. To validate the two point calibration method, an O.D.C. of haemoglobin with a pCO_2 of 40 mmHg, pH 7.33 and at 37 °C was measured and compared with a published O.D.C. under the same conditions. The agreement between measured and published curves confirmed the accuracy of this method of oxygen saturation measurement.

The reflection and transmission spectra of a sample with different levels of oxygenation were measured and compared. The ratio of the haemoglobin index calculated from its reflectance spectrum to that calculated from its transmission spectrum was approximately constant (2.05 ± 0.15) for all oxygenation. The average of the ratio of the LIR to the transmission absorbance at the haemoglobin peak (540 nm) was 2.03 ± 0.07, and at longer wavelength (670 nm) was 1.59 ± 0.19. The experimentally derived ratio of the geometrical light path lengths in reflection to those in transmission when measured with the same geometry and a clear solution of $CuSO_4$ was 2.3. These results show that the effective path length in a suspension of red cells is 69% and 88% of the geometrical path length at 670 and 540 nm respectively. The decrease in the effective path length with increasing wavelength indicates that in the reflectance spectroscopy of blood samples the effective path length decreases with increasing

scattering or decreasing absorption.

Finally, the specific absorption coefficient of oxy and reduced haemoglobin has been measured and compared with the published spectra. The observed discrepancy is attributed to the difference in band pass of the instrument used in this study and that of the published curves, nevertheless the general agreement confirms the validity of our measurements.

CHAPTER 6

6 - IN-VIVO REFLECTANCE SPECTROSCOPY

It was shown in chapter 5 that diffusely reflected light at the surface of the simulated skin sample has a significant effect on the haemoglobin index (section 5-3-2). In in-vivo measurements this reflectance component has no information about the skin pigments and is dependent on skin texture at the measurement site. In this chapter instrumental improvement of the in-vivo measurement of skin reflectance and the stability of the instrument will be discussed. The effect of light scattering in the epidermis and dermis on the accuracy of measurements will then be studied. Finally it is shown that in in-vivo reflectance measurements the average penetration depth of radiation (550 nm) in tissue is about 0.5 mm, and not more than 1.2% of the tissue volume in the ear lobe is occupied by the blood.

6 - 1 Exclusion of specular reflection

In order to measure the net back scattered light from within the skin, the measured reflected signal should be corrected for the contribution of stray light. Two types of stray light may contribute to the signal, one is the stray light inside the reflectance probe and the other is the specular reflection from the surface of the skin. The measured signal is corrected for stray light inside the reflectance probe by measuring the reflectance of a black surface as described in chapter 4. The specular reflection is dependent on the surface topology of the stratum corneum and varies from site to site in an individual, therefore a simple correction made by subtracting a constant value from the reflected signal cannot be used. Two different methods for excluding specularly reflected light from the measured

signal are described below:

1) suppression of specular reflection

2) use of polarised light

In the first method the 1 cm viewing aperture of the reflectance probe is covered with a thin microscope slide. The skin surface is then optically matched to this microscope slide for each measurement by using glycerine or any clear substances with a refractive index between the refractive index of stratum corneum (1.55) and that of crown glass (1.48 -1.61). When the refractive index of the microscope slide and the clear substance are exactly the same as the stratum corneum there would be no specular reflection at the skin surface, therefore any radiation which passes through the microscope slide would penetrate into the skin, and light back scattered within the skin layers would be collected in the signal channel. Any specular reflection from the surface of the microscope slide inside the reflectance probe would then be accounted for in the stray light measurement made using a black surface. Figure 6.1 shows the in-vivo spectra of skin on the palm of the hand measured with and without the suppression of specular reflection by use of glycerine as an optical coupling agent.

The LIR spectrum of naturally desquamated epidermis following excessive exposure to solar radiation, placed on a black surface was also measured and plotted in Fig. 6.1. The proportion ($R_{spec,\lambda}$) of light specularly reflected from desquamated epidermis to that from a white diffusing surface may be estimated from measurements of the LIR spectrum of the specimen if it is assumed that the specimen does not scatter light within itself and the black surface is a perfect absorber. Under these conditions:

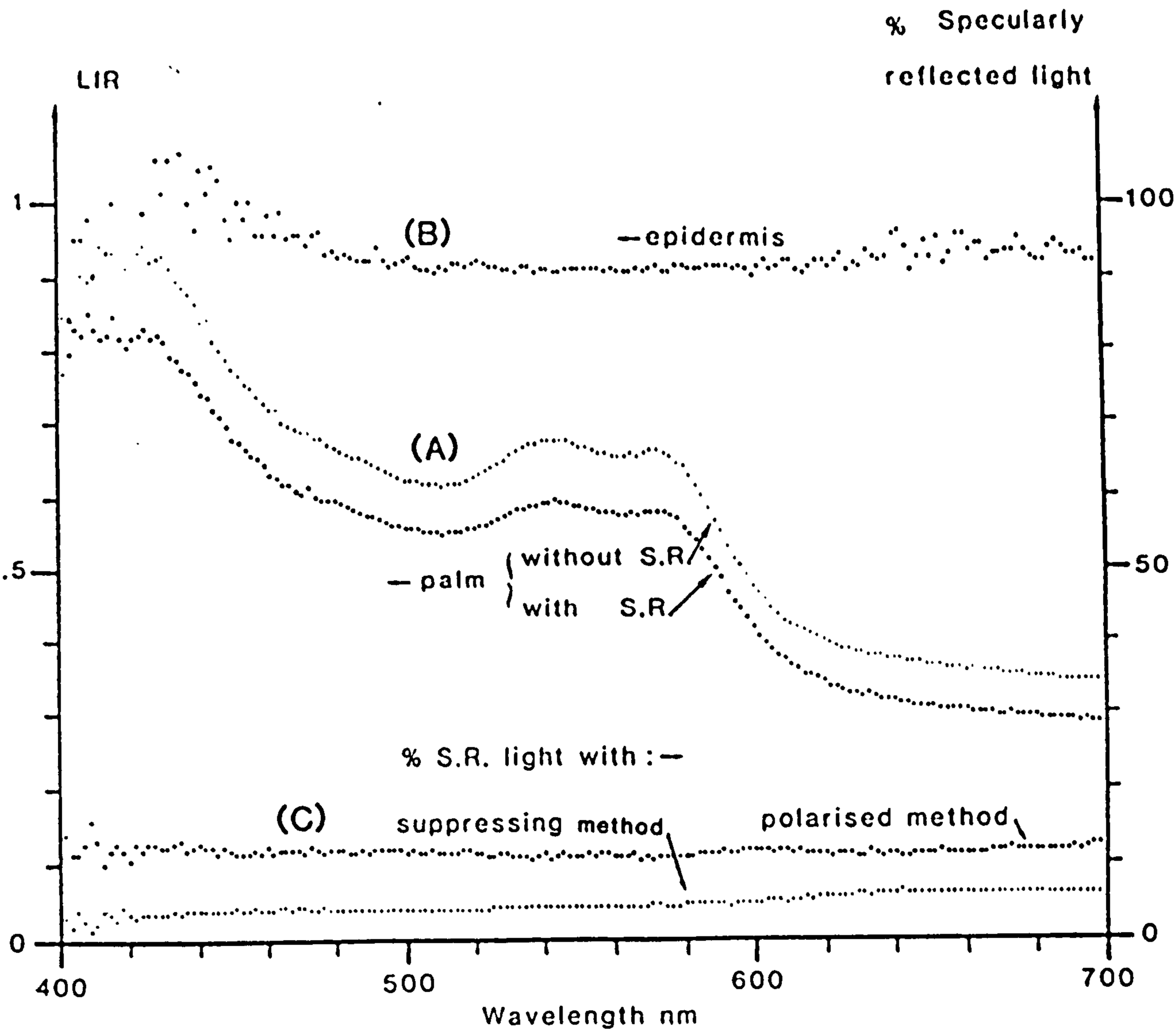

Fig. 6.1- A) LIR spectrum of a palm with and without suppression of specular reflection (S.R.) by use of glycerine, B) LIR spectrum of desquamated epidermis on a black surface, C) the proportion of specularly reflected light from a palm surface as measured by two methods.

$$LIR = \text{Log}\left(\frac{I_w}{I_{spec}}\right) \qquad 6\text{-}1$$

where "I_{spec}" is the intensity of specularly reflected light, "Iw" is the diffusely reflected light from a white surface. Hence, for the wavelength range 480-700 nm:

$$R_{spec,\lambda} = I_{spec}/I_w = 10^{-LIR} = 10^{-.905} = 12.4\%$$

The amount of specular reflection at wavelength λ from the in-vivo skin surface may be calculated from the following expression:

$$R_{spec,\lambda} = 10^{-A'_\lambda} - 10^{-A_\lambda} \qquad 6\text{-}2$$

"A_λ" and "A'_λ" are the LIR values of the skin reflectance spectrum with and without suppression of the specular reflection at each wavelength, "λ". The calculated specularly reflected light by this method (Fig. 6.1) is about 4-5% for all the spectrum and is less than that measured from the desquamated epidermis on the black surface. This is because the refractive index of glycerine n=1.473 (Tennent 1971) is less than that of stratum corneum, so the skin surface was not precisely optically matched to the microscope slide.This method has two disadvantages, firstly the difficulty of finding a coupling fluid and a microscope slide with the same refractive index as that of the stratum corneum (1.55) and secondly the possibility of changing the blood content and oxygenation through contact with the skin at the measurement site. In practice this method cannot totally suppress the specular reflectance.

The second approach utilizes the differences in the polarisation

properties of diffusely and specularly reflected light. Specularly reflected light retains a regular relationship with its incident polarisation whilst diffusely (multiple) scattered light becomes randomly polarised. To apply this method, two linear polarisers were mounted at the tips of the optical fibres in the reflectance probe, their axes of polarisation perpendicular to each other. Hence specularly (singly) reflected light is not collected. The principal problem in utilizing this method is the attenuation of the signal due to the light passing twice through the polarisers which decreases the signal to noise ratio, especially at shorter wavelength. This difficulty was overcome by increasing the light intensity in the signal fibre by mounting a concave mirror at the back of the light source.

The specular reflectance of a palm measured using polarised light is also shown in Fig. 6.1. This curve is calculated from equation 6.2 by using the LIR value from the skin reflectance spectra with and without the polarisers for each wavelength. As can be seen in this figure, the fraction of the incident light that is specularly reflected, as measured by this method, (12%) is in close agreement with that measured from the desquamated epidermis placed on a black surface. It was concluded that the crossed polariser method is the preferred approach to overcoming the effects of specularly reflected light from the in-vivo LIR spectrum. As described in chapter 4, the collecting fibre was mounted at 45 degrees to the illuminated surface, this angle was chosen to minimise the collection of specular reflection light, however when using polarisers the fibre can be fixed at any angle.

6 - 2 Optimisation of the light collecting angle

In order to find the best collecting angle for the in-vivo reflected signal, ie where the back scatter signal from within the skin layers is greatest, the LIR spectra of a forearm at different angles were measured with and without the polarisers. The LIR value of an in-vivo skin surface at a given wavelength "λ", as described in chapter 4, is defined as $A_L = \mathrm{Log}(I_{W\lambda\Phi}/I_{S\lambda\Phi})$, where "$I_{W\lambda\Phi}$" and "$I_{S\lambda\Phi}$" are the reflected intensities of light at an angle of Φ to the normals from a $MgCO_3$ tablet and the skin surface respectively. The total back scatter signal from the skin at the collecting angle Φ can then be calculated from the following formula:

$$I_{S\lambda\Phi} = I_{W\lambda\Phi} \times 10^{-A_L} \qquad 6\text{-}3$$

If it is assumed that the $MgCO_3$ tablet has a fully diffusing surface, then the angular distribution of "$I_{W\lambda\Phi}$" will obey Lambert's law and for a collecting angle "Φ":

$$I_{W\lambda\Phi} = I_{W\lambda O} \times \cos\Phi \qquad 6\text{-}4$$

"$I_{W\lambda O}$" is the intensity of light reflected normal to the surface. Specularly reflected light can be excluded from the total reflected light if the LIR is measured using crossed polarisers. In this case "$I_{S\lambda\Phi}$" is the back scattered light from within the skin layers and is denoted by "$I_{s,exc}$". In other situations the total reflected light would include the specularly reflected light and is denoted "$I_{s,inc}$". The back scattered light from within the skin layers ($I_{s,exc}$) and the total reflected light ($I_{s,inc}$) for collection angles of 15, 30, 45, 60, and 75 degrees were calculated by using equation 6.3 for each

collection angle Φ. The data are obtained from LIR spectra of a forearm which were measured at those angles with and without the polarisers. The results for two different wavelengths (540 and 670 nm) are shown in Fig. 6.2. In this diagram the intensity of the normally reflected light from the $MgCO_3$ surface ($I_{W\lambda o}$) was assumed to be 100 for all wavelengths and the radius of the reflectance probe was 2.5 cm. The curves which are fitted to the data points, are cosine functions and their intersection point at 90 degrees shows that there was 5% residual stray light in the system. The relative intensity of specularly reflected light can be measured by subtracting "$I_{s,exc}$" from "$I_{s,inc}$". The following conclusions can be drawn from this experiment:

A) Back scattered light from within the skin layers and specular reflection from the stratum corneum of a forearm increase with decreasing the angle of collection. The ratio of the intensity of specularly reflected to back scattered light is independent of the angle of measurement, viz 0.41 and 0.16 at 540 and 670 nm respectively.

B) Back scattered light from within the skin layers ($I_{s,exc}$) at 670 nm is greater than at 540 nm. As light of longer wavelength is more forwardly scattered in skin the fact that it produces a stronger back scattered signal indicates that the back scattered light at 540 nm suffers from greater absorption by blood in the skin.

C) The specularly reflected light at the skin surface, unlike the reflection from a smooth plane surface, spreads in all directions. For normally incident radiation, there is some specular reflection at large angles which is dependent on the skin surface morphology.

These results show that the diffuse reflected signal from within

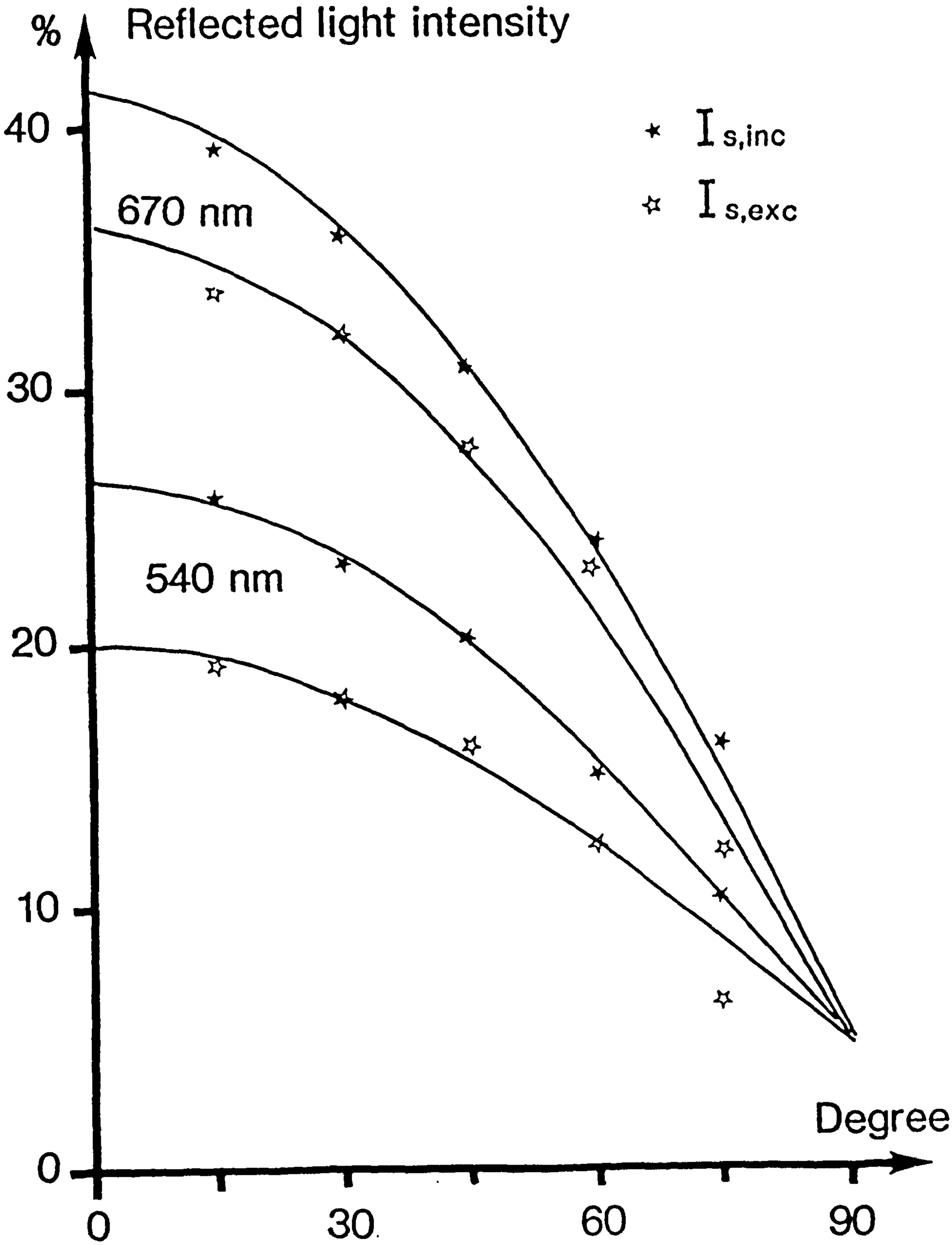

Fig. 6.2- Reflected light intensity from within the skin layer with and without the specular reflection at different angles (normal to skin).

the skin layers has a Lambertian distribution, as reported by Hardy (1956), and hence the smaller the collecting angle, the greater the signal would be.

6 - 3 Design of a new reflectance probe

The measurement of diffusely reflected light from within the skin layers can be improved by using polarisers to exclude the specularly reflected component and by reducing the collection angle as much as possible. The light delivery fibre is fixed perpendicularly to the surface in the reflectance probe, as described in chapter 4. The minimum angle at which the light collecting fibre can be mounted is when the tip of the collection fibre is touching the tip of the delivery fibre in the reflectance probe (Fig. 6.3). To decrease this collection angle still further the radius of the reflectance probe, R_p, has to be increased, as shown in Fig. 6.3. But increasing the radius of the reflection probe will decrease the light intensity at the skin surface and consequently will reduce the reflected signal. In order to find the optimum geometry for the light delivery and collecting fibres, so that the reflected signal is maximum, the total irradiance at the surface of the collecting fibre was calculated for different dimensions of the reflectance probe. Based on these calculations, a new reflectance probe was designed to improve the reflectance signal.

If the divergent angle of the fibre is assumed to be "α" (33^o), and the light emerges from the fibre tip with the irradiance "E_o" (mw/cm^2), the total power emerging from the fibre tip would be spread over a larger area on the diffusing surface, hence the mean irradiance on the illuminated surface is calculated from:

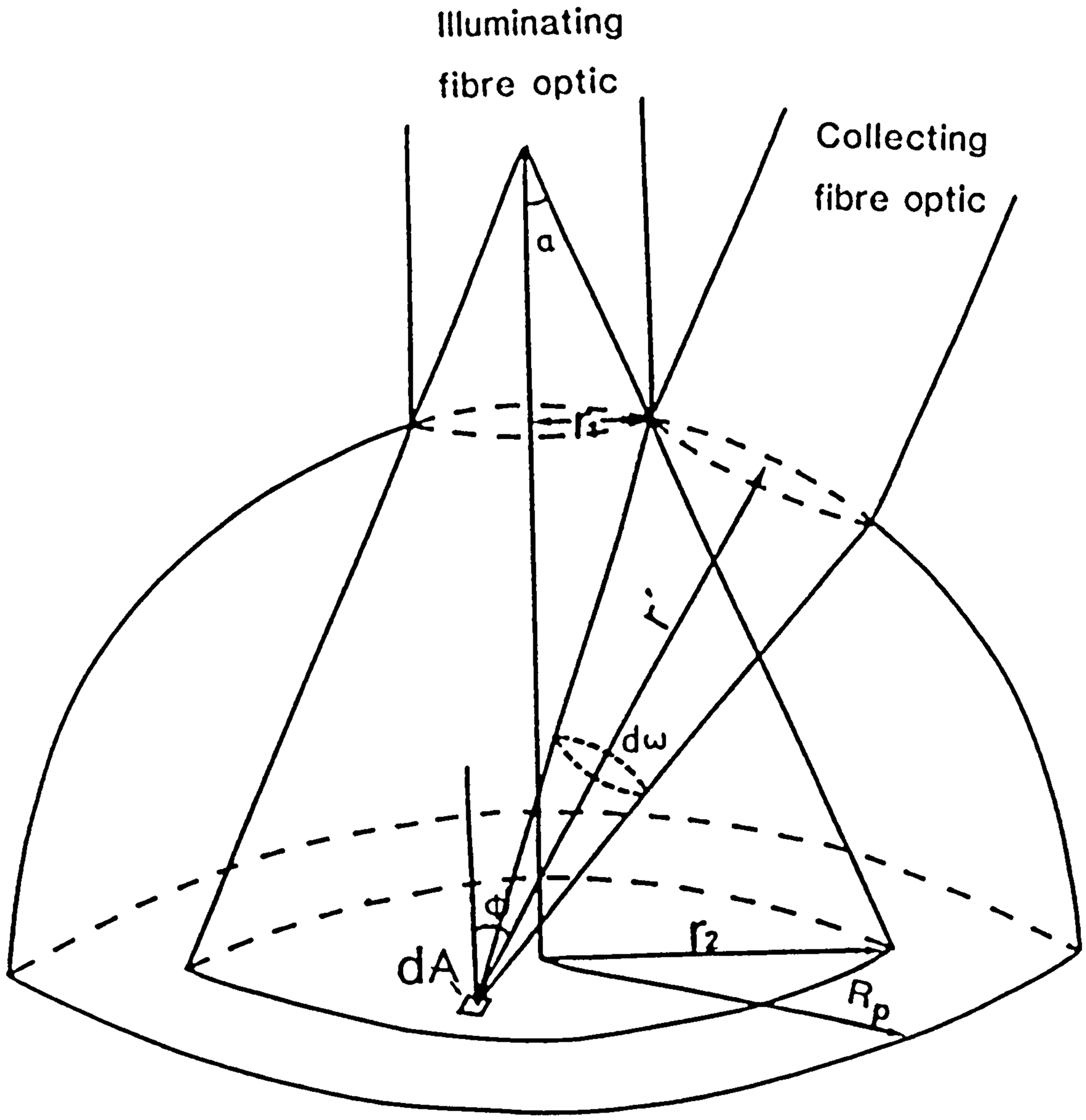

Fig. 6.3- Illustration of incident and collection geometry of light in the reflectance probe.

$$E_{(mw/cm^2)} = (\frac{A_1}{A_2})E_o = (\frac{r_1}{r_2})^2 E_o \qquad 6\text{-}5$$

where "A_1" is the area of the fibre tip with radius "r_1", and "A_2" is the illuminated area with radius "r_2". "r_1" and "r_2" are related by the following formula:

$$r_2 = r_1 + \sqrt{(R_p^2 - r_i^2)} \times \tan\alpha \qquad 6\text{-}6$$

"R_p" is the internal radius of the reflectance probe head. The white diffuse reflector is not an absorbing surface and reflects all the incident radiation with a Lambertian distribution. The emitted irradiance of the surface is thus the same as that of the illumination (E). The total radiant power from the surface is distributed over 2π steradian, hence the radiance (emitted power per unit solid angle per unit projected area) in all directions is:

$$L_{(mw/cm^2\ sr)} = E/2\pi \qquad 6\text{-}7$$

To calculate the radiation at the surface of the collecting fibre, let an element area "dA" emit radiation with a radiance "L", the radiant power (dp) in direction "Φ" from its normal will then be:

$$dp = L\ dA \cos\Phi\ d\omega \qquad 6\text{-}8$$

"$\cos\Phi$" is introduced because the projected area of "dA" in direction "Φ" is $dA \cos\Phi$, and "$d\omega$" is the solid angle of the collecting fibre viewed from the emitting point. The radiant power "dp" falls upon the collecting fibre with area "A_1" at a distance "r'"

from the emitting point (Fig 6.3); the solid angle is:

$$d\omega = A_1/r'^2 \qquad 6\text{-}9$$

The irradiance falling on the collecting fibre (dE_c) is calculated from the following formula:

$$dE_c = \frac{dp}{A_1} = \frac{L\ dA\ \cos\Phi}{r'^2} \qquad 6\text{-}10$$

substituting eqtns 6.5, 6.6, and 6.7 in 6.10 gives:

$$dE_{c_{(mw/cm^2)}} = \left(\frac{r_1}{r_1 + \sqrt{(R_p^2 - r_1^2)}\ \tan\alpha}\right)^2 \frac{E_o\ \cos\Phi}{2\pi r'^2}\, dA \qquad 6\text{-}11$$

The relative irradiances of the signals from a non-absorbing surface were calculated for different radii of the reflectance probe by computer numerical integration of eqtn 6.11 over the illuminated aperture in the reflectence probe, and are presented in Fig. 6.4. In this calculation the diameter of the fibre's tip is 4.5 mm and the divergence angle of the fibre is $\alpha = 33^o$. Although decreasing the collection angle would increase the reflected signal, it can be seen that increasing the radius, which decreases the collecting angle, would decrease the reflected signal. Maximum signal will obtain when the radius of reflectance probe is 4.5 mm. In this case the collection angle is 54 degrees. A new reflectance probe was therefore designed for in-vivo measurement of LIR from skin surface, as shown in Fig. 6.5. The internal radius of this probe is 5 mm and the light is exposed normally to the surface and is collected at an angle of 54 degrees.

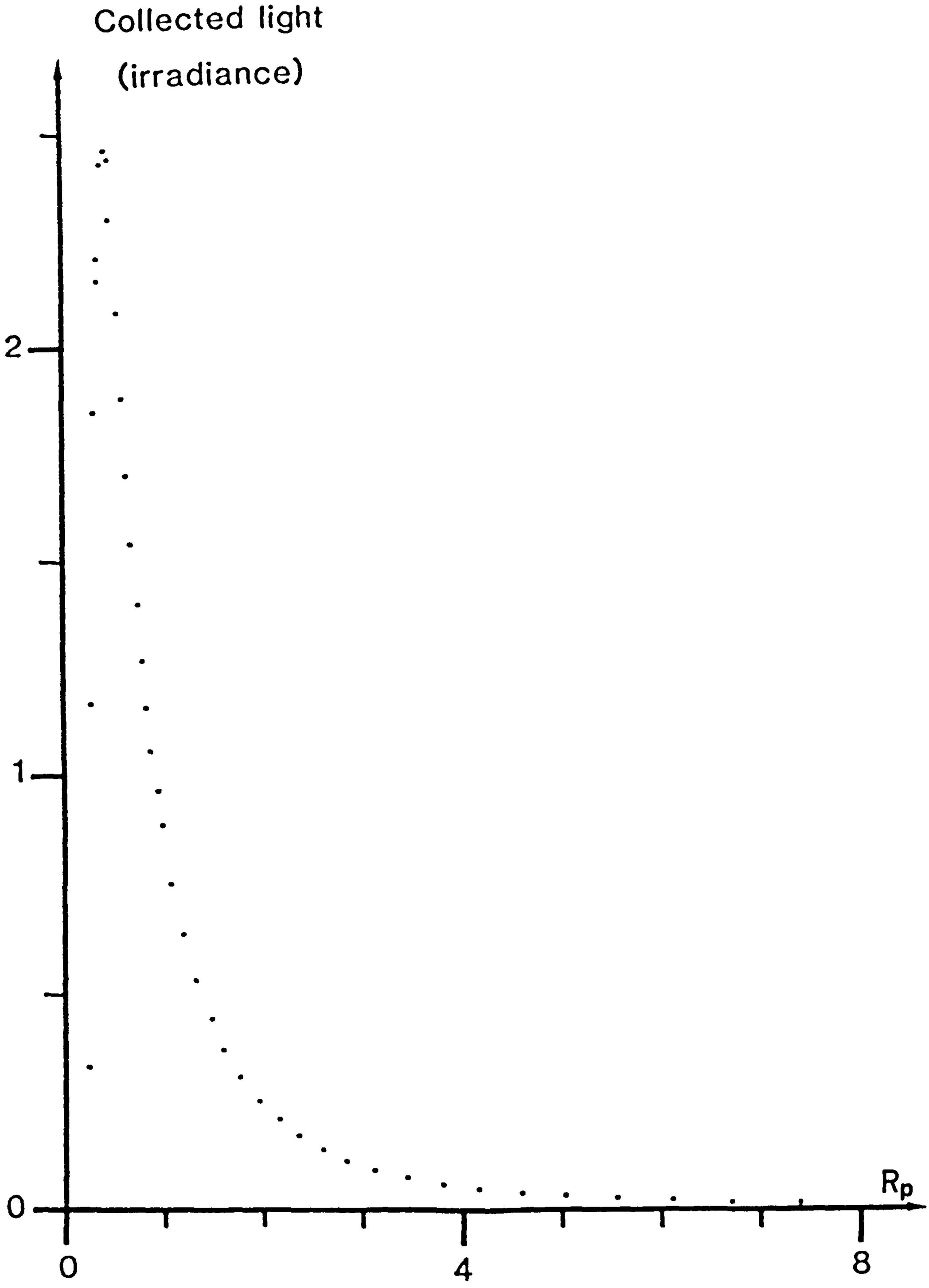

Fig. 6.4- Effect of different radii of reflectance probe on light collection efficiency.

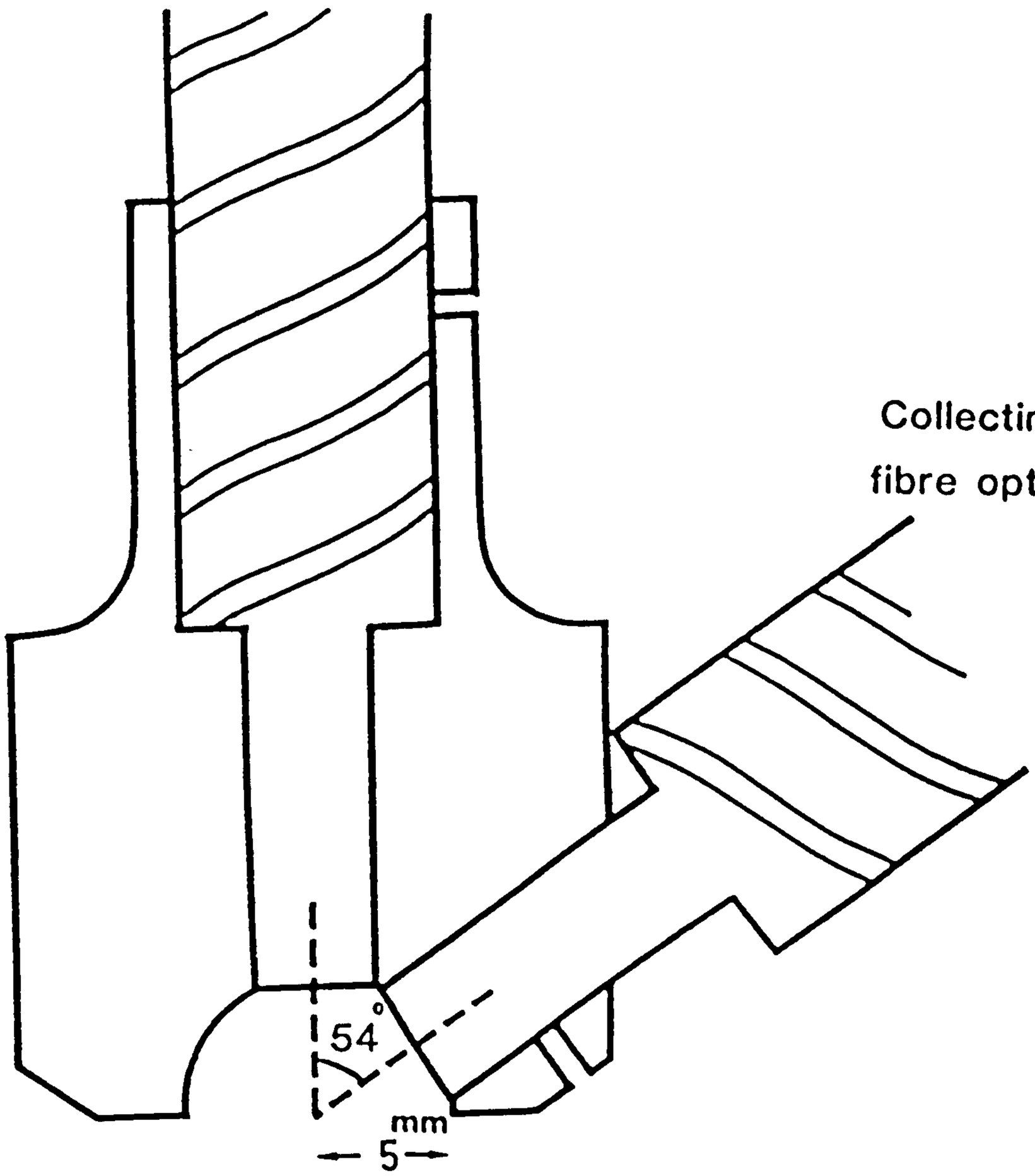

Fig. 6.5- Geometry of the reflectance probe for in-vivo measurement of LIR from skin surface.

6 - 4 Dependence of the indices on biological changes

In order to assess the in-vivo performance of the reflectance spectrophotometer described in chapter 4, the variation in the haemoglobin index and oxygenation produced by biological changes in the reflected signal was studied. Factors affecting the diffusely reflected signal, and consequently the haemoglobin index and oxygenation, are described below:

a) The dermis is a vascular bed, it expands during the systolic period of the circulation when the blood is pumped to the tissue, and relaxes during the diastolic cycle. The expansion and relaxation of tissue generate changes in the light path which will modify the detected signal. The frequency of this pulsation, which is produced by the heart beat and changes from person to person, is normally about 60 to 70 beats per minute. The period of each scan for measuring the LIR spectrum with the present instrument is 2.8 s, of which 0.5 s is occupied in measuring the wavelengths used to calculate the haemoglobin index and oxygenation. The variation in the detected signal is a systematic variation, but in the present instrument, which is not synchronised with the blood circulation pulses, it can be assumed to be a random variation.

b) The dermis is a highly scattering medium and the light is scattered by the collagen fibres, arterioles, venules, red cells, fatty tissue and other substances. The back scattered light is composed of part of the incident light which has been scattered along different pathways through the medium. There is a likelihood that some light will be returned without passing through red cells. This part of the back scattered light is effectively stray light in the measurement of haemoglobin. It is dependent on the property of the

measurement site and changes from site to site on the skin surface. Therefore any change in the biological conditions such as temperature and blood pressure during the measurement, and also movement of the reflectance probe can be considered as potential sources of variation in the reflected signal.

As the biological structures of any two measurement sites are not exactly the same, the contribution of the different sources of variation to the reflected signal will not be the same for all measurements. The effective variability will therefore be assumed to be a random variation in the reflected signal. The effect of this variation on the haemoglobin index and oxygenation will now be examined. Any variation in the detected signal (ΔIs) will create a variation in the LIR which can be calculated from the following formula:

$$\Delta \text{ LIR} = \text{Log}_{10}(1 \pm \frac{\Delta I_s}{I_s}) \qquad 6\text{-}12$$

Substituting eqtn 6.12 in the definition of the haemoglobin index, "H" (eqtn. 5.3) and assuming that ΔLIR is the same for all wavelengths, will give:

$$\Delta H = 11.79\ \Delta \text{LIR} \qquad 6\text{-}13$$

Details of the calculations are presented in appendix B. The coefficient of variation of the haemoglobin index may be calculated from eqtn 6.14:

$$\frac{\Delta H}{H} = \frac{11.79}{H} \text{Log}_{10}(1 \pm \frac{\Delta I_s}{I_s}) \qquad 6\text{-}14$$

Equation 6.12 may also be incorporated into the definition of the oxygenation index (eqtn. 5.7) to give:

$$\Delta OX = \frac{1}{H}\sqrt{(285.37 + 139.04\ OX^2)}\ \Delta LIR \qquad 6\text{-}15$$

Since the oxygen saturation (Sa%) is calculated from equation 5.8, the coefficient of variation for oxygen saturation may be expressed as:

$$\frac{\Delta Sa\ O_2}{Sa\ O_2} = \frac{50.76}{H}\sqrt{\left(\frac{19.47}{Sa\ O_2} - 0.1155\right)^2 + 0.0406}\ \Delta LIR \qquad 6\text{-}16$$

The total biological variation in the diffusely reflected signal was measured in-vivo by setting the spectrometer at 540 nm and placing the reflectance probe very gently on the finger tip. The diffusely reflected light was recorded on a chart recorder. Two distinct types of variation in the recorded signal were detected, one was a regular variation which may be attributed to the biological variation in the skin, ie the blood flow, and the other was an irregular variation due to the movement of the reflection probe. The regular variation is about 0.5% of the signal. In a measurement of the haemoglobin index and oxygenation of a finger tip where the haemoglobin index is 0.3 and oxygen saturation 98%, the fluctuations led to coefficients of variation of 8.51% for the haemoglobin index and 7.99% for oxygenation. Equations 6.14 and 6.16 show that the coefficient of variation for both the haemoglobin index and oxygenation will decrease with increasing haemoglobin index. The prediction of this theory will

be verified experimentally by changing the amount of haemoglobin in the skin using chemical or heat treatment (see chapter 7).

6 - 5 Effect of the epidermis

The epidermis has two important effects on the light transmitted through it. Firstly, absorption by melanin and secondly scattering by cells or membranes. In order to study the absorption of light by melanin an index will be defined to quantify the relative amount of melanin in the skin by either reflection or transmission. This index is called the melanin index and will be explained in the next chapter. Scattering of light by epidermis was studied by measuring the angular distribution of light scattered by a thin sheet of epidermis.

The light reflected from within the skin layers passes twice through the epidermis, and on each passage it will be absorbed by melanin and scattered by cells or membranes. In order to investigate the effect of scattering, an experiment was set up to measure the angular distribution of light scattered by the epidermis illuminated with an Argon dye laser. To prepare a sheet of epidermis, a sample of abdominal skin was immersed in water at 70 °C for two minutes. The epidermis was then separated, mounted on a frame and placed at the centre of a 500 ml spherical flask as shown in Fig. 6.6a. In order to simulate optically the dermis, the flask was filled with 0.9% saline. A spherical flask was used to reduce the effect of the step change between the refractive indices of saline with the flask and the flask with an air interface on the observed angular distribution of the scattered light. The flask was placed at the centre of a rotatable plate and the sample irradiated with a narrow light beam (4 mm in diameter) from an argon/dye laser at 630 nm. A silicon photodiode was

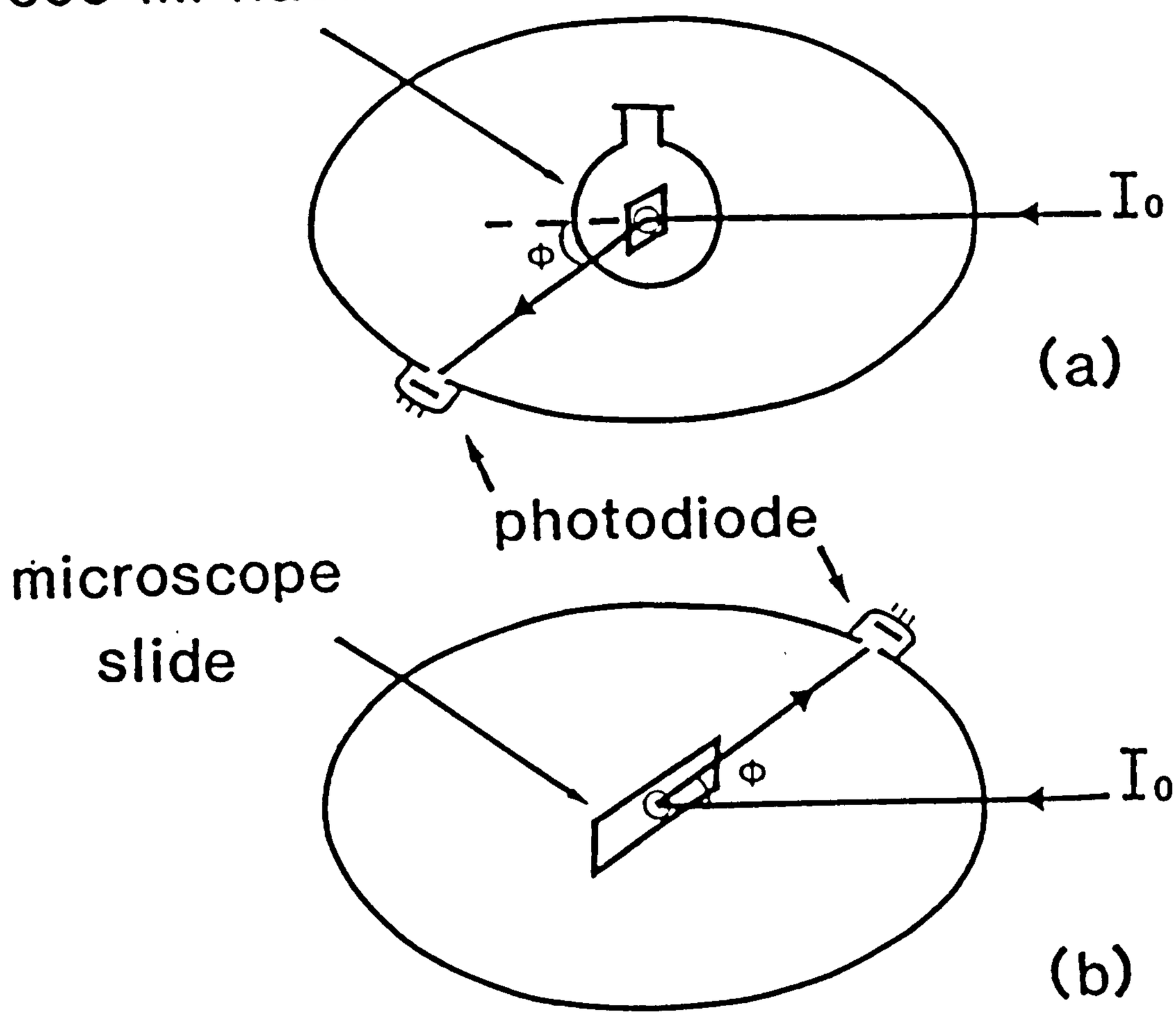

Fig. 6.6- Geometries used for measuring a) scattered transmittance, b) back scattered reflectance of epidermis.

used to measure the intensity of light scattered by the epidermis. The whole apparatus was enclosed in a dark chamber. The photodiode, which has a detecting area of 5 mm^2, was rotated around the sample at a radius of 197 mm. The detector was mounted with its sensitive surface at right angles to the radius connecting it to the sample. The stratum corneum side of the sample was illuminated normally with a radiation power of 14 mW from the laser; the scattered light was measured at 5 degree intervals. To account for changes in the incident power or in other parameters, which may vary between measurements, the radiance of the scattered light can be normalised by expressing it as a fraction of the radiation incident on the sample. This is calculated from the following formula:

$$\underset{(cm^{-2}\ sr^{-1})}{\text{Fractional scattered radiance}} = \frac{V_{out}}{p.P_r.d\omega} \qquad 6.17$$

where "p" is the incident power of the laser (14 mw), "P_r" is the photodiode responsivity at 630 nm (160 V mw^{-1} cm^2), "V_{out}" is the photodiode output (V), and "$d\omega$" is the solid angle of the detector which is centred around direction ϕ ($1.29x10^{-4}$ sr). The fractional scattered radiance of the epidermis and of a perfect diffuser (Comar 25 DO 00, Flashed opal disc) are presented in Fig 6.7. Measurement at 175 and 180 degrees was not possible due to interception of the incident beam by the detector. By extrapolating the data the intensity of reflected light at these angles was estimated. Comparison of the light scattered by epidermis and by a perfect diffuser shows that. 1) most of the incident radiation will be transmitted through the epidermis, suffering scattering of less than 20 degrees and a small amount will be back scattered. 2) there is an increase in the back

scattered light at large angles which may be due to the specularly reflected light from the rough surface of the epidermis.

The reflection from the surface of the sample when immersed in saline is different from that of dry stratum corneum, therefore the reflectance was measured again with the epidermis placed on a microscope slide as shown in Fig. 6.6b. In this measurement the incident radiation power was 58 mW and the horny side of the sample was dry while the other side was on a wet microscope slide. The results of this measurement are also shown in Fig. 6.7b. Measurements were made only between 90^{o} and 180^{o} as the transmitted light would be deflected at the interface of the microscope slide with air.

To determine the importance of the contribution of radiation scattered by a given angle "Φ" to the total amount of scattered light, the spatial distribution of radiation will be calculated. The fraction of the total incident radiation scattered into a ϕ-ring, shown in Fig 6.8, can be calculated from the following formula:

$$\% \text{ of scattered radiation at angle } \Phi \qquad S_r = \frac{V_{out}\, dA}{p.P_r}\, 100 \qquad 6\text{-}18$$

where "S_r" is the fraction of the scattered radiation in the ϕ-ring between $\phi \pm 2.5$ degrees, "dA" is the area of the ϕ-ring, "Φ" is the angle of scattering from the laser beam, "p", "P_r" and "V_{out}" are the same as defined in eqtn 6.17. The results are shown in Fig. 6.9. Since the intensity of the transmitted light at zero degrees is much higher than that at other angles, ie there is a rapid decrease in a few degrees, smaller ϕ-rings were used between 0 and 2.5 degrees. The first point was integrated over the area between 0 to 0.5 degrees, and the second point between 0.5 to 2.5 degrees.

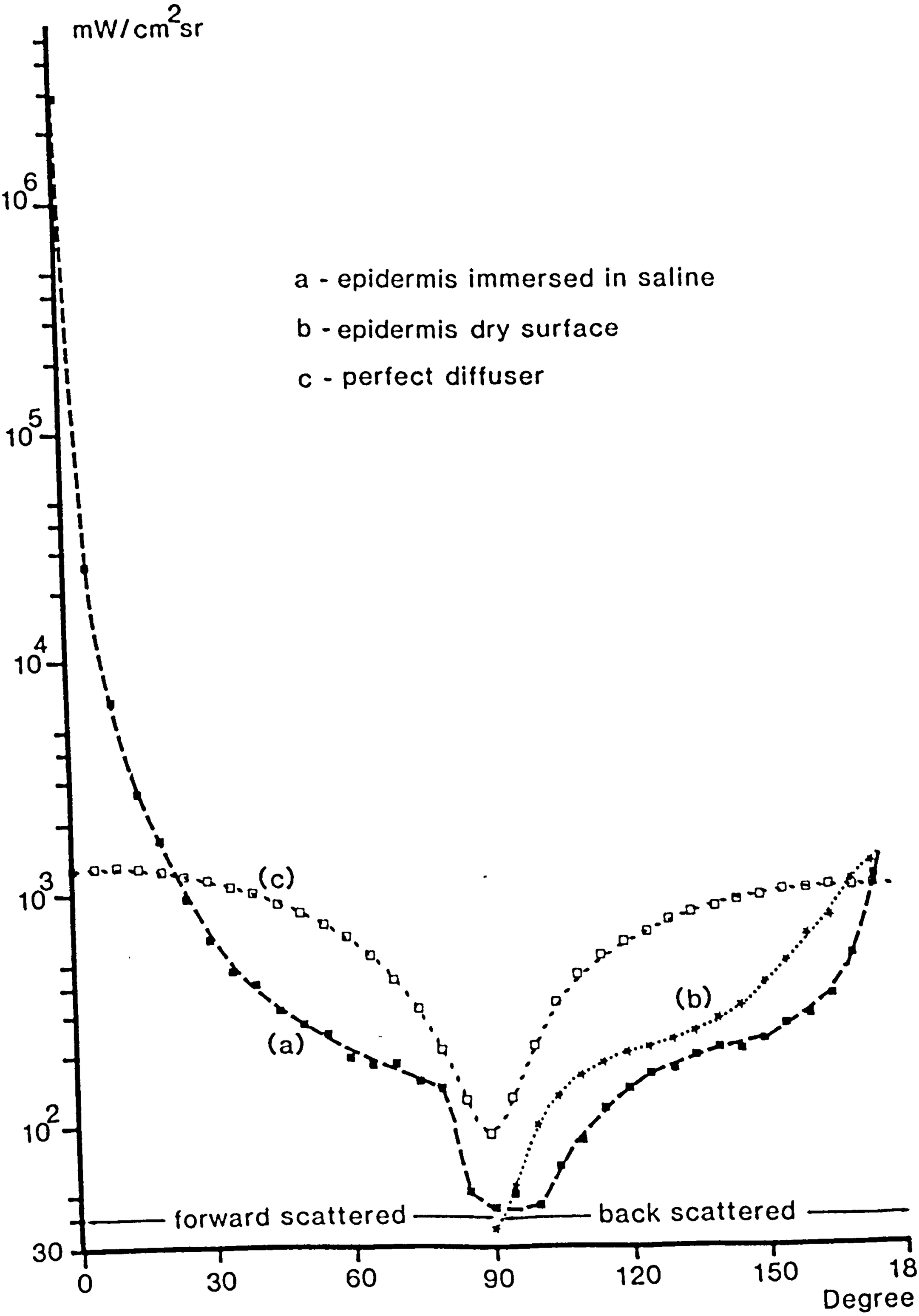

Fig. 6.7- Angular distribution of radiation (radiance) scattered by epidermis and a perfect diffuser.

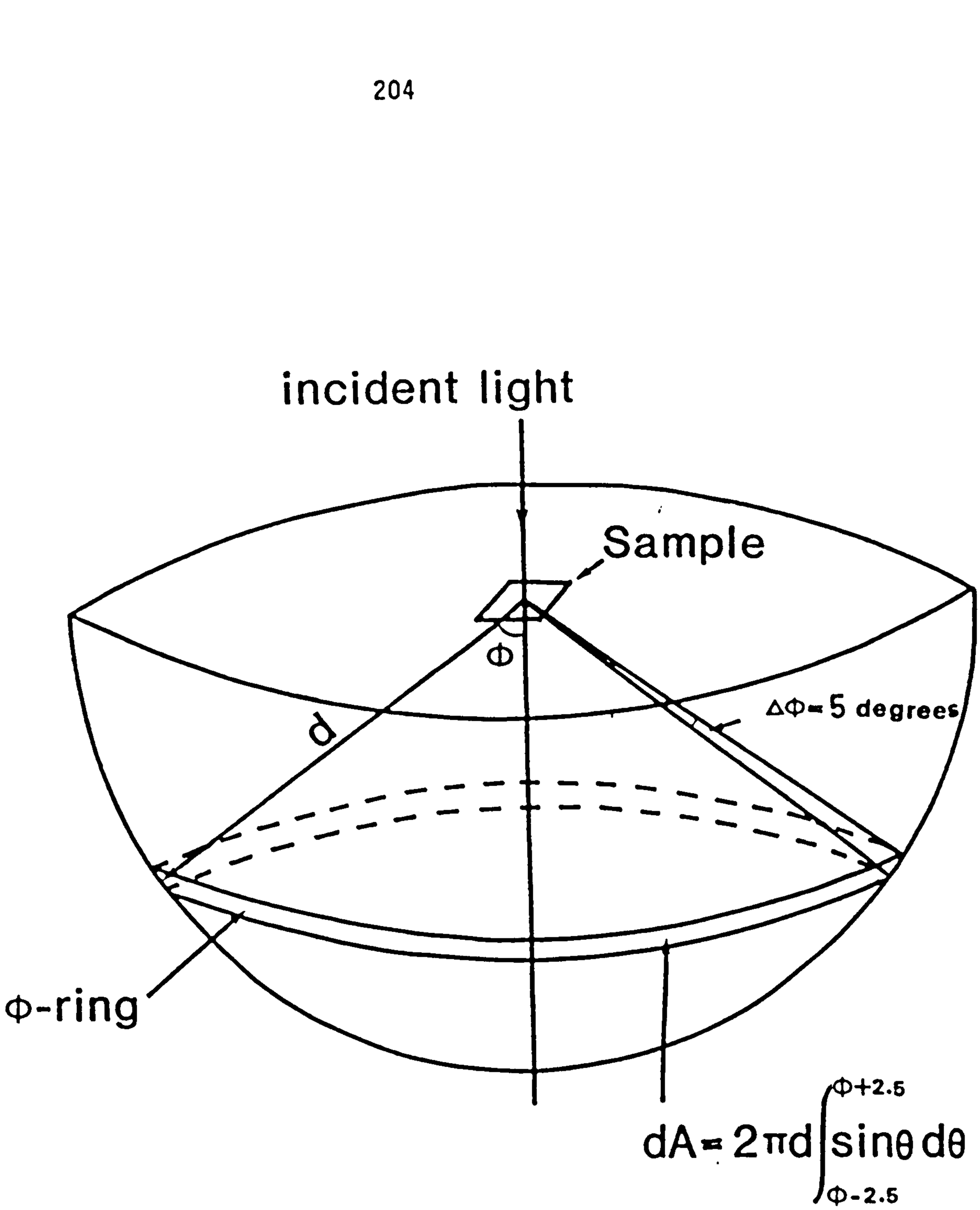

Fig. 6.8- Illustration of computation of the amount of energy scattered into a Φ-ring.

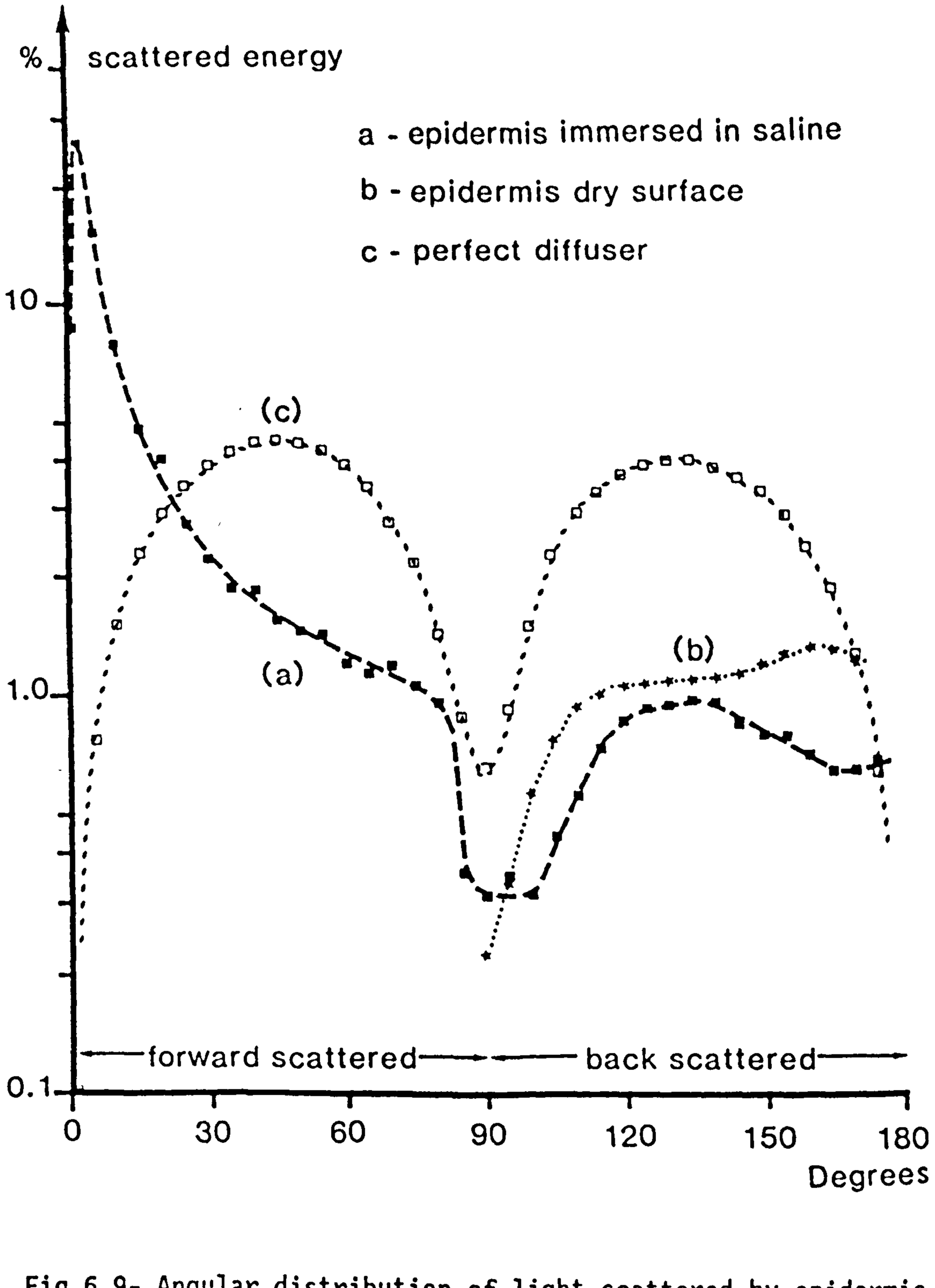

Fig 6.9- Angular distribution of light scattered by epidermis, as a fraction of incident radiation.

Because the surface area of the ϕ-ring increases rapidly with increasing "ϕ", the largest fraction of the scattered radiation is not present at ϕ=0, but at a larger angle. It is found that for epidermis the largest amount of radiation is present at 1.5 degrees while for a perfect diffuser it is at 45 degrees.

The scattering properties of the epidermis can be more clearly demonstrated if the fraction of the total incident energy transmitted within a certain solid angle be quantified. This fraction can be computed by summing the radiation scattered in all angles within the solid angle from Fig 6.9 . The results for epidermis and a perfect diffuser are tabulated in Table 6.1. The total intensity of light back scattered from the dry surface of epidermis was found to be 16.9% of the incident radiation. This measured reflectance from a dry epidermis is greater than the expected specular reflectance of stratum corneum, ie 4% to 7%, and may be attributed to additional back scattered light from within the viable layer of the epidermis (malpighian layer). 67% of the incident radiation is scattered within 22.5 degrees of the incident light beam. Comparison with the value that can be computed for a perfect diffuser (7.5% within 22.5 degrees from the normal) confirms earlier observations that most of the radiation transmitted through the epidermis is forwardly orientated. Bruls et al (1984) measured the angular distribution of the radiation transmitted through the stratum corneum and epidermis. They determined the fraction of energy transmitted within an angle of 22.5 degrees of the normal at several wavelengths. For stratum corneum this fraction ranged from 83% at 546 nm to 75% at 254 nm, and for full-thickness epidermis from 59% at 546 nm to 44% at 302 nm. These results are in general agreement with those found in this work and show that the radiation scattered by

Table 6.1- Transmitted and back scattered light from epidermis and perfect diffuser integrated over solid angle 2Φ (Fig. 6.8), expressed as a fraction of incident radiation.

Forward transmitted light (% of incident intensity)			Back scattered light (% of incident intensity)			
angle Φ	epidermis wet	perfect diffuser	angle Φ	epidermis		perfect diffuser
				wet	dried	
0.25	8.61	0.004				
1.50	34.47	0.05				
5	50.39	0.82	95	0.35	0.34	0.91
10	58.21	2.35	100	0.66	0.90	2.38
15	62.98	4.62	105	1.10	1.66	4.66
20	67.05	7.53	110	1.66	2.58	7.60
25	69.82	10.97	115	2.38	3.57	10.90
30	72.01	14.86	120	3.22	4.60	14.50
35	73.86	19.08	125	4.14	5.64	18.34
40	75.71	23.52	130	5.04	6.69	22.25
45	77.23	27.99	135	5.98	7.75	26.17
50	78.67	32.38	140	6.93	8.84	29.92
55	80.09	36.59	145	7.75	9.98	33.47
60	81.24	40.51	150	8.53	11.17	36.72
65	82.36	43.89	155	9.31	12.44	39.57
70	83.56	46.64	160	10.00	13.76	41.93
75	84.59	48.79	165	10.64	15.08	43.76
80	85.55	50.22	170	11.27	16.20	45.00
85	85.90	51.08	175	11.96	16.84	45.63
90	86.21	51.72	180	12.19	16.95	45.71

the epidermis is forwardly orientated and wavelength dependent, the fraction of incident light reaching the surface of the dermis decreasing at shorter wavelengths.

6 - 6 Effect of the dermis

It has been shown, section 6.5, that in the case of 630 nm radiation 67% of a collimated beam incident on a skin surface will enter the dermis within an angle of 22.5 degrees of the incident direction. Since the dermis is a highly scattering medium, the penetrating radiation will become more diffuse the deeper it penetrates. Hardy et al (1956), in a study of spectral transmission and reflectance of excised human skin, found that the shorter the wavelength the thinner the sample required to change the incident collimated radiation into fully diffused light. They also showed that, for excised skin specimens with a thickness of 0.43 mm, visible light becomes fully diffused and follows Lambert's law. For thickness as great as 1 mm scattering is complete for all wavelengths.

In order to study the effect of scattering in dermis in-vivo, the transmission and reflectance spectra of an ear lobe were measured. The LIR spectrum was measured with the normal procedure of the instrument described in section 4.4. To measure the transmission of the ear lobe, the tips of the light delivery and collection fibres were removed from the reflectance probe and mounted face to face in a piece of perspex with an air gap between them. Transmitted light could then measured by placing the ear lobe in the gap and shining the light on to one surface via a light delivery fibre and measuring the transmitted light at the other surface with the collecting fibre. To measure the absorbance spectrum with the present instrument, initially a white

translucent fully diffusing disc (Comar 25 DO 00, Flashed opal disc) was placed in the gap and the transmitted light was measured for all visible wavelengths. These data were taken to be the incident radiation for each wavelength and stored in the microcomputer (I_w). The diffuser was used to decrease the intensity of the incident radiation uniformly for all wavelengths to be measured by the photodiode detector. A neutral density filter was not used for this purpose because of its absorption spectrum. The diffuser was removed and an ear lobe of a volunteer was placed in the gap and the transmitted light was measured again (I_s). The absorbance was calculated by a computer program using equation 4.2. Since half of the incident radiation will be back scattered from the perfect diffuser (Table 6.1), "I_w" is under estimated for all wavelengths, hence the absorption spectrum requires correction. To determine the absolute absorbance spectrum, the absorption of the ear lobe at the 630 nm line of a Neon laser was measured. In this measurement the intensity of the incident radiation was calibrated by inserting a known neutral density filter into the gap, hence the true absorbance of the ear lobe could be measured. The difference between the true absorbance at 630 nm and that measured when using the diffuser was calculated. This difference was added to the measured absorbance at all wavelengths. The LIR and absorbance spectra of the ear lobe with a thickness of 3.75 mm are shown in Fig. 6.10.

The haemoglobin index as calculated from the transmission spectrum is 1.423 and that measured by reflectance is 0.523. These two spectra may be compared if first the LIR spectrum is multiplied by 2.72 (ratio of the haemoglobin index measured by transmission to that by reflection) to represent the same amount of haemoglobin in both

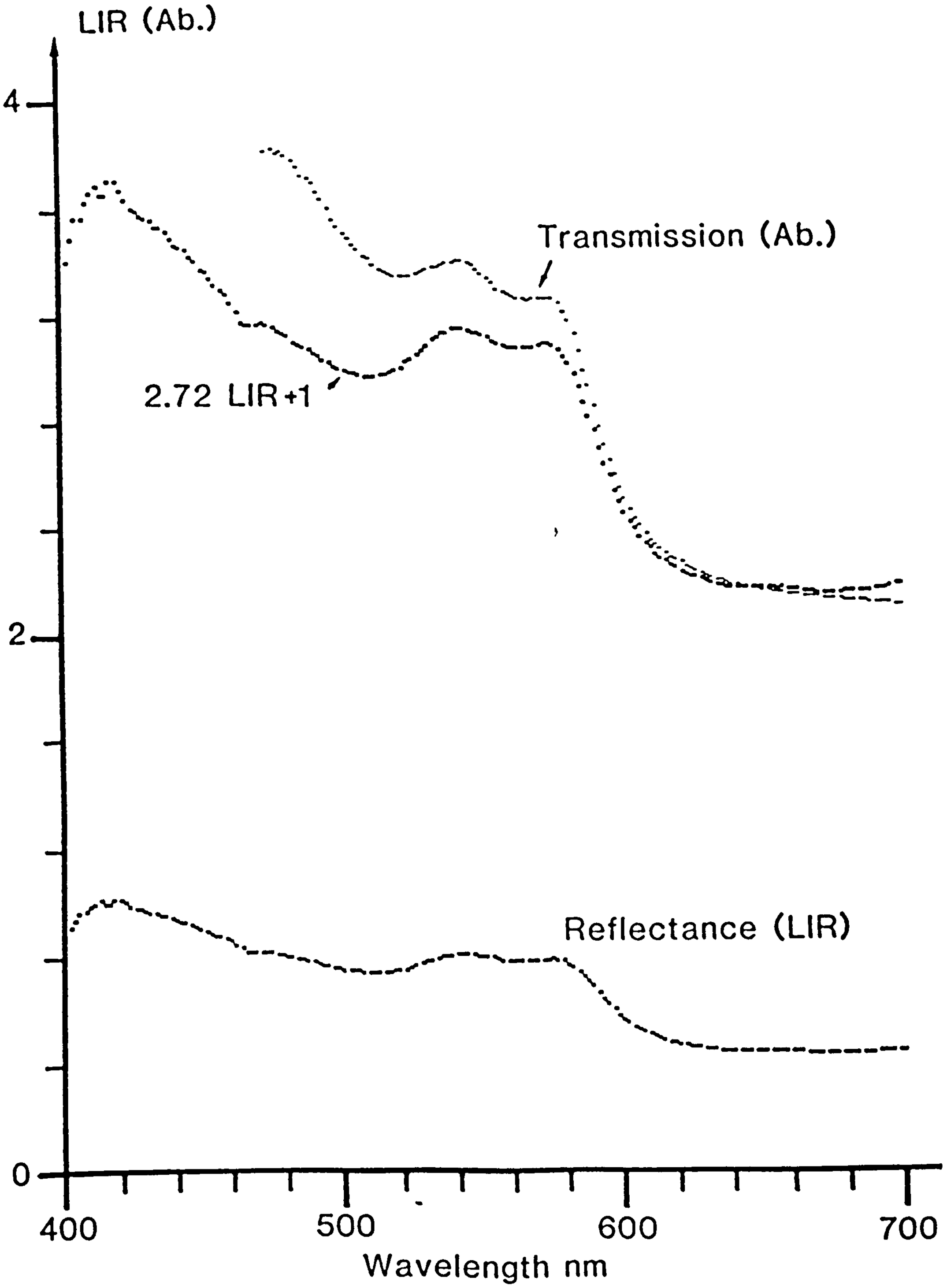

Fig. 6.10- Comparison between LIR and absorbance spectra of an ear lobe (0.375 cm thick).

measurement modalities and then a constant value (+1) is added to all LIR to overlap the transmission spectrum at long wavelengths, as shown in Fig 6.10. It can be seen that the absorbance spectrum is steeper than the corrected LIR spectrum. This may be attributed to the effects of wavelength dependent scattering in the dermis which will decrease the LIR and increase the absorbance value. Increases in the scattering at shorter wavelengths will increase the back scattered 'stray' light which causes the LIR to be decreased. The transmitted light would then decrease due to increase in the path length of light which increases the absorption and also causes some light to be lost.

A parameter, the half value layer ($t_{1/2}$), of the tissue may be used to quantify the effect of scattering and absorption in the dermis. The half value layer is the thickness of a layer required to reduce the light intensity passing through it to one half. It will be decreased by increasing the absorption and scattering coefficients of the medium. The transmission of a medium as a function of the half value layer can be written as:

$$T_{(t)} = 2^{-t/t_{1/2}} \qquad 6\text{-}19$$

where "$T_{(t)}$" is the transmission of a layer of thickness "t" and "$t_{1/2}$" is the thickness of the half-value layer. The absorption coefficient of blood in tissue and the scattering in the dermis increases as the wavelength decreases. The in-vivo half value layer of tissue will therefore decrease at short wavelength.

6-6-1 Estimation of half value layer, average penetration depth, and fractional blood volume in skin

A) Half value layer

The in-vivo half value layer can be calculated from the absorbance spectrum of the ear lobe (t = 3.75 mm) with the following formula:

$$\text{Half value layer (mm) } t_{1/2} = \frac{t.\text{Log}2}{\text{Ab.}} = \frac{1.129}{\text{Ab.}} \qquad 6\text{-}20$$

where "Ab." is the absorbance measured by transmission of light through an ear lobe. It consists of attenuation both by scattering and absorption in the skin. The results between 500 nm to 700 nm are presented in Fig 6.11. For wavelengths shorter than 480 nm no transmitted light could be detected.

B) Average penetration depth

To estimate the average penetration depth of light in skin, first the haemoglobin index and oxygenation of an ear lobe were computed, using 15 successive measurements of LIR and absorbance spectra. These values and their standard deviations are shown in Table 6.2.

By assuming a uniform distribution of blood throughout the ear tissue, the haemoglobin index per mm of tissue in transmission measurement is 0.3, which is almost equal to the haemoglobin index measured by reflection. Hence, one can deduce that in reflectance measurement the average light path length in the ear is almost 1.08 mm at those wavelengths around 550 nm that are used for calculating the haemoglobin index. The reflected light from within the tissue is the back scattered radiation from various depths and the average penetration depth of radiation is defined as half the average light

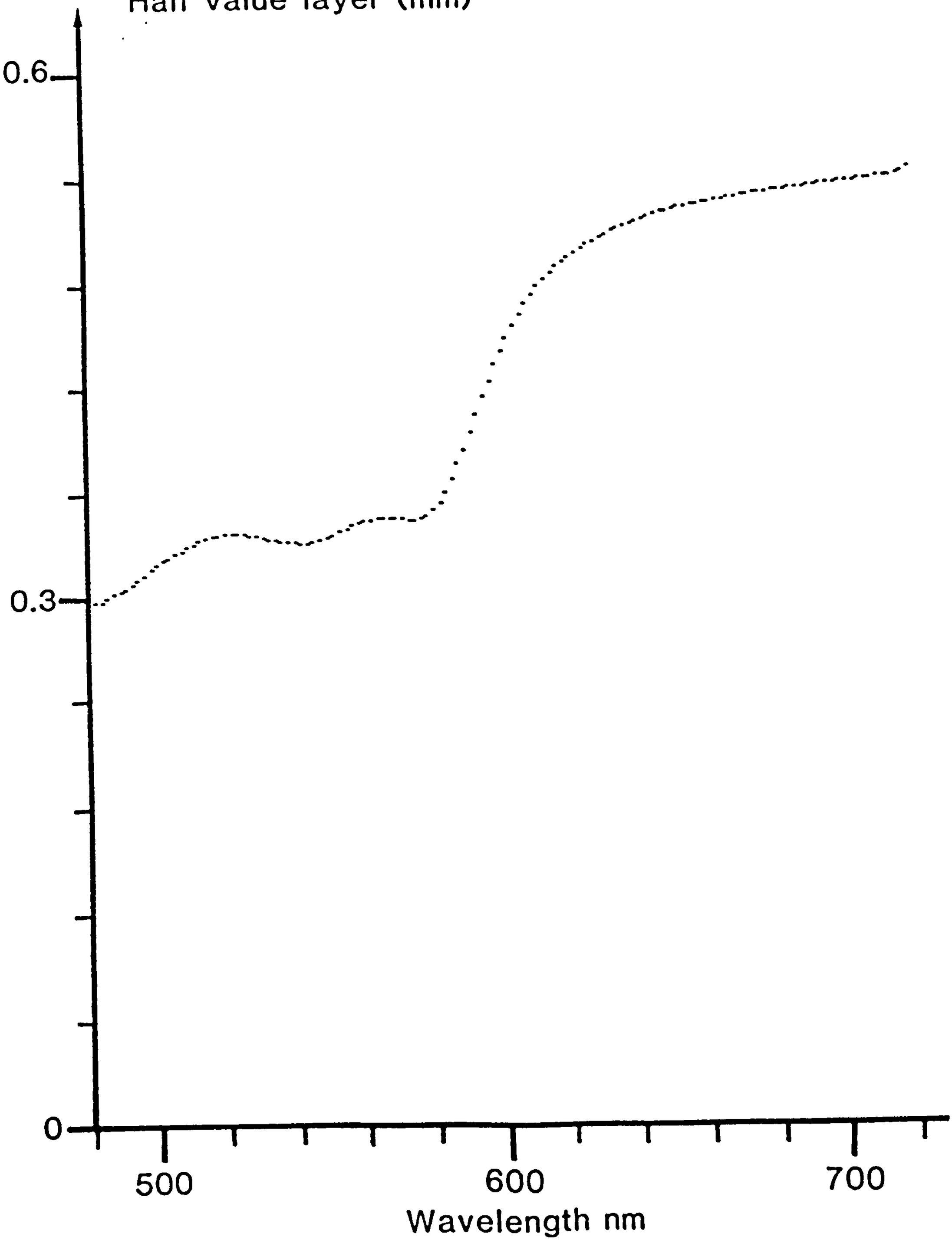

Fig. 6.11- In-vivo half value layer calculated from the transmission spectrum of an ear lobe (3.75 mm thick).

Table 6.2- Haemoglobin index and oxygenation of an ear lobe measured by transmission and (t =3.75 mm) reflection spectroscopy.

	H index (Ab./nm) Mean ± S.D.	Oxygenation % Mean ± S.D.
Transmission	1.12 ± 0.18	95.7 ± 8.7
Reflectance	0.32 ± 0.03	86.2 ± 6.2

path length. Therefore, wavelengths around 550 nm have an average penetration depth of 0.54 mm in the ear tissue. This value can be verified by using the results of in-vitro LIR measurement of diluted blood samples and assuming that the blood occupies 1.2% of the tissue volume. The in-vitro haemoglobin index measured from the LIR spectra of a sample of 4% diluted blood (2% red cells in 0.9% saline) in a 1.166 mm thick cuvette is 2.21 (Table 5.4). Hence the in-vitro haemoglobin index per mm of whole blood is 47.4 (2.21/1.166x0.04). Therefore, the value 0.32 which was obtained from in-vivo LIR measurement (Table 6.2), indicates that a thickness of 6.7×10^{-3} mm of whole blood was sampled. This thickness is equivalent to 0.56 mm tissue if blood occupies 1.2% of the tissue volume.

The average depth of penetration of 0.5 mm indicates that the oxygen saturation, as measured by reflectance spectroscopy, is the oxygen saturation of the superficial blood present in the capillaries of the papillary dermis. Oxygen saturation measured by transmission spectroscopy would be the oxygen saturation of deeper blood. Table 6.2 implies that the oxygen saturation of superficial blood is lower than that of deeper blood and may be attributed to the slower blood flow in capillaries than in the deeper arterioles and venules.

C) Fractional blood volume in skin

The in-vivo haemoglobin index, as measured by transmission of light through 3.75 mm of an ear lobe is 1.12, which is equal to the in-vitro haemoglobin index, measured by transmission of light through 1.16 mm of 4% diluted oxygenated blood (2% red cells) in 0.9% saline. By assuming that blood is uniformly distributed throughout the tissue, a thickness of 0.046 mm (1.16x0.04), would be required to give the same haemoglobin index from undiluted blood. This means that at the

most only 1.2% (0.046/3.75) of the tissue volume in the ear lobe is occupied by blood. No estimate of the blood content of human skin has been made in the literature, but the total blood of the skin for rats and mice has been quoted as varing from 19 to 30 µl/g wet tissue (Altman 1958). These figures, which are about 1.9% to 3%, are close to the 1.2% measured for human skin.

6 - 7 Summary and conclusions

In this chapter some instrumental improvements for the in-vivo measurement of skin reflectance have been described. Two different methods for excluding specularly reflected light from the measured signal were suggested. One is the suppression of specular reflection and the other is the use of polarised light. In practice the polariser method is easier and more reliable. Further, the collecting fibre can be mounted at any angle in the reflectance probe. A study was then undertaken to determine the best collection angle, to maximise the signal from the diffusely reflected light from within the skin. This study led us to design a new reflectance probe as shown in Fig. 6.5.

The reflected signal from a skin surface might change due to changes in the biological condition of the measurement site, such as temperature, blood pressure or any movement in the reflectance probe during each measurement. Hence, the stability of the indices against random variation in the reflected signal was studied. The coefficients of variation of the haemoglobin index and oxygen saturation were calculated from equation 6.14 and 6.16 in terms of any variation in the reflected signal; errors of the order of 8 and 9% were observed.

The transmission of light through epidermis and dermis was

studied. Epidermis has two important effects on the radiation passing through it: a) absorption of light by melanin and b) scattering by cells or membranes. The scattering properties of epidermis were studied by measuring the angular distribution of light scattered by a sheet of epidermis. The scattered radiation was forwardly orientated and wavelength dependent.

In dermis with a thickness of 1 mm or more scattering is complete and follows Lambert's law. The transmittance of dermis has a wavelength dependence which may be attributed to two different effects. One is the wavelength dependence of scattered radiation passing through the epidermis, and the other is the effect of the combination of absorbance and scattering in the dermis at shorter wavelengths. The latter effect was explained in terms of the half-value layer. The half-value layer at shorter wavelengths is decreased due to the increase in the specific absorption coefficient of blood and also to the increase of scattering in the dermis. An in-vivo estimation of the thickness of the half value layer between 500 -700 nm was shown in Fig 6.11.

Finally, it is concluded from in-vivo reflectance and transmission measurements of an ear lobe, that in reflectance measurements the average penetration depth of radiation (550 nm) in tissue is about 0.5 mm. Therefore, the oxygen saturation observed by reflectance measurement is that of superficial blood. This was found to be less than the oxygen saturation of deeper blood, and was attributed to the slower blood flow in the capillaries than in the deeper arterioles and venules. It was also shown that not more than 1.2% of the tissue volume in the ear lobe is occupied by the blood.

CHAPTER 7

7 - IN-VIVO MEASUREMENT OF SKIN INDICES

To test the instrumentation, the validity of the indices and their usefulness in quantifying "skin colour" changes, a series of in-vivo measurements were made. Their results are discussed in this chapter. An additional index, a melanin index will be introduced in this chapter. The dependence of the melanin index upon the haemoglobin and oxygen saturation of blood in skin, and the melanin pigmentation levels of different ethnic groups will be presented. The haemoglobin index and oxygen saturation of superficial blood under various conditions will then be discussed. The effect of the application of a topical vasodilator chemical on the cutaneous blood content and its oxygen saturation will be reported as will the results of a study on the amount of superficial blood at different body sites. Finally, an evaluation of the suitability of the reflectance spectrophotometer for measurement of the haemoglobin in terms of g/dl blood will be presented.

7 - 1 Melanin index

Erythema, increased blood volume in the superficial and deep vascular plexi in the dermis, has been widely used as an indication of inflammation in the study of cutaneous response to UV radiation. Skin colour is an important factor in determining erythemogenesis, and the detectability of erythema varies according to the degree of constitutive or facultative pigmentation present. Resistance to the induction of erythema by UV radiation is conferred by both racial pigmentation and by facultative tanning. Fair-skinned people require 3

to 4 times less UVB (290 -320 nm) radiation to induce erythema than people with moderately pigmented skin and up to 10 times less than people with darkly pigmented skin. Four weeks of intensive UVB radiation treatment for psoriasis can cause an eight fold rise in minimum erythema dose MED (Cripps 1981). This photoprotective effect of tanning is partly the result of increased cutaneous melanin and partly the result of increased thickness of the stratum corneum. An objective measurement of the melanin level present in the skin could be a useful factor to be used in determining the end point of the therapeutic UV radiation dosage given to -different coloured skin during the course of treatment.

In addition to the haemoglobin index and oxygenation, a melanin index can be derived from the reflection spectrum of the skin surface. The absorption spectrum of melanin in the visible spectrum (400 -700 nm) is a smooth, gradual curve without any peak (Fig 7.1). The melanin index is defined as a function of the slope of the melanin absorption spectrum by the following formula:

$$M_{\bar{\lambda}} = \frac{\Delta A_L}{\Delta \lambda} \qquad 7\text{-}1$$

"$M_{\bar{\lambda}}$" is the melanin index at average wavelength "$\bar{\lambda}$" of two defined wavelengths, "ΔA_L" is the difference in LIR value of the two wavelengths, and "$\Delta \lambda$" is the difference between those wavelengths. Dawson et al (1980) used 650 and 700 nm to calculate the melanin index. It can also be calculated at the haemoglobin peak (about 540 nm).

The in-vivo absorption spectrum of melanin can be determined by measuring the reflectance spectrum of an unpigmented skin and

subtracting it from the pigmented one with the same amount of haemoglobin, ie. equal H index. Figure 7.1 shows the absorption spectra of a synthetic melanin compound and of in-vivo melanin measured from a Negro and an Indian skin. A layer of pig fat, with its residual haemoglobin, a few mm thick, was used as an unpigmented sample. To obtain the in-vitro spectra sample of 0.35 g/l synthetic melanin compound in 0.05% NaOH was prepared and the LIR spectrum of that was measured using a 1 mm thick cuvette. The LIR values of the synthetic melanin spectrum were then multiplied by 1.6 to give the same slope in the spectral range 500 -700 nm as that of the in-vivo Negro skin and by 0.75 for the Indian skin. LIR values at short wavelengths (400- 500 nm) in all spectra were decreased due to the effect of stray light. The upward displacement of the in-vivo spectra may be attributed to the scattering properties of the pigmented and unpigmented skin.

Two different approaches to the in-vivo measurement of a melanin index are discussed below. The purpose of these approaches is to derive a melanin index that is independent of cutaneous blood and its oxygenation.

Option 1) Since the calibration curves of both absorbance and haemoglobin index against red cell concentration are linear and pass through the origin, their ratio will be constant and independent of the concentration or amount of blood, but will be dependent upon the oxygenation state of haemoglobin. For any in-vitro measurement of a blood sample:

$$Y(\lambda,oxy) = \frac{H}{A_{b,\lambda}} \qquad 7\text{-}2$$

where "H" is the haemoglobin index, "$A_{b,\lambda}$" absorbance by blood at

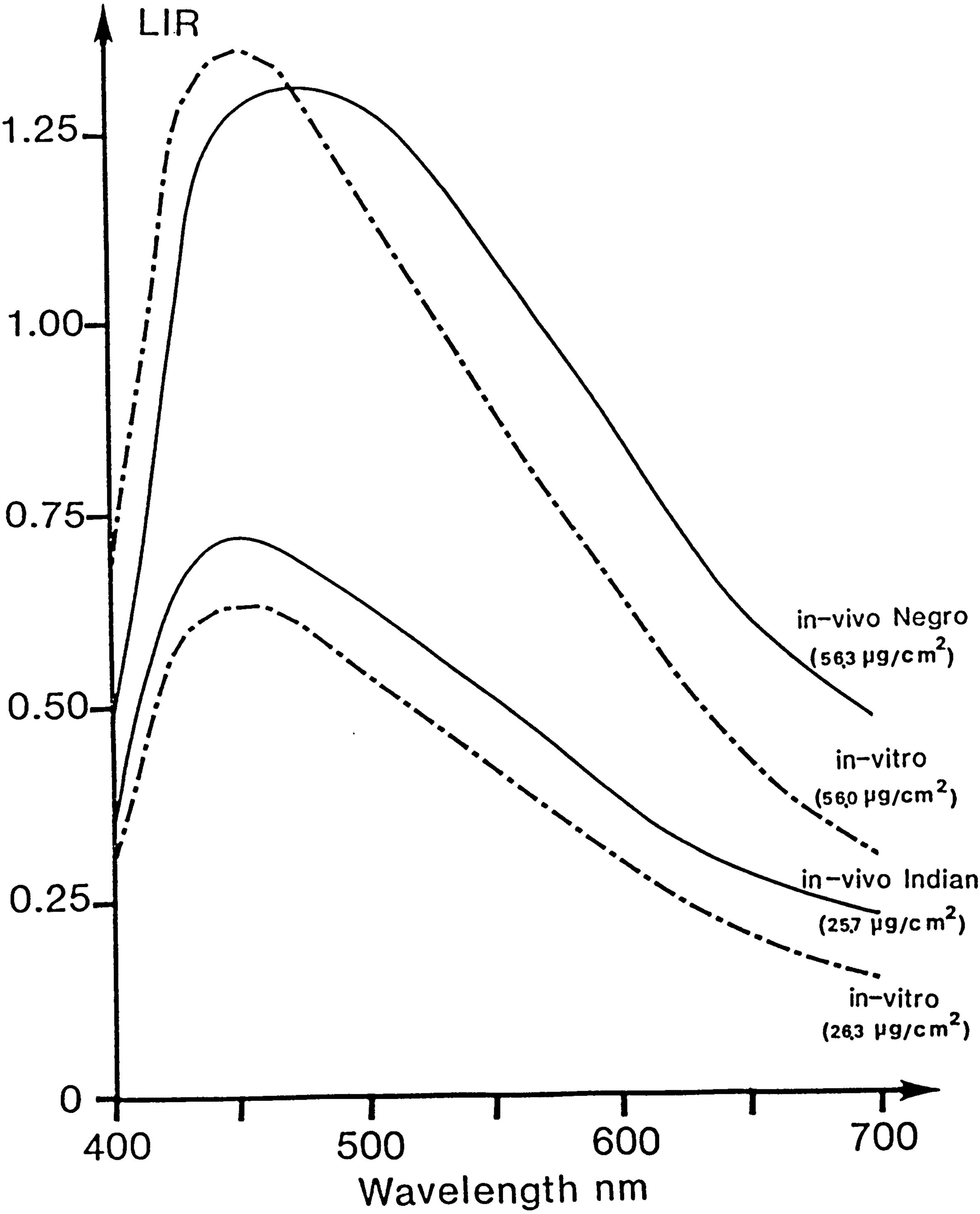

Fig. 7.1- LIR spectra of melanin; full line) in-vivo spectra (difference between LIR of two pigmented skins and LIR of pig fat); broken line) spectra of synthetic melanin compound in 0.05% NaOH.

wavelength "λ" and "Y" is a constant for each wavelength and oxygenation state of blood. The LIR of in-vivo skin ($A_{s,\lambda}$) at wavelength "λ" consists of absorbance by subcutaneous blood ($A_{b,\lambda}$), melanin ($A_{m,\lambda}$) and an effective absorbance due to scattering of light out of the field of view of the detector "U_λ". They are related as follows:

$$A_{s,\lambda} = A_{b,\lambda} + A_{m,\lambda} + U_\lambda \qquad 7\text{-}3$$

The absorbance (LIR) of subcutaneous blood can be calculated from:

$$A_{b,\lambda} = \frac{H_s}{Y_{(\lambda,oxy)}} \qquad 7\text{-}4$$

where "H_s" is the in-vivo haemoglobin index of the skin and $Y_{(\lambda,oxy)}$ is calculated for each wavelength from in-vitro data using equation 7.2, and provided that the in-vitro sample has the same oxygenation as subcutaneous blood. Assuming that the oxygenation of blood is "X", then equation 7.2, for wavelengths more than 580 nm (the isobestic point at the longest wavelength in the visible region), can be written as:

$$Y_{(\lambda,oxy)} = H/\{(1 - X/100)(A_{d,\lambda} - A_{o,\lambda}) + A_{o,\lambda}\} \qquad 7\text{-}5$$

$A_{o,\lambda}$ and $A_{d,\lambda}$ are the LIR values for fully oxidised and reduced samples respectively at wavelength "λ". By subtracting equation 7.3 for two different wavelengths, the melanin index ($M_{\bar{\lambda}}$) at the mean wavelength "$\bar{\lambda}$", can be calculated from the following formula:

$$M_{\bar{\lambda}}\Delta\lambda = (A_{m,\lambda} - A_{m,\lambda'}) \qquad 7\text{-}6$$

$$= (A_{s,\lambda} - A_{s,\lambda'}) - (A_{b,\lambda} - A_{b,\lambda'}) - (U_\lambda - U_{\lambda'})$$

Since the component of absorbance due to light lost within the tissue, mostly by scattering, is nearly constant for small differences between wavelengths, $(U_{\lambda} - U_{\lambda'})$ is approximately zero and by substituting 7.4 and 7.5 in 7.6 gives:

$$M_{\overline{\lambda}} = \frac{(A_{s,\lambda} - A_{s,\lambda'})}{\Delta\lambda} - \{(1 - \frac{X}{100}) [(A_{d,\lambda} - A_{d,\lambda'}) - (A_{o,\lambda} - A_{o,\lambda'})] + (A_{o,\lambda} - A_{o,\lambda'})\} \times \frac{H_s}{H\,\Delta\lambda} \qquad 7\text{-}7$$

By substituting the in-vitro haemoglobin index (H) and the absorbances of 100% oxy and deoxy haemoglobin at 650 and 700 nm in equation 7.7, an expression for a corrected melanin index at the mean wavelength (675 nm) is created as below:

$$M_{\overline{675}} = \{(A_{s,700} - A_{s,650})/50 + [.062(1 - X/100) + .0098] \times H_s/82.3\ \} \times 100 \qquad 7\text{-}8$$

Option 2) An alternative basis for obtaining a corrected melanin index is by using the isobestic points of the haemoglobin spectrum instead of correcting the melanin index for oxygenation. For isobestic points "Y" in equation 7.2 is not dependent on oxygenation and hence equation 7.7 for isobestic points is modified to:

$$M_{\overline{\lambda}'} = \frac{(A_{s,\lambda} - A_{s,\lambda'})}{\Delta\lambda} - \frac{(A_{\lambda} - A_{\lambda'})}{\Delta\lambda} \times \frac{H_s}{H} \qquad 7\text{-}9$$

By using the two isobestic points at 573 and 500 nm in equation

7.9:

$$M_{\overline{536}} = \frac{(A_{s,573} - A_{s,500})}{73} - \frac{(A_{573} - A_{500})}{73} \times \frac{H_s}{H} \qquad 7\text{-}10$$

"$A_{s,\lambda}$" is the LIR value of skin at wavelength "λ", and "$A\lambda$" is the in-vitro absorbance of blood sample at the isobestic points with the wavelength λ, "H_s" and "H" are the haemoglobin indices of skin and in-vitro blood samples respectively. By substituting in eqtn. 7.10 the in-vitro value of the haemoglobin index and LIR at wavelengths 573 and 500 nm a simple expression for melanin index is created as follows:

$$M_{\overline{536}} = \{(A_{s,573} - A_{s,500})/73 - .0036H_s\} \times 100 \qquad 7\text{-}11$$

The melanin index, as defined in eqtn 7.8 and 7.11, is slightly positive for unpigmented skin due to wavelength dependence of scattering, and becomes negative for pigmented skin. Since the in-vivo LIR spectrum of melanin is similar to that in-vitro (Fig 7.1), melanin indices could be expressed in terms of the amount of synthetic compound in the unit area of the surface. To achieve that, consider the in-vivo melanin spectrum of black skin in Fig 7.1, the corresponding synthetic melanin concentration (c=0.560 mg/ml), and the cuvette thickness (t=0.1 cm) are known. Therefore, the amount of melanin per unit area could be calculated from the following formula:

$$\text{Melanin } (\mu g/cm^2) = \frac{c\ t}{M_s} (M_{\overline{\lambda}} - M_w) \qquad 7\text{-}12$$

where "$M_{\overline{\lambda}}$" is the melanin index of the subject under

investigation (measured from eqtn 7.8 or 7.11), "M_w" is the melanin index of unpigmented sample and "M_s" is the slope of synthetic melanin compound at the same wavelength as the melanin indices. "M_w" measured from a layer of pig fat is 0.0744 and 0.0541 using eqtn 7.11 (536 nm) and 7.8 (675 nm), and "M_s" is -0.9886 and -0.4702 at those wavelengths respectively. Substituting eqtn 7.8 and 7.11 in 7.12 with the corresponding values will give the following formula:

$$\text{Melanin } (\mu g/cm^2) = -56.6(M_{\overline{536}} - 0.0744) \qquad 7.13$$

$$\text{Melanin } (\mu g/cm^2) = -119.1(M_{\overline{675}} - 0.0541) \qquad 7\text{-}14$$

The amount of melanin ($\mu g/cm^2$) for the Negro and Indian skin (Fig 7.1) were calculated from eqtns 7.13 and 7.14 and compared with the corresponding synthetic melanin compound in Table 7.1.

Although a melanin index measured at 536 nm is more sensitive than one measured at 675 nm, because the LIR spectrum of melanin is steeper, it can be seen that for in-vivo measurements it gives a lower estimate of the melanin content. This is because scattering in the skin is wavelength dependent and increasing the scattering at short wavelength increases the stray light which decreases the slope of the LIR spectrum. However, in-vivo melanin can be measured at 675 nm by means of equation 7.14. The independence of this index upon the haemoglobin and oxygen saturation of blood in skin, and also the melanin pigmentation levels of different ethnic groups will be presented in the next section.

Table 7.1- Comparison between measurements of in-vitro synthetic melanin and in-vivo melanin of Negro and Indian skin at two wavelengths.

	In-vitro synthetic ($\mu g/cm^2$)	In-vivo ($\mu g/cm^2$)	
		675 nm	535 nm
Negro	56.0	56.3	37.5
Indian	26.3	25.7	20.4

7-1-1 Measurement of the melanin index

To examine the independence of this index with respect to changes in the haemoglobin content and oxygen saturation of blood in the skin, LIR spectra of a volunteer's forearm were measured at different heights relative to the heart. The height of the measurement site on the inner forearm, 15 cm from the wrist, are quantified relative to the horizontal plane passing through the heart. Positive value indicates that the measurement site is raised, and negative values are used for lowering the arm. Raising or lowering the limb alters the blood content of the skin and its oxygenation. The average haemoglobin, oxygenation and melanin content ($\mu g/cm^2$) were calculated from ten successive measurements at +45, 0, -15, -25, and -45 cm and plotted in Fig. 7.2a. It can be seen that changes in the haemoglobin index from 0.125 (raised arm) to 0.605 (lowered arm) and nearly 46% variation in oxygenation (from 62% to 16%) have only a small effect on the melanin index. This experiment was repeated by measuring 24 successive LIR spectra from a raised forearm (+30 cm) that was lowered almost 3 cm after each measurement down to position -30 cm, followed by rapid raising to position +30 cm for the last three measurements. The results are shown in Fig. 7.2b. In this series of measurements the haemoglobin index changed from 0.16 (raised arm) to 0.4 (lowered arm) and on raising returns to its original value. The observed oxygenation increased in the first six successive measurements of the raised arm, which may be due to draining of the deoxy blood out of the arm. It tends to decrease as the arm is lowered but because the skin surface becomes slightly warm due to keeping the reflection probe on the skin surface throughout the measurement time (3 minutes), it remains at a higher level than in previous measurements when the probe was only placed on the arm for short measurement periods. In all these

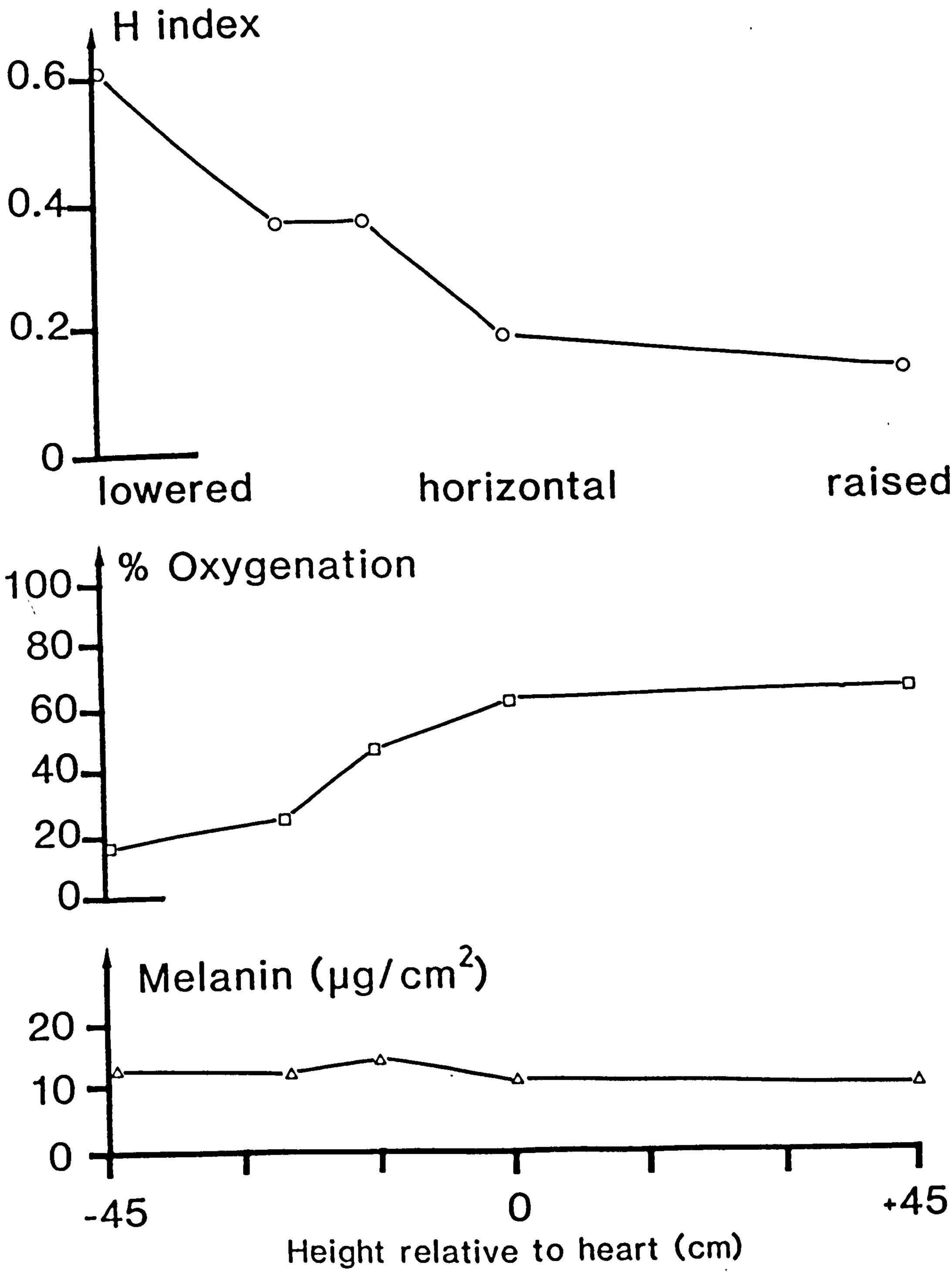

Fig. 7.2a- Haemoglobin index, oxygenation and melanin content of a forearm at different heights relative to the heart.

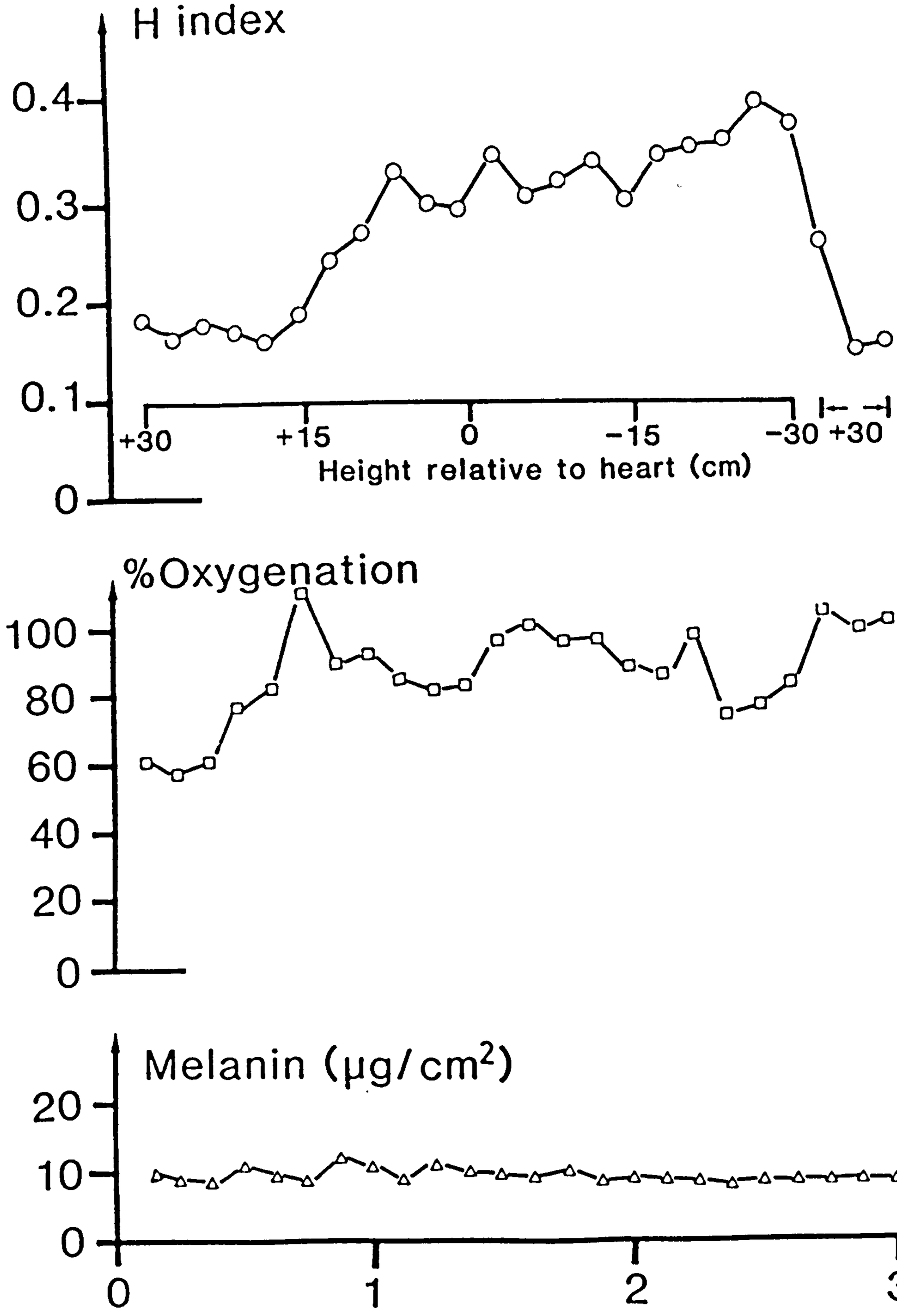

Fig. 7.2b- Haemoglobin index, oxygenation and melanin content of a raised forearm (+30 cm) that was lowered down to -30 cm relative to the heart, followed by rapid raising to its original position.

measurements the melanin content ($\mu g/cm^2$) remained almost constant and independent of changes in skin blood content and its oxygenation.

Two further experiments were carried out to assess the sensitivity of the melanin index. First, different sites on a hand of a single subject were measured and second, the melanin content ($\mu g/cm^2$) of several subjects with different racial pigmentation was measured and compared.

In the first approach, five successive LIR spectra of the finger tip, palm, forearm, dorsum of hand, and backarm of an Asian and two African subjects were measured. The average values of the haemoglobin index, oxygenation and melanin content ($\mu g/cm^2$) are plotted in Fig. 7.3. It can be seen that the melanin content measured at forearm, dorsum of hand, and backarm of the Asian subject is nearly the same as that measured at finger tip and palm, while it has increased almost three fold in the African subjects.

In the second approach, ten successive LIR spectra of the forearm of several subjects with different endogenous pigmentation were measured. All subjects were healthy male volunteers, aged between 21 and 35 years old. They have lived in U.K. for at least the previous six months, consequently it was assumed that they had received little exposure to UV radiation. Therefore it was hoped that the melanin pigmentation measured was the genetically determined level of melanin present in the absence of stimulation by environmental UV radiation. The average haemoglobin index, oxygenation and melanin content was calculated for each subject. The subjects were grouped in terms of their country of birth as a cold, medium, and hot country. The average of haemoglobin index, oxygenation, and melanin content of each group is calculated and shown in Table 7.2. A systematic decrease in H index and oxygenation with increase in melanin pigmentation could suggest

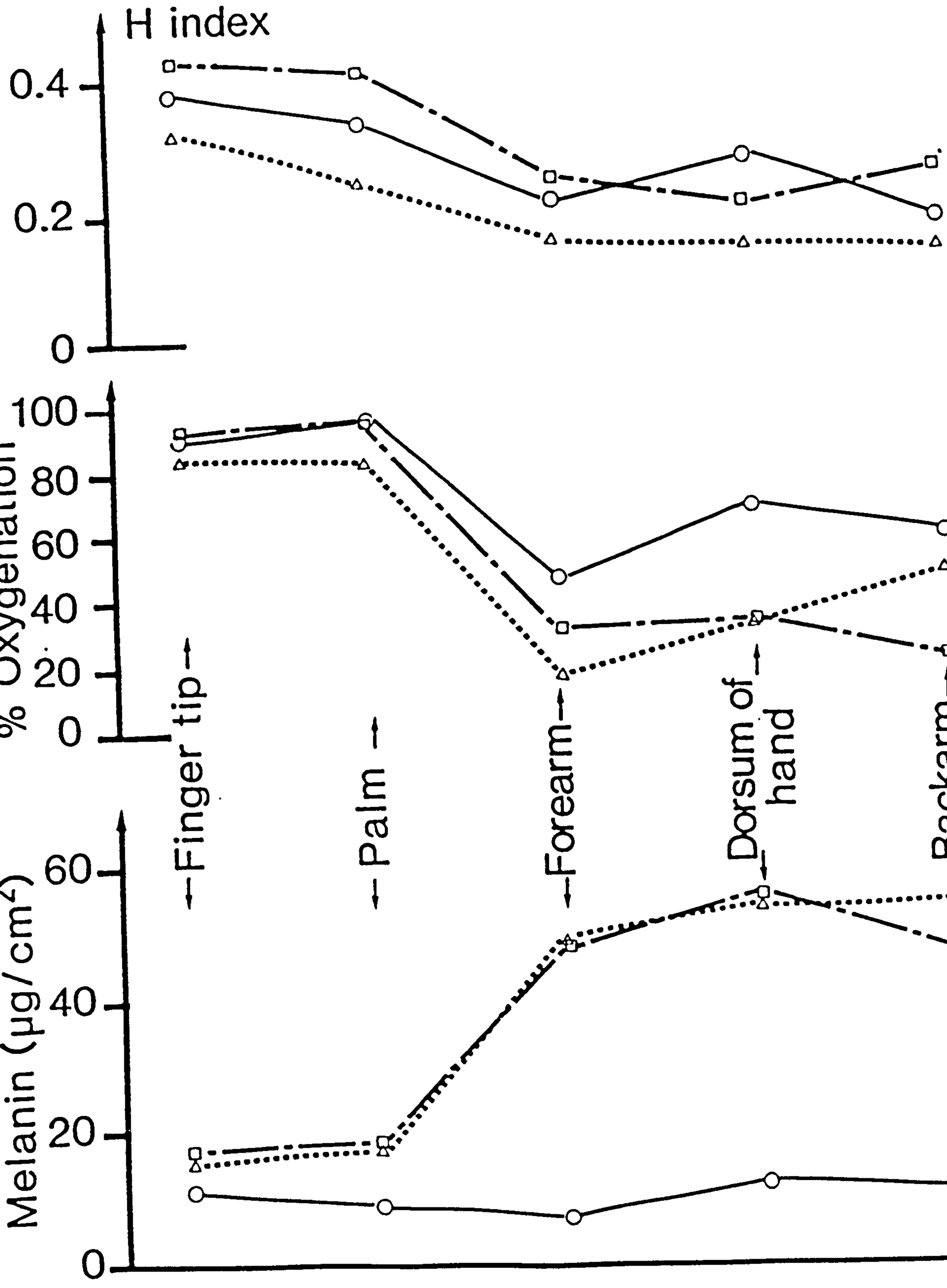

Fig. 7.3- Haemoglobin index, oxygenation and melanin content of different sites on a hand of an Asian (full line) and two African (broken line) subjects.

Table 7.2- Average haemoglobin index, %oxygenation and melanin content ($\mu g/cm^2$) measured from the forearm of different skin pigmented subjects.

Country of origin	H index Mean ± S.D.	% Oxygenation Mean ± S.D.	Melanin Mean ± S.D.
Cold (Caucasian)	0.220 ± 0.035	38.9 ± 9.2	6.3 ± 2.31
Medium (Indian)	0.207 ± 0.038	36.9 ± 10.8	10.1 ± 1.65
Hot (Negro)	0.186 ± 0.027	27.5 ± 3.7	47.2 ± 2.03

that melanin affects the haemoglobin index and oxygenation. But it does not seem likely to be the case because, firstly, the H index and oxygenation is very much dependent on the measurement conditions which might not be exactly the same in all of these measurements. Secondly, the differences between H index and oxygenation values are comparable with standard deviation of the measurements.

Feather (1986) introduced a melanin index based on the slope of the LIR spectrum of skin surface between 650 nm and 700 nm. He measured the melanin pigmentation of seven sites (thigh, palm, nail, forearm, shin, sole, and forearm) on 30 subjects with four different ethnic groups (Caucasian, Chinese, Indian and Negro). The ratio of the average of all sites of Negro to Caucasian is 8, which is the same as that measured from the forearm in this study. Large differences in cutaneous melanin content between peoples (6.3 -47.2 $\mu g/cm^2$) is generally believed to be related to the adaptation of man to his environment. Many theories have been advanced to explain the biological significance of melanin pigmentation in man. Thermoregulation, vitamin D3 regulation via cutaneous photosynthesis, and protection from solar UV radiation has been reviewed by Feather (1986). Since the solar energy received to the earth's surface is latitude dependent, the possible relationship between melanin pigmentation and the native geographical region of the ethnic groups was investigated. The melanin content of the subject is plotted against the latitude of their family origin in Fig. 7.4a. A non-linear dependance between melanin content and latitude can be seen.

7-1-2 Ethnic / latitude effect

It is widely accepted that the major function of melanin in skin is to provide protection from the acute and chronic effects of sunlight. This belief has been strengthened recently by

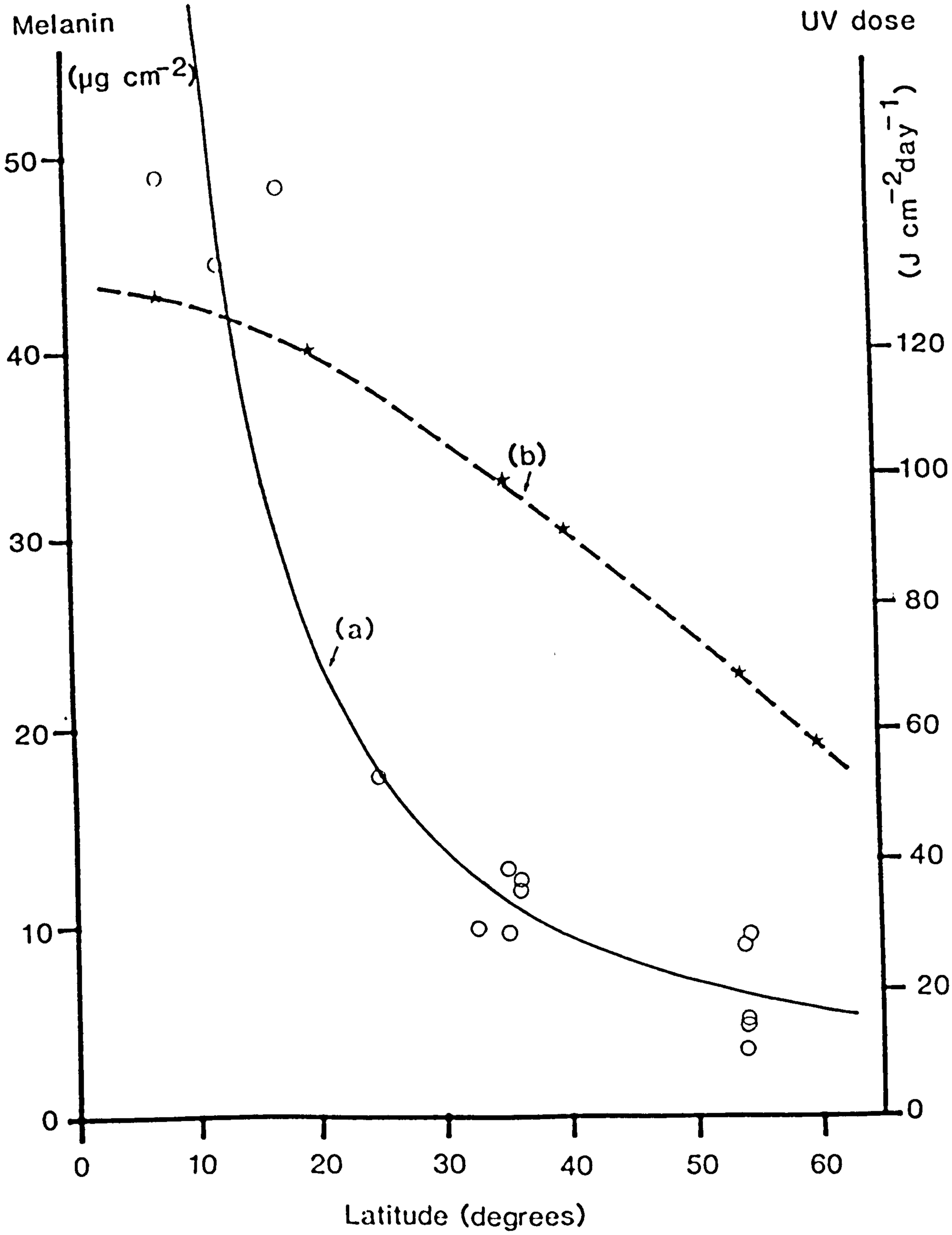

Fig. 7.4a- Latitude dependence of: a) melanin content (μg/cm^2), b) average annual UV dose (J cm^{-2} day^{-1}).

epidemiological studies which strongly support the role of sunlight in the induction of skin cancer. Among equally pigmented persons skin cancers are more common in those regions of the world that receive most sunlight and they occur predominantly on light exposed areas of the body such as the head and neck (Feather 1986).

Since the melanin content is quantitatively measured by the present method, we studied possible relationships between the melanin index and external characteristics of the native geographical regions of the ethnic groups, such as the average annual UV dose, ambient temperature and cutaneous blood flow.

Feather (1986) studied the dependence of the melanin on the native geographical latitude of four groups with different levels of melanin pigmentation. He assumed that the total number of absorbed photons by blood determines the degree of damage to the red cells, and not the rate at which they are absorbed, and hence expected that the melanin index would be linearly proportional to the logarithm of the annual UVB dose. He found, however, that the melanin index increases more rapidly than would be required to control the annual radiation dose to a constant vulnerable target tissue. Therefore, he concluded that further latitude dependent factors such as temperature play a part in the geographically determined levels of melanin pigmentation.

A possible explanation of the high melanin content of the Negro is that, with increasing ambient temperature, the body attempts to lose heat by firstly, before the onset of sweating, increasing the cutaneous blood flow and redistributing the blood to the upper dermis, to increase convectional heat exchange with the environment. Since UV radiation penetrates only to the upper dermal levels, then this redistribution of blood could greatly increase the amount of blood exposed to light, particularly the shorter wavelength, less

penetrating UV radiation. If blood is the target tissue then an increase in melanin with increasing ambient temperature would be required to provide the necessary level of protection.

The average annual dose of UV radiation (sum of UVA and UVB) at the earth's surface and the average annual temperature at different latitudes were calculated and plotted in Figs. 7.4a and 7.4b respectively. Data for UV radiation was calculated from the formulae of Diffey (1977), and the data for the temperature was derived from Philip (1946). Based on these ambient temperatures the average blood flow at each latitude was estimated using the data provided by Fetcher et al (1949). These workers measured the blood flow in a finger, using a plethsmographic method, at different ambient temperatures (7, 21 and 32 ^{o}C). Figure 7.4b shows the calculated skin blood flow against latitude. It can be seen that the blood flow and the measured melanin content of different ethnic subjects against their native latitudes follow almost the same pattern. The ratio of blood flow to melanin content (Bf/M) and the inverse of the melanin content (1/M) for different latitudes are calculated and plotted in Fig 7.5. They are seen to be linearly related to the latitude. This observation is consistent with the early work done by Feather (1986) and supports the hypothesis that melanin pigmentation is an evolutionary development to protect blood from UV radiation.

7 - 2 In-vivo measurement of the haemoglobin index and oxygen saturation

As was shown earlier (chapter 6), our reflectance spectrophotometer measures superficial blood i.e. blood lying less than approximately 0.5 mm below the skin surface. Physiological factors affecting the measured indices will now be examined.

The effects of temperature and of the height of the measuring

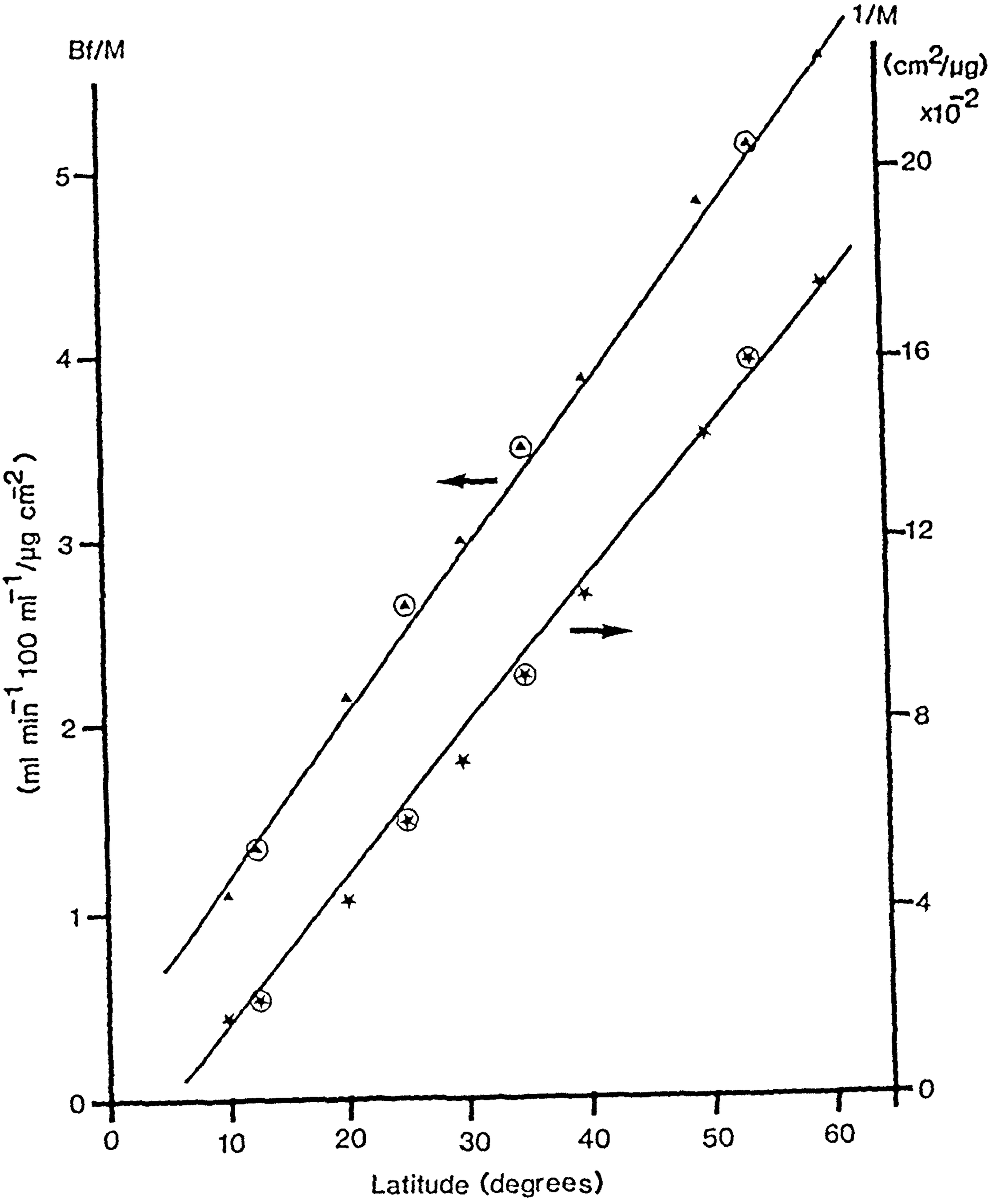

Fig. 7.5- Ratio of blood flow to melanin content (Bf/M) and inverse of melanin (1/M) against latitude. (circled points are those in which the melanin was measured experimentally).

site · relative to the heart on the amount and oxygen saturation of superficial blood in the skin surface were studied by measuring the haemoglobin index and oxygen saturation of a forearm. The heights of the measurement sites are quantified relative to the heart as described in section 7.1.1. Table 7.3 shows the average values from 14 successive measurements of a forearm under seven different conditions. Firstly, the arm was held horizontal to maintain the blood content of the tissue constant. The blood content and oxygenation of the arm was then altered by slapping, cooling, heating, and lowering or raising the limb. The values shown for the horizontal arm (H= 0.1514, Sa O_2= 44.9%) were measured with the arm resting on a bench at the same height as the heart. Holding the arm lower than the heart (-45 cm) causes the blood to pool in the tissue and become deoxygenated. This effect is shown in Table 7.3 by an increase in the "H" index and a decrease in oxygenation (ΔH= +0.224, ΔSa O_2= -25.4%). Raising the arm (+45 cm) causes the deoxy blood to drain out and oxy blood to flow in due to the higher arterial blood pressure. Hence, a decrease in the haemoglobin index and an increase in oxygen saturation is observed (ΔH= -0.064, ΔSa O_2= +29.7%). Cooling the surface of the skin causes the blood supply to decrease and the level of oxygenation falls but on cooling further the skin surface become visually red and more oxygenated blood is supplied. In this experiment the skin surface was cooled by a plastic bag filled with cold water (10 - 12 °C) which was placed on the skin surface around the reflection probe. Variation in the haemoglobin index (ΔH=+0.042) and oxygenation (ΔSa O_2= -3.1%) was not noticeable. The skin surface was further cooled by placing a piece of ice on the arm separated from the skin by a plastic sheet to keep the arm dry. In this case increase in the haemoglobin index and oxygenation (ΔH= +0.121, ΔSa O_2= +59.2%) confirms that more

Table 7.3- Forearm skin indices measured under different conditions (room temperature 23 ^{o}C).

condition of the thumb	height relative to heart, cm	haemoglobin index Mean ± SEM	% of oxygen saturation Mean ± SEM
Horizontal	0	0.151 ± 0.008	44.9 ± 3.2
Lowered	-45	0.375 ± 0.015	19.5 ± 1.6
Raised	+45	0.087 ± 0.002	74.6 ± 4.1
Superficial cold	0	0.193 ± 0.003	41.8 ± 0.7
Deep cold	0	0.272 ± 0.009	104.1 ± 2.0
Slapped	0	0.214 ± 0.007	99.8 ± 1.4
Warmed	0	0.309 ± 0.008	94.5 ± 1.4

oxygenated blood was observed. A value of oxygenation of more than 100% in this case may be attributed to possible error in the calibration of the oxygenation index using data obtained from in-vitro measurement in which the blood sample was not representative of this in-vivo situation. Slapping or heating also causes more oxygenated blood to come to the upper dermis (ΔH= +0.110, $\Delta Sa\ O_2$= +52.3%).

As can be seen in Table 7.3, the measured oxygen saturation for the horizontal arm is less than 75% which is the oxygen saturation of mixed venous blood (Brodsky, 1986). This can be attributed to the broad and meandering capillary loops of the forearm, as mentioned in chapter 2, which produce slow blood flow in the capillaries and hence greater oxygen exchange with tissue. This effect was investigated at three other sites: thumb, palm and finger tip, where the capillary loops are different from those of the forearm. The averages of 20 successive measurements of the haemoglobin index and oxygenation of thumb, palm, and finger tip of a horizontal hand are shown in Table 7.4. Values shown as "pressed" were measured when the reflectance probe was pressed onto the skin surface. In this situation the superficial blood was trapped inside the small hemisphere in the reflectance probe where the light delivery and collection fibres are mounted and therefore the oxygen saturation drops and the haemoglobin index increases. These variations in the haemoglobin index and oxygenation are significant (mean variation of 8.0% and 6.9% respectively), hence in reflection measurement minimum force should be exerted on the skin surface. The values obtained for oxygen saturation are reasonable ($Sa\ O_2$= 94.3%) and indicate that the superficial blood supply in these areas is different from that in the forearm ($Sa\ O_2$= 44.9%). In the palm and finger tips there are long and relatively straight capillary loops which produces fast blood flow and hence less

Table 7.4- Haemoglobin index and oxygen saturation of different sites on a horizontal hand (room temperature 23 ^{o}C).

		Haemoglobin index Mean ± SEM	% of oxygen saturation Mean ± SEM
Thumb	relaxed	0.271 ± 0.009	96.0 ± 1.7
	pressed	0.282 ± 0.010	88.0 ± 2.3
Palm	relaxed	0.242 ± 0.005	92.6 ± 2.8
	pressed	0.274 ± 0.005	84.5 ± 2.6
Finger tip	relaxed	0.282 ± 0.011	94.3 ± 1.4
	pressed	0.301 ± 0.008	91.0 ± 1.5

oxygen exchange with tissue. The effects of different heights and temperatures on the amount and oxygen saturation of blood in the thumb were studied using the reflectance probe with minimum pressure on the skin surface. Table 7.5 shows the results of 20 successive measurements of the thumb when the hand was horizontal, raised (+45 cm) or lowered (-45 cm) at room temperature (23 ^{o}C). Also it was cooled by contact with an ice-cooled plastic sheet, and warmed to about 45 ^{o}C with hot air from a hair drier. The hand was horizontal when the cooling and warming experiments were carried out. The blood content of the thumb measured in the horizontal position (H= 0.271) is more than that observed on the forearm (H= 0.151, Table 7.3), but its variation due to raising, lowering, cooling or warming is less than that measured at the forearm. This effect may be due to a lower capacity of the thumb capillaries to dilate than those in the forearm. Variation in the oxygen saturation of the thumb is different from that of the forearm. Since the oxygen saturation measured in the thumb (94.3%) is almost the same as the arterial saturation a fast blood flow is implied; it is not increased by cooling or warming the measurement site as was the case for the forearm. Indeed, raising the hand causes the oxygen saturation of the thumb to decrease and may be attributed to a decrease in blood flow due to a decrease in arterial pressure.

7 - 3 Study of skin superficial blood content

To assess the clinical value of the reflectance measurement of the haemoglobin index and oxygen saturation, vasodilation induced by a topical analgesic was studied. In this study the local circulation in the capillaries was increased by means of a vasodilator chemical, and the variation in the amount of blood and its oxygen saturation observed. The chemical used for this purpose was ALGIPAN RUB, which is

Table 7.5- Haemoglobin index and oxygen saturation of a horizontal thumb (room temperature 23 ^{o}C).

	Height relative to heart, cm	Haemoglobin index Mean ± SEM	% of oxygen saturation Mean ± SEM
Horizontal	0	0.271 ± 0.009	96.0 ± 1.7
Lowered	-45	0.312 ± 0.008	55.9 ± 2.1
Raised	+45	0.252 ± 0.010	85.0 ± 3.0
Cooled surface	0	0.305 ± 0.009	92.1 ± 1.6
Warmed surface	0	0.339 ± 0.008	93.3 ± 1.3

a perfumed cream containing:

10% glycol salicylate

1% methyl nicotinate

0.1% capsicum oleoresine

Glycol salicylate is readily absorbed percutaneously and therefore is used as a vehicle for the transport of the other active ingredients. Application of methyl nicotinate and capsicum to the skin is rapidly followed by an increase in skin temperature and blood flow (Alcun 1987). Fulton et al (1959) in a study of the mechanism of the action of rubefacients reported that the topical application of a vasodilator chemical causes the vasodilation response to occur more widely than where the arterioles are solely in direct contact with the rubefacient. Varying concentrations of rubefacients such as ethyl nicotinate were found to produce essentially constant vasodilation, though the latent periods and duration of response differed. The types of blood vessels participating in the responses were arterioles and precapillary sphincters. The capillaries and non-muscular venules do not increase in diameter in response to rubefacients. Although rubefacients frequently improved the rate of blood flow through capillaries, the only changes in size were due to slight passive distention (Fulton 1959). Fountain et al (1969) reported that the rate of absorption of methyl nicotinate varies at different sites and temperatures, and also that the slower the absorbance, the more prolonged is the action.

In this study the cream was applied to three different sites, forearm, palm and finger tip, and oxygen saturation and the haemoglobin index were then measured at different times after application. Each value for haemoglobin and oxygen saturation is the

average of ten successive measurements taken over a 1.2 minutes interval. To carry out the experiment, first the haemoglobin index and oxygen saturation of a site were measured. The cream was then applied to the site in a thin circular layer with a diameter of about 1.5 cm. After a short time it was wiped off and the indices were measured. Following the measurement another thin layer of cream was then applied to the site. This procedure was repeated three or four times until the intensity of the erythema became substantial. The haemoglobin index and oxygen saturation of finger tip, palm and a forearm were measured on two separate occasions and their results are presented in Figs. 7.6, 7.7, and 7.8 respectively. The duration of the application of the vasodilator chemical to the skin is recorded on the X-axes of each diagram. In all measurements the ambient temperature was kept constant at 23 ^{o}C.

The stratum corneum is the main barrier to the passage of the chemical through the skin and its thickness affects the rate of penetration. The rapid initial rise in the haemoglobin index curve measured on the forearm and the shorter duration of the action is consistent with the view that the chemical has penetrated more quickly through the thinner stratum corneum of the forearm than that of the palm or finger tip and is demonstrated by comparing Fig 7.8 with Figs 7.6 and 7.7.

In Fig 7.6, 7.7, and 7.8 there is some indication of periodic variations in the haemoglobin index. The variation in the haemoglobin index, which is proportional to the amount of blood in the tissue, is produced by repeated cycles of constriction and dilatation of the arterioles. This type of constriction was noticed by Fulton (1959). He reported that occasionally, limited and localized vasoconstriction was

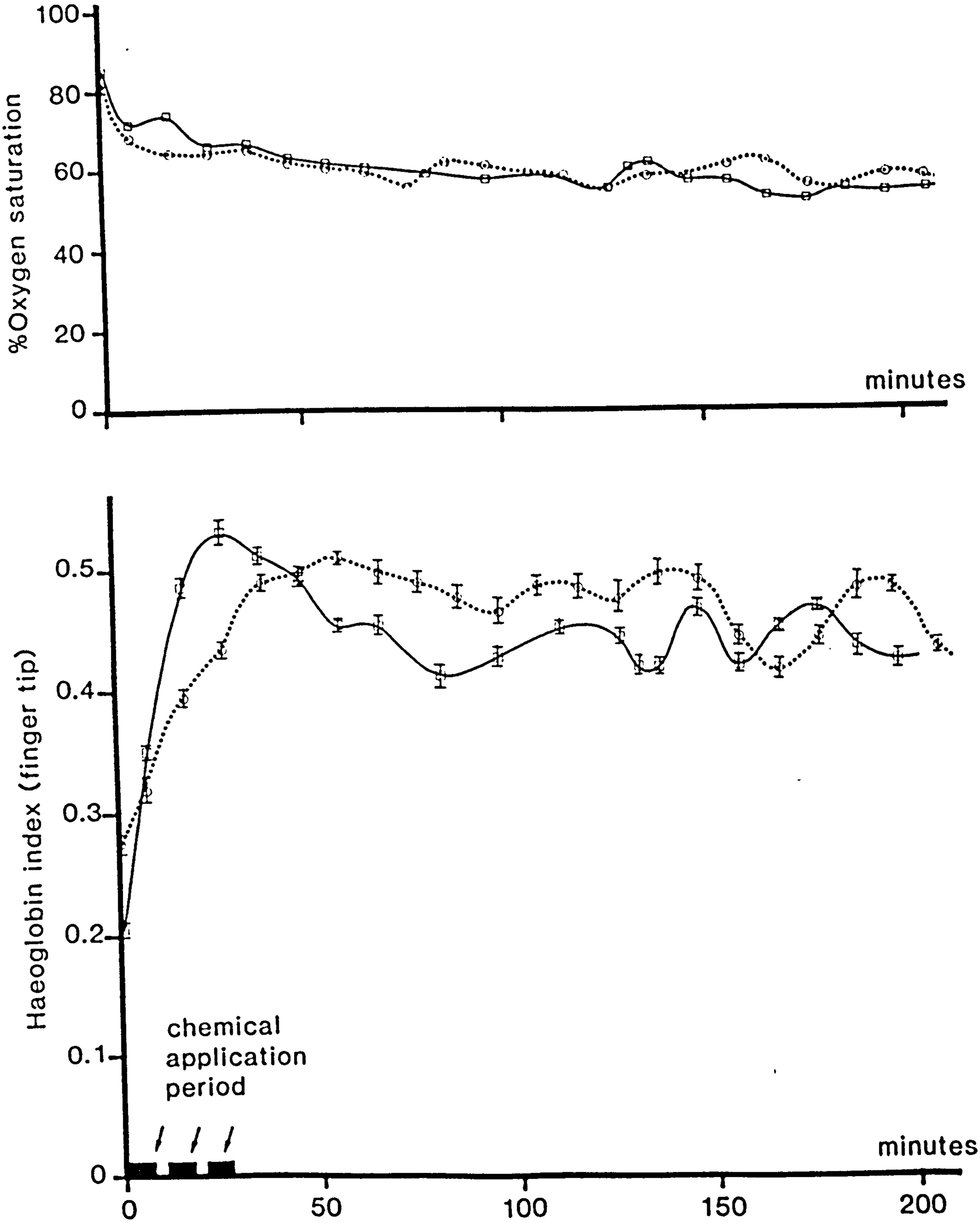

Fig. 7.6- Haemoglobin index and oxygenation of a finger tip after applying a vasodilator chemical, measured on two separate occasions.

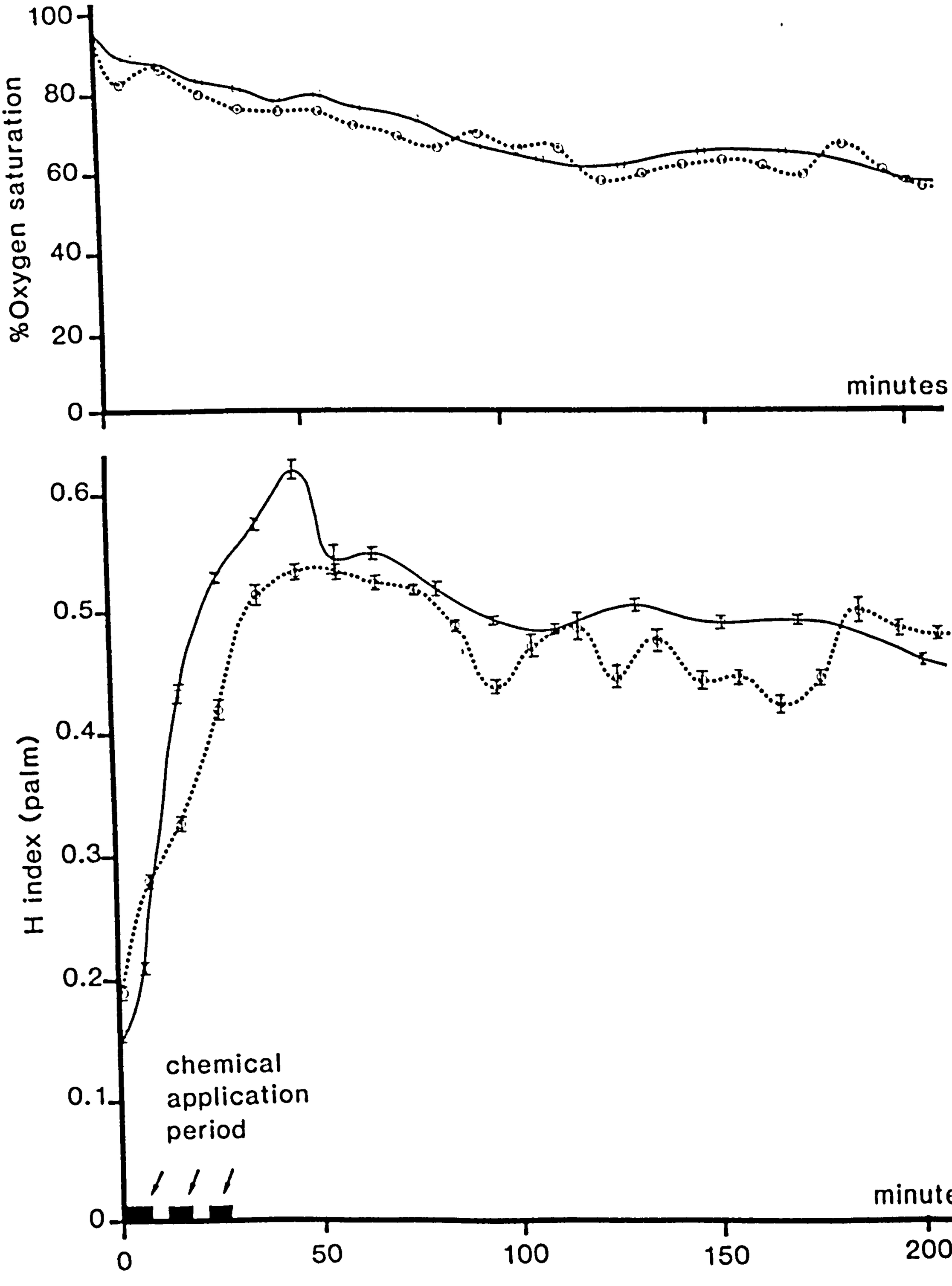

Fig. 7.7- Haemoglobin index and oxygenation of a palm after applying a vasodilator chemical, measured on two separate occasions.

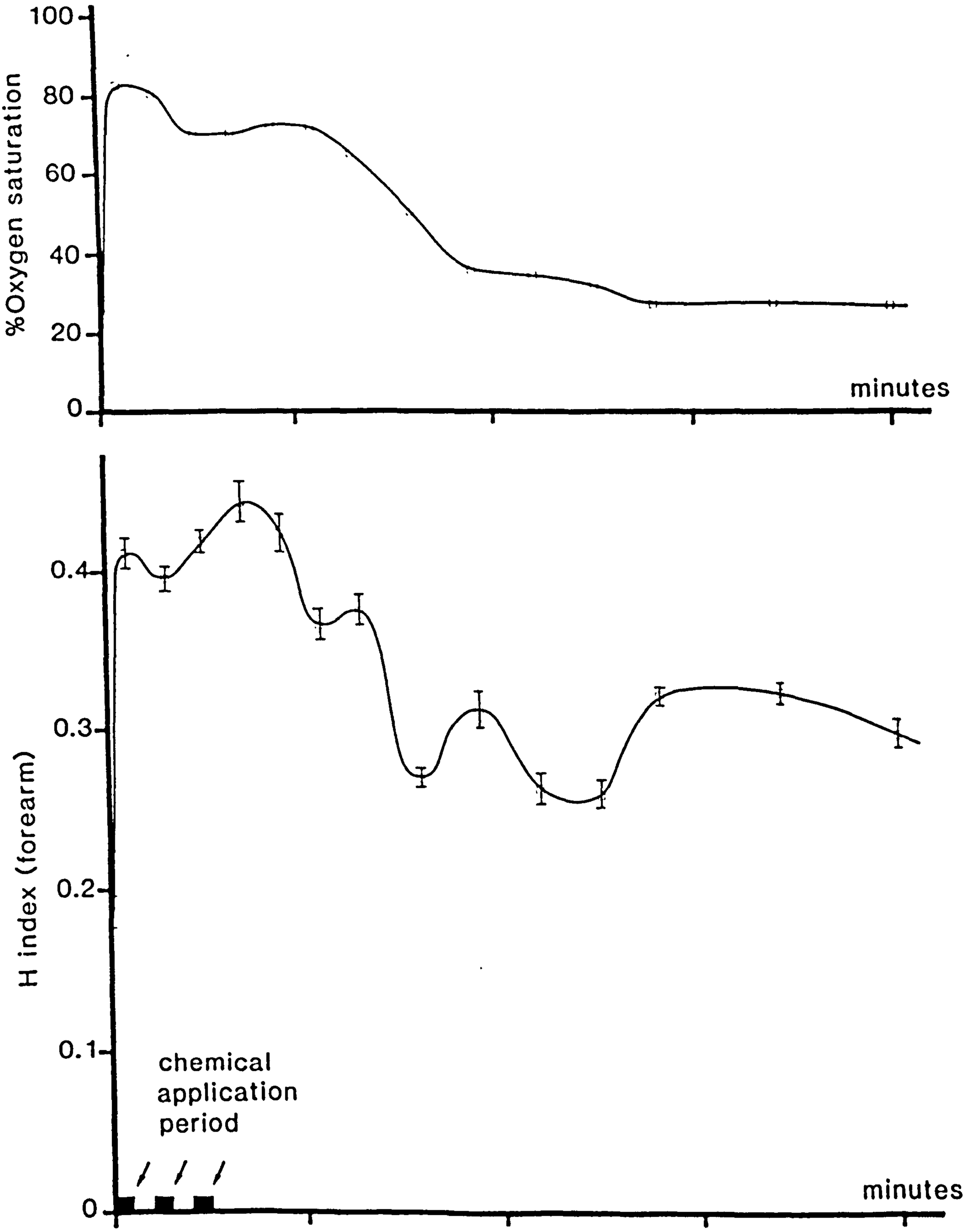

Fig. 7.8- Haemoglobin index and oxygenation of a forearm after applying a vasodilator chemical.

produced even at low concentration of rubefacient. These fluctuations may be attributed to different regulatory functions generated by blood flow.

Gimmerikh (1965) has reported that "haemoglycolysis", ie glycolysis in erythrocytes, is a powerful activator of the release of oxygen, attributable primarily to the decrease in the pH. He found that cold in the form of a shower or bath or the action of nicotinate acid increased heamoglycolysis. Hence, in this work, in the local area where the applied cream (methyl nicotinate) has penetrated to the capillaries of the dermis, more oxygen may be released. Consumption of the released oxygen by the tissue produces heat. An increase in blood flow is then required to remove the heat and regulate the skin temperature. The increase in blood flow causes more oxygen to be released and in turn more heat to be produced. Therefore the thermal regulatory function of blood by periodical constriction and dilatation of the arterioles may control the increase of blood flow through the capillaries and consequently regulate the skin temperature. This regulatory function may be affected by several other factors, hence the period of fluctuation, 20 - 30 minutes, in the measured haemoglobin index varies from one set of measurements to another.

In order to measure the thermal effect of the vasodilator chemicals, the skin temperature of a finger tip was measured before and after application of the cream. To measure the temperature a thermocouple with an amplifier circuit which was sensitive to 0.01 ^{o}C was used, and the skin temperature was measured at different time intervals. The average of 10 measurements (one every minute) before application of the cream was 35.46 ^{o}C, and the average of 10 measurements (one every two minutes) commencing 15 minutes after application of the cream was 36.2 ^{o}C. The increase of 0.74 ^{o}C was

constant for a longer period than the measurement time and may be attributed to the consumption of the released oxygen by the tissue. The oxygen saturation of blood in the finger tip and palm, as shown in Figs. 7.6 and 7.7, was reduced after application of the cream. This reduction is consistent with the release of more oxygen at the measurement site. The haemoglobin index and oxygen saturation of the forearm, as shown in Fig. 7.8, increased immediately on application of the vasodilator cream and then gradually decreased. This may be attributed to vasodilatation of the arterioles and increase in the blood flow of the capillaries which causes more oxygenated blood to pass to the upper dermis. After 100 - 120 minutes the haemoglobin index and oxygen saturation decreased to the same level as before applying the cream. This period which is called the "period of action" of a vasodilator chemical, is dependent on the vehicle used and therefore on the rate of absorption of active ingredients in different sites, so that the slower the absorption, the more prolonged is the action (Fountain 1969).

To show the effect of an increase in the blood flow of the capillaries in the forearm, the study was extended by using different amounts of chemical and by measurement of skin temperature as well as haemoglobin index and oxygen saturation. The results of the repeated measurements are shown in Fig. 7.9. In this figure, the curves identified by a full line were measured with more chemical applied to the same site but over a larger area than in curves with a broken line. The increase in skin temperature of the forearm, due to an increase in blood flow, was maximally 2.8 ^{o}C which is different from the 0.74 ^{o}C increase in skin temperature observed for the finger tip. The forearm skin temperature gradually increased whilst the chemical was applied and after that decreased to normal by the end of the

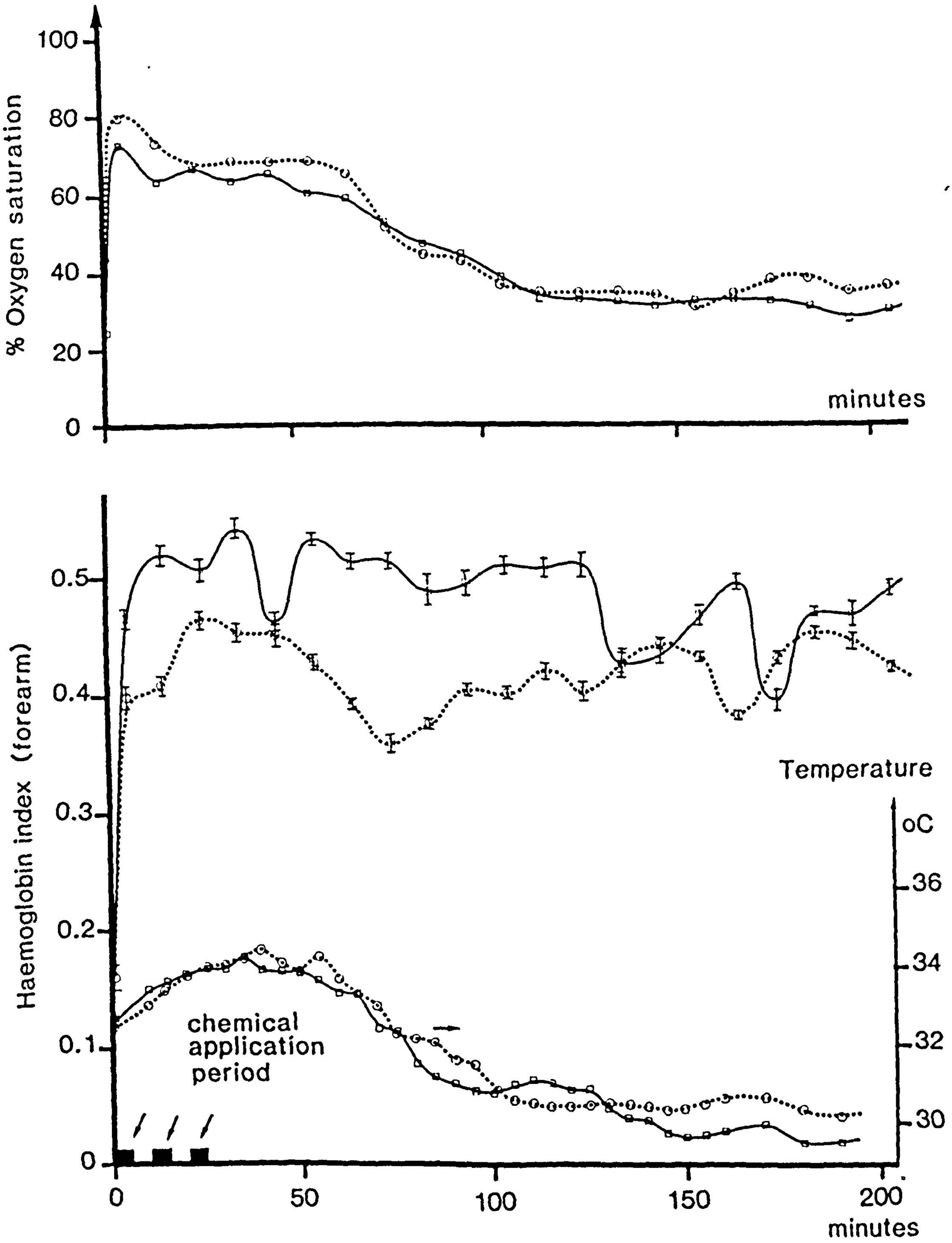

Fig. 7.9- Haemoglobin index, oxygen saturation and skin temperature of a forearm after applying a vasodilator chemical. (full lines were measured with more chemical than broken lines)

period of action of the chemical (120 minutes). The increase in the skin temperature is not as fast as the increase in oxygen saturation which may be due to skin thermal conductivity, but the decrease is simultaneous with the decrease in oxygen saturation of the skin blood. This effect confirms that the blood flow in the capillaries was increased by the application of the chemical and then decreased by the end of the period of action of the chemical; the haemoglobin index shows that the blood content of the skin remains elevated. There is no significant difference in the skin temperature between the two sets of measurements especially with respect to the period of action of the chemical. This indicates that the blood flow has increased to the same level for different amounts of chemical. The initial sudden increase in the oxygen saturation is attributed to an increase in the blood flow, which brings more oxygenated blood to the measurement site. By the end of the period of action of the chemical the flow decreases to its initial level. Comparison of the maximum oxygen saturation achieved in the forearm, measured 5 minutes after applying the chemical, as shown in Figs. 7.8 and 7.9 (84% in Fig. 7.8, 80% and 74% for curves with broken and full lines in Fig. 7.9) indicates that the application of more chemical causes a greater reduction in the oxygen saturation. This may be attributed to haemoglycolysis and release of oxygen from the red cells.

It is found that the more chemical that is used, the more extended is the induced erythema and the greater is the increase in the haemoglobin index. This effect is shown in Fig. 7.9, and indicates that the degree of dilatation is to some extent dependent upon the total area treated by the chemical which is contrary to the observations of Fulton (1959) on animals. In contrast to the result of the first measurements on the forearm (Fig. 7.8), the haemoglobin index in both of these repeated measurements did not return close to

its initial value at the end of the period of action of the chemical, and implies that the arterioles remained in a dilated state. This effect may be attributed to a saturation of the vasodilating capacity of the arterioles.

7 - 4 Clinical use of the reflectance spectrometer

In order to compare the haemoglobin indices of forearm and thumb with the true amount of haemoglobin in the blood in g/dl, reflectance measurements and blood samples were taken from patients who attended a blood clinic. The amount of haemoglobin in their blood was measured by a Coulter S plus IV blood analyzer. Figures 7.10 and 7.11 show the correlation of haemoglobin index vs haemoglobin content (g/dl) for the forearm and thumb respectively. The haemoglobin index values measured from the thumb are higher than of the forearm which indicate more blood in the thumb than the forearm in all subjects as was noted earlier (section 7.2). The correlation coefficient of 0.4 between the haemoglobin content and haemoglobin index as measured on the forearm and of 0.2 from the thumb show that the relationship between the haemoglobin index and haemoglobin content in g/dl is weak. This may be attributed to the difficulty of defining the volume of blood observed when measuring the "H" index. At different sites the amount of blood varies according to biological conditions such as temperature or blood pressure at the time of measurement and also variation in the thickness of the epidermis. The lower value of the correlation coefficient for the haemoglobin index when measured on the thumb (0.2) may be attributed to greater variation in the thickness of the thumb epidermis than that of the forearm. To examine the effect of biological change on the haemoglobin index, the finger tip and forearm of a single subject were measured at different times throughout one day. The results of these measurements are shown in Table 7.6 and indicate that haemoglobin index changes depend on the

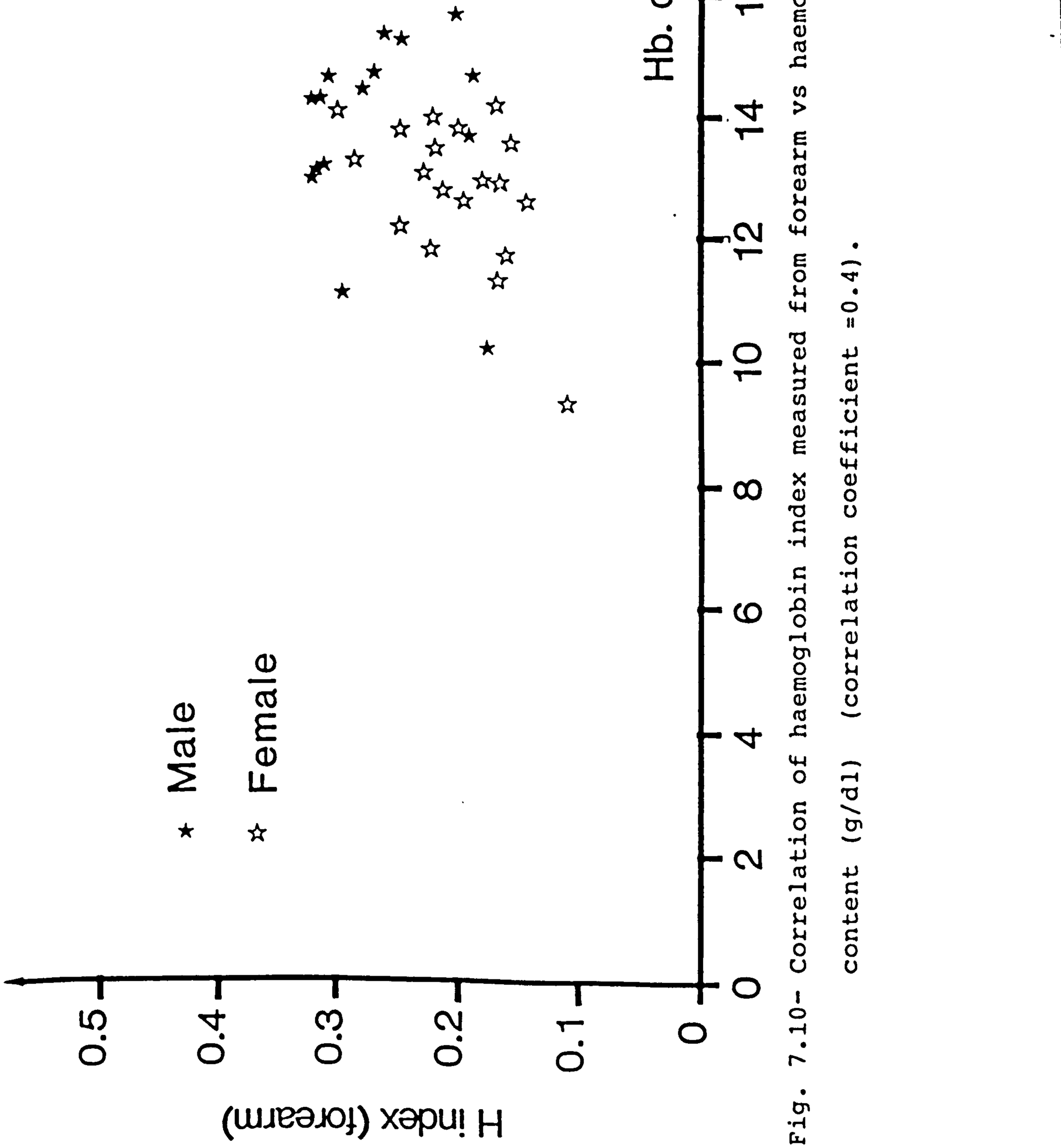

Fig. 7.10- Correlation of haemoglobin index measured from forearm vs haemoglobin content (g/dl) (correlation coefficient =0.4).

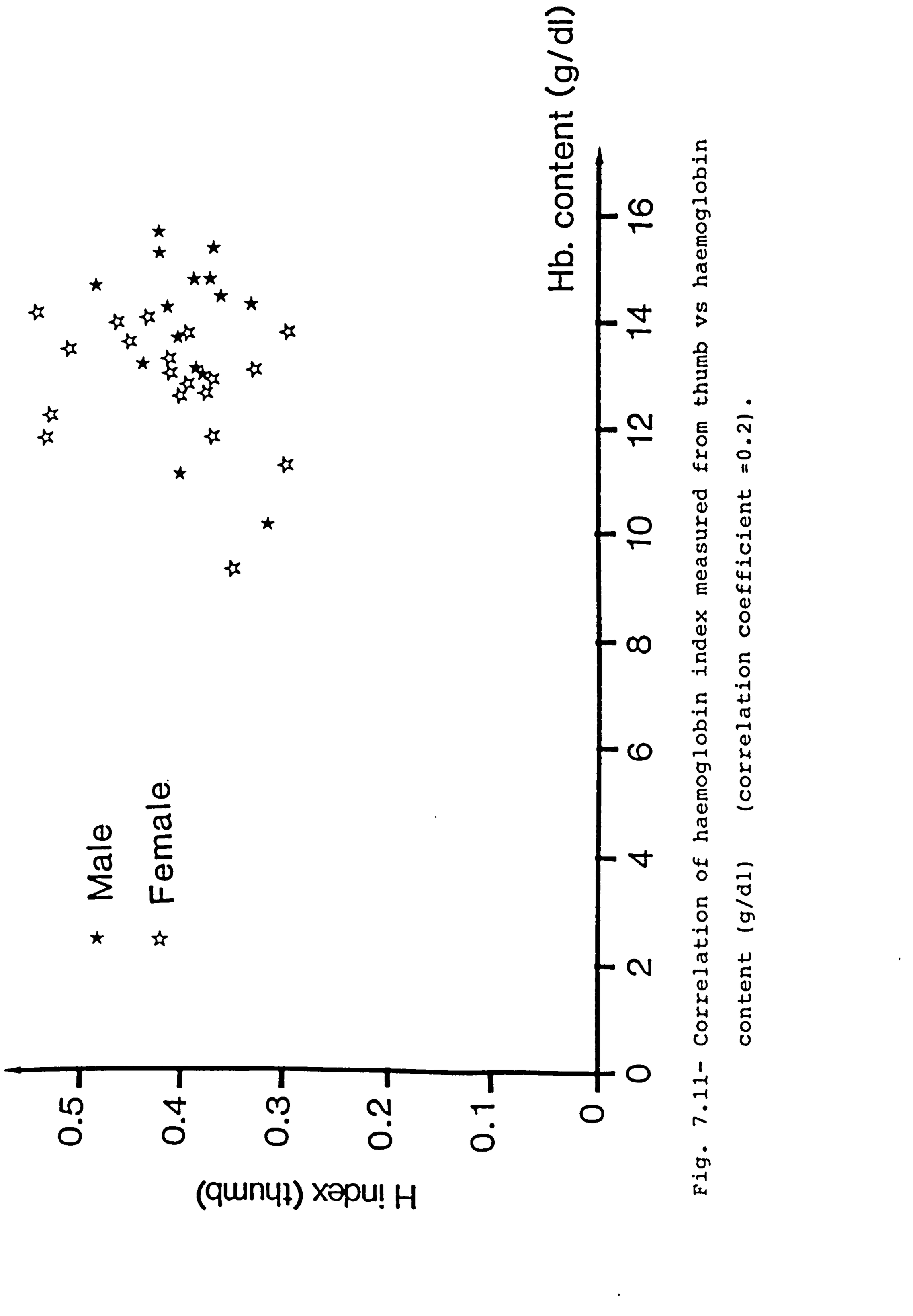

Fig. 7.11- Correlation of haemoglobin index measured from thumb vs haemoglobin content (g/dl) (correlation coefficient =0.2).

Table 7.6 - Amount and oxygen saturation of superficial blood in forearm and finger tip of a single subject at different times of day.

	Forearm		Finger tip	
Time	H index	oxygenation	H index	oxygenation
morning (9 am)	0.147 + 0.010	50.5 + 4.1	0.352 + 0.006	93.8 + 1.3
midmorning (10 am)	0.151 + 0.010	44.9 + 3.7	0.384 + 0.009	98.1 + 1.4
night (8 pm)	0.286 + 0.011	69.3 + 2.0	0.442 + 0.016	78.4 + 2.0

skin treatment before the measurement. It increases as the subjects get warm and tired. Therefore, to achieve a better correlation between the haemoglobin index and the amount of haemoglobin (g/dl) in the blood much further study of the biological factors determining the blood content of skin and of the physical factors affecting the measured value of the "H" index will be required.

7 - 5 Summary and conclusions

In this chapter, to facilitate the study of the absorption properties of the epidermis a new index called the "melanin index" was introduced and quantified using a synthetic melanin compound for calibration purposes. The independence of this index with respect to changes in the amount and degree of oxygen saturation of haemoglobin in the skin was examined. To assess the sensitivity of the melanin index, firstly, different sites on the hand of a single subject were measured and secondly, the melanin content ($\mu g/cm^2$) of several subjects with different racial pigmentation levels were measured and compared. It was found that the melanin content of the skin correlated well with the computed cutaneous blood flow corresponding to the native latitude of the subject.

The effects of the height of the measurement site relative to the heart and of the temperature of the site on the amount and oxygen saturation of superficial blood in the skin surface were studied by measuring the haemoglobin index and oxygen saturation of three sites; forearm, finger tip and palm. The results show that when the hand is lower than the heart the blood accumulated in the tissue and became deoxygenated, ie there was an increase in the haemoglobin index and a decrease in oxygen saturation. Raising the hand drained away the deoxygenated blood hence the haemoglobin index decreased and the oxygen saturation increased. Cooling the skin surface caused the blood supply to decrease, on further cooling the skin became red and more

oxygenated blood was measured. Slapping and heating the surface also caused more oxygenated blood to come to the upper dermis. These variations in haemoglobin index and oxygen saturation were observed on the forearm and a finger tip where similar responses were found.

The effect of topical application of a vasodilating chemical to a finger tip, palm and forearm was studied by measuring the haemoglobin index, oxygen saturation and skin temperature of the sites at different times after application. Penetration of the chemical to the dermis was rapidly followed by erythema whose rate of increase was related to the thickness of the stratum corneum. A decrease in oxygen saturation observed in the finger tip and palm was attributed to haemoglycolysis in the presence of methyl nicotinate. This process reduces the oxygen affinity of the haemoglobin and causes more oxygen to be released at the treated site. The increase in the haemoglobin index and skin temperature is attributed to vasodilation and the increased blood flow in the capillaries.

Finally, to compare the haemoglobin index with the true amount of haemoglobin in the blood in g/dl, reflectance measurements were made on the forearm and thumb of different patients and compared with the amount of haemoglobin in their blood (g/dl) as measured by a conventional spectrophotometric method. Correlation coefficients between the two methods were 0.4 for forearm and 0.2 for thumb and indicate that the haemoglobin content of blood cannot be measured transcutaneously by the present instrument.

From the experiments reported in this chapter it is clear that the haemoglobin index and oxygenation of the skin are very sensitive to changes in experimental conditions hence when undertaking reflectance measurements on skin great care must be taken to standardise and control those conditions.

CHAPTER 8

8 - SUMMARY, CONCLUSIONS AND FUTURE WORK

The work detailed in this thesis describes the design and construction of a multiwavelength reflectance spectrophotometer for the in-vivo measurement of skin pigments. This instrument, which scans the visible spectrum rapidly from 400 to 700 nm in 2.8 seconds, was used to study the amount and oxygen saturation of superficial blood, and the melanin pigmentation level of the epidermis by measuring the reflectance spectrum of the skin surface.

In the first chapter, the importance and some clinical applications of reflectance skin colour measurements were discussed. Literature reports of experimental measurements of light reflection and transmission were reviewed. The structure and optical properties of skin, blood flow and its significance as a distributor of oxygen, and methods for the measurement of oxygen saturation were reviewed in chapter 2.

Based on the optical properties of skin, a theoretical model for light propagation in scattering and absorbing media such as whole blood or skin was developed in chapter 3. This theory, which is considered as a special case of the more general photon diffusion theory, is called the "Kubelka-Munk" theory and is based on two simultaneous differential equations of the first order. It describes the attenuation of light intensity within the sample due to scattering and absorption. The equations were solved for two different boundary conditions. One is the situation where the sample is optically thin and the transmitted light is reflected back from a white surface or absorbed on a black surface placed beneath the sample, the other is

for strongly absorbing material or very thick samples. The first situation fulfils the in-vitro measurement conditions and the second, the in-vivo conditions of this study.

In chapter 4, details of the reflectance spectrophotometer were presented. According to the theory described in chapter 3, the instrument should measure only the component of light which is diffusely reflected from within the skin. Light from the light source is carried by fibre optics to the reflectance probe head where it illuminates the skin surface perpendicularly and the diffusely reflected light is collected at an angle of 54 degrees to the skin surface. The wavelength of the reflected and reference light is selected by passing through a variable wavelength interference filter prior to conversion to an electrical signal via two Si photodiodes. The electric signals are then digitized to be read by a BBC master microcomputer. The LIR of the skin surface, which is the logarithm of the ratio of the diffusely reflected light from a non-absorbing white surface divided by that from the skin surface, is then calculated by the computer for a series of visible wavelengths.

In chapter 5, the application of the instrument to the study of the optical properties of diluted red cells is reported. Using the LIR values measured at selected wavelengths, two independent indices proportional to the amount of haemoglobin and to the oxygenated state of the sample were derived and defined as the "haemoglobin index" and the "oxygenation index". The in-vitro calibration curve of the haemoglobin index against red cell concentration for both collimated and diffuse incident light was linear. The independence of the indices from each other was also verified. The oxygenation index may be converted into percentage oxygen saturation by comparing the

measured oxygenation index of the sample with that of reduced and fully oxygenated blood. The validity of the method was examined by measuring the oxygen dissociation curve of human blood at 40 mm Hg pCO_2, pH = 7.33 and 37 ^{o}C and comparing it with a published curve obtained under the same conditions. The agreement between the measured and published curves confirmed that the oxygen saturation can be measured accurately by the present method. The measured haemoglobin index is affected by the thickness of the epidermis which changes in different parts of the body, therefore, no attempt was made to express the index in terms of the amount of blood (g/dl) in the measurement site.

In chapter 6, some instrumental improvements for in-vivo measurement of skin reflectance were suggested. Polarised light was used to exclude the signal from any specularly reflected light, hence, the collecting fibre can be fixed to any angle relative to the normal to the surface. A study was undertaken to determine the light collecting angle at which the diffusely reflected light was a maximum. This study led to the design of a new reflectance probe. The stability of the indices against random variations in the reflected signal, and the effect of epidermis and dermis on the light transmission and reflection were studied. Studies of the angular distribution of the scattered radiation by the epidermis showed that the scattering in the epidermis is forwardly orientated and wavelength dependent, whereas in the dermis with a thickness of 1 mm or more it is completely diffused and follows Lambert's law (Hardy et al 1956). A comparison between in-vivo reflectance and transmission measurements of an ear lobe indicated that in reflectance measurements the average penetration depth of radiation (at 550 nm) in tissue is about 0.5 mm. Therefore

the measured oxygen saturation by this method is that of superficial blood. These measurements also showed that not more than 1.2% of the tissue volume in the ear lobe is occupied by blood.

To demonstrate the absorption property of the epidermis a new index called the "melanin index" was introduced in chapter 7. This index was expressed relative to the amount of a synthetic melanin compound per unit area of producing the same LIR spectrum. The independence of the melanin index from the amount of blood in skin, as indicated by the haemoglobin index, and its oxygenation was demonstrated, and the in-vivo melanin pigmentation levels of different racial subjects were measured.

Also in chapter 7, variations in the amount and oxygen saturation of superficial blood were studied when the measurement site was at different heights relative to the heart, temperatures or pressures. Raising or lowering the hand causes the blood to drain out of or flow into the tissue; cooling or warming also caused reduction or increases in the blood flow in the tissue. All these variations of blood contained in a finger tip or forearm were quantified by measuring the haemoglobin index and oxygen saturation. The correlation between the haemoglobin index as measured by this method at two different sites, forearm and thumb, and the haemoglobin content (g/dl) of the blood as measured by direct spectrophotometry for 34 different patients was determined. The correlation coefficients (0.40 for forearm and 0.19 for thumb) were found not to be significant. The effects of the topical application of a vasodilating chemical were studied by measuring the haemoglobin index and oxygen saturation at different time intervals after application at three different sites. An immediate increase in the haemoglobin index (blood content) and

decrease in oxygenation index (saturation) indicates that penetration of the chemical stimulates more oxygen release from the haemoglobin. Consumption of the released oxygen increased the skin temperature and thereby stimulated the thermal regulatory function of blood. This function operates by periodically increasing and decreasing blood flow in the capillaries.

The work described in this thesis demonstrates that the new reflectance spectrophotometer is suitable for in-vivo non-invasive study of the melanin pigmentation and the haemoglobin and oxygen saturation of superficial blood. It can also be used in a transmission mode to measure these factors by transmission of light through a thin piece of tissue such as an ear lobe. By attenuating the infra-red portion of the incident radiation to avoid thermal injury, and increasing the intensity of the light delivered, information may be obtained from deeper in the skin. The present method has been used to investigate tumour and normal tissue responses to porphyrin mediated photodynamic therapy of cancer. Preliminary results using rats as experimental subjects indicate a large decrease in tumour blood oxygenation during treatment with little recovery up to 2 hours post treatment in photosensitised animals, suggesting a decrease in tumour blood flow. After an immediate reduction in the haemoglobin index at the start of illumination, haemoglobin levels progressively rose throughout the treatment period and up to 2 hours post treatment. No significant changes occurred in non- photosensitised animals (Feather et al 1988). It was also found by Feather et al (1988) that an absorbance peak at around 500nm was consistently present in photosensitised animals and absent in animals without drug. This observation confirms the possible application of reflectance

Appendix A

Computer program

As noted in chapter 4, a BBC Master microcomputer was interfaced with the reflectance spectrophotometer to measure the LIR spectrum of the skin surface. The computer program has been written using two languages: BASIC and Machine Code. The main program which is written in BASIC, in addition to carrying out all functions which are not involved with timing operations such as calculation, printing or plotting the results, and saving the data on floppy discs, also controls the measurement procedure which was written in Machine Code in four separate sections. These sections are called: reset (for reseting the filter), test (for testing the A/D's output at selected wavelength), acquire (for data acquisation), and drive (for driving the stepper motor forward). The following flow-charts show the detail of each section (cf pp 108-113).

Reset:

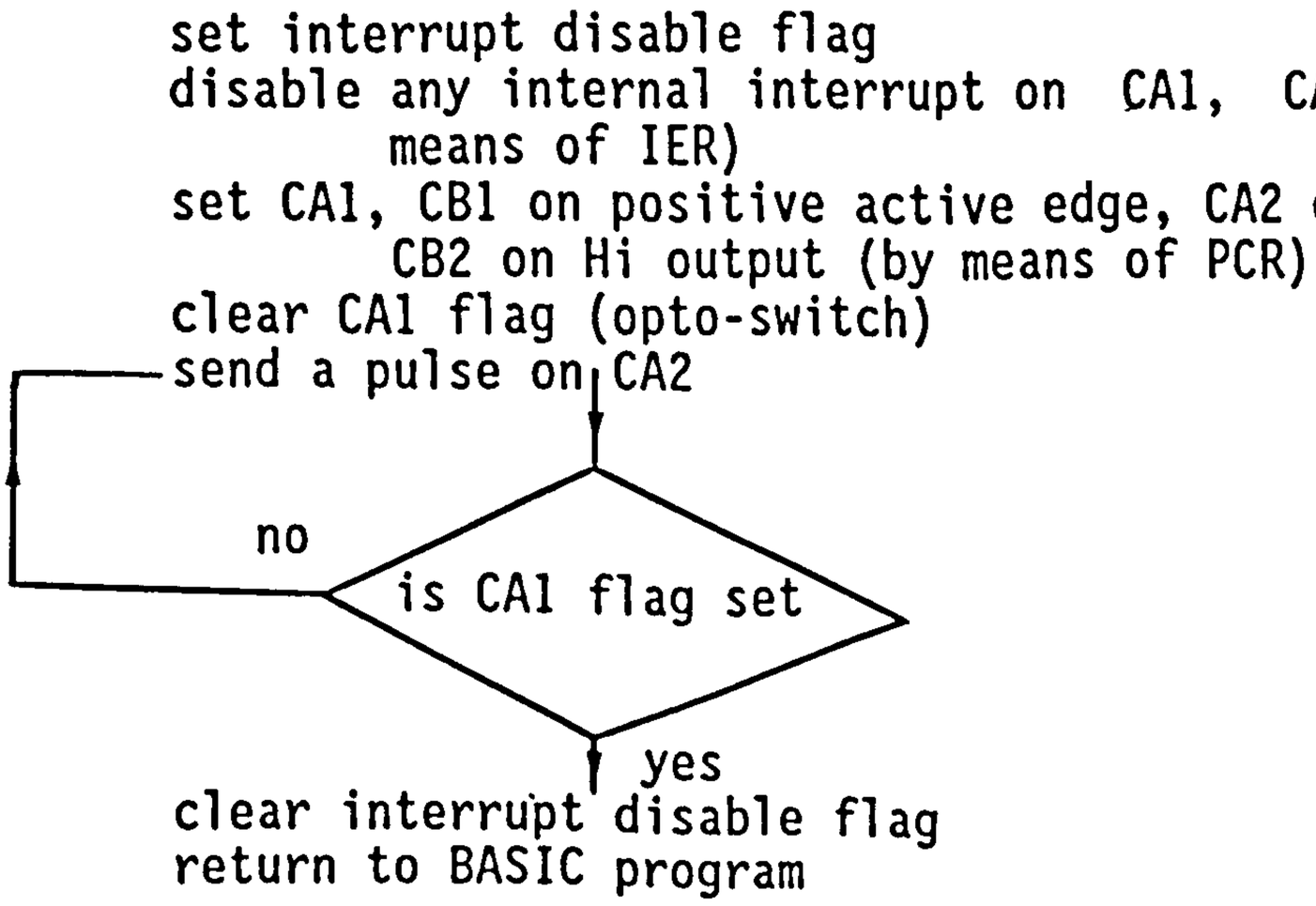

Acquire:

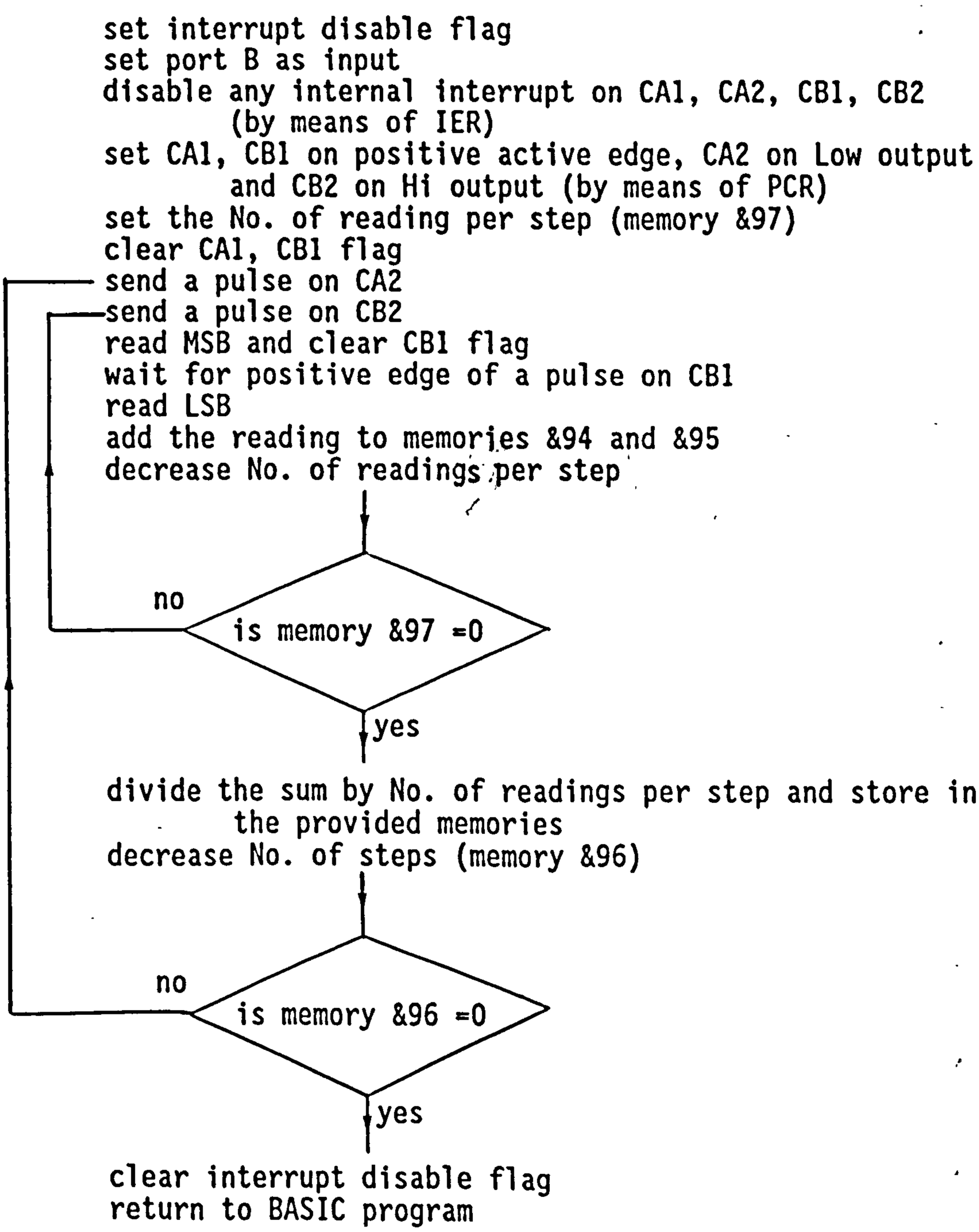
set interrupt disable flag
set port B as input
disable any internal interrupt on CA1, CA2, CB1, CB2
(by means of IER)
set CA1, CB1 on positive active edge, CA2 on Low output
and CB2 on Hi output (by means of PCR)
set the No. of reading per step (memory &97)
clear CA1, CB1 flag
send a pulse on CA2
send a pulse on CB2
read MSB and clear CB1 flag
wait for positive edge of a pulse on CB1
read LSB
add the reading to memories &94 and &95
decrease No. of readings per step
is memory &97 =0
no
yes
divide the sum by No. of readings per step and store in
the provided memories
decrease No. of steps (memory &96)
is memory &96 =0
no
yes
clear interrupt disable flag
return to BASIC program

Test:

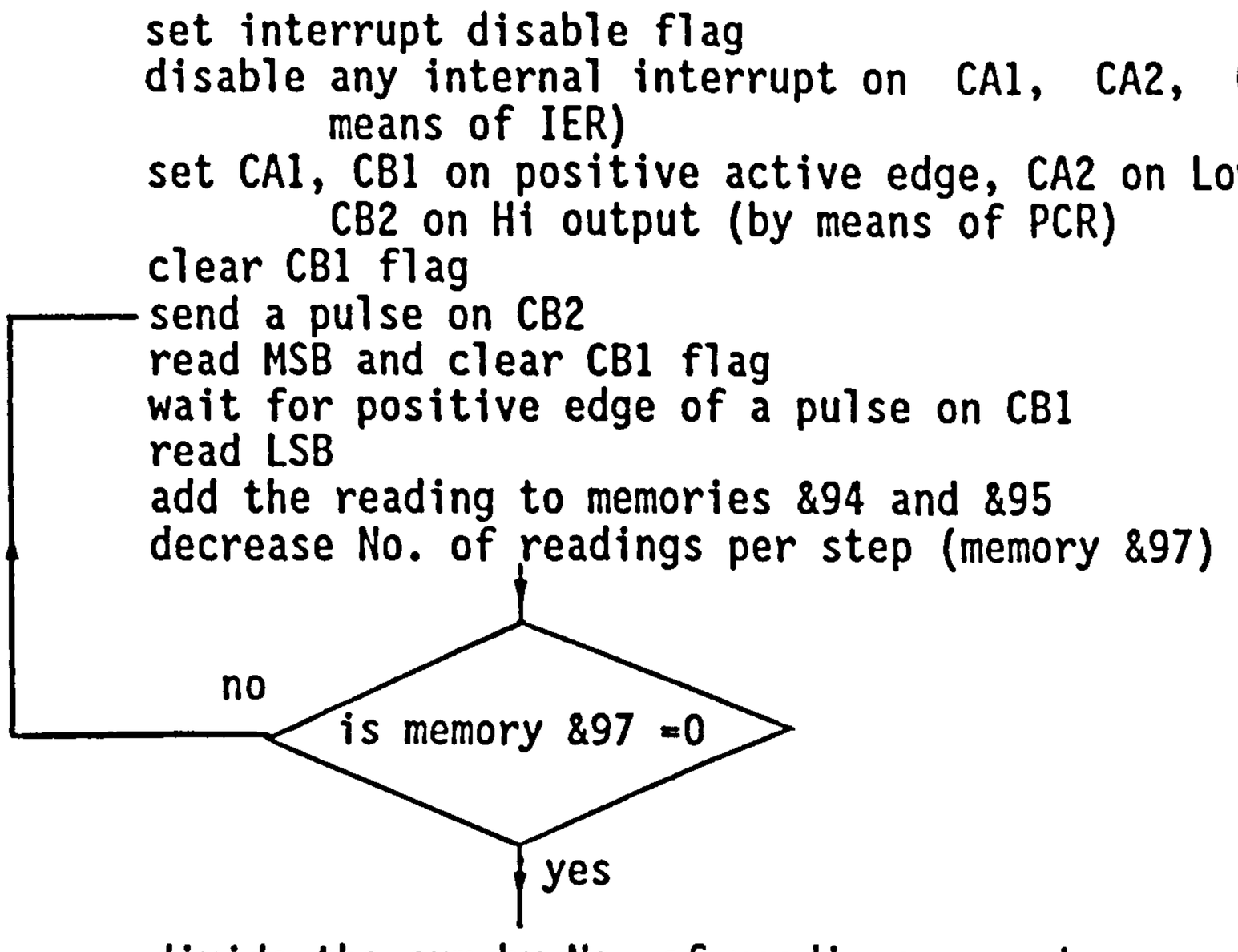
set interrupt disable flag
disable any internal interrupt on CA1, CA2, CB1, CB2 (by means of IER)
set CA1, CB1 on positive active edge, CA2 on Low output and CB2 on Hi output (by means of PCR)
clear CB1 flag
send a pulse on CB2
read MSB and clear CB1 flag
wait for positive edge of a pulse on CB1
read LSB
add the reading to memories &94 and &95
decrease No. of readings per step (memory &97)
no
is memory &97 =0
yes
divide the sum by No. of readings per step
set the No. of readings per step (memory &97)
clear interrupt disable flag
return to BASIC program

Drive:

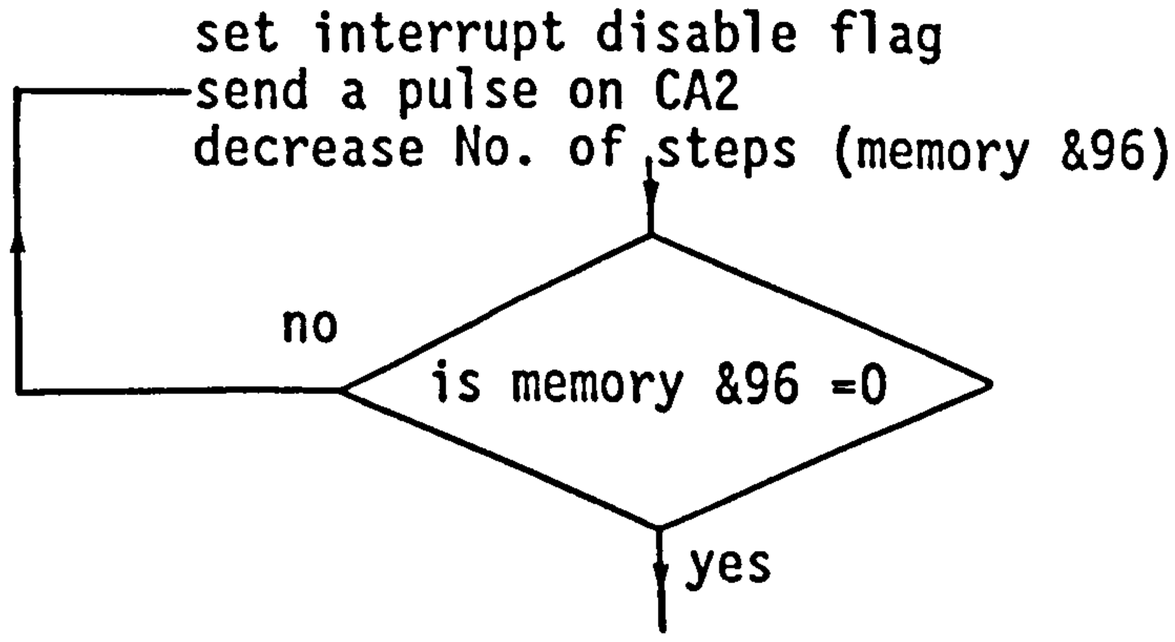
set interrupt disable flag
send a pulse on CA2
decrease No. of steps (memory &96)
no
is memory &96 =0
yes
clear interrupt disable flag
return to BASIC program

The main program is listed below:

```
 2 REM
 4 REM      ┌──────────────────────────────────┐
 6 REM      │ Program for the measurement of the
 8 REM      │ LIR spectrum of skin surface with
10 REM      │ the reflectance spectrophotometer.
            └──────────────────────────────────┘
20 LOMEM=&3200
30 DIM AW(200),A(200),B(200)
40 PROCmachinecode
 50 PRINT TAB(10)"OPTIONS:"
 60 PRINT TAB(13)"1) Test"
 70 PRINT TAB(13)"2) Reset"
 80 PRINT TAB(13)"3) Acquire "
 90 INPUT OPTION:ON OPTION GOTO 100,110,120
100 PROCtest:GOTO 50
110 PROCreset:GOTO 50
120 Z=200:PRINT TAB(10)"OPTIONS:"
130 PRINTTAB(13)"1) Black surface"
140 PRINTTAB(13)"2) White surface"
150 PRINTTAB(13)"3) Corrected spectrum"
160 PRINTTAB(13)"4) Other options "
170 INPUT  OPTION:IF OPTION=4:GOTO 210
180 PROCacquire:
190 IF OPTION=3:PROCcalculation
200 GOTO 120
210 PRINTTAB(10)"OPTIONS;"
220 PRINT TAB(13)"1) Printing Ab."
230 PRINT TAB(13)"2) Plotting Ab."
240 PRINT TAB(13)"3) Saving data "
250 INPUT OPTION:ON OPTION GOTO  260, 270,280
260 PROCprint:GOTO120
270 PROCplot:GOTO120
280 PROCsave:GOTO120
290 END
300 REM   ------------ PROC reset ------------
310 DEFPROCreset
320 CALL RR:?&76=202:CALL FF
330 ENDPROC
340 REM   ------------ PROC  test ------------
350 DEFPROCtest
360 INPUT"Which step ",S
370 IF S>255 THEN PRINT "Out of range":GOTO 360
380 ?&76=S:CALL FF:A=&74:CLS
390 PRINT TAB(1,7)"Sig."TAB(1,8)"----- ="TAB(1,9)"Ref."
400 CALL TT:X=?A*256+?(A+1):PRINT TAB(8,8)~X
410 IF ?&EC=0 THEN GOTO400
420 ENDPROC
430 REM   ------------ PROC acquire ----------
440 DEFPROCacquire
450 INPUT "Number of step ",S
460 IF S>255 THEN PRINT "Out of range":GOTO 450
470 Z=Z-S:?&76=S
480 IF Z<0 PRINT "Only  ";Z+S;"  Step left":Z=Z+S:GOTO 450
```

```
  500 CALL AA:IF Z>0 GOTO 450
  510 B=&31F9:FOR I=1 TO 200:Y=?B*256+?(B-1):B=B-2
  520 IF Y>4094 PRINT" A/D Saturated at step ";I
  530 IF OPTION=1 THEN B(I)=Y:GOTO 600
  540 IF OPTION=2 THEN AW(I)=Y:GOTO 600
  550 IO=AW(I)-B(I)
  560 IF IO<=0 PRINT" Intensity  of white <= black surface at
step";I:IO=0.00001
  570 IS=Y-B(I)
  580  IF  IS<= 0 PRINT"  Signal  <  Black  tile  at  step";I
:IS=0.00001
590 A(I)=LOG(IO/IS)
600 NEXT I:?&76=200:CALL FF:ENDPROC
610 REM   --------- PROC calculation ---------
620 DEFPROCcalculation
630 A94=(A(93)+A(94)+A(95))/3
640 A103=(A(102)+A(103)+A(104))/3
650 A111=(A(110)+A(111)+A(112))/3
660 A119=(A(118)+A(119)+A(120))/3
670 A162=(A(161)+A(162)+A(163))/3
680 A189=(A(188)+A(189)+A(190))/3
690 E=(A103-A119)/16+(A103-A94)/9
700 OX=(A119-A111)/8+(A103-A111)/8
710 OXY=(OX/E+0.821)*100/1.97
720 ME=((A189-A162)/27+(.062*(1-OXY/100)+.009)*E/8 2.3)*100
730 MELAN=-119.1*(ME-0.0541)
740 CLS:PRINT TAB(6);" Haem.=";100*E;TAB(25);" Oxy% =";OXY;
  750 PRINT TAB(6);" Melanin ug/cm2 =";MELAN
  760 ENDPROC
  770 REM   ------------ PROC  plot ------------
  780 DEFPROCplot
  790 INPUT"Title ",Title$
  800 INPUT"Max. Scale ";MAXS:CLS
  810 X=50:Y=250:YM=850:VL=YM-Y
  820 VDU23,240,192,0,0,0,0,0,0,0,0
  830 VDU5:MOVE X,Y:PLOT5,X,YM+75:MOVE X,Y:PLOT5,1300,Y
  840 FOR I=Y TO YM STEP VL/10:MOVE X-15,I:PLOT5,X,I:NEXTI
  850 FOR I=Y TO YM STEP VL/2:MOVE X-30,I:PLOT5,X,I:NEXTI
  860 FOR I=X TO X+1200 STEP 200:MOVE I,Y-15:PLOT5,I,Y:NEXTI
  870 FOR I=X TO X+1200 STEP 400:MOVE I,Y-30:PLOT5,I,Y:NEXTI
  880 FOR I=25 TO 189:MOVE 1200*(I-25)/164+X,500*A(I)/MAXS+Y
:PRINT CHR$240:NEXT I
  890 MOVE X,YM+80: PRINT Title$:MOVE  0,YM+30:PRINT;  MAXS:
MOVE 0,Y+VL/2+30:PRINT; MAXS/2:MOVE 0,Y+30: PRINT; 0
  900 MOVE X-25,Y-50:PRINT;"400":MOVE X+375,Y-50:PRINT;"500"
  910 MOVE X+775,Y-50: PRINT;"600": MOVE X+1175,Y-50: PRINT;
"700"
  920 MOVE X+500,Y-100:PRINT;"Wavelength  nm":VDU4
  930 INPUT TAB(50);"Plot on paper";C:IF  C=1  GOTO 940 ELSE
ENDPROC
  940 CALL &900:ENDPROC
  950 REM   ------------ PROC print ------------
  960 DEFPROCprint
  970 FOR I=1 TO 200 STEP 5
  980 PRINT I; TAB(13);A(I); TAB(26);A(I+1); TAB(39);A(I+2);
TAB(52);A(I+3); TAB(65);A(I+4)
```

```
 990 NEXTI
1000 ENDPROC
1010 REM   ------------ PROC  save ------------
1020 DEFPROCsave
1030 INPUT"File name ",A$
1040 X=OPENOUT A$: FOR I=1  TO  200:  PRINT #X,A(I): NEXTI:
CLOSE#X
1050 ENDPROC
1060 REM   --------- PROC  machinecode ---------
1070 DEFPROCmachinecode
1080 FOR J=0 TO 3 STEP 2
1090 P%=TOP
1100 [ OPT J
1110  .AA   SEI:LDA#0:STA&FE62:LDX#0:LDY#&FA  \PB INPUT
1120        LDA&FE6E:AND#&E4:STA&FE6E          \IER  CA1,CA2
CB1,CB2 DISABLE
1130        LDA&FE6C:AND#&FC:ORA#&FC:STA&FE6C \PCR CA1-CB1+
CB2 HIO/P CA2 LO/P
1140      LDA#&31:STA&71:LDA#0:STA&70:LDA#&10:STA&77:LDA#&8
:STA&78           \No/STEP
1150       LDA&FE60:LDA&FE61              \CLEAR CA1,CB1 FLAG
1160  .A1  LDA#0:STA&74:STA&75
1170       LDA&FE6C:ORA #&07:STA&FE6C     \CA2 HI
1180  .A2  DEX:BNE A2
1190       LDA&FE6C:AND #&FD:STA&FE6C     \CA2 LO
1200  .A3  DEC&78:BNEA3:LDA#8:STA&78:DEX:BNEA3:LDA#8:STA&78
\DELAY
1210  .A4  LDA&FE6C:AND #&1F:ORA #&C0:STA&FE6C     \CB2 LO
1220  .A5  DEC&78:BNE A5:LDA#8:STA&78     \DELAY
1230       LDA&FE6C:ORA #&E0:STA&FE6C     \CB2 HI
1240       LDA&FE60:STA&72:JMP A7         \MSB
1250  .A6  JMP A1
1260  .A7  LDA&FE6D:AND #&10:BEQ A7       \WAIT  FOR Ao  HI
ON CB1
1270       LDA&FE60:STA&73                \LSB
1280      LSR&72:ROR&73:CLC:LSR&72:ROR&73:CLC:LSR&72:ROR&73
:CLC:LSR&72:ROR&73:CLC
1290       LDA&73:ADC&75:STA&75:LDA&72:ADC&74:STA&74
1300       DEC&77:BNE A4                  \16 READING/STEP
1310      LSR&74:ROR&75:CLC:LSR&74:ROR&75:CLC:LSR&74:ROR&75
:CLC:LSR&74:ROR&75;CLC
1320       LDA#&10:STA&77:DEY:LDA&74:STA(&70),Y:DEY:BEQ A9:
LDA&75:STA(&70),Y
1330  .A8  DEX:NOP:BNE A8                 \DELAY
1340       DEC&76:BNE A6                  \NEXT STEP
1350       CLI:RTS
1360  .A9  LDA&75:STA(&70),Y:DEC&71:DEC&76:BNE A6
1370  .FF  SEI:LDX#0
1380  .F1  DEC&78:BNE F1:LDA#6:STA&78:DEX:BNE F1   \DELAY
1390       LDA&FE6C:ORA #&07:STA&FE6C     \CA2 HI
1400  .F2  DEX:BNE F2                     \DELAY
1410       LDA&FE6C:AND #&FD:STA&FE6C     \CA2 LO
1420  .F3  DEC&78:BNE F3:LDA#6:STA&78:DEX:BNE F3   \DELAY
1430       DEC&76:BNE F1
1440       CLI:RTS
1450  .RR  SEI:LDX#0:LDA&FE6E:AND#&E4:STA&FE6E     \IER CA1
```

```
CA2, CB1,CB2 DISABLE
 1460       LDA&FE6C:AND#&FC:ORA#&FC:STA&FE6C  \PCR CA1-CB1+
CB2 HIO/P CA2 LO/P
 1470       LDA#0:STA&FE63:LDA&FE61         \CLEAR CA1 FLAG
 1480  .R1  DEC&78:BNER1:LDA#6:STA&78:DEX:BNER1:LDA#6:STA&78
\DELAY
 1490       LDA&FE6C:ORA #&07:STA&FE6C      \CA2 HI
 1500  .R2  DEX:BNE R2         \DELAY
 1510       LDA&FE6C:AND #&FD:STA&FE6C      \CA2 LO
 1520  .R3  DEC&78:BNER3:LDA#6:STA&78:DEX:BNER3:LDA#8:STA&78
\DELAY
 1530       LDA&FE6D:AND #&2:BEQ R1         \OPTO  SWITCH  ON
CA1
 1540       CLI:RTS
 1550  .TT  SEI:LDA&FE6E:AND#&E4:STA&FE6E  \IER CA1,2  CB1,2
DISABLE
 1560       LDA&FE6C:AND#&FC:ORA#&FC:STA&FE6C  \PCR CA1-CB1+
CB2 HIO/P CA2 LO/P
 1570       LDA#0:STA&74:STA&75
 1580  .T1  LDA&FE60                        \CLEAR CB1 FLAG
 1590       LDA&FE6C:AND #&1F:ORA #&C0:STA&FE6C     \CB2 LO
 1600  .T2  DEC&78:BNE T2:LDA#8:STA&78      \DELAY
 1610       LDA&FE6C:ORA #&E0:STA&FE6C      \CB2 HI
 1620       LDA&FE60:STA&72                 \MSB
 1630  .T3  LDA&FE6D:AND #&10:BEQ T3        \WAIT  FOR Ao  HI
ON CB1
 1640       LDA&FE60:STA&73                 \LSB
 1650      LSR&72:ROR&73:CLC:LSR&72:ROR&73:CLC:LSR&72:ROR&73
:CLC:LSR&72:ROR&73:CLC
 1660       LDA&73:ADC&75:STA&75:LDA&72:ADC&74:STA&74
 1670       DEC&77:BNE T1                    \16 READING/STEP
 1680     LSR&74:ROR&75:CLC:LSR&74:ROR&75:CLC:LSR&74:ROR&75
:CLC:LSR&74:ROR&75:CLC
 1690       LDA#&10:STA&77
 1700       CLI:RTS:]
 1710 NEXT J
 1720 ENDPROC
```

Appendix B

Effect of random variation in reflected signal on the haemoglobin index and oxygen saturation measurement

The coefficient of variation of the haemoglobin index and oxygenation can be calculated by assuming a random variation in the reflected signal (ΔI_s) as explained in section 6.4. Details of the calculations (cf page 197) are presented here. The LIR is defined as the logarithm of inverse of reflectance, LIR = $\log(I_w/I_s)$, hence, ΔI_s will create a variation in the LIR which can be calculated from the following formula:

$$\Delta LIR = Log_{10}(1 \pm \frac{\Delta I_s}{I_s}) \qquad 1$$

To apply this equation in the haemoglobin index (eqtn 5.3), it can be written as below:

$$H = \{(A_{L2} - A_{L1})/16.5 - (A_{L3} - A_{L2})/29\}\ 100$$

$$= -6.06\ A_{L1} + 3.45\ A_{L2} + 9.51\ A_{L3} \qquad 2$$

where A_{L1}, A_{L2}, and A_{L3} represent the LIR value at wavelength 527.5, 544, and 573 nm. If it is assumed that there is no association between the fluctuations in LIR at different wavelengths, then:

$$(\Delta H)^2 = (6.06\ \Delta A_{L1})^2 + (3.45\ \Delta A_{L2})^2 + (9.51\ \Delta A_{L3})^2 \qquad 3$$

Assuming that the variation in the signal (ΔI_s) for wavelengths 527 to 573 nm are the same, the variation in the LIR would then be the

same and hence:

$$\Delta A_{L1} = \Delta A_{L2} = \Delta A_{L3} = \Delta A_L$$

$$= \text{Log}_{10}(1 \pm \frac{I_s}{I_s}) \qquad 4$$

substituting 4 in 3 gives:

$$\Delta H = 11.79 \Delta A_L \qquad 5$$

The coefficient of variation of the haemoglobin index is then calculated from the following:

$$\frac{\Delta H}{H} = \frac{11.79}{H} \text{Log}_{10}(1 \pm \frac{\Delta I_s}{I_s}) \qquad 6$$

Biological variation in the diffusely reflected signal measured in-vivo at a finger tip at 540 nm is 0.5%. This variation leads to a coefficient of variation of 9.0% for a finger tip haemoglobin index of 0.282 (Table 7.4).

To calculate the coefficient of variation of oxygen saturation, the oxygenation index (eqtn 5.7) is written as below:

$$OX = \{(A_{L3} - A_{L4})/14.5 - (A_{L4} - A_{L5})/14.5 \} 100/H$$

$$= (6.9A_{L3} - 13.8A_{L4} - 6.9A'_{L5})/H$$

$$= Nu/H \qquad 7$$

A_{L3}, A_{L4}, and A_{L5} represents the LIR value at wavelengths 573, 558.5, and 544 nm, and "Nu" represents the numerator. ΔNu can be calculated the same as ΔH, the result is:

$$\triangle Nu = 16.89\ \triangle A_L \qquad 8$$

From equation 7 it can be written that:

$$\left(\frac{\triangle OX}{OX}\right)^2 = \left(\frac{\triangle Nu}{Nu}\right)^2 + \left(\frac{\triangle H}{H}\right)^2 \qquad 9$$

substituting 7 in 9 and rearranging the result will give the following:

$$\triangle OX = \frac{1}{H}\ (\triangle Nu^2 + OX^2 x\ \triangle H^2) \qquad 10$$

substituting 8 and 5 in 10 gives the following:

$$\triangle OX = \frac{1}{H}\ (285.37 + 139.04\ OX^2)\ \triangle LIR \qquad 11$$

Since the percentage of oxygen saturation is calculated from the following formula (eqtn 5.8)

$$Sa\ O_2 = 50.76\ OX + 41.675 \qquad 12$$

hence:

$$\triangle Sa\ O_2 = 50.76\ \triangle OX \qquad 13$$

and the coefficient of variation of oxygen saturation is calculated from the following formula:

$$\frac{\Delta Sa\ O_2}{Sa\ O_2} = \frac{50.76\ \Delta OX}{50.76\ OX + 41.675} \qquad 14$$

substituting 11 and 12 in 14 gives:

$$\frac{\Delta Sa\ O_2}{Sa\ O_2} = \frac{50.76}{H}\sqrt{\left(\frac{19.47}{Sa\ O_2} - 0.1155\right)^2 + 0.0406}\ \Delta LIR \qquad 15$$

0.5% variation in the reflected signal from a finger tip with haemoglobin index =0.282 and oxygen saturation =94% (Table 7.4) will give a coefficient of variation of 8.6% in the oxygen saturation measurements.

REFERENCES

Alcun Li W.P., 1987, "Non-prescription drugs", Blackwell Scientific Publisher.

Altman P.L., Gibson J.F., and Wang C.C., 1958, "Handbook of respiration" W.B.Saunders, Philadelphia and London.

Anderson N.M., and Sekelj P., 1967, Phys. Med. Biol., 12, a) 173, b) 185.

Anderson R.R., and Parrish J.A., 1981, Laser Surg. Med., 1, 263.

Baumberger J.P., and Goodfriend R.B. 1951, Fedn. Proc. Fedn. Soc. Exp. Biol. 10, 10.

Bell G.H., Davidson J.N., and Scarborough H., 1961, "Textbook of physiology and biochemistry", fifth edition, P 577, E & S Livingston Ltd. Edinburgh and London.

Brinkman R., and Wildschut J.H., 1938, Acta Medica Scandinavica, 94, 459.

Brodsky J.B., September 1986, Seminars in Anesthesia, 5, 180.

Bruls W.A.G., and Van der leun J.C., 1982, Photochem. Photobiol., 36, 709.

Bruls W.A.G., and Van der leun J.C., 1984, Photochem. Photobiol., 40, 231.

Brunsting L.A., and Sheard C., 1929, J. Clin. Invest., 7, a) 559, b) 575, c) 593.

Buckley W.R., and Grum F., 1961, Arch. Dermatol., 83, 111.

Comroe J.H. Jr., 1974, "Physiology of respiration, An introductory text", second edition, year book Medical Publishers, Inc, Chicargo.

Cripps D., 1981, J. Invest. Dermatol. 76, 154.

Dawson J.B., Barker D.J., Grassam E., Cotterill J.A., Fisher G.W., and Feather J.W. 1980, Phys. Med. Biol., 25, 695.

Diffey B.L., 1977, Phys. Med. Biol., 22, 309.

Drabkin D.L., and Austine J.H., 1932, J. Biol. Chem., 98, 719.

Farrington D.Jr., and Van der leun J.C., 1968, Arch. Derm. 97, 553.

Feather J.W., 1986, "A reflectance spectrophotometric study of the interaction of visible and ultraviolet radiation with skin", Ph.D. thesis, Leeds University, England.

Feather J.W., Driver I., Leslie G., Hajizadeh-Saffar M., Gilson D., King P.R., and Dixon B., 1988, Proc. Int. Soc. Opt. Eng. (SPIE), 906, (In press).

Fetcher E.S., Hall J.F., and Shaub H.G., 1949, Science, 110, 422.

Flock S.T., Wilson B.C., and Patterson M.S., 1987, Am. Assoc. Phys. Med., 14, 835.

Fountain R.B., Baker B.S., Hadgraft J.W., and Sarkany I., 1969, Br. J. Der., 81, 202.

Fulton G.P., Farber E.M., and Moreci A.P., 1959, J. Invest. Dermot., 33, 312.

Gimmerikh F.I., June 1966, NASSA TT, F420, 35.

Goldie E.A.G., 1942, J. Sci. Inst., 19, 23.

Gordy E., and Drabkin D.L., 1957, J. Biol. Chem., 227, 285.

Groenhuis R.A.J., Ferwerda H.A., and TenBosch J.J., 1983, Appl. Opt., 22, 2456.

Ham A.W., Axelrad A.A., and Cormac D.H., 1979, "Blood cell formation and the cellular basis of immune responses", J.B. Lippincott Co., Philadelphia and Toronto.

Hardy J.D., Hammel H.T., and Murgatroyd D., September 1956, J. Appl. Physiol., 9, 257.

Hardy C., and Perrin F.H., 1932, "The principles of optics", McGraw -Hill Book Company, New york, London.

Horecker B.L., 1943, J. Biol. Chem., 148, 173.

Jacquez J.A., and Huppenhem H.F., March 1955, J. Appl. Physiol., 7, 523.

Janssen F.J., 1972, Med. & Biol. Engng., 10, 231.

Jonxis H.P., 1938, Acta Medica Scandinavica, 94, 467.

Keenan R.L., September 1986, Seminars in Anesthesia, 5, 175.

Kramer K., Elam J.O., Saxton G.A., and Elam W.N., April 1951, Amer. J. Physiol., 165, 229.

Keramer K., Graf K. and Overbeck W., 1956, Pflugers Arch. Ges. Physiol. 262, 285.

Kubelka P., May 1948, J. Opt. Soc. Am., 38, 448.

Kubelka P. and Munk F., 1931, Z. Techn. Physik, 2, 593.

Longini R.L., Zdrojkowski R. January 1968, IEEE Transaction Bio-Medical Engineering, BME-15, 4.

Major Gy., 1980, Acta Physica Academiae Scientiarum Hungaricae, 48, 3.

McKelvey J.P., Longini R.L., and Brody T.P., July 1961, Phys. Rev., 123,51.

Millikan G.A., October 1942, Rev. Sci. Inst., 13, 434.

Montagna W. and Parakkal P.F., 1974, "The structure and function of skin", (3d edition), Academic Press, New York.

Montgomery G.E. Jr., Geraci J.E., and Wood E.H., 1948, Federation Proc., 7, 81.

Mook G.A., Osypka P., Sturm R.E., and Wood E.H., 1968, Cardiovaso. Res., 2, 199.

Parrish J.A., Anderson R.R., Urbach F., and Pitts D., 1978, "UV-A,

Biological effects of ultraviolet radiation with emphasis on human responses to longwave ultraviolet", Plenum Press, New York.

Patterson M.S., Wilson B.C., Feather J.W., Burns D.M., Pushka W., 1987, Photochem. Photobiol., 46, 337.

Philip G., 1946, "Philips' Modern School Atlas", 37 th edition, George Philip & son Ltd., London.

Pisharoty N.R., 1971, "Optical scattering in blood", Ph.D. Thesis, Carnegio-Mellon University, Pittsburgh.

Regan J.D., and Parrish J.A., 1982, "The science of photomedicine", Plenum Press, New York and London.

Russell N.J., Powell G.M., Jones J.G., Winterburn P.J., and Basford J.M., 1982, "Blood biochemistry", Croom Helm Ltd. London and Canada.

Ryatt K.S., Feather J.W., Dawson J.B. and Cotterill J.A., 1983, J. Am. Acad. Dermatol., 9, 558.

San van, Anderson R.R., and Parrish J.A., 1981, Photochem. Photobiol., 34, 493.

Shockley W., 1962, Phys. Rev., 125, 1570.

Schuster A., 1905, Astrophysics J., 21, 1.

Sulzberger M.B., 1968, Arch. Derm. 97, 564.

Tennent R.M., 1971, "Science data book", C. Nicholls & Company Ltd, Manchester.

Twersky V., 1962, J. Opt. Soc. Am., 52, 145.

Wendlandt N.WM., and Hecht H.G. 1966 "Reflection spectroscopy", Interscience Publishers, New York, London, Sydney.

West J.B., 1974, "Respiratory physiology - the essentials", Blackwell Scientific Publications, Oxford, London, Edinburgh, Melbourne.

Wood E.H., and Geraci J.E., 1949, J. Lab. Clin. Med., 34, 387.

Mathematical Symbols

Ab.	Absorbance (Log 1/T)
A_L	LIR value at wavelength λ
A_1	Area of the tip of the fibre optic
A_2	Illuminated area
A_b	LIR value of saline on black surface
A_m	Measured absorbance
A_s	LIR value of sample
A_λ	LIR value of reflectance spectrum at wavelength λ
$A_{b,\lambda}$	LIR value of blood sample at wavelength λ
$A_{d,\lambda}$	LIR value of deoxygenated blood at wavelength λ
$A_{m,\lambda}$	LIR value of melanin at wavelenth λ
$A_{o,\lambda}$	LIR value of fully oxidised blood at wavelength λ
$A_{s,\lambda}$	LIR value of in-vivo skin at wavelength λ
$A_{(x)}$	Incident collimated photon flux at any point in the sample
Bf	Blood flow (ml min^{-1} dl^{-1} tissue)
C	Velocity of light (m/s)
c	Concentration of red cells (g/cm^3 or mol/cm^3)
Ca O_2	Oxygen content of arterial blood (ml/dl of blood)
D	Diffusion coefficient (cm^2/s)
d	Distance of detector from the sample (cm)
E	Irradiance (mW/cm^2)
E_0	Irradiance of light at the surface of the illuminated fibre
E_c	Irradiance of light at the surface of the collecting fibre
F	Photon flux (photons cm^{-2} s^{-1})
$G_{(x)}$	Photon generation function
Hb	Haemoglobin content (g/dl blood)
Hs	In-vivo haemoglobin index of the skin
h	Haematocrit
I	Intensity of light in the Kubelka-Munk model
I_o	Incident light intensity (mW/cm^2)
I_ϕ	Diffusely reflected light at an angle ϕ
I_{ow}	Diffusely reflected light from white surface at normal angle
I_b	Stray light or reflected light from black surface
I_{dr}	Diffusely reflected light from the surface of scatterer
I_r	Diffusely reflected light intensity
I_s	Back scattered light from the sample
I_{spec}	Specular reflected light intensity
$I_{s\lambda\phi}$	Diffuse reflected light from a skin surface at wavelength λ, and at angle ϕ
I_t	Transmitted light intensity
I_w	Diffuse reflected light from white surface
$I_{w\lambda o}$	Diffuse reflected light from white surface at wavelength λ, and normal to the surface
$I_{w\lambda\phi}$	Diffuse reflected light from white surface at wavelength λ, and at angle ϕ
i	Angle of incident
J	Intensity of light in Kubelka-Munk model (opposite to incident)

K, k	Absorption coefficient (K -Ln10 k)
L	Radiance (mW cm^{-2} sr^{-1})
LIR	LIR of in-vivo skin surface
l	Mean photon free path before absorption
M	Melanin content ($\mu g/cm^2$)
$M_{\bar{\lambda}}$	Melanin index defined at average wavelength λ
M_s	Slope of the synthetic melanin compound spectrum
M_w	Melanin index of unpigmented sample (pig fat)
m	Mean photon free path before scattering
N	Number of steps of the stepper motor
Nu	Numerator (appendix B)
n	Refractive index
P	Photon density (photon cm^{-3})
P_i, P_j	Density of photons which are travelling in the incident and opposite direction (Kubelka -Munk model)
P_r	Photodiode responsivity (V mW^{-1} cm^2)
p	Power of incident radiation (radiant power mW)
pO_2, PCO_2	Partial pressure of oxygen and CO_2 (mmHg)
R	Diffused reflectance
R_p	Internal radius of the reflectance probe
R_{spec}	Specular reflectance
R_w	Reflection coefficient of white surface
r	Refraction angle
r_1	Radius of the tio of the fibre optic boundle
r_2	Radius of the illuminated area inside the reflectance probe
r'	Distance of the collecting fibre from an emitting point on the illuminated surface
S, s	Scattering coefficient (S -ln10 s)
Sa O_2	Oxygen saturation (%)
S_r	Fraction of scattered radiation
T	Transmittance (transmitted flux)
t	Thickness (cm)
$T_{1/2}$	Half value layer (cm)
U_λ	Non-specific absorption in skin
u	Path length of small portion of light in a medium (Monte Carlo method)
V_{out}	Output voltage (V)
X	Used as a variable for oxygenation of blood samples
x	Used as a variable for thickness (Kubelka -Munk model)
$Y_{(\lambda,oxy)}$	Ratio of haemoglobin index to absorbance of blood at wavelength λ and certain oxygenation
α	Divergent angle of the light emerging the fibre tip
Θ	Angle of observation (in a plane surface)
Φ	Angle of observation (with normal to the surface)
ω	Solid angle (sr)
τ	Photon life time
ε	Specific absorption coefficient (cm^2/mol)
ρ	Radius
λ	Wavelength (nm)